A LIQUEFACTION KINETIC RESEARCH NEEDS ASSESSMENT

J. Ferrance, and R. P. Warzinski
U. S. Department of Energy
Pittsburgh Energy Technology Center
Pittsburgh, Pennsylvania 15236

Keywords: Direct liquefaction, kinetic modeling assessment, processing variable effects

INTRODUCTION In February 1989, the Department of Energy released its assessment of the research needs for coal liquefaction.[1] Under direct liquefaction, 4 of the 12 recommendations focused on developing models and determining kinetics. Reasons accompanying these recommendations stressed the need to understand the retrograde reactions, the reactions taking place as the coal is heated to the reaction temperature, and the effects of coal types and solvent on liquefaction reactions. By understanding the liquefaction process better, suggestions for improving the process may be made. A good kinetic model would provide a basis for testing suggestions which would attempt to control reactions or effects in the development of improved liquefaction technologies. Brandes et al. suggests that a kinetic model could also possibly have a large impact on the economics of coal liquefaction.[2] Cost factors which could be studied using a kinetic model include: coal preparations, reactor throughput, hydrogen usage, catalyst usage, product yields and selectivity, and process control.

The purpose then of a kinetic model is to have a tool for evaluating the liquefaction process as the inputs and the processing conditions are changed. The model has to be able to account for the effects of these changes and provide valuable results to someone using the model. As a starting point for the development of this type of kinetic model, the assessment described in this work was carried out. The assessment included an intense review of earlier kinetic models found in the literature, along with reviews of the current work being carried out in this area. It was meant to discover the strengths, weaknesses, and limitations of available models and provide guidelines for future models. At the same time, the assessment looked at questions of who uses liquefaction models, why they use them, and what they expect the model to do.

SMALL-SCALE MODELS At the level of small-scale processes, most kinetic models for batch reactors use a variation on the simplified reaction scheme shown in Figure 1. Reaction rate constants are determined in each of these studies by fitting liquefaction results obtained in that particular set of experiments. Because of this, no consistent set of rate constants or activation energies has been found for these reactions. Even within a single study, changing coal or solvents required new rate constants to be determined. More complicated reaction schemes, based more on the actual chemistry taking place during the liquefaction process, have also been developed. A scheme by Suzuki, shown in Figure 2, includes a free radical pool as the first product of coal dissolution.[3] This allows retrograde reactions to be included as one of the important reactions taking place during liquefaction.

Weller found four problems with these types of kinetic models.[4] First, the reactions listed are not elementary and therefore cannot be described by simple rate laws. Second, the liquefaction system is not a single phase. Third, the quantities used in rate laws must be described in terms of liquid-phase concentration, not just masses in the reactor. Fourth, the reactivity of the intermediate products change with time. This assessment has revealed three additional problems with these models. One, they do not include hydrogen as a reactant but assume hydrogen is present in excess and does not affect the rates. Two, reactions during heat-up times are usually ignored, but even for fast heat-ups (1-2 min) significant amounts of the coal will break down during this period. Three, these models do not fulfill the basic purpose of a model because they have little predictive value for determining results of liquefactions run under different processing conditions.

This situation has been partially corrected in a current model containing additional retrograde reactions and calculations during the heat-up time.[5] The reaction scheme for this model is shown in Figure 3. The kinetic expressions derived from this scheme are based not on mass, but on liquid-phase concentrations. This can be done because thermodynamic calculations are also included in the model to account for the three-phase nature of the liquefaction process. Hydrogen is included directly in the necessary expressions, and the gas-phase contribution to this concentration is determined through the mass transport calculations which are also part of the model. Processing variables are incorporated directly into these calculations in one or more ways. An example is the type of solvent, which affects mass transport through its viscosity, thermodynamics through its partition coefficient, and kinetics through its hydrogen donating ability. The effects of changing some processing variables can be predicted, but some important variables, such as the type of catalyst used, have not yet been incorporated into this model.

Like most of the earlier models, this model also suffers from the fact that the reactions are not truly elementary and the reactivity of the intermediate products change. Lack of

elementary reactions in the scheme is inherent in any model dealing with coal. Because of the large number of reactions actually taking place within the coal, there is no real way to include and write kinetic expressions for all of these reactions (see Current Models below). In models which lump the products as preasphaltenes, asphaltenes, and oils, these simple product definitions give no indication of the internal nature of each product. Reactions within a single product, which change the quality and reactivity of that product, cannot be included in the model. Inclusion of more product fractions in the model would be one way of handling this problem. The small amounts of material recovered in small-scale batch reactors, however, often prevent further fractionation of the products.

In continuous reactors, sufficient product can be recovered for separation into additional fractions, but this is not always done. Many of the models for continuous reactors therefore also use solubility-defined products and suffer from the same problems as the batch models. Studies which have fractionated the oil into more species by boiling point ranges usually then lump the widely different preasphaltene, asphaltene, and nondistillable oil fractions as a single fraction. This single product is usually called resid or solvent refined coal (SRC). Though reactions and reactivities of the distillate fractions can be defined in models using such products, the major changes which take place within the resid product are now lost.

One of the better continuous models was given by Singh et al.[6] This model defined three distillate products based on boiling point ranges along with a SRC product. The kinetic expressions developed in the model included terms for both the hydrogen pressure and the mineral matter content of the slurry. Inclusion of these terms made the model applicable to more situations, but no justification was given as to the final form of these terms which were based on empirical fitting of experimental data. In addition, the kinetic parameters were still limited by a simplified reaction scheme, containing an instantaneous initial reaction and no retrograde reactions and experimental data from only a single coal.

LARGER SCALE MODELS Kinetic modeling of large-scale liquefaction processes was carried out using both Wilsonville and HTI pilot plant data. The Wilsonville model was developed in two parts using data from both the actual plant and a specially designed batch reactor.[7] For the thermal liquefaction unit, the reaction scheme, shown in Figure 4, considered light and heavy hydrocarbon gas products along with a resid fraction, but lumped all of the liquid product into a single distillate fraction. Heteroatom gases were also included as products since much of the hydrogen used in the liquefaction process goes into these products. In setting up the actual kinetic expressions, the Wilsonville model developers used the results of tracer studies which showed that the thermal liquefaction unit could be modeled as a CSTR. However, two different residence time definitions were used in the various kinetic expressions. The actual residence time above 370°C, including both the reactor and part of the preheater, was used in the hydrocarbon gas formation expressions, but the nominal residence time, just over the reactor, was used in the heteroatom expressions. These choices came purely from data fitting and had no theoretical basis.

The hydrotreating unit part of the Wilsonville model included a set of secondary reactions considered to be purely catalytic. These reactions, shown in Figure 5, included hydrotreated resid and hydrotreated distillate products. Internal reactions within these two products are included in the model to account for changes in their reactivity and composition. No indication was given, however, on how these hydrotreated products could be separated or identified, and kinetic expressions were not developed for these reactions. Catalyst deactivation terms were included in the kinetic expressions which were determined from this reaction scheme.

The overall Wilsonville model was thus not only specific for the processing condition being used, but suffered from the same problems as the small-scale models. Two-phase effects were accounted for in some of the expressions by using actual residence times, but not for all of the reactions, and the choice of residence time definition for a reaction was not justified. The reaction scheme was also too simplified with product lumps which were too encompassing.

The model developed at HTI, shown in Figure 6, is significantly different from the Wilsonville model.[8] Two distillate products, a high boiling gas-oil, and a low boiling naphtha, were defined, along with resid and gaseous products. High, low, and unreactive coal fractions were defined, and the reactions scheme included both parallel and implied sequential reaction pathways leading from coal to all of the products. This represents a move towards a reaction scheme based more on the underlying liquefaction mechanisms. Two problems remain, however. First, there are no retrograde reactions specified, and, second, no secondary reaction scheme is established.

Coal type was taken into account in the model by the amounts of high, low, and unreactive fractions (a, b, and c), and by the distribution of products formed in the initial parallel reactions during coal dissolution (f-j). One would then expect that if a-c and f-j could be determined independent of the model, then liquefaction using any coal type could be predicted by this model. Unfortunately, the rate constants (k_1 and k_2) used in the coal breakdown reactions were also made coal dependent. Catalyst deactivation rates, included for reactions which were

found to be catalyst dependent, were made coal dependent as well.

Additional problems with the HTI model included inconsistencies in both the reaction scheme and the rate constants which required changes in the model when it was applied to batch autoclave liquefactions. The model developers suggest that their product lumps are too large and that significant changes occur within the individual product fractions during liquefaction. No reactions describing this process are included in the model, however. There are no kinetic expressions for heteroatom removal or hydrogen consumption, and gas-oil kinetics are only found by difference in the model rather than through a direct expression.

CURRENT WORK In addition to the current model for small-scale batch processes described above,[5] work is also being conducted on statistical models. These models represent coal by a large number of random chain molecules which have the same statistical characteristics (carbon content, aromatic content, etc,) as the original coal. Rules for breaking bonds within the chains are specified and a Monte Carlo simulation is run to follow the breakdown of the coal molecules with time. By defining products based on specific chain characteristics, the production of individual products with time can also be followed. To be comparable to experimental data, the products defined in the model must be characterizable by methods currently available for analyzing coal liquefaction products.

Monte Carlo simulations require significant amounts of computer time to carry out. This time increases greatly as the number of initial molecules in the simulation increases, as the number of possible reactions increase, or as simulation time is increased. This limits the starting point to a small representative sample of all possible coal chain molecules. Reactions which take place within a single product fraction, such as naphtha, can be included, but will not really be detectable at the actual experimental level. In addition, these simulations usually represent purely kinetic descriptions of the process and do not account for transport or thermodynamic considerations of the reaction system.

MODEL USERS Two groups of researchers are expected to be the predominant users of coal liquefaction kinetic models: those who use them for economic analysis, and those who use them for scientific or engineering analysis. For economic analysis of large-scale processes, the structure or organization of the model itself is not usually important. What is needed is for the model to accept specific characteristics of input streams and predict the expected compositions of the output streams. If the type of reactor and separation units to be used are known, cost analysis will focus mainly on changes in the amounts of useful product in the exit stream as processing conditions are changed. Catalyst cost is a major factor, however, so both economic and scientific users are interested in the rate at which catalyst must be replaced in the reactor.

Scientific users are more interested in what is going on inside the reactor and how various conditions affect the process. The model must be able to show what happens as the space velocity is changed, as the reactor temperature is changed, or as the hydrogen treat rate is changed. It would be beneficial to separate the kinetics of the reactions from the physical effects of the reactor, such that the model is applicable to any reactor system design. By having an accurate description of what is going on inside the reactor, it may also be possible to adjust conditions to control the particular reactions taking place.

RESULTS This assessment has helped to identify a number of specific areas important to the development of future kinetic models. Decoupling of the processing variables from the kinetic parameters is needed to make the model applicable over a wider range of experimental conditions. To do this, intrinsic rate constants must be determined for the various reaction steps which are independent of the coal, solvent, reactor, and all other processing conditions. Since the model must still be able to predict the effects of changing these processing conditions, other ways must be found to incorporate these variables.

Some of the models described above have begun to take these variables into account, but this is only a start. In the model of Ferrance and Holder, literature correlations based on coal characteristics are used to determine ultimate conversions and hydrogen availability.[5] These correlations, however, were developed using data from a limited range of coals. More basic research is needed to extend the applicability of such correlations to the entire range of coal types. Similar correlations, independent of the model itself, will also be needed to determine initial product distributions and the hydrogen donating ability of both coals and solvents.

Decoupling the reaction rates from the design of the reactor will make the kinetics applicable to all reactor setups. This means that the model will have to be able to handle and incorporate the mixing and mass transport characteristics within the reactor. Mass transport calculations will require accurate predictions of the viscosity and hydrogen gas solubility of the slurry, two areas in which further work needs to be carried out. In addition to solubilities, other areas of the thermodynamics of liquefaction systems also need work. In particular, studies are needed on partitioning of the solvent and light products into the vapor-phase since these may represent the hydrogen donating or hydrogen shuttling species in the reactor.

While modeling of both small-scale and large-scale reactors would be possible, much more work is needed for development of a large-scale model which can be used for both economic and engineering purposes on a commercial level. For work at this scale, inclusion of the preheater in the model was determined to be of great importance. Simulation of pilot plant preheaters have shown that up to 90% of the total coal conversion may be complete by the time the slurry exits the preheater.[9] The rates of the coal dissolution reactions are very fast and produce large changes in the characteristics of the slurry. Free radical and retrograde reactions which occur as the slurry is heated may have an influence on the final product yields. The possible presence now of dispersed catalyst in the preheater, fed or recycled with the slurry, adds to the complexity of the reactions occurring in this unit.

Product definitions have also been found to be an important area in which improvements are needed, because the reaction scheme and kinetic expressions depend on the products. What is needed, is standardization of a choice of product fractions which can be analytically defined and experimentally characterized. For the distillate products, definition of fractions by boiling point ranges will allow use of the various correlations developed by the petroleum industry. For the nondistillable products, additional solubility separations might be possible, or molecular weight separations might be used to give additional fractions. CONSOL has directed a study to evaluate the usefulness of various analytical methods for characterizing coal liquefaction process streams.[10] Though applicable methods have been determined, no set of products which could be defined by these methods has been established.

Enough product fractions must be defined so that each fraction has stable and consistent physical and thermodynamic properties which can be used for engineering analyses. Inclusion of too many product fractions, however, will lead to a large number of reactions and an unwieldy model. A reaction scheme will have to be set up relating how each of these products, plus any additional intermediates are formed and reacted. The scheme must include a set of initial reactions, giving the products formed directly from the coal, as well as a set of secondary reactions describing the further breakdown into low molecular weight products. As this reaction scheme is setup, it is also important to distinguish between those reactions which are purely thermal, those which have both thermal and catalytic components, and those which are only catalytic. The assessment has found that this is the best way to explicitly include the impact of catalysts in the model. Rate constants for the catalytic reactions will always be catalyst dependent and will have to be determined independently for each catalyst. However, incorporation of catalyst variables, such as the amount of catalyst or the catalyst particle size, must be independent of these rate constants for the model to be valuable.

EXPERIMENTAL Experimental work has begun at the Pittsburgh Energy Technology Center in conjunction with the assessment to study some of these areas. Determining a workable reaction scheme was felt to be the most important contribution at this stage. To do this, specific product cuts from a bench-scale continuous facility are being reacted in microautoclave reactors under different conditions. Both the initial and reacted products are being analyzed to determine how fractions can be defined using readily available techniques. How the amounts and types of fractions change during the process will help to elucidate the secondary reactions which take place during liquefaction to convert or produce each fraction.

A second set of experiments has been designed to investigate the initial reactions which take place. In these experiments, coal will be reacted in microautoclave reactors under conditions typically found in a coal liquefaction preheater. Time/temperature profiles determined for pilot-plant preheaters are shown in Figure 7.[11-12] By simulating heating of the coal to different temperatures along this curve in a tubing bomb, the initial reactions which occur as coal is converted to a liquid will be observed. The prevalence of secondary reactions taking place before the slurry exits the preheater will also be determined through these experiments. A true scheme for the formation of light products from coal both directly and through sequential reactions will be developed. This determination of the early reactions taking place in the preheater should help in the design of better preheaters for large-scale processes.

FUTURE WORK The assessment is not complete. Discussions with investigators working at both the bench-scale and larger scale continue to provide additional input on what should be incorporated into future models to make them useful and valuable. This input is solicited through distribution of preliminary reports and on-line through a coal liquefaction kinetic modeling home page (http://www.petc.doe.gov/kinetics.html).

What has become evident already is that kinetic modeling has developed independent of mass transport and thermodynamic considerations which affect the liquefaction process. Future efforts will require assessing the studies carried out in these areas to determine what additional work will be needed to incorporate these results into liquefaction models. Monitoring of current external experimental work relevant to all areas listed will continue. Continuing adjustments of the PETC internal experimental program as data is collected, and as additional input arrives will also be carried out.

REFERENCES

1. "Coal Liquefaction - A Research Needs Assessment," DOE/ER-0400, 1989.

2. Brandes, S.D., Robbins, G.A., Winschel, R.A., Burke, F.P., "Coal Liquefaction Process Streams Characterization and Evaluation, Volume II," DOE/PC/89883-93, 1994.

3. Suzuki, T., "Development of Highly Dispersed Coal Liquefaction Catalysts," Energy & Fuels, 1994, 8, 341.

4. Weller, S.W., "Kinetics of Coal Liquefaction: Interpretation of Data," Energy & Fuels, 1995, 9, 384.

5. Ferrance, J.P., Holder, G.D., "Development of a General Model for Coal Liquefaction," This volume, 1996

6. Singh, C.P.P., Shah, Y.T., Carr, N.L., Prudich, M.E., "Liquefaction of Coal by SRC-II Process, Part I: A New Kinetic Model," Can. J. Chem. Eng., 1982, 60, 248.

7. Catalytic, Inc., "Development of a Simulation Model for Bituminous Coal Liquefaction in the Integrated Process at Wilsonville," DOE/PC/50041-89, 1987.

8. Comolli, A.G., Johanson, E.S., Lee, L.K., Popper, G.A., Smith, T.O., "Final Report," DE-88818-TOP-03, 1993.

9. Brandes, S.D., Lancet, M.S., Robbins, G.A., Winschel, R.A., Burke, F.P., "Coal Liquefaction Process Streams Characterization and Evaluation," DOE/PC/89883-53, 1992.

10. Robbins, G.A., Brandes, S.D., Winschel, R.A., Burke, F.P., "Coal Liquefaction Process Streams Characterization and Evaluation, Volume I," DOE/PC/89883-93, 1994.

11. Catalytic, Inc., "Operation of the Wilsonville Advanced Coal Liquefaction R & D Facility," DOE/ET/10154-122, 1982.

12. Gulf Science & Technology Co., "Slurry Preheater Design: SRC-II Process," Report No. 560RM149, 1981.

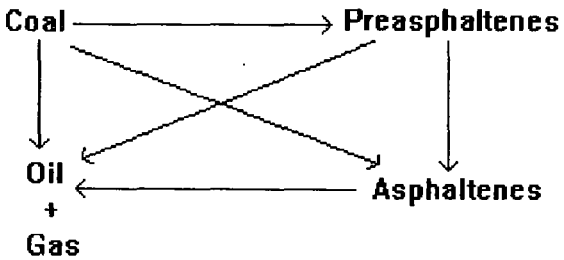

Figure 1 Reaction scheme used in most earlier simple models

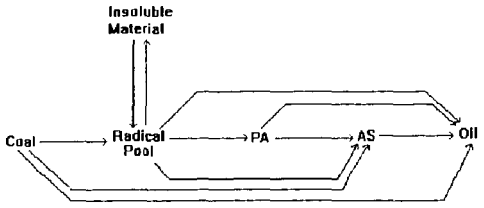

Figure 2 Reaction scheme of a recent model by Suzuki.

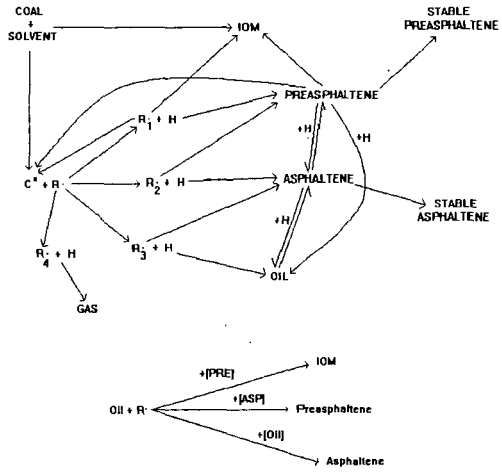

Figure 3 Reaction scheme of Ferrance and Holder

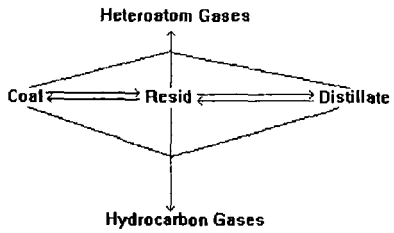

Figure 4 Wilsonville reaction scheme for the thermal liquefaction unit

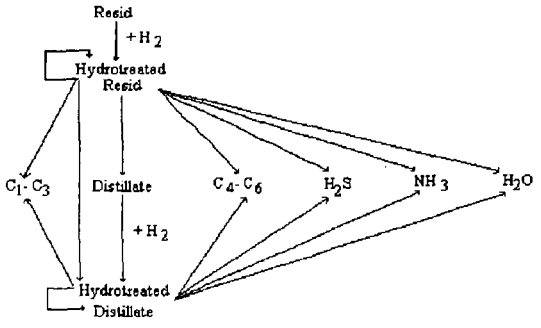

Figure 5 Wilsonville reaction scheme for the hydrotreater unit

$$Coal \xrightarrow{\qquad\qquad} a\,C_1 + b\,C_2 + c\,Unreactive\ Coal$$

$$C_1 \xrightarrow{k_1} f Resid + g Gas\ oil + h Naphtha + i Hydrocarbon\ gases + j Byproduct\ gases$$

$$C_2 \xrightarrow{k_2} f Resid + g Gas\ oil + h Naphtha + i Hydrocarbon\ gases + j Byproduct\ gases$$

$$Resid + H_2 \xrightarrow{catalyst} Products$$

Figure 6 Reactions used in the HTI coal liquefaction model

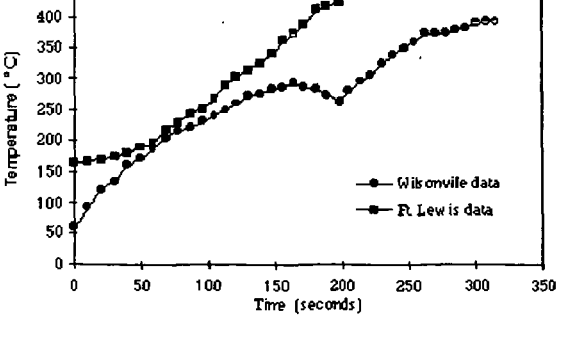

Figure 7 Time/temperature profiles for two pilot-plant preheaters

COAL LIQUEFACTION KINETICS

Shaojie Wang, Keyu Wang, He Huang, Michael T.Klein and William H. Calkins*
Department of Chemical Engineering
University of Delaware, Newark, Delaware 19716

Key words: kinetics, coal liquefaction, modelling

Introduction

Understanding the mechanisms of uncatalyzed direct coal liquefaction by means of reaction kinetics has been a long sought goal. Curran et al. in 1967 (1) and Wiser in 1968 (2) and Neavel in 1976 (3) measured the rates of liquefaction of various coals and postulated a free radical mechanism to explain the data obtained. The kinetics as determined by these and other workers is described in detail by Gorin in Chapter 27 of Elliott's Second Supplementary Volume to the Chemistry of Coal Series (4). However, it has been well known that most coals contain some material extractable by organic solvents. The solvents used in direct coal liquefaction would of course be expected to also extract soluble material as well as effect the liquefaction reaction. If the extractable material were a significant quantity in the coal, it would seriously affect the kinetics. Cassidy et al. (5,6) used a stirred autoclave with a sampling port at the bottom in their kinetic studies. They observed that hot charging the coal rapidly formed an oil which they considered to originate predominantly from the "guest component", i.e., extractables, in the lignite they studied. Also, the free radical nature of the liquefaction process would be expected to produce secondary reaction products which would complicate the kinetics as well as lead to retrograde products.

With this background, it seemed important to measure the kinetics of direct liquefaction at very short contact times where the extractables would be quickly removed and secondary reactions due to the free radical nature of the liquefaction would be minimized. By the use of a special Short Contact Time Batch Reactor (SCTBR), we have been able to show that direct coal liquefaction occurs both thermally and catalytically in at least two separate and distinct stages: an extraction stage and a slower breakdown and liquefaction of the coal macromolecules themselves (7,8). With this equipment, it is possible to study the kinetics of each stage and to measure the kinetic parameters of each. The kinetics of two coals (Illinois #6 bituminous and Wyodak-Anderson subbituminous coals) investigated at reaction times from 10 s to 60 min are reported in this paper.

Experimental

Apparatus. The Short Contact Time Batch Reactor was used to carry out the liquefactions. The design and operation of the reactor system including a schematic diagram have been described elsewhere (9,10). In brief, a 30 cm^3 reactor is constructed of 3/4" o.d. stainless steel tubing of approximately 12" length with wall thickness of approximately 0.433". The 21 ft lengths of coiled stainless tubing used for both the preheater and precooler are 1/4" o.d. with wall thickness of 0.035". The reactor system is capable of containing up to 17 MPa (2500 psi) pressure at temperatures of up to 500°C.

In operation, both the empty preheater and the reactor are immersed in a Techne IFB-52 fluidized sand bath. They are brought up to the reaction temperature prior to the start of the reaction. High pressure hydrogen or nitrogen gas provided the driving force to deliver the slurry mixture of coal-solvent or coal-solvent-catalyst under study from a small blow case at ambient temperature into the empty reactor through the hot preheater tubing. Hydrogen or nitrogen gas was then bubbled through the reactor from the bottom to provide the agitation needed in the liquefaction reaction. The degree of agitation was controlled by the exit gas flow rate from the top of the reactor. In the case of running under hydrogen pressure, the gas bubbles were also used to supply the hydrogen for the liquefaction reaction.

The temperature of the reactants (ca.30 g) initially at ambient temperature, approach the desired reaction temperature to within 5-8°C during the transport process (approximately 0.3 seconds) and reaches the predetermined reaction temperature within 30 seconds. At a preselected time, the high pressure gas is again used to drive the reactor contents from the reactor into a cold receiver through the precooler. Both receiver and precooler are immersed in a water bath. Quenching of the product mixture to about 25°C is achieved during the transport time of about 0.3 seconds.

Coal Studied. Illinois #6 bituminous and Wyodak-Anderson subbituminous coals from the Argonne Premium Coal Sample program were investigated in this study. Proximate and elemental analyses, together with other analytical data, of these coals are available in the User's Handbook for the Argonne Premium Coal Sample program (11).

Workup Procedures of the Reaction Products. The product mixtures were filtered and the solid residues washed with cold fresh tetralin thoroughly and dried in a vacuum oven with a nitrogen purge at 105°C for 48 hours. The filter cake was then rinsed with methylene

chloride and dried in a vacuum oven with a nitrogen purge at 105°C for 12 hours. The solid residue and the liquid filtrate were analyzed separately by various procedures.

Thermogravimetric Analysis. The thermogravimetric analyzer was a Model 51 TGA (TA Instruments, New Castle, Delaware). The TGA which was run on liquefaction residues provided a measure of the amount of volatile matter (VM), fixed carbon (FC) and ash. The mineral matter of the coal was shown to accumulate in the coal residue and not in the coal liquids. Ash in the residue was therefore used to calculate the conversion using the formula:

$$Conversion\ (wt\%) = (1 - \frac{A_0}{A_s}) \times 100\% \qquad (1)$$

where A_0 and A_s are the weight fractions of ash (derived from the coal mineral matter) in a control sample and in the liquefaction residue, respectively.

The volatile matter (VM) in the residue turned out to be only a function of the reaction time and temperature. The fixed carbon (FC), however, is a measure of the retrograde processes occurring during the liquefaction and the kinetics of the FC formation could be followed by TGA.

Results and Discussion

Liquefaction Conversion vs Time. Figure 1 shows conversion vs time curves for Illinois #6 coal without added catalyst in tetralin (8 to 1 tetralin to coal weight ratio) at four temperatures and 1000 psig nitrogen atmosphere. There are several stages in the liquefaction as shown by these curves. There is an initial rapid conversion which is due to the extraction of soluble matter into the tetralin. This is followed by a pseudo-induction period during which little conversion appears to occur. This is not due to the build up of any intermediates such as free radicals as shown by ESR spectroscopy (12). Actually it is due to the simultaneous ending of the extraction stage and the slow conversion of the coal structure to liquid products. As the temperature increases, the extent of the extraction process increases and the pseudo-induction period becomes shorter. At still higher temperatures, particularly in the presence of a strong hydrogenation catalyst, the induction period becomes almost undetectable.

In nitrogen, there is little increase in conversion to liquid products above 408°C, although the reaction mixture is changing rapidly. We have shown that the volatile matter (VM) content decreases steadily as the time and temperature increases. However, the fixed carbon (FC) values increase dramatically at higher temperature, resulting in decreased yield of tetralin soluble materials (8).

Similar conversion curves are obtained for the liquefaction of the Wyodak-Anderson subbituminous coal in tetralin (8 to one tetralin to coal by weight)(8). These curves show the characteristic stages of extraction, induction period and coal liquefaction similar to the Illinois #6 coal.

Conversion vs time curves for both Illinois #6 and Wyodak Anderson coals in tetralin in the presence of hydrogen and added catalysts will be presented with a kinetic analysis in a future paper.

Kinetic Analysis of Coal Liquefaction. As shown in the previous section, three distinct phases in the coal liquefaction process in the absence of hydrogen and a catalyst are observed. The initial rapid conversion (in the first 30 to 60 s) is due to the extraction of a soluble fraction of the coal into the processing solvent. This is followed by a pseudo-induction period and then the slow conversion of the coal structure to liquid products. This pseudo-induction period is a transition interval which is due to the simultaneous occurrence of these two processes, a very rapid extraction which is ending and a relatively slower liquefaction of the coal matrix which is becoming dominant. Based on this hypothesis, the liquefaction conversion observed in experiments, therefore, is the sum of the conversions of these two processes:

$$X = X_s + X_r \qquad (2)$$

where X is the liquefaction conversion determined in the experiments; X_s is the solubilizing conversion which is due to the extraction of the soluble materials in the coal; and X_r is the liquefaction reaction conversion which is due to the chemical breakdown of the coal structure. From Eq. 2, the liquefaction rate is the sum of the derivatives of these conversions, i.e.,

$$\frac{dX}{dt} = \frac{dX_s}{dt} + \frac{dX_r}{dt} \qquad (3)$$

The extraction rate could be expressed by

$$\frac{dX_s}{dt} = k_s(X_{s0} - X_s) \qquad (4)$$

where k_s is the extraction rate constant; X_{s0} is the equilibrium level of extraction of coal under liquefaction conditions; and X_s is the soluble fraction at time t. The breakdown rate for the coal matrix is given by

$$\frac{dX_r}{dt} = k_r' ((1-X_{s0}) - X_r)^{\alpha} C_t^{\beta} P_{gas}^{\gamma} \quad (5)$$

where k_r' is the reaction rate constant; X_r is the liquefaction reaction conversion at time t; C_t is the tetralin concentration; and P_{gas} is the nitrogen or hydrogen pressure. When a large amount of tetralin is used in the liquefaction (for example, 8 to 1 of tetralin to coal ratio was used in this study), C_t is approximately equal to a constant. P_{gas} is held a constant during the liquefaction run in this study. Assuming $\alpha = 1$, Eq. 5 is simplified to

$$\frac{dX_r}{dt} = k_r((1 - X_{s0}) - X_r) \quad (6)$$

Integrating with boundary conditions of $X_s = 0$ and $X_r = 0$ at $t = 0$ and substituting $(1 - X_{s0})$ by X_{r0} which is defined to be the maximum conversion due to liquefaction reactions, Eqs. 4 and 6 become

$$\ln(1 - \frac{X_s}{X_{s0}}) = -k_s t \quad (7)$$

and

$$\ln(1 - \frac{X_r}{X_{r0}}) = -k_r t \quad (8)$$

respectively.

Kinetics of Illinois #6 and Wyodak-Anderson Coal Liquefactions. The plot of $\ln(1-X_s/X_{s0})$ against t for the Illinois #6 coal liquefaction in tetralin under 1000 psig N_2 at 390 °C is shown in Figure 2. The slope gives a measured rate constant for extraction of $k_s = 2.81$ with an r^2 of 0.97. The plot of $\ln(1-X_r/X_{r0})$ against t for the Illinois #6 coal liquefaction reaction process is illustrated in Figure 3. It shows two distinct reaction stages: a rapid one with a rate constant of 0.027 for the first 5 minutes, and a slower one of 0.0054 for times greater than 5 minutes. The kinetic parameters of the Illinois #6 and Wyodak-Anderson coal liquefactions evaluated by the proposed model are summarized in Table 1. As an example, Figure 4 shows experimental data and modelling curve at the reaction times up to 10 min for Wyodak-Anderson coal liquefaction in tetralin at 390 °C under 1000 psig N_2. It shows that the model fits the experimental data very well.

Rate constants of k_s and k_r at three temperatures (358, 390, and 408 °C) were used to estimate activation energies of extraction and liquefaction reaction processes. The plot of $\ln k_s$ against 1/T and $\ln k_r$ vs 1/T shown in Figures 5 and 6 give activation energies of 14 and 22 kcal/mol for the solubilization and liquefaction reaction processes, respectively.

It is of interest to compare these results with those obtained by others at higher conversion. Wiser (2) obtained an activation energy value of 28.8 kcal/mol for Utah bituminous coal liquefaction at 63 to 94% conversion. Curran et al. (1) obtained two values for a rapid and a slow rate with mean values of 30 and 38 kcal/mol on Pittsburgh Seam bituminous coal at 2.5 minutes and 2 hours, respectively. They used a process-derived solvent from 325 to 435°C. While the 22 kcal/mole value seems rather low, coal has obviously both weak and strong bonds which will be broken in order of their bond strength. The process derived solvent may strongly affect the relative amounts of the extraction and liquefaction stages in the Curran work. All of these values are low compared to the strength of carbon-carbon bonds and obviously the activation energies observed by us and others reflects the reaction complexity as well as the particular bonds being broken.

The Retrograde Reactions Occurring during liquefaction. As reported above, increasing temperature results in a levelling off of liquefaction yields due to the production of fixed carbon (FC) which results in lower liquefaction yields and production of tars and coke. Understanding this onset of retrograde reactions is of great importance for improvement of the direct coal liquefaction process. Analysis of these residues show decreasing hydrogen to carbon ratios as the coal residues are exposed to higher temperatures and longer reaction times (see Figure 7). It is not surprising therefore that introduction of a hydrogenation catalyst in the liquefaction process has a profound effect limiting the rate of formation of fixed carbon FC and therefore increasing the liquefaction yields. Interestingly, however, when a good hydrogenation catalyst is used, increasing reaction temperature up to a point actually increases yield and decreases FC formation (8).

Summary and Conclusions

The direct liquefaction of coal shows distinct stages: an extraction stage and multiple slower stages representing the breakdown of various components of the coal structure. These only become apparent with a reactor system capable of accurately distinguishing conversions at reaction times as low as 10 seconds.

The liquefaction conversion observed in the experiments is the sum of the two simultaneous liquefaction processes of extraction and liquefaction of the coal structure. Based on this model, the liquefaction kinetics in each stage of the entire process can be adequately described.

The extraction stages in the bituminous and subbituminous coals studied to date are about two orders of magnitude faster than the structure breakdown stages and have correspondingly lower activation energies. The liquefaction of the coal structure itself also consists of multiple steps of different rate constants and activation energies.

The retrograde reactions can be followed by thermogravimetric analysis of the coal liquefaction residues. They are suppressed by catalytic hydrogenation during the liquefaction process.

Acknowledgements

The support of this work under DOE Contract DE-PS22-93PC93201 is gratefully acknowledged.

References

1. G.P. Curran, R.T. Struck, and E. Gorin *I&EC Process Design and Development* **6**, 1, pp. 166-173 (1967).
2. W.H. Wiser *Fuel* **47** pp. 475-485 (1968).
3. R.C. Neavel *Fuel* **55** pp. 237-242 (1976).
4. E. Gorin *Chemistry of Coal Utilization Second Supplementary Volume* Elliott, M.A. Editor, Chapter 27, pp. 1845-1918, Wiley Interscience (1981).
5. P.J. Cassidy, W.R. Jackson, F.P. Larkins, M.B. Louey, D. Rash and I.D. Watkins *Fuel* **68**, pp. 32-39 (1989).
6. P.J. Cassidy, W.R. Jackson, F.P. Larkins, M.B. Louey and I. Watkins *Fuel* **68** pp. 40-44 (1989).
7. H. Huang, K. Wang, S. Wang, M.T. Klein, and W.H. Calkins *Coal Science and Technology 24: Coal Science*, Proceedings of the 1995 International Conference on Coal Science, Eds J.A. Pajares and J.M.D. Tascon, Vol. II, p. 1207 (1995).
8. H. Huang, K. Wang, S. Wang, M.T. Klein and W.H. Calkins *Energy and Fuels* 1996, in press.
9. H. Huang, W.H. Calkins, M.T. Klein *Energy and Fuels* **8** pp. 1304-1309 (1994).
10. H. Huang, D.M. Fake, W.H. Calkins, and M.T. Klein *Energy and Fuels* **8** pp. 1310-1315 (1994).
11. K.S. Vorres 'User's Handbook for the Argonne Premium Coal Sample Program' *ANL/PCSP-93/1.*
12. W.D. Provine, B. Jung, M.A. Jacintha, D.G. Rethwisch, H. Huang, W.H. Calkins, M.T. Klein, C.G. Scouten, C.R. Dybowski *Catalysis Today* **19**, 3, 409 (1994).

Table 1 The rate constants of the Illinois #6 and Wyodak coal liquefactions

Coal	T,℃	time	Liquefaction stage	Rate constant k	r^2
Illinois #6	358	0 - 2 min	Extraction	0.848	0.996
		0 - 60 min	Reaction	0.00275	0.999
	390	0 - 1.5 min	Extraction	2.81	0.997
		0-5 min	Reaction (R1, fast)	0.0276	0.999
		> 5 min	Reaction (R2, slow)	0.00541	0.998
	408	0 - 1 min	Extraction	6.05	0.998
		0-10 min	Reaction (R1, fast)	0.0458	0.972
		> 10 min	Reaction (R2, slow)	0.00301	0.987
Wyodak-Anderson	390	0 - 0.5 min	Extraction	11.8	0.996
		0-15 min	Reaction (R1, fast)	0.0195	0.995
		> 15 min	Reaction (R2, slow)	0.0161	0.999

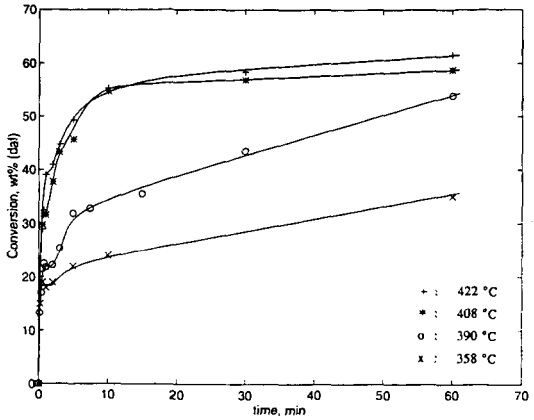

Figure 1 Conversion vs time for Illinois #6 coal liquefaction without added catalyst in tetralin (tetralin:coal = 8:1 mass ratio) under 1000 psig N_2

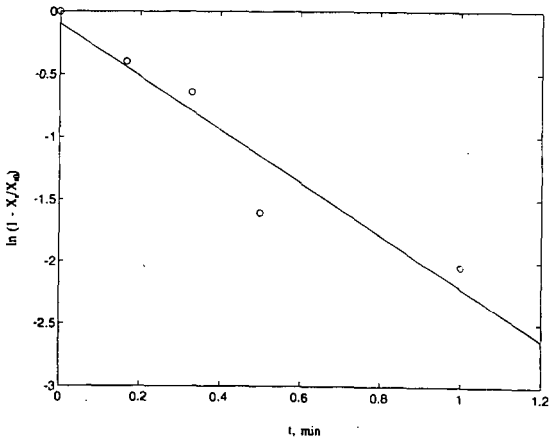

Figure 2 $\ln(1-X_r/X_{r0})$ vs t for the Illinois #6 coal liquefaction in tetralin under 1000 psig N_2 at 390 °C

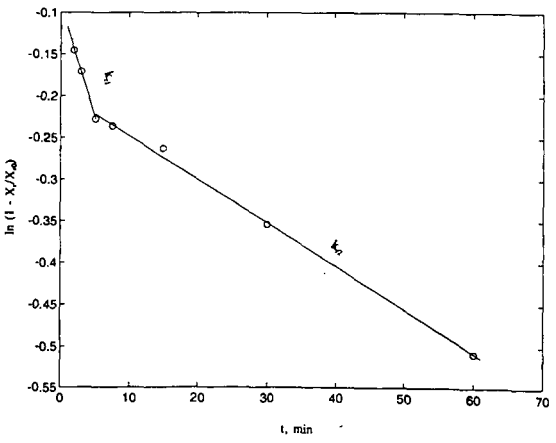

Figure 3 $\ln(1-X_r/X_{r0})$ vs t for the Illinois #6 coal liquefaction in tetralin under 1000 psig N_2 at 390 °C

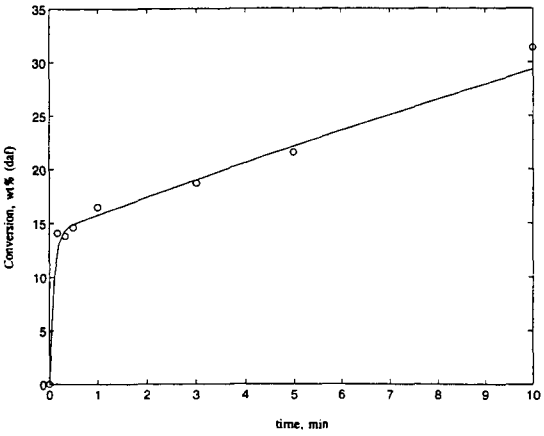

Figure 4 Plot of the experimental data and modelling curve at the reaction times up to 10 min for Wyodak-Anderson coal liquefaction in tetralin at 390 °C under 1000 psig N_2.

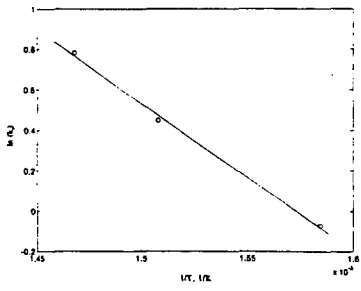

Figure 5 $\ln k_e$ vs 1/T for the thermal liquefaction of Illinois #6 coal (Extraction stage)

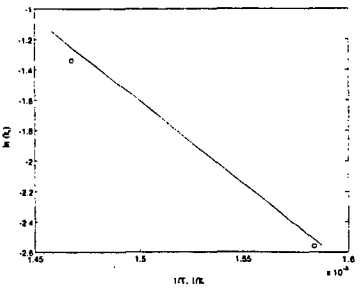

Figure 6 $\ln k_r$ vs 1/T for the thermal liquefaction of Illinois #6 coal (Reaction stage)

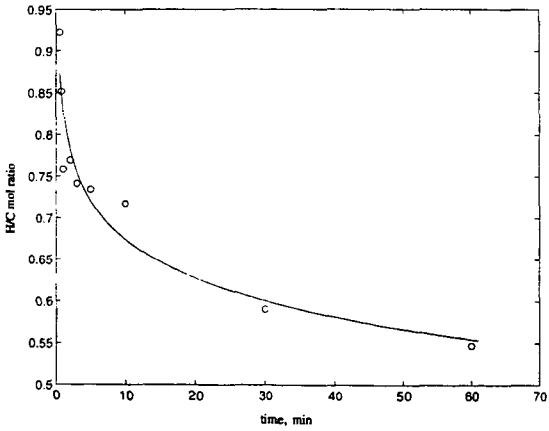

Figure 7 H/C mol ratio of the liquefaction residues of Illinois #6 coal without added catalyst in tetralin (tetralin:coal = 8:1 mass ratio) under 1000 psig N_2 at 422 °C

DEVELOPMENT OF A GENERAL MODEL FOR COAL LIQUEFACTION

Jerome P. Ferrance and Gerald D. Holder
Department of Chemical Engineering
University of Pittsburgh
Pittsburgh, PA 15261

Keywords: Kinetic modeling, coal liquefaction simulation, processing condition effects

INTRODUCTION One goal of coal liquefaction kinetic models is to be able to predict the results of coal liquefaction experiments in order to identify optimal processing conditions. A second goal is to be able to define experimental conditions that provide the greatest amount of information per experiment. This is especially important in comparing catalysts. A third goal is simply to be able to identify those processing variables which will have the greatest effects in a given system. This will reduce the number of actual experiments needed to investigate new systems by focusing on only the most important variables.

Previous investigators have taken into account the effects of a number of variables in development of their kinetic models.[1] These effects include temperature, coal type, solvent type, and hydrogen pressure. Temperature is readily taken into account through determination of activation energies from rate constants found at different temperatures. Coal type and solvent type were sometimes taken into account through ultimate conversions, but most often were included by adjusting the rate constants for each coal or solvent. Hydrogen pressure was included as a separate term in the rate equations in some models.

These models could not fulfill the three goals listed above, because the rate constants determined in each of these models was specific for the conditions of the experiment. Changing conditions in these models meant redetermining the kinetic parameters in the rate expressions. These new parameters could only be obtained by first doing actual experiments under the new conditions. Figure 1 shows the model and rate constants determined by Giralt et al. for a system in which only the solvent was changed.[2] The widely different reaction rate constants for some of the reactions indicate that no predictions of how the system would have performed when the solvent was changed would have been possible.

A model which is to fulfill the above goals must be able to account for the effects which take place when processing conditions are changed without resorting to redetermining the kinetic constants from experimental data. One approach has been to include additional terms directly in the kinetic equations used in the calculations. For example, basing ultimate conversion on coal type provides a way to include the type of coal directly into the models predictions. The ultimate conversion is related to characteristics of the coal being used. Such advances provide a partial answer, but coal type affects more than just the ultimate conversion, as different coals have different solubilities, amounts of mobile phase, numbers of free radicals, and donatable hydrogen. Solvent, solvent/coal ratio, reactor type, heat-up time, mixing speed, coal treatment, and gas phase pressure and composition must also be included in the model. As shown in Table 1, all of these variables have been included in this general model which has been developed.

GENERAL MODEL

NEW CALCULATIONS Two things included in the kinetics of this model, which had not been included in previous models, are the basing of reaction rates on the *concentration* of reactants in the liquid phase and inclusion of an explicit hydrogen concentration. Earlier models used masses of reactants in the reactor, and ignored variable phase volumes and distribution of components between phases. Earlier models also assumed that hydrogen was not limiting in their systems and the hydrogen supply was considered constant. That prevents these models from being applied to systems in which the amount of hydrogen does influence the results of the reactions.

To include the effects of concentration and hydrogen pressure into the kinetic calculations required two additional sets of calculations to be simultaneously carried out. To determine reactant concentrations, both the volume of the liquid phase and the amount of each component in the liquid phase has to be determined. This required that the thermodynamic state of the system be continuously determined in conjunction with the kinetics, as changes in the reactor contents take place. Mass transfer calculations are also required to determine the rate at which solid coal particles dissolve into the liquid phase, and the rate at which hydrogen gas dissolves into the liquid phase. Mass transfer calculations require the thermodynamics calculations to set the maximum solubilities of coal and hydrogen gas in the liquid phase. Mass transfer also depends on kinetic calculations, through the viscosity of the liquid phase which changes as the liquefaction reactions take place. Thus the mass transfer, thermodynamic, and kinetic calculations are completely dependent on each other.

The model was set-up to be as accurate as possible in terms of mass transport and thermodynamic calculations. Figure 2 shows partition coefficients calculated by the model for

the hydrogen/tetralin system along with experimental data.[3] Figure 3 shows calculated and experimental viscosities for a coal liquid at three pressures for a range of temperatures.[4] These figures reflect the different kinds of experimental data which were incorporated into the development of this model. By including thermodynamics and mass transport, the properties of the solvent being used, such as its solubility parameter, vapor pressure, and viscosity became intimately connected with the calculations. The processing variables, solvent/coal ratio and mixing speed, are also directly taken into account through these calculations.

NEW REACTION SCHEME As mentioned above, hydrogen concentration was used in the reaction rate equations. To do this, a new scheme had to be developed for the liquefaction mechanism in which hydrogen directly participated in some of the reactions. The reactions were based more on the underlying chemistry which has been determined to take place, through both model compound and liquefaction studies. One of the major improvements in this model was the inclusion of free radical reactions as a significant part of the coal breakdown mechanism. The free radical intermediates could be either capped in reactions in which hydrogen participated, or recombined in retrograde reactions. The numbers of free radicals present was determined from both the coal type and the temperature in the reactor using correlations developed from literature data.

As in some earlier models, we assume a fixed fraction of the coal is unreactive. This amount is based on the coal type, but it does not have to be experimentally determined in this new model. Instead, a literature correlation of maximum conversions based on coal characteristics has been adapted to provide this value for any coal used in the model. In addition to the unreactive coal, the retrograde reactions form some material which will be unreactive; some fraction of the preasphaltenes and asphaltenes produced in the liquefaction are also considered to be stable. Empirical correlations were developed to determine the stable fractions also based on the coal characteristics. Data from a large number of liquefactions run under different conditions was used to determine the final coefficients in these correlations.

Both parallel and serial reactions were included in the scheme to allow for the production of asphaltenes and oils directly from the coal. Two separate coal breakdown reactions were specified, representing the two types of bonds which are normally broken in the coal structure, ether bonds and alkyl linkages between aromatic structures. The amounts of each fraction formed by these initial reactions was also set up to be dependent on the type of coal used in the model. The series reactions, including preasphaltenes to asphaltenes to oils and preasphaltenes to oils, were also made hydrogen dependent since hydrogen addition is a big part of the conversion to lower molecular weight products. In the model, hydrogen for these reactions comes from three sources: the coal, the solvent if it has donatable hydrogen, and hydrogen gas if present. The amount of hydrogen available from the coal is also determined from a literature derived correlation.

COMPUTER PROGRAM To make the model useable, a computer program was written to carry out all of the simultaneous kinetic, mass transport, and thermodynamic calculations. Including all of the various correlations for stable fractions, free radicals, coal solubility parameter, and the amount of donatable hydrogen from coal, allows the user to specify only the type of coal without having to first do all of these calculations to use the model. This required storing default values of the coal characteristics for each type of coal within the program. Solvent characteristics were also stored within the program for use in both the thermodynamic and transport calculations.

The final computer program which was produced is designed such that the user does not have to understand the inner workings of the model or the calculations included in the model. The user interacts with the program answering questions about the processing conditions which are to be used. Variables which must be input to the program include the reaction temperature, the type and amount of coal, the coal particle size and if the coal has been dried, the type and size of the reactor, the mixing speed and heat-up time, the type and mass of solvent, and the type of and pressure of the gas phase. The computer program calculates all necessary parameters which are dependent on the users input, then simulates the experiment using the model's calculations. Results of the simulation are given as preasphaltene, asphaltene, oil, gas, and THF insoluble material.

PARAMETER FITTING As with other kinetic models, the activation energies and frequency factors for each of the reactions had to be determined from experimental data. This model had a number of additional parameters which also had to be fitted. What is unique about this model is that data from experiments run under widely varying conditions was combined to carry out this parameter fitting. The data covered temperatures from 300 to 480°C, 6 different types of coal, 4 different solvents, in both stirred autoclave and microautoclave reactors; short and long heat-up time experiments were included. Both hydrogen and inert gas phases were represented at pressures from 0 to 2000 psi, and solvent to coal ratios from 1/1 to 8/1 were covered.

Figure 4 shows a parity plot of experimental versus predicted coal conversions for 100 data points. Figure 5 shows a parity plot of the oil yields for those same data points. Because these points were used in fitting the model parameters, it is not surprising that the model predicts these results well. The diversity of conditions under which these simulations were run using the same set of kinetic constants, however, shows that the model has been able to incorporate a wide variety of processing conditions.

RESULTS The real test for this model was to show that the effects reported in the literature for changes in processing conditions could be reproduced by the model. A simulation was run using a set of conditions selected as the base case. The processing variables were then varied one at a time and the simulation results compared with experimental results for similar changes. The effects of temperature and solvent to coal ratio are predicted by this model. An effect of solvent is predicted, but comparison with experimental data shows that all properties of the solvent have not been fully incorporated into the model. Changes in product yields due to changes in coal type are predicted by the model, but do not follow the exact pattern seen in experimental studies. This was not completely unexpected, as the literature correlations used for taking coal characteristics into account in the model were determined over limited ranges of coal types. The effects of changing hydrogen pressure are predicted by the model, with less of a hydrogen effect seen in good hydrogen donating solvents as expected.

CONCLUSIONS A first generation general model for coal liquefaction has been developed in which the model parameters are not dependent on the liquefaction conditions. This allows the effects of changes in processing variables to be modelled without having to first run experiments to get the necessary kinetic parameters. Inclusion of both mass transport and thermodynamic calculations, along with the kinetic calculations, was needed to incorporate these processing variables into the model predictions. Development of a computer program proved to be the best way to carry out all of the simultaneous calculations which are needed in the model. The interactive nature of the computer program makes the model accessible for use by those unfamiliar with the underlying concepts on which the model was designed.

REFERENCES

1. Ferrance, J. P.,Ph.D. Thesis, University of Pittsburgh, 1996

2. Giralt, J., Fabregat, A., Giralt, F., Ind. Eng. Chem. Res., 1988, 27, 1110.

3. Simnick, J.J., Lawson, C.C., Lin, H.M., Chao, K.C., AIChE J, 1977, 23, 469.

4. Hwang, S.C., Tsonopoulos, C., Cunningham, J.R., Wilson, G.M., Ind. Eng. Chem. Process. Des. Dev., 1982, 21 127.

Table 1 Processing variables included in the model

Variable	Incorporated into model through:
Temperature	Influence on reaction rates Influence on ultimate conversion Influence on hydrogen availability from the coal and solvent Influence on the thermodynamics of the system
Coal type	Influence on ultimate conversion Influence on hydrogen available from coal Influence on initial production fractions Influence on the number of free radicals Influence on coal solubility
Solvent (type and amount)	Influence on the amount of available solvent hydrogen Influence on the system thermodynamics Influence on the coal and hydrogen gas solubilities Influence on the concentrations of reactants Influence on the viscosity
Pressure and gas phase composition	Influence on the system thermodynamics Influence on the amount of hydrogen available from the gas phase Influence on the hydrogen solubility
Reactor (type, size, and mixing speed)	Influence on the thermodynamics of the system Influence on the cold volume in the reactor Influence on the coal and hydrogen dissolution rates
Heat-up time	Reaction rates change during non-isothermal operation Amount of available hydrogen changes with temperature

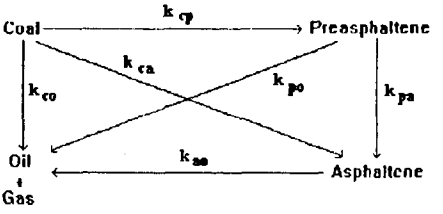

	400°C		350°C	
	Tetralin	Anthracene oil	Tetralin	Anthracene oil
k_{cp}	.0964	.0978	.0575	.0766
k_{ca}	.0540	.0044	.0283	.0022
k_{co}	.0241	.0235	.0191	.0195
k_{pa}	6.2E-6	.0066	2.7E-6	.0039
k_{po}	1.8E-4	0	7.4E-5	0
k_{ao}	.0080	.0125	.0027	.0054

Figure 1 Reaction scheme and rate constants in two different solvents for a kinetic model by Giralt et al.

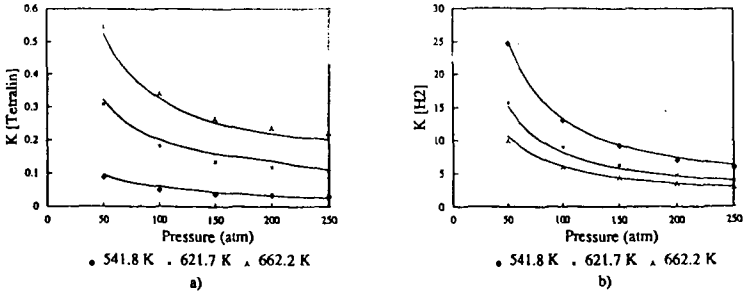

Figure 2 Predicted and experimental partition coefficients for hydrogen/tetralin system: a) tetralin, b) hydrogen.

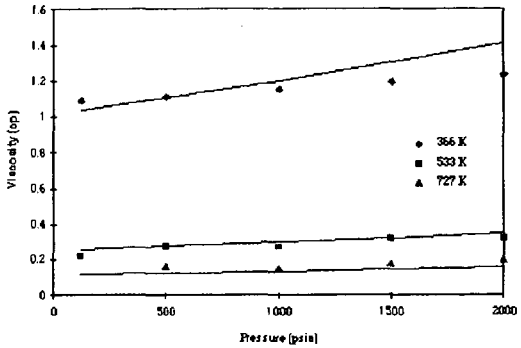

Figure 3 Viscosity of a coal liquid versus pressure at three different temperatures.

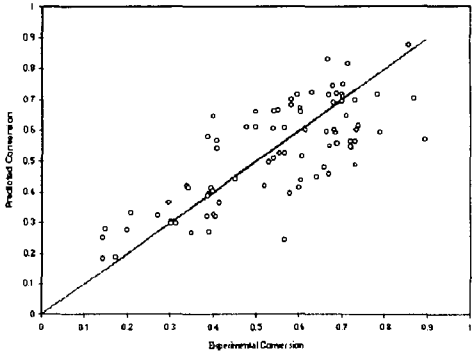

Figure 4 Parity plot of experimental and predicted coal conversions.

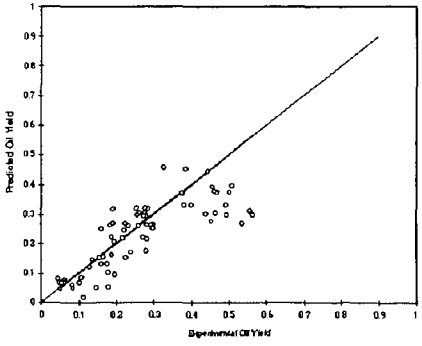

Figure 5 Parity plot of experimental versus predicted oil yields.

DISPERSED SLURRY CATALYSTS FOR HYDROCONVERSION OF CARBONACEOUS MATERIALS

L.K. Lee, V.R. Pradhan, G. Popper, and A.G. Comolli
Hydrocarbon Technologies, Inc.
Lawrenceville, NJ 08648

Keywords: Dispersed Catalysts, Coal Liquefaction, Coal/Waste Coprocessing

ABSTRACT

Dispersed slurry catalysts, based upon the *in situ* sulfided forms of transition metals such as iron and molybdenum, have been developed and successfully employed in the multi-stage hydroconversion of various carbonaceous materials including coal, heavy petroleum resid, waste plastics, and different combinations of these feedstocks. For example, using HTI's proprietary iron-based catalyst and commercial Molyvan-A additive, over 95 % maf coal conversion has been obtained accompanied by over 90 % maf conversion of 524°C+ residuum and over 65 % maf yield of C_4-524°C distillate yield in a fully back-mixed high pressure reaction system. The use of an in-line fixed-bed hydrotreater in such a hydroconversion process that relies only on dispersed slurry catalysts for conversion allows to selectively upgrade the light distillate products (IBP-400°C) from the process resulting in premium quality naphtha and mid-distillate products with less than 10 ppm nitrogen, an H/C ratio of 1.9, and about 20 ppm sulfur. The use of dispersed catalyst for such hydroconversion processes has a significant positive impact (as much as 20 % cost potential reduction) on the process economics because the reactor throughput can be increased by as much as 70 % while maintaining the equivalent residence time and the cost associated with the expensive high pressure catalyst addition/withdrawal system, used for supported extrudate catalyst, and that associated with expensive ebullating pumps can be reduced or eliminated completely.

INTRODUCTION

Two-stage catalytic conversion of coal and other carbonaceous feedstocks have been studied extensively using Ni/Mo or Co/Mo supported catalysts. The low/high temperature mode of operations was demonstrated in 3 ton/day scale at both the Wilsonville advanced Coal Liquefaction facility and Hydrocarbon Research, Inc. This mode of operations in combination with an in-line hydrotreater yields liquids of premium quality containing less than 20 ppm of nitrogen. The high conversion was achieved at the expense of high replacement rate of the supported catalysts which became deactivated with carbon and heavy metal depositions. The deactivation rate of supported catalysts for feedstocks, that contain high degree of heavy metals, such as vanadium and nickel and materials that have high tendency to form coke, is one of the key factor affecting the design and cost of the conversion facility.

Dispersed slurry catalysts, which offer better contact with the reactants than the supported extrudate catalysts, have drawn much attention in recent years. Hydrocarbon Technologies, Inc. has been studied the use of anion modified iron based catalyst at its bench scale (30 Kg/day) multi-stage unit located at Lawrenceville, New Jersey. It is observed that the use of dispersed catalyst, with or without supported catalyst, in conjunction with an in-line hydrotreater increase the throughput of a system significantly without compromising much in the product qualities. This paper discusses the use of HTI's proprietary dispersed catalysts in processing coal and other carbonaceous feedstocks, such as heavy oil and waste plastics. Due to the high activity of these dispersed iron-based catalysts, they can be used in small concentrations of 0.1-1.0 wt% iron relative to weight of feed for the various hydrogenation and hydroconversion reactions mentioned above, and are preferably recycled with the unconverted or partially converted high boiling fraction (454°C+) back to the reactor for further reaction. Because these dispersed fine-sized iron catalysts are produced based on use of available relatively inexpensive materials and since the principal component is cheap and environmentally friendly iron, they are usually disposable for large scale processes and do not require recovery and regeneration. HTI's proprietary dispersed catalyst can be used either as a wet cake consisting of a gel of precipitate particles in water containing 50-80 wt% water or as a dry powder obtained after drying and/or calcination of the oxyhydroxide precipitates. In the gel mode of usage, the precipitates from hydrolysis are not filtered or dried, but are used as is. The catalyst gel form reduces the catalyst cost significantly and also does not compromise at all on its activity for relevant hydroprocessing reactions. These catalysts, either in the dry powder form or in the wet-cake form, have been successfully tested (in the presence of a sulfiding source) both at a 20 cc microautoclave reactor scale and at a 30 kg/day continuous two-stage bench-scale operation, under hydrogen pressures of 5-20 MPa and operating temperatures of between 400 to 460°C. The key to the higher activity of these HTI's catalysts as compared with some other iron-based catalysts disclosed in literature, is believed to be their initial fine size, high surface area, a high extent of catalytic dispersion, and their ability to preserve the state of high dispersion under reaction conditions due to presence of anionic modifiers which are known to prevent sintering or agglomeration of fine-sized particles at high temperatures.

EXPERIMENTAL

The activity of catalyst was tested in a 20 cc vertically shaken microautoclave unit and in a two-stage bench scale continuous flow system of nominal capacity of 30 Kg/day. The bench-scale operations, employing dispersed catalysts, were conducted in HTI's fully back-mixed reaction system employing off-line pressure filtration for solids separation; a simplified schematic of the hydroconversion process used during this work is shown in *Figure 1*. As shown in *Figure 1*, the hydroconversion process, followed here, is based upon a catalytic multi-stage reactor system supported by an independent feed preparation/handling section, high pressure product fractionation section, light distillate refining and solids separation/heavy distillate recovery sections. The hydroconversion reactors could be operated in a close-coupled mode or an interstage product fractionator could be used for taking the lights off the feed going to the second stage hydroconversion reactor. The light product fraction (400°C- material) from the hydroconversion reactors was selectively processed through an in-line fixed-bed hydrotreating unit. This step achieves a significant function of improving the quality of distillable products from the process. The heavier product fraction (400°C+ material) is substantially recycled and unreacted feed (including solids in case of coal) is either partly recycled or rejected from the process completely with minimal loss of organics. The HTI iron based catalyst is an anion modified oxyhydroxide catalyst prepared in either a dry or a gel form which contains about 50-80 w% water. Molybdenum catalyst was added in form of Molyvan A at the desired concentration levels. Coal used in this study is from Wyoming Black Thunder Mine. The coal was prepared by Empire Coke Company of Alabama and was used in the last run of the DOE Proof of Concept program. The heavy oil is a California Hondo vacuum tower bottom, while the waste plastic was a curb side plastic waste containing mostly high density polyethylene, polystyrene and polypropylene.

RESULTS AND DISCUSSION

The activity screening of dispersed slurry catalysts, performed using shaken microautoclaves, is summarized in *Table 1*. From the *Table 1* results, it is seen that the HTI's dispersed slurry catalysts, used in either a wet cake (gel) form or a dried particulate form, provided hydroconversion results superior to those obtained using the two known iron oxide catalysts. Specifically, the percent coal conversion based on tetrahydrofuran (THF) solubility and percent conversion of 524°C+ resid fraction were both significantly greater than for the commercial iron oxide catalysts. The addition of about 100 ppm of molybdenum to HTI's iron catalyst improved both the coal and the resid conversions; the gel form of iron catalyst appeared slightly better than the dry powder form. The best performance of HTI's dispersed catalyst was almost equivalent to that obtained using a more active supported NiMo catalyst, Akzo AO-60, with which a shade better performance was obtained at same temperature but for a longer reaction time (60 minutes).

The dispersed iron-based catalysts described in this paper have been used extensively in continuous bench-scale two-stage operations with throughput up to 30 kg/day of moisture and ash-free (maf) coal feed for direct catalytic two-stage liquefaction of coal. As shown in *Table 2*, under the prevailing operating conditions, for the direct liquefaction of a sub-bituminous Wyoming Black Thunder Mine coal, dispersed catalyst containing 615-10000 ppmw of iron and 50-200 ppmw of molybdenum was used, relative to maf coal feed, in the form of HTI's iron-based dispersed catalysts. The dispersed catalysts were used either in an all-dispersed slurry catalyst mode, or in a hybrid system utilizing dispersed catalyst in one of two close-coupled hydroconversion reactors and the extrudate supported catalyst in the other reactor. The use of iron and molybdenum containing dispersed catalysts has resulted in a coal conversion range of 93-96 wt%, a 524°C+ residuum conversion range of 83-92 wt%, and C_4-524°C distillate liquid yields of 60-66 wt% (all on maf coal basis). When evaluated on the basis of the maf coal feed, this performance provides up to 4 barrels of C_4-524°C distillate liquid products per ton of the maf coal feed. Specifically, the direct comparison between the data from Bench Run 83 Condition 4 and Run 91 Condition 1B shows that in an hybrid catalytic mode of operation, higher molybdenum loading (100 vs. 50 ppm) results in better liquid distillate yields (66.3 vs. 63.4) and higher conversions of coal (94.7 vs. 92.8) and resid (90.0 vs. 87.4). The performance of HTI's dispersed slurry catalysts has been compared with some other dispersed and supported type catalysts for direct coal liquefaction as shown in *Figure 2*. The process performance has been compared on the basis of total coal conversion (based on quinoline solubility of the products), 524°C+ residuum conversion, and C_4-524°C distillate yield. The first bar (None-Cat) in *Figure 2* represents process performance with a thermal first stage reactor and an expanded supported catalyst bed in the second stage reactor; the second bar (Cat-Cat) represents process performance with supported catalysts in both the reactor stages; the third bar (Mo-Cat) represents molybdenum dispersed catalyst in first stage reactor and an expanded supported catalyst bed in the second stage reactor; the fourth bar (HTI-Cat) represents performance with HTI's iron-based dispersed catalyst in the first stage reactor and an expanded supported catalyst in the second stage reactor; the fifth bar (HTI-HTI) represents the performance of an all-dispersed slurry catalyst two-stage reactor system utilizing the HTI's dispersed catalyst It can be clearly seen from *Figure 2* that the reactor configurations utilizing HTI's dispersed catalysts alone result in the highest extent of total coal and 524°C+ residuum conversion, and C_4-524 C distillate

yields. The result obtained with the 'all dispersed catalyst' mode of operation were also better than those obtained with 'Supported catalyst-catalyst' or 'hybrid mode'of operations. At 5000 ppm of iron and 50 ppm of molybdenum, 2 % higher coal conversion, higher light distillate products were obtained; the yield of light gases was also higher in an 'all dispersed' catalyst mode. The use of dispersed catalyst allows the higher volume of reactor for thermal cracking.

Bench-scale continuous multi-stage operations were also conducted to evaluate the performance of HTI's dispersed iron-based catalysts for hydroconversion of (a) heavy petroleum oil (California Hondo resid vacuum tower bottoms), (b) mixtures of heavy petroleum resid oil and mixed plastics (containing high density polyethylene, polypropylene, polystyrene, and other organic/inorganic impurities) from municipal solid waste streams, © mixtures of Wyoming Black Thunder Mine coal and Hondo resid, and (d) combinations of coal, Hondo resid, and the mixed plastics feeds. Significant process performance was obtained with all of these varied feedstocks with dispersed catalysts in each stage reactor, under conditions similar to those employed for direct coal liquefaction. The prevailing operating conditions, feed type and composition, dispersed catalyst metal loadings, and process performance and yields are summarized in *Table 3*. As shown in *Table 3*, consistently high feed conversions and light distillate oil yields have been realized in the bench-scale operations. With the bench-scale operations involving either heavy petroleum resid, Hondo resid alone or in a mixed feed with coal, as high as 99 wt% feed conversion to quinoline soluble products was obtained, with as high as 75 wt% C_4-524°C distillate liquid yields. During the operations, involving mixed plastics from a municipal solid waste stream, either with coal or with heavy resid or mixtures of coal and heavy resid, over 93 wt% total feed conversions were realized with about 75 wt% distillate liquid yields.

CONCLUSION

Based upon the data presented in this paper, it is evident that the sulfate-modified iron-based dispersed catalysts, HTI has developed, are very effective in achieving the levels of performance that is tantamount to or better than that obtained using the conventional supported extrudate catalysts. The iron-based dispersed slurry catalysts were also very effective for the hydroconversion of organic wastes such as heavy petroleum resids and MSW plastics, in combination with coal, into the value-added distillate products.The higher activity of these HTI's catalysts as compared with some other iron-based catalysts disclosed in literature, is believed to be due to their initial fine size, high surface area, a high extent of catalytic dispersion, and their ability to preserve the state of high dispersion under reaction conditions due to presence of anionic modifiers which are known to prevent sintering or agglomeration of fine-sized particles at high temperatures. The overall high levels of yields and conversions are obtained with HTI's proprietary dispersed catalyst, especially at the metal loadings that potentially make the use of these catalysts possible on a disposable basis. The replacement of supported extrudate catalysts by fine-sized dispersed slurry catalysts also allows for operations at significantly higher throughput under similar overall reaction severity. It is anticipated that the use of dispersed catalysts would lower the overall cost of hydroconversion of coal and other organic feeds discussed in this paper.

ACKNOWLEDGMENT

The financial support provided for this work by the U.S. Department of Energy under the Contract Nos. DE-AC22-93PC92147 and DE-AC22-92PC92148 is gratefully acknowledged.

Table 1. Activity of Dispersed Catalyst in Microautoclave Testing*

Coal: 2 g, Solvent: 6g, DMDS: 0.2 g 427°C @ 14 MPa for 30 min. Fe: 5000 wppm

Catalyst Type	THF Conversion [%]	524°C+ Conversion [%]
Fe_2O_3 (Aldrich)	76.1	34.1
Fe_2O_3 (Mach I)	80.6	42.8
Fe/SO_4^{2-} (dry)	83.3	53.3
Fe/SO_4^{2-} (gel)	86.2	55.1
$Mo.Fe/SO_4^{2-}$ (dry)	86.8	59.6
$Mo.Fe/SO_4^{2-}$ (gel)	89.9	63.3

***The THF Conversion under similar reaction conditions (but 60 minute long reaction time) for a supported extrudate $NiMo/Al_2O_3$ catalyst (fresh Akzo AO-60) was 92.1 w% and the 524°C+ residuum conversion was 64.4 w%.**

Table 2 Process Performance using Dispersed and Supported Catalysts
Wyoming Black Thunder Mine Coal
Dispersed Catalyst: HTI sulfated Iron; Supported Catalyst: Shell S-317

Run I.D. Condition	CMSL-6 4	PB-02 1B	CMSL-11 1	PB-1 1
Process Conditions				
Mode	Thm/Cat	Thm/Cat	All Disp.	All Disp.
Recycle/Coal ratio	1.3	1.0	1.0	1.0
Space Velocity, Kg mf coalh/M³	640	665	703	694
1st Stage Temperature, °C	449	447	441	433
2nd Stage Temperature, °C	429	427	449	449
Catalyst Concentration				
Iron, w%	0.0615	0.500	0.500	0.500
Molybdenum, wppm	100	50	50	50
Process Performance W% maf Coal				
C_1-C_3	11.3	10.3	15.7	12.4
C_4-177°C	18.2	20.8	19.7	21.2
177°-343°C	33.5	26.4	32.1	28.0
343°-524°C	14.9	16.2	9.0	12.7
524°C+	4.5	5.4	3.7	6.6
C_4-524°C Distillate	66.6	63.4	64.6	61.9
Coal Conversion	94.5	92.8	95.5	94.7
524°C+ Conversion	90.0	87.4	91.5	88.0
H_2 Consumption	7.0	7.3	6.9	6.4

Note: Thm/Cat = Thermal/Catalytic two-stage mode; All Disp. = All Dispersed Catalyst two-stage mode

Table 3 Hydroprocessing of Mixed Feeds using HTI's Iron Based Dispersed Catalyst

Run I.D. Condition	CMSL-9 9	CMSL-11 3A	CMSL-11 4B	PB-1 4	PB-1 9	PB-1 7
Feed Composition,w%						
Black Thunder	50	67	75	0	0	33.3
Waste Plastics	50	33	25	0	50	33.3
Hondo VTB	0	0	0	100	50	33.4
Process Conditions						
Space Velocity, Kg mf coalh/M³	669	687	662	1059	1250	1033
1st Stage Temperature, °C	449	450	447	441	451	450
2nd Stage Temperature, °C	462	459	461	451	460	461
Catalyst Concentration						
Iron, w%	1.00	0.500	0.500	0.500	0.500	0.500
Molybdenum, wppm	300	100	100	50	50	50
Process Performance W% maf Coal						
C_1-C_3	7.5	8.6	7.4	5.0	4.3	7.6
C_4-177°C	30.0	16.8	13.4	16.2	21.4	26.2
177°-343°C	26.2	24.9	26.1	27.7	24.3	24.6
343°-524°C	18.1	25.3	28.1	32.2	30.5	22.0
524°C+	8.9	11.4	11.2	16.5	15.7	10.9
C_4-524°C Distillate	74.3	67.0	67.6	76.1	76.2	72.8
Coal Conversion	97.0	95.3	94.7	N.A.	N.A.	96.3
524°C+ Conversion	88.1	83.9	83.5	83.3	84.0	85.4
H_2 Consumption	3.5	4.1	4.9	1.7	1.8	3.4

Figure 1. Simplified Schematic of HTI's Catalytic Multi-Stage Hydroconversion Process

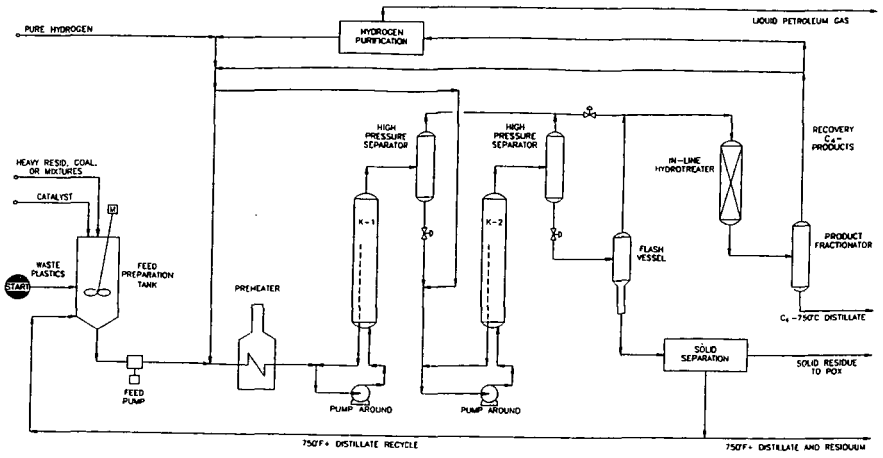

Figure 2. Comparison of Catalyst Performance in Bench-Scale Direct Coal Liquefaction

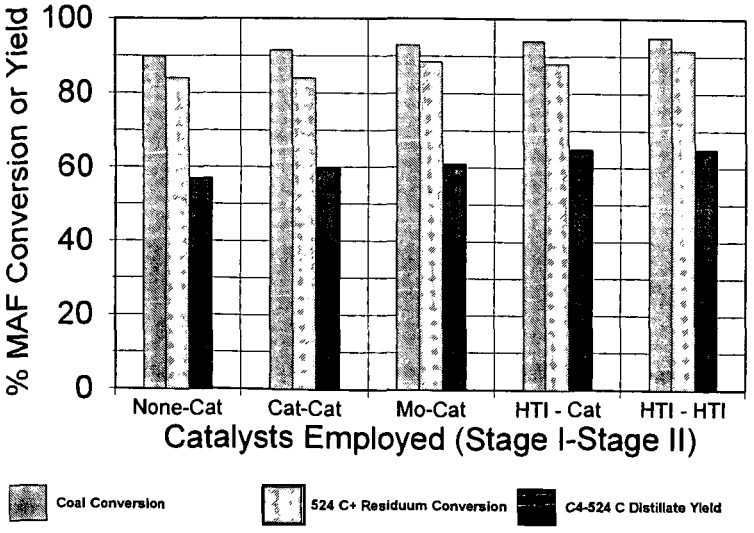

RESULTS OF HYDROTREATING THE KEROSENE FRACTION OF HTI'S FIRST PROOF OF CONCEPT RUN

Frances V. Stohl, Stephen E. Lott, Kathleen V. Diegert, David C. Goodnow
Process Research Dept. 6212
Sandia National Laboratories
P.O. Box 5800
Albuquerque, NM 87185-0709

Keywords: Hydrotreating coal liquids; Factorial experimental design; Continuous reactor studies

ABSTRACT

The objective of Sandia's hydrotreating study is to determine the relationships between hydrotreating conditions and product characteristics for coal liquids produced using current technologies. The coal-derived liquid used in the current work is the kerosene fraction of the product from Hydrocarbon Technologies Inc.'s first proof-of-concept run for it's Catalytic Two-Stage Liquefaction Technology. Sandia's hydrotreating experiments were performed in a continuous operation, microflow reactor system using aged HDN-60 catalyst. A factorial experimental design with three variables (temperature, pressure, liquid hourly space velocity) was used in this work. Nitrogen and sulfur contents of the feed and hydrotreated products were determined using an Antek 7000 Sulfur and Nitrogen Analyzer. Multiple samples were collected at each set of reaction conditions to ensure that each condition was lined out. Hydrotreating at each set of reaction conditions was repeated so that results could be normalized for catalyst deactivation. The normalized results were statistically analyzed. Increases in temperature and pressure had the greatest effects on nitrogen removal. The highest severity condition (388°C, 1500 psig H_2, 1.5g/h/g(cat)) gave a measured nitrogen value of <5 ppm.

INTRODUCTION

DOE/PETC's refining of coal liquids program is aimed at determining the most cost effective combination of existing refinery processes and blending options necessary to upgrade direct and indirect coal liquids into transportation fuels that meet year 2000 specifications. A main reason for this program is that coal liquefaction processing has improved significantly since the last refining evaluation was done by Sullivan and Frumkin[1] at Chevron in the early 1980s. In addition, a recent publication by Zhou, Marano and Winschel[2] indicates that blending coal liquids with petroleum may allow refiners to produce specification products with less refining than if each fraction was processed separately.

The objective of Sandia's refining of coal-derived liquids project is to experimentally evaluate options for hydrotreating coal liquids and various distillate cuts of coal liquids, and to develop a database relating hydrotreating parameters to feed and product quality. The hydrotreating effort is being conducted using a bench-scale, continuous flow, trickle-bed reactor that enables us to evaluate many hydrotreating options in a rapid and cost effective manner. The coal-derived liquid used in this work was produced in Hydrocarbon Technologies Inc.'s (HTI) first proof-of-concept run (POC #1) in their 3 ton/day Process Development Unit using their Catalytic Two-Stage Liquefaction Technology. This 57 day run used Illinois #6 coal and produced up to 5 barrels of distillate liquid product/ton moisture-ash-free coal. After completion of this run, HTI shipped 2500 gallons of coal liquids to Southwest Research Inc. (SwRI) for characterization, fractionation, and evaluation. The kerosene fraction that Sandia hydrotreated was obtained from SwRI as was the aged Criterion HDN-60 catalyst used in Sandia's hydrotreating study. This work is being done in conjunction with DOE/PETC's Refining and End-Use Study of Coal Liquids project (Bechtel, SwRI, Amoco, M. W. Kellogg). Results from Sandia's hydrotreating work will be analyzed by Bechtel using the PIMS refinery model as part of their effort to determine the best way to incorporate coal liquids into an existing refinery.

EXPERIMENTAL SECTION

Sandia's experimental procedures included using a factorial experimental design, hydrotreating the kerosene fraction of the POC #1 whole coal liquid, characterizing the feed and products, and reporting results to other program participants.

Reactor Feeds and Catalyst. The POC #1 kerosene fraction that was hydrotreated at Sandia was collected when HTI's in-line hydrotreater was not in operation. The nitrogen and sulfur contents of this fraction were 645 ppm and 239 ppm respectively. The initial boiling point was 385°F and the final boiling point was 489°F. The nitrogen and sulfur values are Sandia's values and the boiling points are from SwRI. The hydrotreating experiments used aged HDN-60 catalyst that was obtained from SwRI.

Continuous Operation Hydrotreating System. Sandia's hydrotreating experiments are being conducted using a bench-scale, continuous flow, trickle-bed reactor. The system has all required safety features to enable it to be operated unattended. Ranges of operating conditions for this system are as follows: liquid flow from 0.05 to 4 cm^3/min; gas flows up to 2 L/min for N_2 and H_2 and up to 0.5 L/min for H_2S; maximum temperature of 620°C; maximum pressure of 1800 psig; reactor volume of 59 cm^3; and

maximum catalyst loading of 25 cm^3. For this kerosene hydrotreating run, 10g of aged HDN-60 catalyst was used as received from SwRI, and the actual hydrogen flow rate was 4600 ft^3/bbl. Four samples can be collected automatically during unattended operation. With a 45 minute sample collection time and liquid hourly space velocities (LHSV) of 1.5 and 3 g/h/g(cat), the amounts of sample collected would weigh about 11 g and 22 g respectively.

Factorial Experimental Design. Based on experience, three parameters were chosen for the factorial experimental design used for hydrotreating the kerosene fraction (Figure 1): temperature ranging from 327°C to 388°C, pressure from 500 to 1500 psig H_2, and LHSV from 1.5 to 3 g/h/g(cat)). Nitrogen and sulfur contents of the hydrotreated products were monitored during the hydrotreating experiments to ensure that activity was lined out at each set of reaction conditions. After line-out was attained, multiple samples were collected over a 24 hour period. All reaction conditions were tested at least twice so the effects of catalyst deactivation could be determined for each condition and appropriate corrections could be made. An Analysis of Variance (ANOVA) was used to model the results, which had been normalized for differences in catalyst deactivation and extrapolated to a total of 28,000 g of feed processed. The controlled variables used in the ANOVA are the measured temperature, pressure, and LHSV. In addition, SwRI requested that we test the center points of the cube edges parallel to the temperature axis. These points were also included in the ANOVA.

Nitrogen and Sulfur Analyses. Small samples were collected either manually or automatically throughout the run. Nitrogen analyses were used to determine when line-out was achieved at each reaction condition. These analyses were performed using an Antek 7000 Sulfur & Nitrogen Analyzer with an automatic sampler. Standards were prepared using phenanthridine for nitrogen, thianthrene for sulfur, and toluene for the solvent. Six standards prepared by serial dilution were used in the analysis. Standards were measured at least twice. A polynomial fit of the intensity versus concentration data was used for analysis of nitrogen, and a linear fit of the intensity versus concentration data was used for sulfur. Results will only be shown for nitrogen because sulfur values are very low with only one sample having a measured value >20 ppm.

RESULTS AND DISCUSSION

This run was very successful. There was one unplanned shutdown on the second day of the run due to an operator error. The reactor was restarted and operated continuously for 55 days until the end of the run. The letters at each data point in Figure 2 show the order in which the various conditions were evaluated. The first number after the letter is the average ppm nitrogen at that condition. The number in parentheses is the total amount of feed in grams that had been processed through the reactor from the start of the evaluation of the experimental design to the time the samples were collected. All eight corners and the center point of the cubic design were run at least twice so that the rate of catalyst deactivation could be determined for each condition. The four points at the center points of the cube edges parallel to the temperature axis were only tested once because of lack of feed.

Catalyst Deactivation Correction. Results for each condition (Figure 2) show that the measured nitrogen contents get higher as the amount of feed processed increases, thus indicating catalyst deactivation. The first step in the analysis of the results was to normalize the results for catalyst deactivation so that all results could be compared based on an equal amount of feed processed. This was accomplished by plotting nitrogen values for each lined-out sample collected at a given condition versus the total amount of feed processed from the start of the run until that sample was collected. For example, the numbers of lined-out samples collected at 388°C, 500 psig H_2, and 1.5 g/h/g(cat), were 8 for point A, 3 for point J, and 6 for point R. The equation for the straight line calculated for these 17 samples was $Y = 0.00705X + 49.3$ with $r^2 = 0.97$. The slope of this equation (0.00705 ppm/g of feed processed) was then used to extrapolate the nitrogen content of each individual sample obtained at this condition out to 28,000 g of total feed. This was approximately the total amount of feed processed in this hydrotreating run. This analysis was performed for each reaction condition. These normalized nitrogen values for all conditions were then used in the ANOVA to give a model for the remaining nitrogen at 28,000 g total feed processed. The slopes of the lines for the various conditions are shown in Figure 3. The slopes used to correct the values at the center points of the cube edges parallel to the temperature axis were the averages of the high temperature and low temperature slopes at the same LHSV and pressure. The negative deactivation slope at 327°C, 500 psig H_2, 3 g/h/g(cat) is due to the collection of only two samples, which gave poor reproducibility in the nitrogen analysis, at the second repeat of this test condition.

Model for Nitrogen Remaining at 28,000 g Total Feed Processed. The ANOVA model for nitrogen contents of samples at 28,000 g of total feed processed is shown in Table 1. Results show a good fit of the model to the data as indicated by an r^2 value of 0.95. Calculated nitrogen values vary from 7.9 ppm at the highest severity condition (388°C, 1500 psig H_2, 1.5 g/h/g(cat)) to 599.7 ppm at the lowest severity condition (327°C, 500 psig H_2, 3.0 g/h/g(cat)). The greatest impacts on the nitrogen content are due to the individual effects of temperature and pressure. Changing LHSV by itself has the least effect on nitrogen content. Figure 4 gives a comparison of the calculated and measured results for all reaction conditions. The biggest difference between the calculated and measured results is at the lowest severity condition 327°C, 500 psig H_2, 3 g/h/g(cat). The calculated value for nitrogen at this condition is 675.6 ppm, whereas the amount of nitrogen in the feed is 645 ppm. This discrepancy is probably due to higher variability in

analytical results as nitrogen contents get higher. Efforts are currently underway to quantify and decrease the sources of variability in the nitrogen analysis procedure.

CONCLUSIONS

Results of hydrotreating a coal liquid produced using HTI's Catalytic Two-Stage Liquefaction process show that good denitrogenation and good desulfurization can be obtained under relatively mild conditions. Processing at the highest severity condition (388°C, 1500 psig H_2, 1.5 g/h/g(cat)) decreases nitrogen from 645 ppm in the feed to 7.9 ppm in the hydrotreated product. Sulfur contents were very low for all hydrotreated products. The feed had 239 ppm sulfur whereas all hydrotreating conditions gave <20 ppm sulfur. The results of this work will be used by Bechtel in their Refining and End-Use Study of Coal Liquids project to determine the best way to introduce direct coal liquids into an existing refinery.

Acknowledgment: This work was supported by the U.S. Department of Energy at Sandia National Laboratories under contract DE-AC04-94-AL85000.

REFERENCES

1. Sullivan, R. F., Frumkin, H. A., ACS Div. of Fuel Chem. Preprints 31(2), 325, 1986.
2. Zhou, P.-Z., Marano, J. J., Winschel, R. A. ACS Div. Fuel Chem. Preprints 37(4), 1847, 1992.
3. Comolli, A. G., Lee, L. K., Pradhan, V. R., Stalzer, R. H., Proceedings of Coal Liquefaction and Gas Conversion Contractors' Review Conference, Pittsburgh, PA, August 29-31, 1995.

Table 1. Model for Nitrogen Content of Reaction Products (Normalized to 28,000g of Feed Processed)

	NITROGEN (ppm)		
Parameter	**Model Estimate**	**Meas'd. Average**	**Std. Error**
Constant*	599.3		9.3
Temperature	-330.7		14.4
Pressure	-331.0		16.9
LHSV	0.4		0.2
Temp. x Press Int.	70.3		24.9
Temp. x LHSV Int.	169.5		17.3
Press. x LHSV Int.	87.3		19.6
Temp. x LHSV x Press. Int.	-192.1		33.3
Experimental Error	46.5		
327°C, 500 psig, 1.5**	599.3	520.0	13.0
388°C, 500 psig, 1.5	268.6	246.8	3.1
327°C, 1500 psig, 1.5	268.3	254.6	4.6
388°C, 1500 psig, 1.5	7.9	1.4	0.9
358°C, 1000 psig, 2.25	326.4	360.4	2.5
327°C, 500 psig, 3.0	599.7	675.6	6.3
388°C, 500 psig, 3.0	438.5	412.6	20.1
327°C, 1500 psig, 3.0	356.0	361.8	5.2
388°C, 1500 psig, 3.0	72.9	73.9	3.2
358°C, 500 psig, 1.5	434.0	439.8	8.3
358°C, 1500 psig, 1.5	138.1	139.0	2.7
358°C, 500 psig, 3.0	519.1	565.1	10.7
358°C, 1500 psig, 3.0	214.4	181.0	4.3
R^2	0.95		

* Value calculated for 327°C, 1.5 g/h/g(cat), 500 psig H_2

** g/h/g(cat)

Figure 1: Factorial Experimental Design (Temperature = °C, Pressure = psig H_2, LHSV = g/h/g(cat))

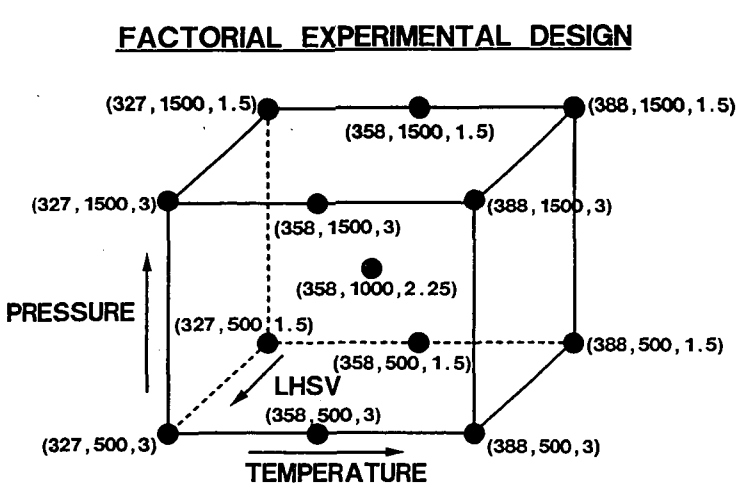

Figure 2: Testing Sequence, Measured Average Nitrogen Values, and Total Amount of Feed Processed From Start of Run Until Sample Collected

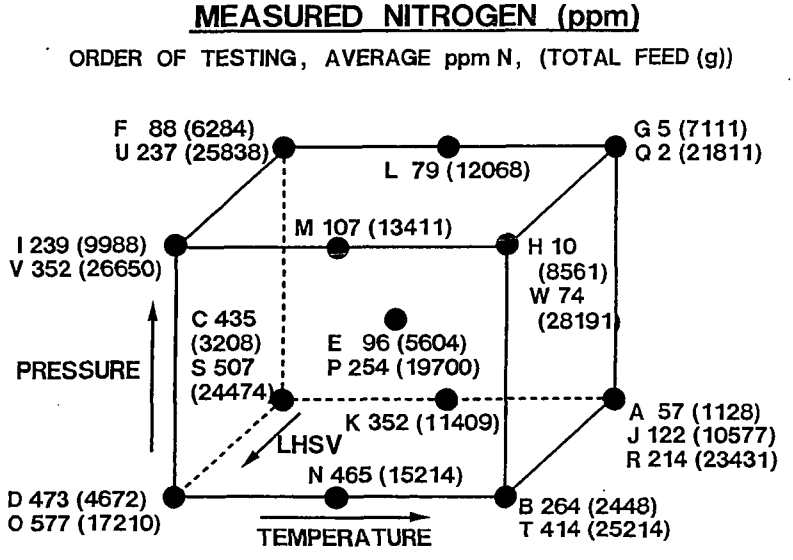

Figure 3: Deactivation Rates for Each Experimental Condition
(ppm N/1000 g Feed)

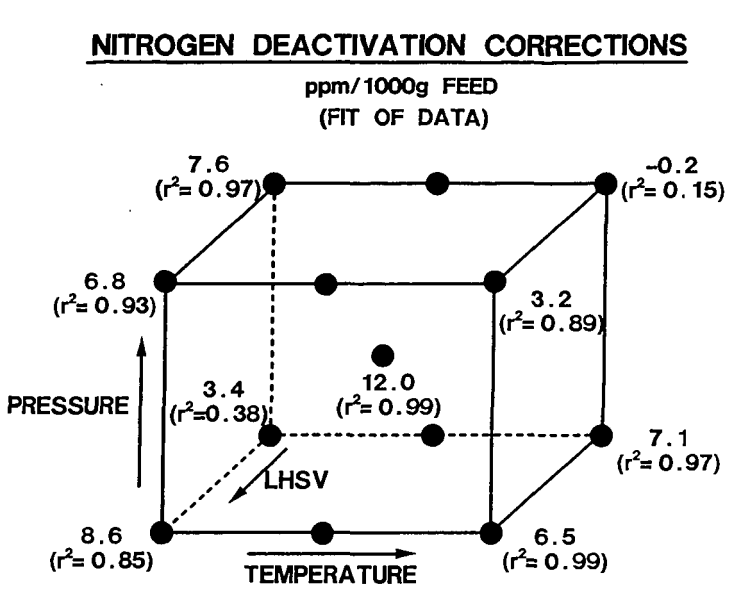

Figure 4: Measured and Calculated Nitrogen Values
(At 28,000g Total Feed Processed)

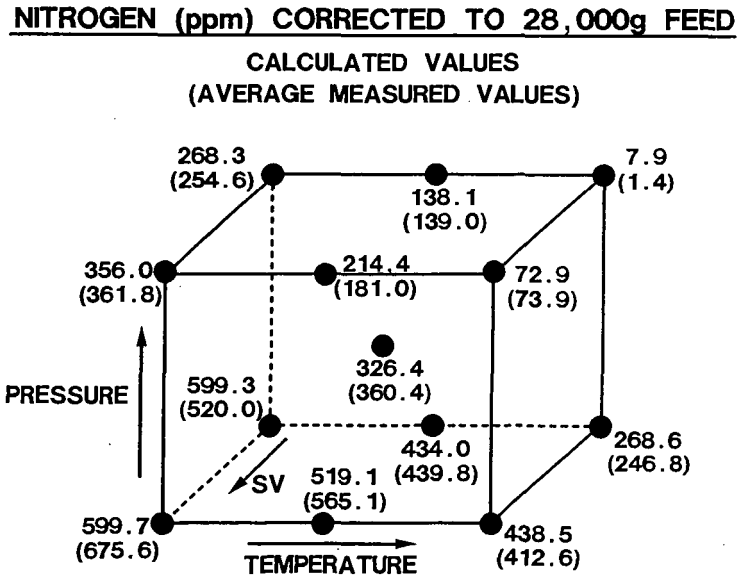

THE EFFECT OF H_2 PARTIAL PRESSURE AND COAL CONCENTRATION ON *CATALYTIC COAL LIQUEFACTION AND COPROCESSING*

Anthony Cugini, Kurt Rothenberger, Donald Krastman, Robert Thompson, and Ray Bernarding
U.S. Department of Energy, Pittsburgh Energy Technology Center
Pittsburgh, PA 15236

KEYWORDS: Liquefaction, Hydrogenation, Coprocessing

INTRODUCTION

An effort is under way at PETC to study the potential of reducing pressure in coal liquefaction. The objective of this effort is to reduce pressure and maintain overall coal conversions, yields and product quality. Several observations have been made during this study and have been reported. [1,2,3] The potential for reducing pressure appears to be tied to a combination of solvent quality and catalyst concentration. Other observations were made concerning the hydrogenation of products from reactors containing coal. These include suppression of two-ring aromatic hydrogenation in the presence of coal and the large consumption of hydrogen observed in the earliest stages of coal liquefaction.

Cugini et al.[1] and Rothenberger et al. [2] reported that catalytic hydrogenation of naphthalenes is suppressed in the presence of coal (using supported or unsupported catalysts). This effect was also observed in several other studies.[4,5,6] The efforts of Cugini et al[3] also indicated the need for a combination of catalyst and donor solvent system to reduce pressure. They found that the donor solvent/low pressure/no catalyst system resulted in consistently lower coal conversions than the non-donor solvent/high pressure/catalyst system. Also, high hydrogen consumption was observed during the early stages of catalytic coal liquefaction. Approximately 50% of the hydrogen consumption during a 30-minute test occurred during the heat-up (~ 2 minutes) and subsequent 2 minutes of the test.

The current effort attempts to provide more information regarding the suppression of catalytic hydrogenation of aromatic compounds by coal and the high initial consumption of hydrogen in catalytic liquefaction. The observation of suppression of catalytic hydrogenation of two-ring aromatic compounds is extended to other multi-ring aromatic compounds. These include phenanthrene and pyrene. Also, short-time liquefaction tests are being studied to determine the differences between donor/non-catalytic and non-donor/catalytic systems.

The remainder of the study was directed toward the investigation of coal/oil coprocessing. The effect of coal concentration, catalyst concentration and pressure were investigated as part of this study. The earlier results from coal liquefaction studies had indicated that pressure and catalyst concentration were interrelated. This phase of the effort attempts to extend the results from the coal liquefaction efforts to coal/oil coprocessing. Essentially, it is hoped that catalyst could (to some extent) be used to compensate for pressure reduction as was observed in coal liquefaction applications. Lower coal concentrations were also investigated because of earlier results that had indicated that a synergism to distillate product was observed at low concentration and that coal could be used to effectively remove the metals from the liquid products even at relatively low coal concentrations.[7]

EXPERIMENTAL

Materials. Purified grade 1-methylnaphthalene (1-MN), phenanthrene, pyrene, and tetralin from Fisher Scientific Company were used in these studies. Hondo residual oil, vacuum tower bottoms obtained from Paramount Petroleum Corporation, was used. Blind Canyon coal, DECS-6, from the U.S. Department of Energy's Coal Sample Program and Illinois No. 6 coal were used. A supported molybdenum catalyst, Akzo AO-60, obtained from HTI, Inc. was used in the microautoclave catalytic tests. An unsupported MoS_2 catalyst prepared at PETC[2] was also used in the microautoclave tests. Aqueous ammonium heptamolybdate (AHM) was used as the precursor for MoS_2 in the 1-L semi-batch tests.

Reactions. Microautoclave reactions were completed in a stainless steel batch microautoclave reactor system (42 mL) constructed at PETC. Semi-batch 1-L reactions were completed in a stainless steel 1-L autoclave. A 97% H_2 / 3% H_2S gas mixture was used in the 1-L tests to sulfide the catalyst. Sample work-up and coal conversions for both the microautoclave and 1-L autoclave tests were calculated by a procedure described previously.[8]

Gas and Pressure Analyses. At the completion of each run, product gases were collected and analyzed at PETC by a previously published method.[3] Hydrogen consumption was determined by a method developed at PETC.[4]

GC-Mass Spectrometry (GC-MS). The THF soluble material from the autoclave runs was analyzed by GC-MS to determine the amount of solvent which had been hydrogenated. The samples were run as 1% solutions (w/w) in methylene chloride on a HP 5890A gas chromatograph equipped with a 50 m capillary column of 50% phenylmethylsilicone and a HP 5970 mass selective detector. The integrated areas of hydrogenated solvent peaks were compared against those of unconverted solvent peaks.

RESULTS

The initial studies were directed toward the effect of solvent type. As indicated, coal was found to suppress the catalytic hydrogenation of 1-MN. Two other aromatic solvents, pyrene and phenanthrene, were tested to evaluate the effect of coal addition on aromatic hydrogenation. The results from testing the two solvents as well as the earlier data with 1-MN are shown in Table 1. The data indicate that catalytic hydrogenation of pyrene and phenanthrene is suppressed by the presence of coal as shown by comparing tests B and C for the two cases. Further, exposure to coal continues to suppress the catalytic hydrogenation of phenanthrene even after coal is removed from the system, as shown by a comparison of tests B and D for phenanthrene. However, the results from the pyrene system are not as straightforward, because the tests using fresh catalyst and catalyst recovered after exposure to coal (tests B and D for pyrene) both appear to reach equilibrium[9] within the reaction time. Figure 1 shows the pressure as a function of time for the two tests with pyrene, fresh catalyst and catalyst exposed to coal. In the case with fresh catalyst, the pressure drops rapidly to 1,470 psig before the pressure levels off for the remainder of the test. This indicates that equilibrium is rapidly achieved during the test. On the other hand, with the catalyst that had been exposed to coal, the pressure drops continuously over the course of the test. This indicates that equilibrium was achieved only after the full reaction time. The net result is that the rate of catalytic hydrogenation of pyrene was also suppressed by exposure of the catalyst to coal just as in the other two examples.

Table 1. Effect of Blind Canyon Coal Addition on Catalytic Hydrogenation of Aromatic Solvents

	Percentage of Product					
Microautoclave Sample	0-H	2-H	4-H	6-H	other	% Hydrog.
Pyrene:						
(A) pyrene only	96	4	0	0	0	4
(B) with catalyst	68	21	2	8	1	32
(C) with coal + catalyst	85	14	0	0	1	15
(D) with THF insols from (C)	66	23	2	6	2	34
Phenanthrene:						
(A) phenanthrene only	97	2	0	1	0	4
(B) with catalyst	47	12	10	24	7	53
(C) with coal + catalyst	80	13	5	1	1	20
(D) with THF insols from (C)	67	16	13	0	4	33
1-Methylnaphthalene:						
(A) 1-MN only	100	----	0	----	0	0
(B) with catalyst	47	----	52	----	1	53
(C) with coal + catalyst	92	----	7	----	1	8
(D) with THF insols from (C)	86	----	12	----	2	14

425°C, 0.5 h, 1000 psig H_2 (cold), and 1000 ppm Mo

Short-time tests were made to compare the effects of catalyst and tetralin on coal conversion. Fast heat-up rates and 2-minute and 30-minute duration tests were conducted. The results of these tests are shown in Table 2. These results indicate that, in this time interval, coal conversion was enhanced in the catalytic case over the tetralin case. Detailed analyses of the insoluble products are being conducted to determine if more coke or hydrogen-deficient species are observed in the tetralin case.

Table 2

Effect of Solvent Quality, Pressure, and Catalyst on Blind Canyon Coal Conversion

					Coal Conversion
A	Tetralin	400 psig (cold)	No Catalyst	2 minutes	70%
B	Tetralin	1000 psig (cold)	No Catalyst	2 minutes	73%
C	Tetralin	400 psig (cold)	No Catalyst	30 minutes	85%
D	Tetralin	1000 psig (cold)	No Catalyst	30 minutes	86%
E	1-MN	1000 psig (cold)	AO-60	2 minutes	79%
F	1-MN	1000 psig (cold)	AO-60	30 minutes	89%
G	1-MN	1000 psig (cold)	MoS_2	30 minutes	93%

The effects of pressure and coal concentration in coal/oil coprocessing were studied in batch autoclave tests. The results are shown in Figure 2. The results indicate that there does appear to be an area at low coal concentration (between 0 and 10% coal) where the distillate conversion is higher than with no coal. Above 10% coal, the distillate conversion falls with increasing coal concentration. This trend was observed at two pressures, 1,000 and 2,500 psig. As catalyst concentration was increased from 100 ppm Mo to 300 ppm Mo, conversion increased. It appeared that, like in the coal liquefaction system, catalyst concentration could be used to compensate for the effect of pressure reduction.

SUMMARY

The results obtained indicate that the catalytic hydrogenation of two-ring aromatic compounds and several types of multi-ring compounds are suppressed in the presence of coal. It appears that the suppression is the result of a combination of competition and poisoning of specific catalytic sites. This is due to the fact that catalytic hydrogenation of aromatics remains suppressed even after coal is removed from the system.

In the case of tetralin as a donor solvent for coal liquefaction, it seems that that there is insufficient hydrogen donated during the early stages of coal liquefaction to prevent the formation of hydrogen deficient species. This results in lower coal conversion compared to catalytic cases. This may contribute to the consistently lower conversions observed in tetralin tests compared to catalytic tests.

Coal/oil coprocessing may be most effective at lower coal concentrations. The distillate yields are higher at coal concentrations between 0 and 10%. At higher coal concentrations the distillate conversion drops with increasing coal concentration. The potential for reducing pressure in coal/oil coprocessing is enhanced by increasing catalyst concentration. At lower pressures, increasing catalyst concentration increases conversions and distillate yield.

DISCLAIMER

Reference in this manuscript to any specific commercial product or service is to facilitate understanding and does not necessarily imply its endorsement or favoring by the United States Department of Energy.

REFERENCES

1. Cugini, A.V., Rothenberger, K.S., Ciocco, M.V., McCreary, C. In *Coal Science, Proceedings of the Eighth International Conference on Coal Science, Volume II*; Pajares, J.A.; Tascon, J.M.D. Eds.; Coal Science and Technology Series, Volume 24; Elsevier: Amsterdam; 1995; pp 1299-1302.
2. Rothenberger, K.S., Cugini, A.V., Schroeder, K.T., Ciocco, M.V., Veloski, G.A., Am. Chem. Soc., Fuel Chem. Div., Prepr. Pap. **39**(3), 688-694 (1994).
3. Cugini, A.V., Rothenberger, K.S., Ciocco, M.V., Veloski, G.A., Martello, D.M.,, Am. Chem. Soc., Fuel Chem. Div., Prepr. Pap. **39**(3), 695-701 (1994).
4. Suzuki, T., *Energy & Fuels*, **8**(2), pp. 341-347 (1994).
5. Ikenaga, N., Kobayashi, Y., Saeki, S., Sakota, T., Watanabe, Y., Yamada, H., Suzuki, T., *Energy & Fuels*, **8**(2), pp. 947-952 (1994).
6. Schroeder, K.T., Bockrath, B., Miller, R., Davis, H., AIChE Summer Meeting, 1991.
7. Cugini, A.V., Lett, R.G., and Wender, I., *Energy & Fuels*, **3**(2), pp. 120-126 (1989).
8. Cugini, A.V., Krastman, D., Lett, R.G., and Balsone, V.D., *Catalysis Today*, **19**, pp. 395-408 (1994).
9. Stephens, H.P. and Kottenstette, R.J., Am. Chem. Soc., Fuel Chem. Div., Prepr. Pap. **30**(2), 345-353 (1985).

Figure 1

Effect of AO-60 Exposure to Coal on Pyrene Hydrogenation

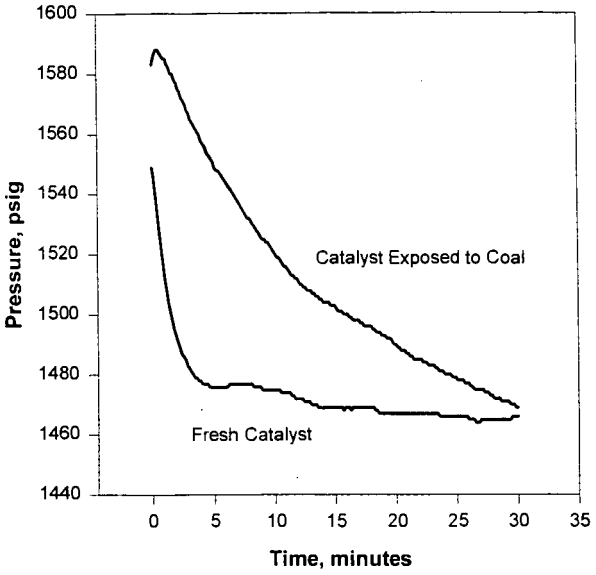

Microautoclave 425°C, 30 minutes, and 1000 psig H_2 (cold)

Figure 2

Effect of Coal Concentration and Pressure in Coprocessing

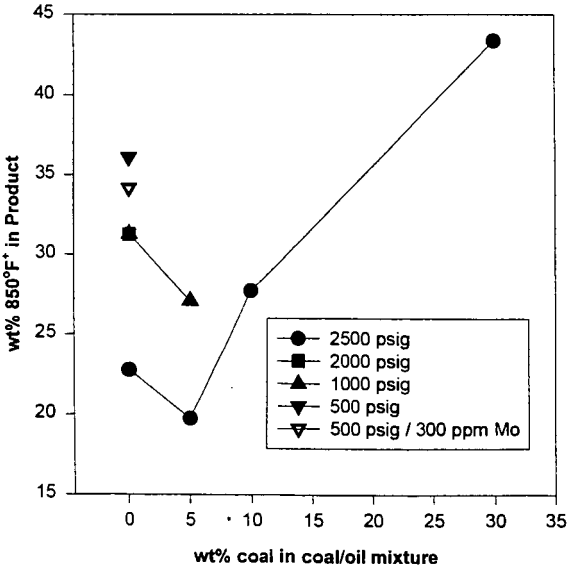

Semi-Batch 1-L Autoclave 425°C, 1 h, 100 ppm Mo (added as AHM), 2:1 Hondo Resid to Illinois No. 6 Coal

EFFECT OF SOLVENT CHARACTERISTICS ON COAL LIQUEFACTION

He Huang, Shaojie Wang, Keyu Wang, Michael T. Klein and William H. Calkins*
Department of Chemical Engineering
University of Delaware, Newark, Delaware 19716

Key words: liquefaction solvent, hydrogen donor, solubility parameter

Introduction

It has been known for a long time that the characteristics of the liquefaction solvent has a profound effect on direct coal liquefaction. The amount of hydrogen consumed during the liquefaction process, the degree and quantity of retrograde reactions that occur, and the quality of the liquid products are all influenced by the process solvent (1). A number of analytical approaches have been developed to determine the important characteristics of the solvent for coal liquefaction (1). The hydrogen donor ability has clearly been important (2). However, such other characteristics of a liquefaction solvent as solubility parameter (1), content and type of higher aromatic hydrocarbons (3), and phenolic content have also been found to be significant (1). Finseth et al. (4) have shown that the bulk of the hydrogen consumed from an uncatalyzed donor solvent liquefaction above 400 °C is consumed in gas generation, heteroatom removal and hydrogenolysis of the coal matrix. Wilson et al. (5) have also shown that the major role of hydrogen in uncatalyzed liquefaction is consumed by alkyl fission and hydrogenolysis reactions and not with hydrogenating aromatic rings. McMillan et al. (6) have postulated that a radical hydrogen transfer process along with donor solvent capping of thermally produced radicals from the coal as possible processes involved with the hydroaromatic donor solvents in coal liquefaction.

With the development of a short contact time batch reactor (SCTBR) (7), determining the influence of the processing solvent on the liquefaction rates, conversion profiles and the quality of the liquid product at a particular time became possible. The influence of type of solvent, combined with other effects, such as gas atmosphere (i.e., in hydrogen and in nitrogen) and catalyst, on the coal liquefaction is reported in this paper.

Experimental

Apparatus. A Short-Contact-Time Batch Reactor (SCTBR) was devised to carry out the coal liquefaction. It allows the heat up of the process stream to reaction temperature in about 0.3 seconds. The removal and quenching of the reaction products occurs in a similar time period. The design and operation of such a SCTBR reactor system have been described in detail elsewhere (7,8).

Solvents Used. Four solvents: 1,2,3,4-tetrahydroquinoline (98%), tetralin (99%), 1-methylnaphthalene (98%), and decahydronaphthalene (99+%) from Aldrich with different hydrogen donor abilities and solubility parameters have been used in the coal liquefaction experiments.

Catalyst Used. Molybdenum naphthenate (6.8 wt% molybdenum from Shepherd Chemical Co.) was the liquefaction catalyst used in this study. The catalyst was prepared by dissolving about 0.5 g molybdenum naphthenate (equivalent to about 0.9 wt% Mo based on the amount of the coal charged) in the processing solvent. The catalyst was then sulfided by reacting the solution with about 1 g of methyl disulfide during the transport into the reactor and liquefaction.

Coal Liquefaction. Illinois #6 bituminous and Wyodak-Anderson subbituminous coals from the Argonne Premium Coal Sample program were used in this study. Proximate and elemental analyses, together with other analytical data, of these coals are available in the User's Handbook for the Argonne Premium Coal Sample program (9). All liquefactions were run as mixtures of processing solvent (S) and coal (C) at a mass ratio of S/C ≈ 8 to minimize the effect of changing processing solvent concentration during the reaction. About 4 grams of coal were used for each reactor run, together with the added processing solvent to make up the reactant slurry.

Workup Procedures of Reaction Products. After a liquefaction run, the product mixture was filtered and the solid residue washed with cold fresh tetralin thoroughly and dried in a vacuum oven with a nitrogen purge at about 105 °C for 48 hours. The filter cake was then rinsed with methylene chloride and dried in a vacuum oven with a nitrogen purge at 105°C for 12 hours. The solid residue and the liquid filtrate were analyzed separately (10). The mineral matter of the coal was shown to accumulate in the coal residue and not in the coal liquids. Therefore, ash in the residue determined by thermogravimetric analysis was used to calculate the conversion (10).

Results and Discussion

Coal Liquefaction Processes. The conversions of Illinois #6 liquefaction in tetralin

without added catalyst under 1000 psig nitrogen at four temperatures (358 °C, 390 °C, 408 °C and 422 °C) for short reaction times (10 s to 10 min) are shown in Figure 1. Three distinct phases in the process were observed: a very rapid conversion followed by an induction period and then a slower liquefaction of the coal structure. The initial rapid conversion in the first 30 to 60 s is due to the extraction of a soluble fraction of the coal into the hot tetralin. The slow conversion after 1 or 2 min is caused by the chemical breakdown of the coal structure to liquid products. The induction period observed is actually a transition interval which is due to the simultaneous occurrence of two processes: a very rapid extraction and a relatively slower liquefaction of the coal structure itself. The amount of extraction increases as the liquefaction temperature increases. The equilibrium extraction of the Illinois #6 coal at 358 °C, 390 °C, 408 °C and 422 °C were about 18.4 wt%, 22.0 wt%, 31.9, and 39.8 wt%, respectively. Similar behavior was also observed in Wyodak-Anderson subbituminous coal liquefaction. The equilibrium extraction of the Wyodak-Anderson coal in tetralin at 390 °C under 1000 psig nitrogen is about 14.1 wt%.

From these observations, a hypothesis of two processes of coal liquefaction was postulated (10). Based on this hypothesis, Wang et al. (11) have developed a model to evaluate the kinetic parameters for each stage. They have reported that the extraction stage is about two orders of magnitude faster than the structure breakdown stages and have correspondingly lower activation energies. The liquefaction of the coal structure itself also consists of multiple steps of different rate constants and activation energies. The rate constant of the extraction stage and the equilibrium extraction fraction are dependent on the solvent characteristics and coal structures as well as liquefaction conditions.

It is important to point out that the coal liquefaction kinetic studies reported in the literature are largely based on liquefaction to high conversions (2,12,13). Therefore, the kinetic measurements are actually combinations of the rapid extraction with the much slower liquefaction of the coal structure.

Effect of Gas Atmosphere on the Coal Liquefaction. Conversions of the liquefaction of Illinois #6 and Wyodak-Anderson coals in tetralin at 390 °C for 30 min under 1000 psig N_2 or 1000 psig H_2 is shown in Figure 2. For the Illinois #6 coal, the liquefaction conversion in hydrogen was higher than in nitrogen. However, there was no difference for the Wyodak-Anderson coal liquefied in hydrogen or in nitrogen. The contents of pyritic sulfur in Illinois #6 and Wyodak-Anderson are 2.81 wt% and 0.17 wt%, respectively. This is a strong indication that pyrite in the Illinois #6 provides some catalysis for the liquefaction in the presence of hydrogen.

Catalysis of Molybdenum Naphthenate. Conversion of the Illinois #6 coal with molybdenum naphthenate (equivalent to 0.9 wt% Mo) was studied in an effort to understand the role of a hydrogenation catalyst relative to the liquefaction solvent in coal liquefaction. Figure 3 summarizes the results of a series of experiments aimed at determining the active species when the molybdenum naphthenate is the added catalyst. The sulfiding agent used was methyl disulfide. Comparison of the conversions in different liquefaction conditions shown in Figure 3 indicates that: 1). sulfided molybdenum naphthenate in the absence of hydrogen is not active; 2). the sulfiding agent itself plays no direct role in coal liquefaction; and 3). only sulfided molybdenum naphthenate (presumable as Mo_2S_3 or MoS_2) in the presence of hydrogen is the active catalyst for coal liquefaction.

Effects of Solvent, Catalyst, and Gas Atmosphere on the Coal Liquefaction. Conversion vs. time curves of the thermal (without added catalyst) liquefaction of Illinois #6 coal in 1,2,3,4-tetrahydroquinoline (THQ), tetralin, and 1-methylnaphthalene, in decreasing order of hydrogen-donor ability, run under 1000 psig nitrogen at 408 °C are shown in Figures 4a and 4b for two different time intervals. The liquefaction conversions using 1-methylnaphthalene as a processing solvent shows distinct stages of liquefaction kinetics: a very rapid extraction and followed by an extremely slow liquefaction of the coal structure. The equilibrium extraction of the Illinois #6 coal using 1-methylnaphthalene was 30.7 wt%. This value is very close to that using tetralin as a processing solvent. The solubility parameters of 1-methylnaphthalene and tetralin are 20.3 and 19.4, respectively. This suggests that the extraction stage in the coal liquefaction is dominated by the solubility characteristics of the processing solvent used. However, the rates of coal structure breakdown in tetralin and in 1-methylnaphthalene were 0.0458 wt%/min and 0.00168 wt%/min, about 27 times difference. For the very strong hydrogen donor solvent of 1,2,3,4-tetrahydroquinoline, the extraction stage becomes indistinguishable from the liquefaction of the coal structure. This is because the rate of coal structure breakdown in the very strong hydrogen donor solvent is close to the rate of extraction. The rate of coal structure breakdown measured in this solvent was 1.41 wt%/min. Comparison of the rates of the coal structure breakdown in 1,2,3,4-tetrahydroquinoline, tetralin, and 1-methylnaphthalene suggests that hydrogen transfer from the solvent is the rate-determining step in uncatalyzed coal liquefaction. This is consistent with the observations that the activation energies for coal structure breakdown is much less than carbon-carbon bond strength (2,11-13).

Effects of solvent on the thermal liquefaction of the Illinois #6 coal in nitrogen and in

hydrogen are illustrated in Figure 5. These data show that the very strong hydrogen donor solvent, such as 1,2,3,4-tetrahydroquinoline, gives much higher conversion than tetralin. More interestingly, the liquefaction conversion in this very strong donor solvent shows no sensitivity to gas atmosphere (i.e., in nitrogen or in hydrogen), indicating little if any hydrogen is derived from the molecular hydrogen in the case of a very strong hydrogen donor solvent used. On the other hand, the liquefaction in the poor hydrogen donor solvents, such as decahydronaphthalene and 1-methylnaphthalene, shows much lower conversion than in tetralin under nitrogen pressure. However, for these very poor hydrogen donor solvents, the liquefaction conversions of the Illinois #6 coal in hydrogen is much higher than that in nitrogen, showing strong sensitivity to gas atmosphere. These results suggest that, in a poor hydrogen donor solvent, the hydrogen needed in the liquefaction process must be mostly derived from molecular hydrogen when a hydrogenation catalyst is present in the parent coal (for example, the pyrite in the Illinois #6 coal) and/or is added (such as sulfided molybdenum naphthenate).

Effect of molybdenum naphthenate catalyst in different solvents on the Illinois #6 coal liquefaction is shown in Figure 6. Liquefaction conversions are always higher in tetralin than in 1-methylnaphthalene for both of the thermal and catalyzed liquefactions. However, with the added catalyst, the conversions in tetralin increased only by a factor of 53%, 31%, and 29% for 30 min liquefaction at 390 °C, 403 °C, and 420 °C, respectively, compared to those in 1-methylnaphthalene by a factor of 123% and 97% for 10 min at 397 °C and 30 min at 410 °C, respectively. These results indicate that the catalysis by an added hydrogenation catalyst in coal liquefaction is more responsive when a poor hydrogen donor solvent is used. It also suggested that a hydrogenation catalyst could be used to compensate for the lack of hydrogen donor ability of a processing solvent.

To quantitatively evaluate the effects of solvent, catalyst, and gas atmosphere for the coal liquefaction, specific liquefaction conversion ratios of α, β, and γ are defined using the coal liquefaction conversion in nitrogen as a reference, i.e.,

$$\alpha = \frac{X_{H_2}}{X_{N_2}}$$

$$\beta = \frac{X_{catalyst}}{X_{N_2}} \qquad (1)$$

$$\gamma = \frac{X_{catalyst}}{X_{H_2}}$$

where X_{N2} is the liquefaction conversion in nitrogen; X_{H2} is the liquefaction conversion in hydrogen; and $X_{catalyst}$ is the catalyzed liquefaction conversion in hydrogen. The α is selected to evaluate the hydrogen gas effect. The larger the α, the stronger the hydrogen gas effect. When $\alpha = 1$, it means there is no hydrogen gas effect in the coal liquefaction. The β is calculated to evaluate the catalyst reactivity and the γ is used to evaluate the net reactivity of the added catalyst. The data to show the combination of the effects of solvent, catalyst, and gas atmosphere on the Illinois #6 and Wyodak-Anderson coal liquefactions, together with the calculated specific ratios of α, β, and γ, are summarized in Table 1. Based on the α values, the order of the hydrogen gas effect on the Illinois #6 coal liquefaction for different solvents was decahydronaphthalene ~ 1-methylnaphthalene > tetralin > 1,2,3,4-tetrahydroquinoline. The stronger the hydrogen donor solvent, the less will be the hydrogen gas effect. In fact, there is no hydrogen gas effect on the Illinois #6 coal liquefaction for the very strong donor solvent of 1,2,3,4-tetrahydroquinoline for which $\alpha = 1$. The Wyodak-Anderson coal shows no hydrogen gas effect ($\alpha = 1$) during the liquefaction in tetralin. Based on the β values, the order of the catalyst influence on coal liquefaction in different hydrogen donor solvents was 1-methylnaphthalene > tetralin. Furthermore, the higher the liquefaction temperature, the lower the catalyst influence on liquefaction conversion. This may be because, as temperature increases, the selectivity to liquid products during the liquefaction decreases. This is also supported by the γ values for the liquefaction of the Illinois #6 in 1-methylnaphthalene.

Summary and Conclusions

The extraction stage in the coal liquefaction is dominated by the solubility characteristics of the processing solvent. The liquefaction of Illinois #6 using 1-methylnaphthalene shows distinct stages of liquefaction kinetics similar to tetralin. However, compared to tetralin, it has an extremely slow breakdown rate of the coal structure. The equilibrium extraction for 1-methylnaphthalene was 30.7 wt% at 408 °C, which is very close to that (31.9 wt%) in tetralin. The extraction and coal structure breakdown stages of the Illinois #6 coal liquefaction in 1,2,3,4-tetrahydroquinoline, however, were indistinguishable.

A hydrogen atmosphere increases the thermal (uncatalyzed) conversion of Illinois #6, but had no effect on Wyodak-Anderson subbituminous coal. This is apparently due to the catalytic

effect of pyrite (or pyrrhotite derived from the pyrite) in the Illinois #6 coal, since this coal contains substantial amounts of pyrite whereas the Wyodak-Anderson coal contains only trace amount of pyrite.

Liquefaction yields and rates of coal structure breakdown are greatly increased by the use of a strong hydrogen donor solvent in which most of the hydrogen is contributed by the solvent rather than molecular hydrogen, suggesting that hydrogen transfer from the solvent is the rate-determining step in uncatalyzed coal liquefaction.

The order of the hydrogen gas effect on the Illinois #6 coal liquefaction for different solvents was decahydronaphthalene ~ 1-methylnaphthalene > tetralin > 1,2,3,4-tetrahydroquinoline. The stronger the hydrogen donor solvent, the less the hydrogen gas effect. When a poor hydrogen donor solvent was used and a hydrogenation catalyst either was present in the coal itself (for example, pyrite in the Illinois #6 coal) or was added (such as sulfided molybdenum naphthenate catalyst), hydrogen is predominantly contributed by molecular hydrogen.

Acknowledgments

The support of this work by the Department of Energy under DE22-93PC93205 is gratefully acknowledged.

References

1. D.D. Whitehurst, T.O. Mitchell and M. Farcasiu in Chapter 9 of *Coal Liquefaction - The Chemistry and Technology of Thermal Processes*, Academic Press (1980).
2. R.C. Neavel *Fuel* **55**, 237 (1976).
3. A. Grint, W.R. Jackson, F.P. Larkins, M.B. Louey, M. Marshall, M.J. Trewhella and I.D. Watkins *Fuel* **73**, 381 (1994).
4. D.H. Finseth, D.L. Cillo, R.F. Sprecher, H.L. Retcofsky and R.G. Lett *Fuel* **64**, 1718 (1985).
5. M.A. Wilson, R.J. Pugmire, A.M. Vassallo, D.M. Grant, P.J.Collin and K.W. Zilm *Ind. Eng. Chem. Prod. Res. Dev.* **21**, 477 (1982).
6. D.F. McMillen, R. Malhotra, S.-J. Chang, W.C. Ogier, S.E. Nigenda and R.H. Fleming *Fuel* **66**, 1611 (1987).
7. H. Huang, W.H. Calkins and M.T. Klein *Energy & Fuels* **8**, 1304 (1994).
8. H. Huang, D.M. Fake, W.H. Calkins and M.T.Klein *Energy & Fuels* **8**, 1310 (1994).
9. K.S. Vorres 'User's Handbook for the Argonne Premium Coal Sample Program' *ANL/PCSP-93/1*.
10. H. Huang, K.-Y. Wang, S.-J., Wang, M.T. Klein and W.H. Calkins *Energy & Fuels* in press (1996).
11. S.-J. Wang, K.-Y. Wang, H. Huang, M.T. Klein and W.H. Calkins see preprints of this symposium.
12. G.P. Curran, R.T. Struck, and E. Gorin *I&EC Prod. Des. & Dev.* **6**, 155 (1967).
13. W.H. Wiser *Fuel* **47**, 475 (1968).

Table 1 Effect of solvent on the thermal and catalytic liquefactions of the Illinois #6 and Wyodak-Anderson coals in 1000 psig N2 or H2

Sample	Coal	Solvent	T C	t min	Gas	Catalyst [Note 1]	X wt% [Note 2]	α	β	γ
DOE00	Illinois #6	Tetralin	390	30	N2	No	42.6	1.09	1.53	1.41
DOE07	Illinois #6	Tetralin	390	30	H2	No	46.3			
DOE14	Illinois #6	Tetralin	392	30	H2	Yes	65.3			
DOE09	Illinois #6	Tetralin	404	30	N2	No	54.4	N.A.	1.31	N.A.
DOE16	Illinois #6	Tetralin	402	30	H2	Yes	71.2			
DOE10	Illinois #6	Tetralin	422	30	N2	No	59.9	N.A.	1.29	N.A.
DOE17	Illinois #6	Tetralin	418	30	H2	Yes	77.1			
DOE14	Illinois #6	1-methylnaphthalene	398	10	N2	No	24.7	1.41	2.23	1.58
DOE15	Illinois #6	1-methylnaphthalene	396	10	H2	No	34.9			
DOE15	Illinois #6	1-methylnaphthalene	395	10	H2	Yes	55.1			
DOE18	Illinois #6	1-methylnaphthalene	409	30	N2	No	33.7	1.63	1.97	1.20
DOE18	Illinois #6	1-methylnaphthalene	412	30	H2	No	55.1			
DOE18	Illinois #6	1-methylnaphthalene	412	30	H2	Yes	66.4			
DOE18	Illinois #6	THQ [Note 3]	412	30	N2	No	85.6	1.00	N.A.	N.A.
DOE18	Illinois #6	THQ	415	30	H2	No	85.5			
DOE23	Illinois #6	Decahydronaphthalene	400	30	N2	No	22.2	1.49	N.A.	N.A.
DOE23	Illinois #6	Decahydronaphthalene	400	30	H2	No	33.0			
DOE08	Wyodak-Anderson	Tetralin	392	30	N2	No	39.6	1.01	N.A.	N.A.
DOE08	Wyodak-Anderson	Tetralin	390	30	H2	No	39.8			

Notes:

1. Catalyst: Molybdenum naphthenate (equivalent to 0.9 wt% Mo) sulfided in-situ by methyl disulfide.
2. X: Liquefaction conversion on the daf (dry-ash-free) basis.
3. THQ: 1,2,3,4 - Tetrahydroquinoline

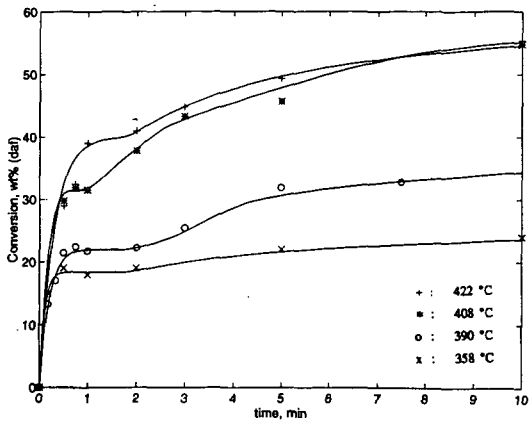

Figure 1 Conversion vs time for Illinois #6 coal liquefaction without added catalyst in tetralin (tetralin:coal = 8:1 mass ratio) under 1000 psig N_2 (for short contact times up to 10 min)

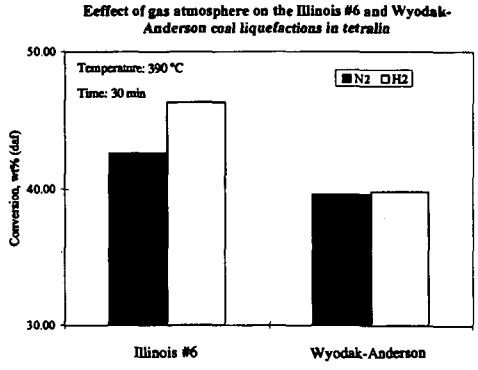

Figure 2

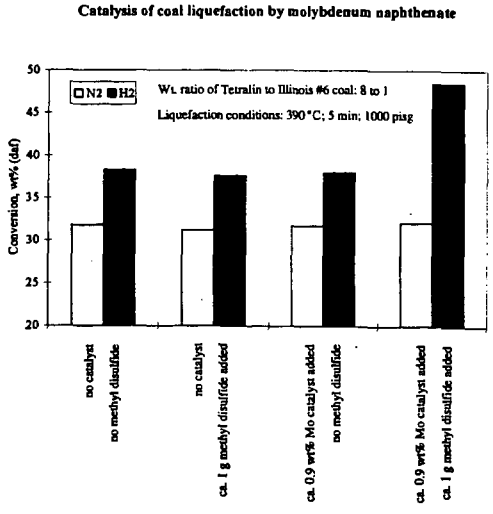

Figure 3

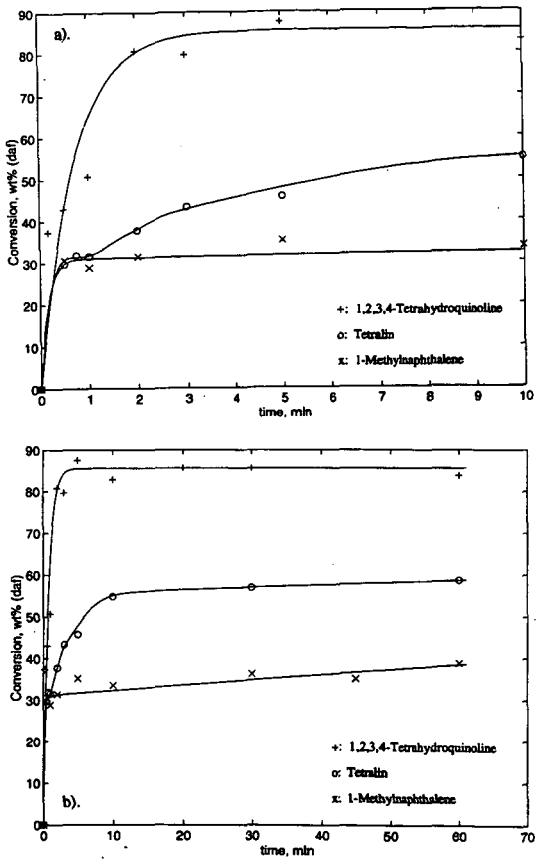

Figure 4 Conversion vs. time curves of the thermal liquefaction of Illinois #6 coal in 1,2,3,4-tetrahydroquinoline (THQ), tetralin, and 1-methylnaphthalene under 1000 psig nitrogen at 408 °C (Solvent:Coal = 8:1): a). for short contact times; b). for up to 60 min

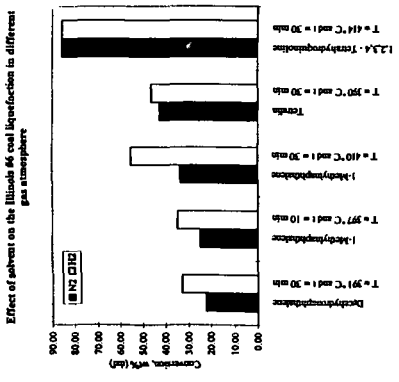

Figure 5

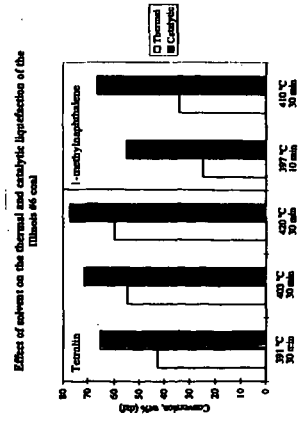

Figure 6

CONTRIBUTION OF MINERAL MATTER TO LOW TEMPERATURE LIQUEFACTION MECHANISMS.

Shona C. Martin, Harold H. Schobert

Fuel Science Program, The Pennsylvania State University, University Park, PA 16802

Keywords: Low rank coals, mineral matter, low temperature liquefaction.

Introduction

The pathways by which coal macromolecules can be depolymerised to give lighter products have long been sought by coal scientists and the precise roles of individual functional groups in the reactions which occur during liquefaction are still not clear. Generally, radical reactions for hydrogen incorporation are dominant at temperatures ≥ 350 °C. However, reactions of coals are not necessarily limited to free radical processes. Recently, the existence of non-radical pathways has been proposed, upon the observation of a higher gas-phase H_2 consumption observed in comparative non-catalytic runs with raw and dried low rank coals at 350 °C [1]. However, the preliminary data largely ruled out the possibility that, under the conditions employed, there was non-radical incorporation of molecular H_2 into coal. It was therefore proposed that the reaction of H_2 may be mineral matter catalysed.

To date, the exact role of much of the mineral matter in coals remains unclear [2-4]. These mineral and inorganic species can act as catalysts or poisons during liquefaction depending on reaction conditions. The physical role of minerals could be to block access to pores or reaction sites. Conversely, the chemical roles of inorganics include: clays which can act as cracking catalysts and the hydrogenation catalyst, pyrite. Catalytic activity, mainly attributed to pyrite, is well documented [2, 5]. Conversely, removal of naturally occurring anions such as Na^+, Ca^{2+} and K^+ has been shown to enhance liquefaction conversions [4,6] and several authors have observed a favorable influence of demineralization on coal depolymerization. Shams et al. [7] reported that the treatment of coals with methanol and HCL removes virtually all of the calcium species, leading to retardation of the retrogressive reactions Ca was proposed to catalyse.

The aim of the work reported here was to evaluate the nature and distribution of coal mineral matter in both untreated and treated (demineralized) samples of Wyodak coal, and consider the influence of these compounds by assessing their possible catalytic effect. To date, a series of experiments has been undertaken to compare the effect of demineralization on coal conversion at low temperatures (*ca* 300-350 °C), where preliminary results indicated that conversions were comparable upon pretreatment.

Experimental

Demineralization Wyodak coal (DECS-8) , ≤60 mesh, was obtained from the Penn State Coal Sample Bank; proximate and ultimate analyses are listed in Table 1[8]. Demineralisation was facilitated by successive acid treatments. The first stage was an HCl wash (10 ml per gram of coal) to remove any alkaline earths which would form insoluble fluorides at the HF wash stage. This was stirred at 60 °C for 1 hour, filtered and washed. In the second stage, a 40% HF solution (10 ml per gram of coal) was digested at 60 °C for 1 hour. The final sample was thoroughly washed with distilled water to ensure removal of residual HF. The filtrate was tested with $AgNO_3$ to indicate the presence of any residual chloride ions.

ICP-AAS Both the untreated and demineralised samples were analysed by ICP-AAS to more clearly identify the mineralogical distribution changes upon acid treatments. Samples were ashed at 950 °C and the ash dissolved using a lithium metaborate fusion technique. Solutions were then analysed using a Leeman Labs PS3000UV inductively coupled plasma spectrophotometer (ICP).

Liquefaction The demineralised coal samples were dried in a vacuum oven at 110 °C for 2 hours prior to use. Liquefaction was carried out in a 25 ml tubing bomb with *ca* 4g coal, at 300 and 350 °C, 1000 psi H_2 or N_2 for 30 min. When solvent was present, the coal:solvent ratio was 1:1 w/w; both H-donor (tetralin) and non-donor solvents (1-methyl naphthalene) were utilised. The gaseous products were collected and analyzed by GC; the liquid and solid products were recovered and separated by sequential Soxhlet extraction into *n*-hexane solubles (oils), toluene solubles (asphaltenes) and THF solubles (preasphaltenes). The THF-insoluble residue was washed with acetone followed by *n*-pentane to remove any residual THF. All recovered products were finally dried under vacuum at 110 °C for *ca* 10 hours. The conversion of coal into soluble products and gases was calculated on the basis of recovered THF-insoluble residue and reported on a dmmf basis. Residues were further analysed by FTIR and ^{13}C NMR.

FTIR Fourier transform infrared (FTIR) spectra of the demineralised coal and liquefaction residues were recorded on a Digilab FTS-60 spectrometer by co-adding 400 scans at a resolution of 2 cm^{-1}. The samples were prepared as KBr discs; predried sample (3 mg) was mixed with KBr (300 mg). All spectra were baseline corrected.

^{13}C NMR Solid state ^{13}C NMR spectra were recorded on a Chemagnetics M-100 NMR spectrometer using the cross polarization magic angle spinning (CP-MAS) technique. The measurements were carried out at a carbon frequency of 25.1 MHz.

Results and Discussion

ICP-AAS

As summarised in Table 2, metal concentration was determined by ICP-AAS in the normal and demineralised Wyodak coal samples. Ash was determined as 8.94 wt%. Upon demineralisation, ash concentration fell to *ca* 0.37 wt%, with the corresponding metal concentrations as indicated. All values are expressed in weight percent on an ash basis with the exception of HTA, which is on an as-received basis.

Liquefaction Data

Results for the reactions conducted at 350 °C, both in the presence and absence of solvent, are reported in Table 3. For purposes of initial comparison, these will be discussed with respect to data with untreated Wyodak coal [1]. It is clearly demonstrated that demineralization imparts no seriously detrimental effects on liquefaction under such conditions.

The overall conversions and liquid product distribution indicates that the most significant changes occur in the presence of solvent, both H-donor and non-donor. In the absence of solvent, conversion can be considered to be solely due to pyrolysis, i.e. there are no solvent dissolution or H donation contributions. Higher conversion is the result of increased gas yield rather than liquid yield and quality. This may be derived from two contributions. If the reduction in Fe concentration, as highlighted by ICP, also comprises pyrite, this would account for the decrease in liquid yield. Moreover, if the increased gas make is due to CO_2, removal of the mineral matter may be considered to promote more facile pyrolysis of -COOH versus -COO$^-$M$^+$.

Reaction in the presence of the non-donor solvent, 1-methyl naphthalene, results in increases in both gas and liquid yield relative to the no-solvent situation. With "normal" coal and 1-MN, the increase in liquid yield for the raw coal is 5.1%. Presumably this increase is the "extra" liquid dissolved out by the solvent. With demineralised coal and 1-MN, the increased liquid yield is 12.4%. Therefore, the solvent is undoubtedly better able to dissolve material from the demineralised coal. This suggests that there is improved access of the solvent to the coal interior upon removal of mineral species.

The best liquid conversion, defined by oil concentration as a fraction of the total liquid yield, occurs upon reaction with tetralin. This is not surprising because tetralin is an H donor, thus any enhancement in tetralin conversion relative to 1-MN can be attributed to H donation. The increase in liquid yield for normal coal in tetralin, relative to 1-MN, is 7.4%; the increase for demineralised coal is 8.6%. The difference in these numbers is within experimental error, ±3%, hence demineralisation has no effect on H transfer from tetralin and there is no mineral matter catalysis of H donation.

Table 4 summarises the results of liquefaction conducted under an inert N_2 atmosphere and those facilitated in H_2. No significant deviation in overall conversion or product distribution was observed, even in the presence of solvent.

There are similarities between the results presented here and those of other studies, not necessarily limited to demineralised samples. Tomic and Schobert [9] also observed solvent effects under mild liquefaction conditions of subbituminous coals; the addition of a solvent was observed to enhance conversion relative to the reaction with no solvent, similar to the results in Table 3. And if, indeed, pyrite concentration has been reduced, the results in Table 4 confirm those reported by Tomic and Schobert [9], Artok [10] and Huang [11] who similarly reported that utilization of H_2(g) is ineffective without a good hydrogenation catalyst, as illustrated by the similarities in the comparitive H_2 and N_2 runs. Serio et al. [4], also reported enhanced conversion for low rank coals following demineralization. This raises questions as to possible contribution of mineral species to low temperature liquefaction mechanisms. Joseph [6] ascribed this phenomenon to cations inhibiting hydrogen transfer from donor solvent/gaseous hydrogen to free radicals, in effect promoting retrogressive reactions. Therefore, it could be that the absence of these species allows for better access to reactive sites in the coal interior.

FTIR Comparative FTIR spectra of the normal and demineralised coal and associated residues are shown in Figures 1 and 2. The spectrum of the whole demineralised coal indicates the presence of most of the groups of interest in this study.

Hydroxyl groups at	3300-3600 cm^{-1}
Aromatics	3030 cm^{-1} and associated bands at 1450-1600 cm^{-1}
Aliphatics	2920, 2850 cm^{-1}
Carboxylic acids	1710-1760 cm-1
Conjugated Ketones	1715 cm-1
Esters	1712-1735 cm^{-1} (present as a shoulder on the C=O band)

After reaction under H_2 at 350 °C, the most notable feature of the whole product spectrum is a decrease in hydroxyl concentration, in part attributed to a loss of H_2O. Further examination of the THF-insoluble residue from this experiment confirms the loss of OH functionality coupled with the disappearance of the ester shoulder. The FTIR spectrum of the THF-insoluble residue from the reaction conducted with tetralin displays somewhat contrasting features. The carboxyl stretching region is much broader; moreover, the ester shoulder is more pronounced and the carbonyl region is much more defined.

The FTIR spectra of the THF-extracted raw coal and the residues from the runs conducted at 350 °C under N_2 demonstrated that under all conditions, i.e. both in the presence and absence of solvent, no marked changes were observed. The residue from these sets of experiments is currently undergoing further analysis by Py-GC-MS, to evaluate in more detail the fundamental differences in speciation resulting from non-catalytic treatment under different regimes.

Solid State ^{13}C NMR The ^{13}C CP-MAS spectra of the normal and demineralised coal is shown in Figure 3. The ^{13}C CP-MAS spectrum of the demineralised Wyodak displays many similarities to that of the untreated coal. The region between 0 and 80 ppm consists primarily of aliphatic carbons, e.g. methoxy groups and the symmetry of this band should be noted. The second region of interest between 90 and 170 ppm is due to the presence of aromatic carbon. The shoulders present on the side of the aromatic band may be attributed to specific functionalities, e.g. catechol groups (at 142 ppm) and phenolic groups (at 152 ppm). The carboxylic functionality is prominent at 180 ppm, similarly for the carbonyl at *ca* 210 ppm. In the aliphatic band, the symmetry observed for the parent coal is lost, and the appearance of a shoulder at ~25 ppm is observed. This may be attributed to a number of groups, including CH_3-Ar side chains (20-21 ppm). Furthermore, the distinct shoulders observed in the aromatic region have virtually disappeared, indicating a loss of oxygen functionalities.

Conclusions

As anticipated, relative to runs at 350 °C with untreated coal, demineralisation affords higher overall conversions; this trend becomes more apparent when either an H-donor (tetralin) or non-donor (1-mn) solvent are used. Specifically, there is no evident mineral matter effect on solvent H donation. Thus, initial results between the two sets of data suggests that the reactions undergone at 350 °C are not mineral matter catalyzed.

With respect to mineral matter identification, further ICP-AAS studies have been conducted, in association with CC-SEM and XRD determinations to identify the mineral phases and species contributing to possible low temperature hydrogenation mechanisms.

References

1. C. Song, A.K. Saini, H.H. Schobert Energy and Fuels **8**, 301 (1994)
2. Maldonado-Hodar, F.J., Rivera-Utrilla, J., Mastral-Lamarca, A.M., Ferro-Garcia, M.A. Fuel **74**(6), 818 (1995) and references therein.
3. Mochida, I., Yufu, A., Sakanishi, K., Korai, Y. Fual **67**, 114 (1988)
4. Serio, M.A., Solomon, P.R., Kroo, E., Bassilakis, R., Malhotra, R., McMillen, D. Am. Chem. Soc., Div, Fuel Chem., Prep. **35**(1), 61 (1990)
5. Garcia, A.B., Schobert, H.H. Fuel **68**, 1613 (1989) and references therein.
6. Joseph, J.T., Forrai, T.R. Fuel **71**, 75 (1992)
7. Shams, K., Miller, R.L., Baldwin, R.M. Fuel **71**, 1015 (1992)
8. Penn State Coal Sample Bank and Database
9. Tomic, J., Schobert, H.H. Energy and Fuels **10** 1996 (in press)
10. Artok, L., Schobert, H.H., Erbatur, O Fuel Proc. Tech. **37**, 221 (1994)
11. Huang, L. PhD. Dissertation Thesis, The Pennsylvania State University, 1995

Table 1. Analysis of Wyodak Subbituminous Coal (DECS-8).

Proximate Analysis (as received)				Ultimate Analysis (wt%, dmmf basis)				
Vol. Matter	Fixed Carbon	Ash	Moisture	C	H	N	S	O
32.4	29.3	9.9	28.4	75.8	5.2	1.0	0.5	17.5

Table 2. Spectrochemical Analysis of Normal and Demineralised Wyodak Coal Samples by ICP-AAS.

Sample	Ash	Metal Concentration (wt%) Fe	Ca	Mg	Na	K
Normal	8.94	5.53	13.2	3.02	1.12	0.78
Demineralised	0.37	56.8	9.23	1.51	0.20	0.24

Table 3. Results of Non-Catalytic Liquefaction of Normal and Demineralised Wyodak Coal at 350 °C for 30 min. Under 6.9 MPa H_2.

Pretreatment	Solvent	Product Distribution (% dmmf basis) Gas	Oil	Asph	Preasph	% Conv.
-	-	3.3	2.1	2.6	4.5	12.5
demineralised	-	10.0	0.8	0.4	5.3	16.6
-	Tetralin	4.2	4.1	7.6	10.0	25.9
demineralised	"	12.0	7.1	6.3	14.4	40.3
-	1-MN	4.0	1.1	5.8	7.4	18.3
demineralised	"	7.7	5.6	3.3	10.3	26.9

Table 4. Results of Non-Catalytic Liquefaction of Demineralised Wyodak Coal at 350 °C for 30 min. Under 6.9 MPa H_2 and N_2.

Gas	Solvent	Product Distribution (% dmmf basis) Gas	Oil	Asph	Preasph	% Conv.
H_2	-	10.0	0.8	0.4	5.3	16.6
N_2	-	10.7	1.2	0.7	5.2	17.8
H_2	Tetralin	12.0	7.1	6.3	14.4	40.3
N_2	"	10.4	10.3	3.6	17.8	42.1
H_2	1-MN	7.7	5.6	3.3	10.3	26.9
N_2	"	8.7	5.8	1.4	8.4	24.4

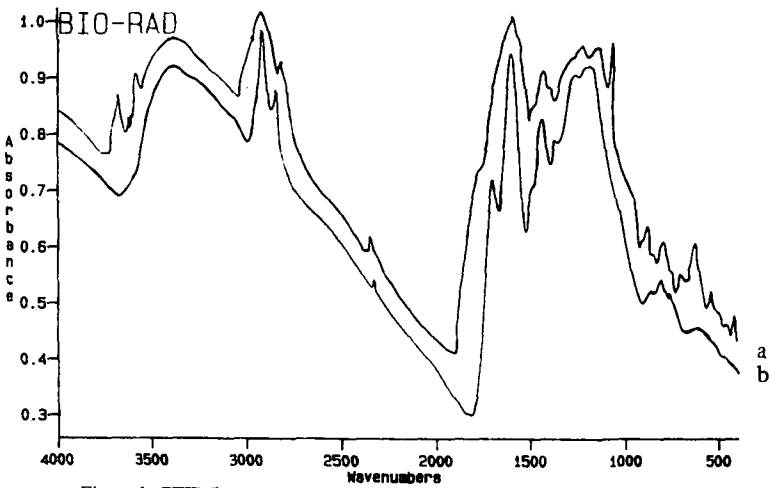

Figure 1. FTIR Spectra of (a) normal and (b) demineralised Wyodak Coal.

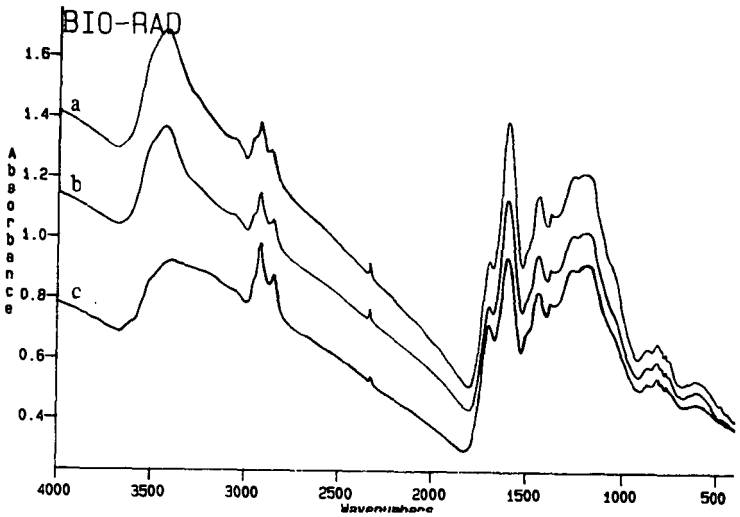

Figure 2. FTIR Spectra of THF-Insoluble Residue from Reaction of Demineralised Wyodak Coal in (a) Absence of Solvent, (b) Presence of Tetralin and (c) Presence of 1-MN.

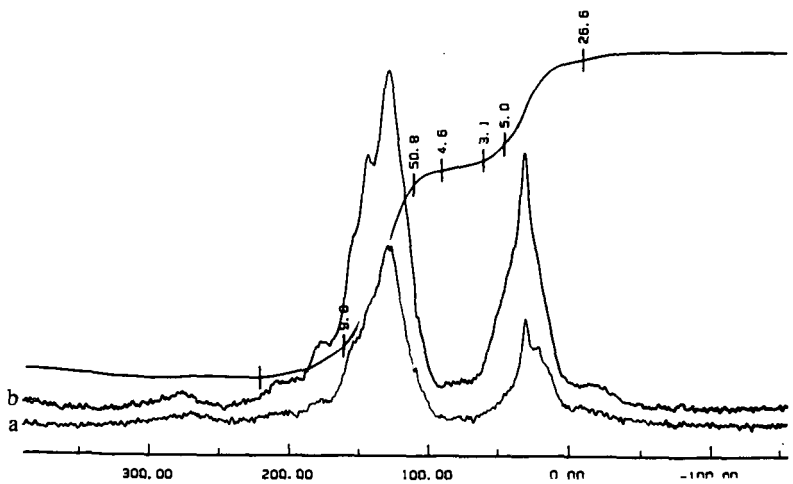

Figure 3. ^{13}C CP-MAS Spectra of (a) Normal and (b) Demineralised Wyodak Coal.

SOLVENT RECYCLABILITY AND HYDROTREATMENT SEVERITY IN DIRECT LIQUEFACTION OF LOW-RANK COAL

Melanie D. Hetland and John R. Rindt
University of North Dakota
Energy & Environmental Research Center
PO Box 9018
Grand Forks, ND 58202-9018
(701) 777-5000

Keywords: Direct liquefaction; solvent recyclability; hydrotreatment severity

INTRODUCTION

A multistep direct liquefaction process specifically aimed at low-rank coals (LRCs) has been developed at the Energy & Environmental Research Center (EERC). The process consists of a preconversion treatment to prepare the coal for solubilization, solubilization of the coal in the solvent, and polishing using a phenolic solvent or solvent blend to complete solubilization of the remaining material. The product of these three steps can then be upgraded during a traditional hydrogenation step.

Research was performed to address two questions necessary for the further development and scaleup of this process: 1) determination of the recyclability of the solvent used during solubilization and 2) determination of the minimum severity required for effective hydrotreatment of the liquid product. The research was performed during two tasks, the first consisting of ten recycle tests and the second consisting of hydrotreatment tests performed at various conditions.

EQUIPMENT

The EERC's time-sampled, batch autoclave system was used during these studies. The system is capable of close-coupled multistage operation. It can be configured to multiple designs with reactor sizes ranging from 1–8 L. Maximum operating conditions are 7500 psig and 510°C. System control and data acquisition are computerized, with the operators and computers located at a control panel separated from the high-pressure, high-temperature system by a steel barricade.

COMPOSITE SOLVENT

Different solvents have proven to be more effective in different steps during the multistep process. It is important that the solvent(s) chosen for the Task 1 testing 1) have the hydrogen donor characteristics needed during the pretreatment and solubilization steps, 2) have the characteristics of the phenolic solvent during the polishing step, and 3) be easily separable from heavier streams for recycling purposes. To meet these criteria, a composite feed solvent was prepared for the recycle tests using equal quantities of phenolic solvent (cresylic acid) and a light fraction of hydrogenated coal-derived anthracene oil (HAO61).

The solvent recycling scheme is summarized in Figure 1. The solubilization solvent initially consisted of equal parts of phenolic solvent and HAO61 light fraction. Heavy fraction HAO61 was added to the product slurry of the polishing step to serve as the vehicle solvent for the hydrotreatment step. The entire mixture was distilled to remove the phenolic solvent, HAO61 light fraction, and light coal-derived liquids (CDLs). The light materials were then recycled to the pretreatment and polishing steps.

SOLVENT RECYCLABILITY TESTS

Ten solvent recyclability tests were performed. In the first test, feed coal and composite solvent were pretreated at 175°C under 1000 psig (cold-charge pressure) CO in the presence of H_2S for 60 min. The pretreated slurry was solubilized at 375°C under 1000 psig (cold-charge pressure) CO and H_2S for 60 min. The product of the solubilization step was polished with additional phenolic solvent under 1000 psig (cold-charge pressure) H_2 for 20 min at 435°C. The polished product slurry was combined with a vehicle solvent and distilled to remove water, solubilization solvent equal to the amount added in the polishing step, and oxygenated light CDLs. If hydrotreatment were part of this task, the bottoms from this distillation would go to the hydrotreatment step. The solubilization solvent was recycled to the pretreatment step for the next test. This scheme was repeated for all ten multistep tests.

Material balances were calculated for all of the processing steps during the solvent recyclability tests. The recoveries for each of the steps were similar. The liquid balance for the pretreatment/solubilization step ranged from 90.4% to 91.7% and from 95.9% to 97.7% for the

polishing step. The overall mass balances for the pretreatment/solubilization step ranged from 96.0% 100.4%, for the polishing step from 98.2% to 99.2%, and for the distillation step from 96.3% to 99.6%. The consistency of the mass balances is indicative of the operational stability of the system. Overall mass balances of at least 96.0% indicate that significant leaks or spills that might have skewed the data did not occur. The data appear to reliably describe the process.

Table 1 shows the distillate yields and solvent balances for each of the solvent recyclability tests. During the original distillation, some of the distillable material from the third test was not collected because of a pressure transducer problem caused by an unexpected power outage. The distillation bottoms were redistilled, and the additional material collected was added to the recycle solvent stream used in the sixth test feed slurry. The table shows that as a result of the lower fraction of light distillate present in the fourth and fifth tests, solvent recovery dropped from approximately 15% excess solvent to about 5% excess solvent. Excess solvent was produced in each of the tests, with an average excess solvent production for all tests of 16.8 wt%. Excluding the low solvent balances for the fourth and fifth tests, the average excess solvent produced was 19.48 wt%.

Detailed analyses were performed to determine the changes in composition of the light solvent as it was recycled during the recyclability tests. Two types of analyses were performed. The first determined the relative aromatic concentration in the recycle solvent, providing an indication of the ability of the solvent to maintain its hydrogen donor characteristics during processing. Fourier transform infrared spectroscopy (FT-IR) was used for this analysis. Table 2 shows that the number of aromatic C-H bonds did not change significantly during the test sequence, indicating that the solvent maintained its hydrogen donor capabilities. The second analysis determined the cresol (or equivalent) concentration in the solvent. The results of this analysis are plotted in Figure 2. As is easily seen from the plot, the cresol concentration appears to be approaching a constant value of approximately 32%-34% wt% of the recycle solvent stream. This concentration agrees with that attained during direct liquefaction research performed in 1983 at the EERC, which indicated that solvent lineout occurred at about 32 wt% phenolics after 40 passes through the system.

Several conclusions can be drawn from the solvent recyclability test results:

- The system is operationally stable. Even when some solvent was not removed for recycle (as in Test 3) or was added back as additional solvent (as in Test 6), little change in product quality was observed.
- Excess solvent was produced for each multistep test.
- Product yield structures were fairly constant for all tests.
- The process produces recycle solvent consisting of approximately 32%-34 wt% cresol (or equivalent).
- The recycle solvent maintains its hydrogen donor capability.

In general, the tests showed that it is possible to produce a consistent, viable recycle solvent stream using the EERC multistep direct liquefaction process.

HYDROTREATMENT SEVERITY TESTS

The purpose of the hydrotreatment severity study was to determine the lowest-severity hydrotreatment conditions that produce high-quality liquid product. A statistical approach to data collection was used so as to predict the lowest-severity conditions in a relatively small number of tests. The results of this type of experimental matrix can be statistically analyzed to develop mathematical equations describing the process. A factorial design consisting of ten tests was employed to test the effects of temperature, pressure, and residence time on product quality. Maximum or minimum conditions of each factor were tested for eight of the tests; tests were performed at temperatures of either 405° or 445°C, at pressures of either 1920 or 3080 psig, and at reaction times of either 34 or 112 min. Two tests were performed at center point conditions (425°C, 2500 psig, and 73 min) to determine lack of fit of the equations. The matrix was randomized to minimize skewing of data that can occur when one variable is held constant for several tests in a row. The liquid product from solvent recyclability Tests 1, 2, 4, and 6 were combined into a single sample to be used as the feedstock for the hydrotreatment severity tests. For each test, composite feed and sulfided Shell 424 catalyst were hydrotreated at experimental matrix-specified conditions.

The analytical and mass balance data from the hydrotreatment severity tests were used to calculate various product quality indicators, including the saturated molar H-to-C ratio of the hydrotreated product; the percent improvement in saturated molar H-to-C ratio of the product over that of the solubilized feed slurry; the distribution of product as pot residue, middle oil, light oil, and cold

trap liquids; the hydrogen consumption of the hydrotreatment step; the yield of hydrocarbon gases from the hydrotreatment step; and the ratio of hydrocarbon gas yield to hydrogen consumption.

The product quality indicators were analyzed using regression analysis. The effect on product quality of each operating parameter or combination of parameters was determined for each indicator by using both backwards elimination and stepwise regression analyses. During a regression analysis, the degree of effect of all independent variables and their combinations on the dependent variable is determined. When the backwards elimination procedure is employed, the independent variable having the least (statistically) significant effect on the dependent variable is dropped. The procedure is repeated until the remaining independent variables are all considered to significantly affect the dependent variable. The stepwise procedure is the reverse of the backwards elimination procedure, in that independent variables are added until one is found not to be statistically significant. The mathematical equation indicated by both regression procedures describes the combined effect of the independent variables on a given dependent variable. Each equation was checked for statistical lack of fit to the data. All of the equations were found to fit the data at a 90% confidence interval.

Spreadsheets were constructed for each product quality indicator by inputting values of the operating parameters over their ranges and calculating the value of a given product quality indicator using the mathematical equation derived during statistical analysis. Nonsignificant operating parameters were held constant at their center point values during these calculations. The calculated product quality indicators were plotted to show what their values would be at various operating conditions that were not actually tested.

The plots showed that a high hydrotreatment temperature (about 440°C) results in the production of hydrocarbon gases at the expense of the production of desirable liquid products, especially when reaction time exceeds 100 min. The plots also showed that an increase in pressure improves total liquid yield.

The various plots were compared to determine the lowest-severity set of conditions that would result in the optimum values for the majority of the product quality indicators. The lowest-severity conditions were determined to be: 405°C temperature, 3000 psig pressure, and 60 min reaction time. A test was performed at these conditions to verify the accuracy of the predictions. The predicted values for each of the product quality indicators are compared with the actual values calculated for the test in Table 3. The data show that the equations predicted the product quality indicator values fairly accurately.

The hydrotreatment temperature at which the verification test was performed was at the lower end of the valid range of the predictive equations. The effect of lowering the temperature below 405°C cannot be determined. Therefore, it is possible that an even lower temperature might effectively hydrotreat the liquid product from the multistep process.

Interpretation of the hydrotreatment severity data led to the following conclusions:

- The mathematical equations derived during statistical analysis of the data effectively predicted the effects of changing the hydrotreatment operating parameters on product quality.
- The composite solvent used during the solvent recyclability test sequence produced solubilized material that could be as effectively hydrotreated as the product of batch tests using optimal solvents for each test.
- Because the production of appropriate distillate material is crucial to a favorable yield structure, it is doubtful that hydrotreatment reaction severity can be reduced by reducing operating pressure. Reductions in hydrotreatment severity must therefore come from reductions in either temperature or reaction time or both.
- Reaction time can probably be reduced to approximately 30 minutes without a substantial reduction in product quality.
- It may be possible to reduce hydrotreatment temperature to less than 400°C while maintaining desired product quality and yield.

It appears that the EERC multistep direct liquefaction process produces a liquid that requires less severe hydrotreatment conditions than are employed during traditional direct liquefaction processing.

ACKNOWLEDGMENT

This research was performed under the U.S. Department of Energy Grant No. DE-FG22-94PC94050.

TABLE 1

Distillate Yields and Solvent Balances for Task 1 Tests

Test No.	Hydrotreatable Solubles, wt% maf[a]		Solvent Yield, wt% maf	Solvent Balance, %
	Liquid Basis[b]	Gas Basis[c]		
1	79.52	87.02	42.01	116.42
2	71.23	86.49	68.17	127.75
3	86.00	86.08	46.27	118.57
4	86.02	85.00	13.67	105.47
5	82.61	83.08	17.12	106.80
6	83.35	79.63	49.53	120.00
7	79.57	83.83	39.52	115.84
8	72.86	79.86	44.88	118.07
9	75.90	79.44	45.03	117.96
10	81.60	81.69	47.20	121.22
Average	79.87	83.21	41.34	116.81

[a] Weight percentage of moisture- and ash-free coal fed to the system.
[b] Yield calculated from liquid stream mass balance data.
[c] Yield calculated by subtracting the gas yield from unity.

TABLE 2

Relative Aromatic Concentrations in Recycle Solvent

Test Number	C-H Absorbance
1	0.35
4	0.34
7	0.36
10	0.35

TABLE 3

Predicted and Actual Product Quality Indicator Values for the Verification Test

Product Quality Indicator	Predicted Value	Actual Value
Saturated Molar H:C	0.3252	0.3306
H:C Improvement, %	48.33	50.82
Pot Residue, wt% of product slurry	10.78	7.72
Middle Oil, wt% of product slurry	80.42	86.16
Light Oil, wt% of product slurry	5.23	1.43
Cold-Trap Liquids, wt% of product slurry	2.91	4.69
Hydrogen Consumption, %	2.97	1.96
Hydrocarbon Gas Yield, %	0.41	0.36
HC Gas Yield:H_2 Consumption	0.1268	0.1822

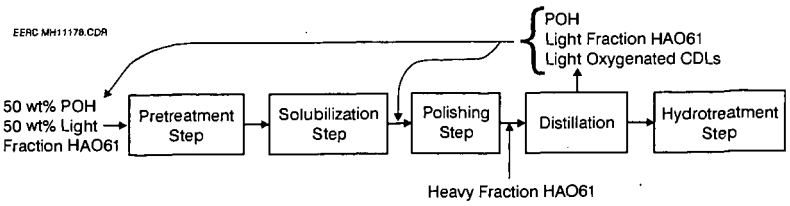

Figure 1. Block diagram summarizing the composite solvent scheme.

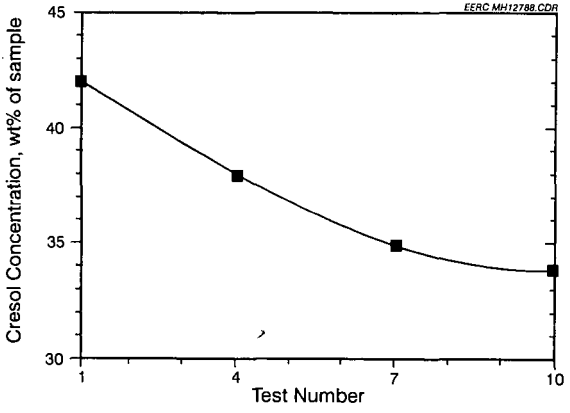

Figure 2. Cresol concentration in recycle solvent as a function of test number.

MDH/djs

EFFECT OF A CATALYST ON THE SOLVENT-FREE LIQUEFACTION OF DECS-17 COAL

R.P. Warzinski, B.C. Bockrath, G.A. Irdi, H.B. Booher, and A.W. Wells
U.S. Department of Energy
Pittsburgh Energy Technology Center
P.O. Box 10940
Pittsburgh, PA 15236.

Keywords: Coal liquefaction, molybdenum sulfide catalysts, reaction mechanism

INTRODUCTION

Dispersed catalysts are important factors in efforts to improve the first stage of direct coal liquefaction processes. Understanding the role of these catalysts is vital to improving their performance. Prior work at the Pittsburgh Energy Technology Center has been devoted to studying the role of a dispersed catalyst, apart from that of added solvent or vehicle, in the first stage of liquefaction (1). In that work, $Mo(CO)_6$ was found to be an excellent precursor for generating dispersed MoS_2-containing catalyst for the solvent-free liquefaction of coal

In the work reported here, solvent-free thermal and catalytic microautoclave experiments with DECS-17 coal were performed at various residence times to investigate the role of the MoS_2-containing catalyst formed from $Mo(CO)_6$ in the initial stages of the liquefaction process. A temperature slightly above that where pronounced catalyst-induced hydrogen uptake was previously observed (375°C) was used in this study. The focus of this paper is on the characterization of the THF-insoluble products. These products were characterized by organic petrology, oxygen speciation analysis, solid-state ^{13}C NMR, and elemental analysis. A more complete account of this work and of similar experiments conducted at 350°C and 400°C is not possible here but will be reported at a later time.

EXPERIMENTAL

All experiments were performed with DECS-17 (Blind Canyon) coal from the Penn State Coal Sample Bank. The elemental analysis (on a dry basis) provided with the coal was as follows: 76.3% carbon, 5.8% hydrogen, 1.3% nitrogen, 0.4% sulfur (0.02% pyritic sulfur), 6.6% ash, and 9.7% oxygen (by difference). The moisture content of the as-received coal was 3.7%. Because this coal contains low levels of pyrite, the influence of native catalyst precursors is minimized.

Microautoclave liquefaction experiments were performed according to previously described procedures in 316-stainless-steel microautoclaves of approximately 46 cm^3 internal volume (1). Separate microautoclaves were used for thermal and catalytic experiments to avoid residual catalytic effects. In the experiments reported here, 6.6 g of coal was used along with a hydrogen/3% hydrogen sulfide gas mixture at 7.2 MPa (1030 psig) cold pressure. In catalytic experiments, $Mo(CO)_6$ was used as the catalyst precursor and was simply added to the microautoclave along with the coal at a level of 1000 ppm Mo based on daf coal. Slow heat-up to a reaction temperature of 375°C and a rapid cool-down were employed. The heat-up time was approximately 55 min. Residence times at temperature of 0, 30, and 60 min were used. All experiments were performed at least in duplicate and the respective products combined to prepare sufficient quantities for subsequent characterization. The products were recovered according to the referenced procedures (1).

Elemental analyses of the liquefaction products were performed at Huffman Laboratories in Golden, Colorado. Extensive characterization of the unreacted coal and the THF-insoluble liquefaction products was performed. This included solid-state ^{13}C NMR spectra, obtained at Western Research Institute in Laramie, Wyoming, following published procedures (2). Oxygen speciation analyses were also performed at PETC. The total hydroxyl contents of the coal and THF-insoluble products were determined by potentiometric titration following reaction with tetrabutylammonium hydroxide. Carboxylic acid contents were determined by exchange with barium ions under nitrogen and in a precisely calibrated buffer solution. The barium was then reacted with standard perchloric acid which was back-titrated to determine the extent of ion exchange. Petrographic analyses were also performed at PETC. The vitrinite reflectance measurements were performed on the vitrinite particles in the raw coal and 0-min residence time samples and on vitroplast (particles derived from heated vitrinite) in the 30-min and 60-min residence time samples according to ASTM procedure D 2798-91.

RESULTS AND DISCUSSION

In prior work with $Mo(CO)_6$ and the DECS-17 coal, the onset of a catalytic effect on hydrogen uptake was detectable at 325°C. The rate of hydrogen uptake due to the catalyst became more pronounced near 370°C (1). In 1-h residence time experiments, the presence of the catalyst promoted conversion of the coal to THF- and cyclohexane-soluble products at temperatures above 325°C and 375°C, respectively. To further define the role of the catalyst, experiments have been conducted at 375°C at residence times of 0, 30, and 60 minutes. This temperature is slightly above that where the pronounced hydrogen uptake caused by the catalyst was observed. To prepare sufficient quantities of material for characterization, twice the usual amount of coal was used. The catalyst loading and initial hydrogen pressure remained the same.

Figure 1 contains the conversion results obtained for the recent experiments with 6.6 g of coal, as well as respective conversions from the previous 1-h experiments at 375°C in which 3.3 g of coal was used. Part A contains the thermal conversions, Part B the catalytic conversions, and Part C the data obtained after subtraction of the thermal conversions from the catalytic data at each residence time. All thermal and catalytic experiments were performed at least in duplicate. The bars on the data in parts A and B represent the range of values obtained and are shown if they are larger than the size of the symbol.

No improvements in the conversions attributable to the catalyst are observed in Figure 1 (part C) after the heat-up to reaction temperature (0 residence time). At the longer times, the catalyst is effective in promoting conversion to THF-soluble products; however, a definite catalytic effect is only observed at the longest reaction time with respect to cyclohexane conversion. With the smaller coal charge, no significant improvement in cyclohexane conversions was noted at 60 minutes. However, at a longer residence time of 8 h (not shown here), a catalytic effect was observed (1). A smaller but significantly lower catalyst-promoted THF conversion was also noted for the liquefaction of the smaller coal charge (part C of Figure 1). This latter observation appears to be due to the lower thermal conversion for the larger coal sample (part A of Figure 1), indicating that in the absence of catalyst, more retrogressive reactions occurred in the larger coal mass. However, with catalyst, the THF conversions were nearly the same for both coal amounts. This highlights the efficacy of the $Mo(CO)_6$ precursor in forming a highly dispersed, active coal liquefaction catalyst.

A procedure has been developed that uses the pressure and temperature data recorded throughout the experiment to monitor the change in gas content of the reactor during solvent-free liquefaction experiments. A description of the procedure used to obtain this representation of the data has been published (1). Figure 2 contains these data for the current 1-h work and for the prior work with 3.3 g of coal. The prior work also showed that the catalyst had little effect on the gases liberated. Therefore, the thermal components, mainly liberation of CO, CO_2, and hydrocarbon gases, have been subtracted from catalytic data to obtain the curves shown in Figure 2 which therefore primarily reflect the hydrogen uptake as a function of time and temperature. The only other major influence on the data in this figure that is unaccounted for is the liberation of water vapor from reactions associated with the catalyst.

Table 1 compares temperatures of the onset of gas uptake, both initial and rapid, and the initial rates of rapid gas uptake obtained from the data in Figure 1.

Table 1. Onset of catalytic activity and rates of gas uptake due to the catalyst for experiments at 375°C with various amounts of DECS-17 coal.

	Amount of Coal	
	3.3 g	**6.6 g**
Onset of Catalyst Activity, °C	345	335
Onset of Rapid Gas Uptake, °C	360	365
Initial Rate of Rapid Gas Uptake, mmol g^{-1}(daf coal) min^{-1}	0.084	0.106

The conversion data and the data in Table 1 show that doubling the loading of the coal had little effect on reactivity. The total pressure in the microautoclave upon reaching reaction temperature with 6.6 g coal charged was about 11.9 MPa (1710 psig) and the total reduction in pressure after

1 h was 1.2 MPa (170 psi). Thus, a pseudo first-order condition with a nearly constant hydrogen partial pressure was maintained even in the case of greatest hydrogen demand.

The change in the slope of the curves shown in Figure 2 during the reaction at 375°C suggests that two major catalytic events are occurring during the course of the liquefaction reaction. This is most evident in the data for the reaction using 6.6 g of coal. Near the end of the heat-up period and for about 15 minutes into the reaction at 375°C, the rate of gas uptake is rapid. After this, the rate of gas uptake drops by about one-third to 0.31 mmol g^{-1}(daf coal) min^{-1}. The change in the apparent rate of hydrogen consumption could be due to different time constants for the various reactions occurring in the liquefaction process. It was observed in thermal experiments that the generation of gas, primarily CO_2 at this temperature, was confined mainly to the early part of the reaction. The release of this gas has been associated with the onset of thermal reactions in the coal which can lead to a more refractory product in the absence of catalyst (3). The high hydrogen demand in the early part of the reaction may be due to the capping of the radicals generated by these thermal reactions. After this event, the lower hydrogen demand could be due to capping of radicals formed from the thermal reactions which occur in parallel with those responsible for the initial burst of activity. This hypothesis is in accord with the idea of an equilibrium between a radical pool and a reactive insoluble product recently used by Suzuki to model the liquefaction of a low-rank coal (4). The catalyst undoubtedly has other roles, especially in the later parts of the liquefaction process. These include heteroatom removal, hydrogenation of aromatic systems, and hydrocracking reactions; all of which would lead to the increase in the lighter, cyclohexane-soluble products observed after 60 minutes (part C of Figure 1).

To obtain additional information on the role of the catalyst, a detailed characterization of the THF-insoluble products from the reactions at 0, 30, and 60 min was performed. The following analytical techniques were used: organic petrography, ^{13}C solid-state NMR, an oxygen speciation technique developed at PETC, and elemental analysis.

Figure 3 shows the change in the H/C ratio and the vitrinite reflectance as a function of conversion of the coal to THF-soluble products. The THF conversion increased with residence time (see Figure 1); however, little change occurred after 30 min in the thermal experiments. The vitrinite reflectance values were determined as part of the petrographic examination of the vitrinite in the raw coal and the vitrinite or vitroplast in the THF-insoluble products. H/C data were also obtained for the same samples and for a sample of the raw coal that had been extracted with THF using the same procedure as for recovering the insoluble residue. The data show that hydrogen is added to the residue in the presence of the catalyst and that the H/C ratio is maintained at a level near that observed for the THF-extracted coal even up to a reaction time of 30 minutes (part A of Figure 3). Without catalyst, the H/C ratio drops even for the 0-residence time sample. The vitrinite reflectance measurements shown in part B of Figure 3 indicate that using catalyst results in a product that is less aromatic and therefore more reactive than in the thermal cases. Even for the 0-residence time sample, the presence of the catalyst resulted in a reflectance value at or even less than that of the starting coal. As with the H/C data, most of the changes in the thermal samples occur within the first 30 minutes at reaction temperature.

The THF-insoluble products obtained from the 0-min residence time experiments still consisted of identifiable macerals. The catalytic samples contained vitrinite particles that exhibited rounding of the edges which may indicate that the catalyst was promoting the initiation of coal softening. Catalytic hydrogenation has been observed to lower the initial softening temperature of coal and extend its plastic range (3). Vitrinite reflectance measurements were also recorded at the centers and edges of the vitrinite particles. In the thermal samples, the reflectance measurements were nearly constant across the particles (0.70% center, 0.69% edge). The values for the catalytic samples were substantially lower and there was a slight increase in vitrinite reflectance from the edge areas (0.58%) to the center (0.61%). Similar observations have been reported in the literature for coal liquefied using naphthalene as a solvent (5). The petrographic and elemental analyses show that, even though the catalyst had not affected the yields of THF-soluble products at 0-min residence time, significant changes had already been induced in the coal by its presence.

The inferences drawn from petrographic and elemental analyses were strengthened by additional information provided by solid-state ^{13}C NMR, summarized in Figure 4. At the onset of liquefaction, the presence of the catalyst limited the increase in the fraction of aromatic carbons in the THF-insoluble product (part A of Figure 4) as compared to the thermal product. This

corroborates the vitrinite reflectance measurements shown in part B of Figure 3. With time, this effect became more pronounced. At the longer reaction times, the catalyst exerted a definite effect on limiting the growth of aromatic clusters in the insoluble product (part B of Figure 4). The presence of the catalyst also resulted in lower attachments per average cluster (part C of Figure 4) and lower molecular weights of the clusters with respect to the amount of conversion that occurred. Liquefaction creates a hydrogen demand that is partially satisfied in the thermal case by condensation and aromatization reactions in the residue. The catalyst provides an alternate source of hydrogen from the gas phase, thus resulting in less condensation and aromatization in the residue.

The effect of catalyst on the oxygen-containing species present in the THF-insoluble products is made evident by the data assembled in Figure 5 from elemental, NMR, and oxygen speciation analyses. Part A contains the atomic O/C ratios as a function of conversion. Only small overall changes are noted and no overall concentration of oxygen-containing species was apparent as more of the coal liquefied. The NMR data in part B and the results of oxygen speciation analyses in part C show that initially the amounts of hydroxyl or phenolic substituted carbon in the THF-insoluble products were similar to that in the starting material. Also, based on data from the potentiometric titrations (not shown), the relative proportion of strong acids in the THF-insoluble products from reactions with catalyst increased. Without catalyst little change was noted.

After 30-min reaction time in the absence of catalyst, the unconverted material does not change in regard to oxygen content or speciation. This is in marked contrast to the extensive increase in aromaticity seen in Figure 4. Catalyst does not seem to have a profound effect on oxygen distribution with the exception that the number of hydroxyl and phenolic substituted carbons becomes somewhat more concentrated in the small fraction of coal left unconverted.

Part D of Figure 5 contains additional information derived from the oxygen speciation analysis and shows that the presence of the catalyst resulted in a small but definite increase in the amount of carboxyl groups in the THF-insoluble products. Virtually no change was observed in the products from the thermal experiments. The carboxyl groups are not formed during the liquefaction reaction but rather through aerial oxidation of the residues during the workup procedure. Catalytic liquefaction apparently renders the remaining residues more susceptible to such oxidation.

CONCLUSIONS

Solvent-free liquefaction with a well-dispersed catalyst provides an excellent opportunity to study its effects on coal without the complications generated by excess extraneous material. The results presented here show that a low level of catalyst addition significantly promotes conversion and the uptake of hydrogen from the gas phase even in the early stages of the liquefaction process. Even before the yields of THF-soluble products are affected, the catalyst causes significant changes in the coal. Petrographic analysis of the liquefaction residues indicates the catalyst promotes hydrogenation and softening. Solid-state ^{13}C NMR analysis reveals pronounced differences between thermal and catalytic residues. The former are more aromatic, contain more aromatic carbons per cluster, and more attachments per cluster. A net effect of catalyst is to protect the unconverted material from thermal reactions leading to the formation of a highly aromatic char. At the conditions of these experiments, reactions involving oxygen functionalities did not seem to be greatly affected by the presence of the catalyst.

ACKNOWLEDGMENTS AND DISCLAIMER

The authors would like to thank Richard Hlasnik and Jerry Foster for performing the microautoclave work. The NMR analyses were performed by Dr. Francis Miknis and Dr. Daniel Netzel of the Western Research Institute in Laramie, Wyoming. Reference in this report to any specific product, process, or service is to facilitate understanding and does not imply its endorsement or favoring by the United States Department of Energy.

REFERENCES

1. R.P. Warzinski; B.C. Bockrath Energy & Fuels **1996**, 10, 612-622.
2. M.S. Solum; R.J. Pugmire; D.M. Grant Energy & Fuels **1989**, 3, 187-193.
3. F.J. Derbyshire; A. Davis; R. Lin Energy & Fuels **1989**, 3, 431-437.
4. T. Suzuki Energy & Fuels **1994**, 8, 341-347.
5. F.J. Derbyshire; A. Davis; M. Epstein; P. Stansberry Fuel **1986**, 65, 1233-1239.

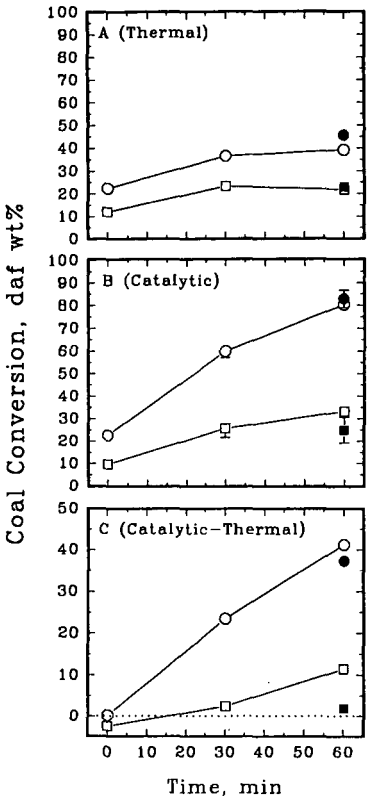

Figure 1. Conversion results for 375°C experiments with DECS–17 coal. (○ , ●) THF conversion; (□ , ■) cyclohexane conversion. Open symbols – 6.6 g coal; closed symbols – 3.3 g coal.

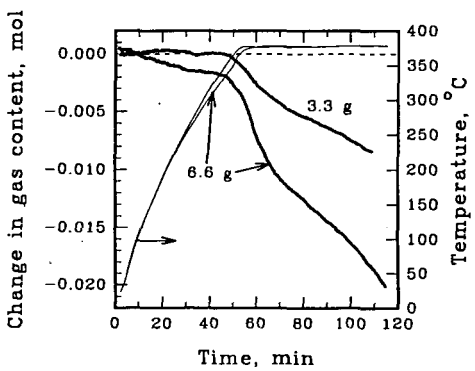

Figure 2. Effect of coal loading on changes in gas content in the microautoclave due to the catalysts for 1–h experiments with DECS–17 coal.

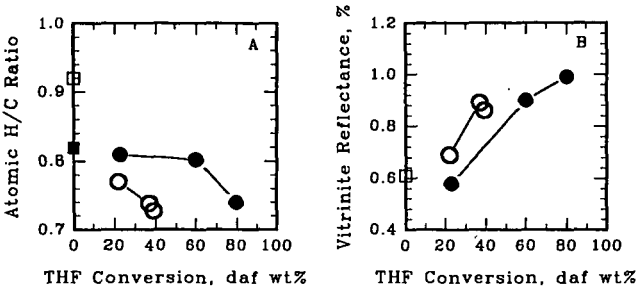

Figure 3. Vitrinite reflectance data and atomic H/C ratios for THF insols from experiments at 375°C with DECS-17 coal. (○ thermal; ● catalytic; □ untreated coal; ■ untreated, THF-extracted coal.)

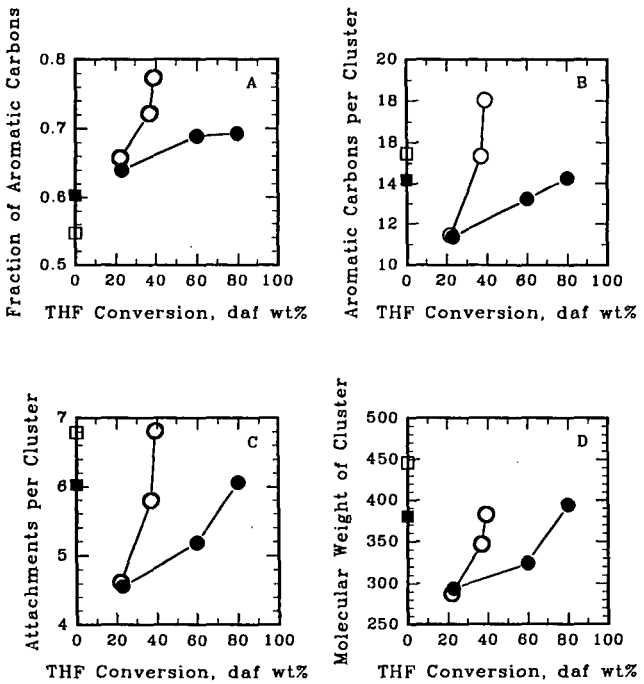

Figure 4. Solid-state ^{13}C NMR data for THF insols from experiments at 375°C with DECS-17 coal. (Symbol definitions are the same as in Figure 3.)

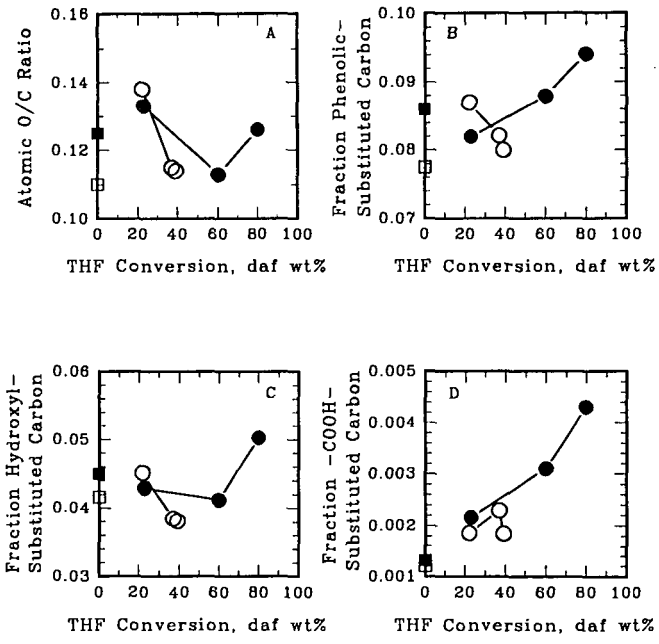

Figure 5. *Oxygen species data for THF insols from* experiments at 375°C with DECS-17 coal. (Symbol definitions are the same as in Figure 3.)

EFFECTS OF SURFACE-ACTIVE AGENTS ON MOLYBDENUM ADSORPTION ONTO COAL FOR LIQUEFACTION

Godfried M. K. Abotsi, Kofi B. Bota, Gautam Saha and Stacey Mayes
Department of Engineering
Clark Atlanta University
Atlanta, GA 30314

Keywords: Surfactants, adsorption, molybdenum catalysts.

INTRODUCTION

The aim of this work is to enhance catalyst loading and dispersion in coal for improved liquefaction by preadsorption of surfactants onto coal. The use of surfactants to increase the dispersion and stability of coal-water slurries and to enhance coal beneficiation is well known. However, the effects of surfactants on catalyst loading and dispersion prior to coal liquefaction have not been investigated. This paper discusses the influence of the cationic surfactant dodecyl dimethyl ethyl ammonium bromide (DDAB) and sodium dodecyl sulfate (SDS, anionic) on the surface properties of Illinois No. 6 coal and its molybdenum uptake from solution.

Extensive investigations on molybdenum and other metals as coal liquefaction catalyst precursors have shown that more effective catalyst loading techniques are required to attain sufficiently high levels of catalyst dispersion in coal for liquefaction on a commercial scale. Studies (1-3) in our laboratory have shown that the surface charge properties of coal exert significant influence on the uptake, dispersion and activities of aqueous soluble calcium and potassium catalysts that were applied to coal char gasification. In general, the surfaces of the three types of coal investigated were negatively charged. The surface charge density was linked to the dissociation of coal surface phenolic and carboxylic groups which promoted the adsorption and dispersion of calcium and potassium ions (1, 2).

Coal surface contains both hydrophobic and hydrophilic sites. The hydrophilic regions consist of inorganic or polar organic surface groups; the hydrophobic surface regions are primarily non-polar organic moieties. When added from aqueous solution, the catalyst will be attracted to the hydrophilic sites on the coal but it will be repelled by the hydrophobic sites. The opposite effect will occur when a catalyst is loaded from organic solution. In either case, a low catalyst dispersion will result, unless the coal surface sites are controlled to optimize the distribution of the catalyst in the coal. The current work examines the application of surface-active agents (surfactants) for controlling coal surface properties with the goal of enhancing molybdenum loading and dispersion prior to liquefaction.

EXPERIMENTAL

The Illinois No.6 coal (DECS-24) used in this study was supplied by the Penn State Coal Sample Bank. Its moisture, ash, volatile matter, and fixed carbon contents were 13.2, 11.6, 35.4, and 39.7 %wt., respectively, on as-received basis. It has an ultimate analysis of 11.6 % ash, 57.3% carbon, 4.0% hydrogen, 1.0% nitrogen, 4.8% sulfur, and 8.1%wt. oxygen (by difference). Coal-water slurries for the study were prepared by adding 2.0g of coal to 25 mL of 0.01M aqueous solution of molybdenum and 25 mL of 0.02M DDAB or 0.02M SDS. A set of six samples were

prepared for each surfactant and the pHs of the slurries ranged from about 2 to 12. Ammonium molybdate (VI) tetrahydrate (AMT) was used as the molybdenum source. After recording the original pHs of the coal dispersions, about 0.5mL of 1M HCl or 0.5M NaOH solution was added to all, except one sample, to adjust the pHs to the desired values. The samples were then shaken on a mechanical agitator for 24h, followed by redetermination of the final equilibrium pHs. The samples were then filtered and the filtrates were analyzed for molybdenum using atomic absorption spectrophotometry. The molybdenum content of the coal residues was measured by Galbraith Laboratories, Knoxville, TN, using inductively coupled argon plasma spectroscopy. Mass balance calculations showed good agreement between the two analytical techniques.

To determine the effects of the coal surface charge on the adsorption of the surfactants and molybdenum, the zeta potentials of coal slurries containing 5g of coal per liter and deionized water were measured. The measurements were conducted on 25 mL samples to which 25 mL of 0.2M, 0.02M, or 0.002M DDAB or SDS solution had been added and the pHs adjusted as described above. The samples were equilibrated for 4h by mechanical agitation, after which the pH values were recorded. The zeta potentials were measured at room temperature using a Pen Kem Model 501 zeta meter.

The interaction of the surfactants with the coal surface was studied using diffuse reflectance FTIR. The coal samples were dispersed in infrared grade KBr that had been dried overnight at 300°C and sieved through a 90 micron sieve. The FTIR spectra were recorded on 10% coal in KBr using a Nicolet Magna IR Spec 750 and 500 scans.

RESULTS AND DISCUSSION

The zeta potential results in Figure 1 show that the parent coal is negatively charged within the pH range investigated and that the charge density increased with increase in the slurry pH. This behavior is attributed to the dissociation of the surface carboxlylic and phenolic acid groups (1, 2). Figure 1 also shows that the coal particles generally produced positive zeta potentials in the presence of DDAB. In solution, SDS ($CH_3(CH_2)_{11}OSO_3^-Na^+$) and DDAB ($CH_3(CH_2)_{11}N(C_2H_5)(CH_3)_2^+Br^-$) will dissociate to produce anionic and cationic surfactants, respectively, which can be denoted as $ROSO_3^-$ and $R'N^+$. Since DDAB is cationic, the positive charge density on the coal can be explained by the coulombic attraction of the surfactant, and its subsequent adsorption, to the negatively charged sites on the coal surface. In contrast to the effect of DDAB, the zeta potentials of the coal particles became more negative than those of the parent coal in the presence of SDS, as shown in Figure 2. The negative charge density increased with increase in pH and in the concentration of SDS. Since the surface of the raw coal is negative, the adsorption of SDS must occur through the hydrocarbon chain of the molecule, with the anionic head oriented towards the aqueous solution.

The effects of the surfactants and pH on molybdenum loading onto the coal are shown in Figure 3. A remarkable dependence of catalyst loading on both parameters was observed. The minimum catalyst loading occurred on the parent, untreated coal in contrast to the DDAB-treated coal which contained the highest molybdenum content. Around pH 2.5, the molybdenum loadings of these samples were about 5 and 15

mg/g of coal, respectively. An intermediate molybdenum loading (~9 mg/g coal) occurred on the SDS-treated sample.

The observed molybdenum adsorption patterns can be explained by the electronic charges on the coal surface and on the molybdenum species. In aqueous solution, AMT will dissociate to form various molybdenum oxyanions which are pH dependent (4). It is reported that $Mo_8O_{26}^{4-}$ predominates below pH 2 whereas $Mo_7O_{24}^{6-}$ exists as the dominant species between pH 2 and 6. MoO_4^{2-} and $Mo_7O_{24}^{6-}$ occur in the pH 6 to 8 range; MoO_4^{2-} predominates above pH 8. Thus, the adsorption of the molybdenum species should be promoted by the positively charged DDAB sites on the coal. It is observed from Figure 1 that at 10^{-3} M DDAB, the zeta potentials are positive and become negative above ~pH 9. At 10^{-2} M DDAB, the zeta potentials are positive within the entire range of pH studied and they increased almost exponentially with increase in pH. This implies progressively stronger adsorption of DDAB onto the coal surface. When the DDAB concentration was raised to 10^{-1} M, the zeta potential increased steadily, passed through a maximum around pH 6-8, and then decreased thereafter. This phenomenon is attributed to strong DDAB adsorption and micelle formation. When the DDAB concentration on the surface exceeded the critical micelle concentration around pH 6-8, the molecules formed aggregates with the polar head of the surfactant oriented towards the interior of the micelle (5). This should decrease the positive charge density on the coal, as was indicated by the decline in the zeta potential values.

The FTIR spectra of the original, untreated coal and those onto which molybdenum and DDAB or SDS were adsorbed are shown in Figure 4. The FTIR spectrum for the original coal after loading with molybdenum is provided in Figure 4A. Significant differences can be seen in the C-H bands at 2800-3000 cm^{-1}. The intensities of these bands are higher for the surfactant-treated samples than for the raw coal (Figure 4B). It is also noted that the intensity of the DDAB-treated coal (Figure 4C) is stronger than for the SDS-treated specimen (Figure 4D). The FTIR spectra confirmed the adsorption of the surfactants onto the coal surface.

In conclusion, it has been shown that the adsorption of molybdenum onto Illinois No. 6 coal (DECS-24) is significantly promoted by preadsorption of dodecyl dimethyl ammonium bromide (DDAB) and sodium dodecyl sulfate (SDS). The former surfactant effected higher catalyst loading since its cationic character favored its adsorption onto the negatively charged coal surface and promoted the uptake of molybdenum oxyanions. This study has shown that the surface properties of coal can be modified for effective catalyst loading onto coal. The influence of the catalyst addition technique on catalyst dispersion and on coal liquefaction activities will be discussed in subsequent papers.

REFERENCES

(1) Abotsi, G. M. K., Bota, K. B., G. Saha, *Energy &Fuels* , 1992, 6, 779.
(2) Abotsi, G. M. K., Bota, K. B., G. Saha, *Fuel Sc. Tech. Intl.*, 1993, 11, 327.
(3) Bota, K. B., Abotsi, G. M. K., L. L. Sims, *Energy & Fuels* , 1994, 8, 937.
(4) Honig, D. S., Kustin, K., *Inorg. Chem.*, 1972, 11, 65.
(5) Rosen, M. J., "Surfactants and Interfacial Phenomena," 2nd Edn., John Wiley, 1989, p. 108.

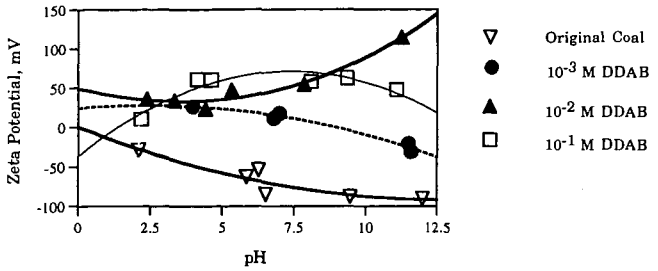

Figure 1. Zeta Potential of DECS-24 Coal as a Function of DDAB Concentration and pH.

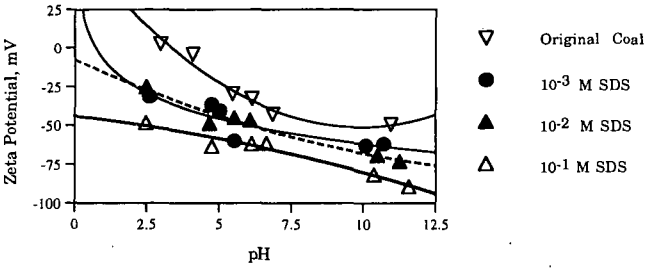

Figure 2. Zeta Potential of the Coal as a Function of SDS Concentration and pH.

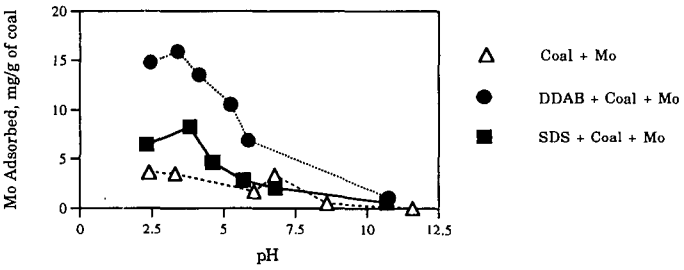

Figure 3. Effect of Surfactant and pH on Molybdenum Adsorption by the Coal.

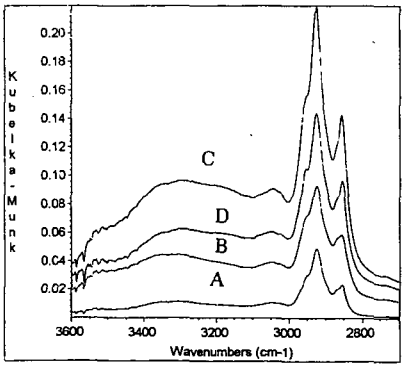

Figure 4. FTIR spectra of the Original and the Surfactant-Treated Coals after Molybdenum Adsorption.
A: Coal + Mo; B: Original Coal only;
C: Coal + DDAB + Mo; D: Coal + SDS + Mo

USE OF DISPERSED CATALYSTS FOR DIRECT COAL LIQUEFACTION

A. S. Hirschon, S. Kim, and R. B. Wilson
SRI International, Menlo Park, CA 94025

and O. Ghaly
Bechtel Corporation, San Francisco, CA 94115

Keywords: Coal liquefaction, syngas, dispersed catalysts

INTRODUCTION

With dwindling supplies of petroleum products, efforts to utilize alternative energy feedstocks such as coal, is essential. Several areas in coal conversion technology have been identified that, if improved, could make coal liquefaction more cost competitive with petroleum.[1-4] The objectives of this project are to address possible improvements in the economics by utilizing low-rank coals, new precursors to dispersed catalysts, and processing variations such as using syngas atmospheres. The purpose of the dispersed catalysts is to better control retrogressive reactions and avoid char formation, while the purpose of the carbon monoxide atmosphere is to improve the economics by simplifying or totally eliminating a separate water-gas-shift step, and perhaps help remove oxygen in the product slate. These possible improvements are being examined and evaluated for potential use in a 2-stage liquefaction process with the goal of converting coal to distillable liquids at a cost competitive to petroleum of $25/bbl.

To evaluate our catalysts and process conditions, we used three types of laboratory-scale operations. In the first operation, we compared the reaction chemistry of various ranks of coals and catalysts in synthetic solvents such as hexadecane. This method allowed us to better compare our catalysts without the complications of solvent initiated chemistry. Once the catalysts were tested in this manner, they were examined for the conversions of a Black Thunder subbituminous coal using a recycle vehicle derived from the same coal as the solvent. Finally, we upgraded selected first-stage conversion products using a conventional hydrotreating catalyst to compare with recent results in two-stage coal liquefaction development. The results were evaluated for economic feasibility through a subcontract with Bechtel Corp.

EXPERIMENTAL

Catalysts: MolyVanL and iron oxide were received from the Wilsonville liquefaction facility. Pentacarbonyl iron was obtained from Aldrich, and the sulfur-containing iron cluster, $(\mu\text{-}S_2)Fe_2(CO)_6$, referred to as Fe_2S_2, was prepared by the method of Bogan et al.[5] Ammonium tetrathiomolybdate, (MoS_4), was obtained from Alfa Chemicals. The organometallic molybdenum catalyst was $(C_5H_5)_2Mo_2(\mu\text{-}SH)_2(\mu\text{-}S)_2$, referred to as Mo(OM), and was prepared by modification of the method of Dubois et al.[6] Nickel biscyclooctadiene [$Ni(COD)_2$] was obtained from Strem Inc. The hydrotreating catalyst Shell 317, obtained courtesy of Criterion Chemical Company, was presulfided under flowing 10% H_2S/H_2 before use.

Coal conversions in synthetic solvents: The model coal liquefaction experiments were conducted in a 300 mL Autoclave Engineers (AE) stirred reactor using 5.0 g of coal, 3 mmol of catalyst, 30 g of solvent, and 500 psig (cold) hydrogen. Reaction temperatures were held at either 400°C or 425°C for 20 minutes.

Black thunder studies: The screening experiments were conducted in a 300 mL autoclave with conversions being run at 425°C for 1 hour. Two autoclaves were used, referred to as autoclave A and B. The properties of autoclave B are such that for a high viscosity medium the conversions are lower in autoclave B than in A. The molybdenum based catalysts were first screened in autoclave B, and then selected reactions were repeated in autoclave A for comparison. The feedstock consisted of 2.5 parts by weight of recycle vehicle (50g) from Wilsonville run #263 to 1 part Black Thunder coal (20g). The total gas charge was up to 1000 psi (cold), and contained 3% H_2S. Carbon monoxide concentrations ranged from 20% to 50%. The simulated 2-stage liquefaction experiments were conducted in a 1 liter autoclave (AE) equipped with an injection port.

RESULTS AND DISCUSSION

Coal conversions using synthetic solvents: The comparison of model coal conversions using various catalysts for a hexadecane solvent system is presented in Table 1. The first three liquefaction experiments listed in Table 1, were conducted at 400°C. They include a noncatalyzed conversion, and conversions using molybdenum (MoS_4 and Mo(OM)) catalysts on an Illinois #6 coal. The fourth liquefaction experiment was conducted in tetralin, for comparison. Most of the conversions are quite low, as expected. For instance, in the absence of catalyst, the Illinois #6 coal was converted to 25% toluene-soluble material.

However, in the presence of the molybdenum catalysts, the conversions were greatly enhanced. For instance, the coal impregnated with $(NH_4)_2MoS_4$ gave a conversion of 41% toluene-soluble material, compared to 54% for the organometallic molybdenum-impregnation [Mo(OM)].

The remaining five experiments, conducted at 425°C using an Argonne lignite coal, compare various soluble iron-, molybdenum-, and nickel-based catalysts. Both the soluble organometallic iron complexes, $Fe(CO)_5$ and $Fe_2S_2(CO)_6$, are effective for the low rank coals, giving toluene-soluble conversions in the range of 40% (carbon-based yields). In previous work we found that these catalysts gave only nominal conversions for the Illinois #6 coal. X-ray analyses of the residues show that both catalysts were converted into pyrrhotite; however, the iron carbonyl also appeared to have been converted into elemental iron and other iron-based products. The Mo(OM) catalyzed reaction gave a higher conversion of 49% for this lignite, consistent with the better efficacy of Mo catalysts over Fe catalysts. Considering the organic chemistry of carboxylates, we also decided to investigate nickel as a potential catalyst for low rank coals. Since iron has a tendency to form dimers during decarboxylation of organic acids,[7,8] and nickel tends to promote decarboxylation without dimerization we speculated that nickel may be a better catalyst for oxygenated coals.[8] Consistent with this premise, the conversion using a Ni-based catalyst [$Ni(COD)_2$] shows that the lignite conversion increased from 40% with the iron catalyst to 60% with the nickel catalyst.

Black Thunder screening tests. The iron oxide catalysts were found to give poorer liquefaction yields than either the iron carbonyl and thiolato iron carbonyl. For instance, under hydrogen atmospheres, the iron oxides gave THF-soluble conversions in the range of 75% compared to over 90% for the iron carbonyl and thiolato iron carbonyl. However, in the presence of syngas, the iron carbonyl gave significantly lower yields than the thiolato iron carbonyl catalyst. Thus the latter catalyst appears to be superior for concepts that take advantage of the carbon monoxide chemistry, and no evidence of methanation was observed.

In a similar manner, Figure 1 illustrates the relative abilities of the MolyVanL and the thiolato Mo catalyst for conversions of the Black Thunder coal. In this case the conversions were conducted in Reactor B, which gives lower conversions than in Reactor A. The molybdenum content in all cases was 500 ppm of Mo. As seen in Figure 2, the MolyVanL gave relatively low conversions in Reactor B, but they were about the same (50%) whether in hydrogen atmospheres or syngas atmospheres. Thus the molybdenum catalyst appears to be able to use the carbon monoxide atmospheres. In the presence of the thiolato molybdenum catalyst, however, the conversion increased from 50% with the MolyVanL catalyst to over 75% conversion showing that the organometallic molybdenum catalyst is a far superior catalyst.

Table 2 compares the conversions using various catalysts in Reactor A. This table lists the best iron-catalyzed conversions described above as well as results from a series of MolyVanL conversions that were repeated in Reactor A for comparison. Prompted by the high conversions obtained for the $Ni(COD)_2$-catalyzed lignite conversions, we also conducted conversions on Black Thunder coal with this catalyst. We investigated both hydrogen atmospheres and syngas atmospheres containing 50% CO; these results are also included in Table 2. The last column of Table 2 lists the coal conversions based on conversions to THF-soluble materials and allows for contributions from the recycle solvent. The nickel-catalyzed reactions both under hydrogen and under 50% carbon monoxide gave very high conversions to THF-soluble material, with overall coal conversions in excess of 90%.

Simulated Two-Stage Conversion. A base-line run was also conducted to simulate a two-stage liquefaction conversion process. For this simulated conversion we used the MolyVanL catalyst in hydrogen atmospheres, and for comparison, in syngas atmospheres. We decided to use this catalyst as a baseline case for comparison with other work that has recently used this commercially available oil-soluble molybdenum compound. Note, however, we have identified other catalysts that are more active than MolyVanL. For instance our thiolato molybdenum catalyst was found to give coal conversions of over 25% greater than that found for the MolyVanL catalyst under mild coal conversion conditions (reactor B). Thus we expect a significant improvement using this catalyst over these base-line conditions.

Tables 3 and 4 list the distillation yields and elemental analyses for the hydrogen atmosphere and syngas atmosphere conversions, respectively. The conversions using the two systems were similar, with the syngas conversion giving a slightly lighter product (C5-650°F product contents were 47.6%) than the hydrogen conversion products (C5-650°F product contents were 40.8%). Furthermore, the amounts of the 1000°F+ fractions were similar, at 25% for the hydrogen conversion and 28% for the syngas conversion. Although there was not enough data using the batch results to obtain a complete economic analysis without a significant amount of approximations, we were able to deduce some effects of the use of syngas in the first stage of the coal conversion. For instance, we found that more value-added products are produced (mainly phenols), the CO shift requirement is reduced, and there is an added effort in the purification of hydrogen for the second stage reactor. The preliminary results suggest that the benefits of syngas in the first stage slightly outweigh the disadvantages.

FUTURE WORK

These preliminary results are encouraging, but economics need to be conducted on the best catalysts. Additionally, we have only used hydrogen in the second stage upgrading step, and thus not achieved the full economic benefits of syngas atmospheres. However, we feel that with proper catalyst and process development, our methods may significantly improve the final product quality and economics during coal liquefaction.

ACKNOWLEDGMENTS

The authors gratefully acknowledge the support of this work by the Department of Energy under Contract DE-AC22-91PC91039.

REFERENCES

1. S. N. Rao, H. D. Schindler, and G. V. McGurl, ACS Fuel Preprints, (1988) 33(3), 145-156.
2. J. M. Lee, O. L. Davies, T. E. Pinkston, and J. R. Gough, ACS Fuel Reprints, (1988) 33(3), 157-171.
3. D. Gray and G. Tomlinson, ACS Fuel Preprints (1988) 33(3), 172-179.
4. S. V. Gollakota, J. M. Lee, O. L. Davies, and T. E. Pinkston, DOE Direct Liquefaction Contractors' Review Meeting, Pittsburgh, Pennsylvania, October 1988.
5. Bogan, L. E. Jr., Lesch, D. A., and Rauchfuss, T. B., J. Organometallic Chem. (1983) 250, 429-438.
6. Cowens, B. A., Haltiwanger, R. C., and DuBois, M. R., Organometallics (1987) 6, 995-1004.
7. J. March, *Advanced Organic Chemistry*, second edition (McGraw-Hill Book Company, NY, 1977), p. 514.
8. S. Patai, "The Chemistry of Carboxylic Acids and Esters" (Interscience-Publishers, NY, 1969), pp. 362-371.

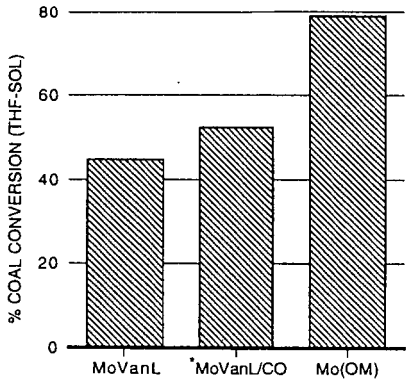

Figure 1. Effect of molybdenum catalysts for Black Thunder coal conversions in Reactor B.

Table 1

CONVERSION TO TOLUENE-SOLUBLE PRODUCTS IN HEXADECANE[a]

Catalyst	Coal	T(°C)	% TS[b]
None	Illinois # 6	400	25
MoS_4	Illinois #6	400	41
Mo(OM)	Illinois #6	400	54
Mo(OM)[c]	Illinois #6	400	61
None	Lignite	425	24
$Fe(CO)_5$	Lignite	425	41
Fe_2S_2	Lignite	425	39
Mo(OM)	Lignite	425	49
$Ni(COD)_2$	Lignite	425	60

[a]Reaction conducted in a 300-mL autoclave with 5 g coal, 3 mmol catalyst, 30 g solvent and 500 psi H_2 for 20 min at temperature.
[b]Yields calculated on daf basis for Illinois #6 coal and on carbon basis for the lignite.
[c]Reaction run in tetralin under identical conditions.

Table 2

DAF YIELDS OF USING VARIOUS METAL CATALYSTS IN REACTOR A[a]

Catalyst	Atmosphere[c]	THF Insol	Preasphaltene	Asphaltene	Oils	% Conv
Recycle	As received	8.7	7.5	60.9	23.2	–
Recycle	1000 psi H_2	6.7	4.4	51.3	29.7	–
$Fe(CO)_5$	1000 psi H_2	5.8	7.5	54.9	21.7	96.5
$Fe(CO)_5$	50% CO	14.9	18.7	34.8	25.4	64.7
$Fe_2S_2(CO)_6$	1000 psi H_2	7.6	11.8	37.5	24.4	90.2
$Fe_2S_2(CO)_6$	50% CO	10.7	11.2	35.4	23.9	79.4
MolyVanL[b]	1000 psi H_2	5.1	10.0	40.2	28.8	98.9
$Ni(COD)_2$[b]	1000 psi H_2	7.2	11.6	41.8	20.7	91.6
$Ni(COD)_2$[b]	50% CO	7.4	11.8	46.3	23.3	90.9

[a]Reaction conducted in a 300-mL autoclave for 1 hr with 20 g Black Thunder Wyodak coal, 2% iron metal in catalyst, 50 g recycle solvent and at 425°C. Atmosphere contained 3% H_2S in H_2.
[b]500 ppm metal added.
[c]Total pressure 1000 psi.

Table 3

ANALYSES OF DISTILLATION PRODUCTS FOR H_2/H_2 TWO-STAGE COAL CONVERSION[a]

Fraction °F	Wt. %	C	H	N	S	H/C
C5-350	4.3	83.63	16.37	b	b	2.332
350-650	21.6	86.24	10.13	0.68	0.17	1.398
650-850	14.9	87.91	9.91	0.64	0.30	1.344
850-1000	15.9	88.48	9.02	0.70	0.49	1.215
1000+	25.0	89.60[c]	6.12[c]	0.97[c]	ND	0.812
Ash	8.5					
H_2O	5.5					

[a]425°C, 30 minutes first-stage, 400°C, 30 minutes second-stage.
[b]Too low for accurate N and S determination.
[c]Calculated on an ash-free basis.

Table 4

ANALYSES OF DISTILLATION PRODUCTS FOR CO/H_2 1ST STAGE, H_2 2ND STAGE TWO-STAGE COAL CONVERSION[a]

Fraction °F	Wt %	C	H	N	S	H/C
C5-350	3.5	85.10	14.34	0.5	0.07	2.008
350-650	20.9	85.05	10.61	0.52	0.05	1.449
650-850	23.2	88.55	9.06	0.60	0.14	1.219
850-1000	8.9	89.87	7.92	0.71	0.24	1.049
1000+	28.3	68.33[a]	4.46[a]	0.87[a]	ND	0.778
Ash	9.6[b]					

[a]425°C, 30 minutes first-stage, 400°C, 30 minutes second-stage.
[b]Calculated on an ash-free basis.

DEVELOPMENT OF AN ALL-SLURRY LIQUEFACTION TEST FOR SCREENING DISPERSED CATALYSTS

Terry Rantell, Richard K. Anderson and Edwin N. Givens
University of Kentucky, Center for Applied Energy Research
3572 Iron Works Pike, Lexington, KY 40511-8433

Keywords: Coal liquefaction, catalysis, molybdenum

ABSTRACT

Exceptionally high distillate yields have previously been achieved in the direct liquefaction of subbituminous coal using dispersed catalysts. As part of a program sponsored by the U. S. Department of Energy, selected dispersed catalysts are being evaluated in continuous bench-scale runs. In consequence, a laboratory test has been developed to screen candidate dispersed catalysts and determine the optimum range of operating conditions to maximize coal conversion and distillate yield. The objectives of the test are to simulate operation in an all-slurry mode with coal conversion and product selectivity at least as good as that achieved in 2-stage operation at the Wilsonville Advanced Coal Liquefaction Facility. Tests are conducted in microautoclaves using pilot plant derived solvents and a Wyodak coal in the ratio of 1.85/1. An Fe-Mo catalyst contained in a Wilsonville process solvent has been used as a reference. The influence of residence time at 440 °C on 524 °C+ resid conversion has been determined and evaluations of various Mo formulations will be discussed.

INTRODUCTION

A DOE sponsored program is currently being conducted, in part, at the CAER to develop viable slurry catalysts for producing a distillate product equivalent to that obtained in a run made at the Wilsonville Advanced Coal Liquefaction R&D Facility in 1992. In the Wilsonville study, Runs 262E and 263J, Wyodak coal from the Black Thunder mine was used as feed. Unlike those runs, which were made in a 2-stage configuration in which the 1st-stage was operated as a thermal reactor, with a Mo-Fe dispersed catalyst, and the 2nd-stage as an ebullated bed reactor, with a Ni-Mo extrudate catalyst,[1] the objective tahe current work[2] is to develop a process involving an all-slurry reactor configuration using only dispersed catalyst. By eliminating the 2nd-stage catalyst, considerable cost reduction can be achieved if a dispersed catalyst can be found that can provide the same level of coal conversion and product selectivity that was obtained in the 2-stage Wilsonville operation.

Various methods for introducing dispersed catalyst precursors into the reaction system is being investigated in this project. One approach is to impregnate the catalytic metal precursors onto coal and activate these metals *in situ*. Such catalysts require that several interrelated process parameters be optimized in order to generate active catalysts. Although Mo is an active component in all these catalysts, the co-metals and their particular salt precursors must be defined as well as the concentration of metal on the coal substrate. In addition, limitations on the amount of the feed coal that must be impregnated, the conditions and reactants necessary to activate the catalyst as well as maintain its activity in the process, and the concentration of the catalyst in the recycle stream must be specified. The effect of each catalyst on product yields and quality must also be determined.

A catalyst screening test is being developed to facilitate the selection of catalysts and their concentration in the reaction system. The test simulates the liquefaction performance in an all-slurry liquefaction mode and expands upon the a catalyst screening test that was recently reported that simulates the first-stage reactor.[3] The active catalyst, which is contained in the ashy resid portion of the recycle solvent from Wilsonville Run 262E, has been used as a reference catalyst. The performance of various test catalysts will be compared to the performance of the Run 262E catalyst, which appears to be far more active than any others that have been tested in our laboratory. Distillate yield and coal conversion are used as a measure of catalyst activity.

EXPERIMENTAL

Wyodak coal, obtained from the Black Thunder Mine in Wright, Wyoming, was ground to -200 mesh, riffled and stored under nitrogen at 4 °C. Proximate and ultimate analyses of the coal are presented in Table 1. Samples of the various components of the recycle solvents from Runs 258 and 262 were obtained from the Advanced Coal Liquefaction R&D Facility at Wilsonville, AL. All of these materials were produced at Wilsonville when the plant was operating in a close-coupled configuration and feeding Black Thunder coal. Run 262E recycle solvent contains sizable concentrations of iron and molybdenum resulting from addition of iron oxide and Molyvan L to the feed slurries. This solvent had previously been described in detail.[4] Molyvan L is an organic-based Mo containing material supplied by R. I. Vanderbilt Co.

Based on previous Mössbauer studies on solids obtained from liquefaction of Black

Thunder coal in Run 262 solvent, the iron in the THF IOM was present in combination with sulfur as pyrrhotite. The molybdenum was presumed to be present as MoS_2. A sample of THF insoluble material in the Run 262 563 °C+ ashy resid was isolated by exhaustively extracting with THF for 2 days.[5] Another sample of catalyst-enriched solids from Run 262 solvent was obtained by filtering a THF slurry at ambient temperature. In both cases the samples were dried overnight at 40 °C at 125 torr.

The catalyst screening tests are run in 50 mL microautoclaves in 2-3% H_2S in H_2 at a nominal total pressure at ambient temperature of 1350 psig which provides a hydrogen to feed coal ratio of about 18 wt % on dry coal. Total pressure at operating temperature is approximately 2500 psig. In the test, approximately 2.4 g dry coal is slurried in a solids-free solvent mixture comprising 33 wt % Run 258B heavy distillate (Wilsonville Vessel Number V-1074) and 67 wt % Run 258 ROSE deashed resid (Wilsonville Vessel Number V-130). Although the deashed resid is a bottoms cut from a 565 °C (1050 °F) vacuum tower, it still contains 8.3% 524 °C- (975 °F-) distillate and 16.0% of the 524-565 °C fraction, as determined in our laboratory. The various distillate cuts and feed coal concentrations in the starting mix are shown in Table 2. The ash contents of the deashed resid and distillate materials were determined to be quite small, i.e., 0.13 wt% and 0.12 wt%, respectively.

Reactions were conducted in 50 cc microautoclaves pressurized with hydrogen at ambient temperature. After pressurization, the reactor was placed in a fluidized sandbath set at the specified temperature and continuously agitated at a rate of 300 cycles per minute. At the end of the reaction period, the reactor was quenched to ambient temperature and the gaseous products collected and analyzed by gas chromatography. The solid and liquid products were scraped from the reactor using THF and the mixture was extracted in a Soxhlet apparatus for 18 hours. The THF insoluble material, which included IOM and ash, was dried (80 °C at 125 torr) and weighed. The THF solubles were concentrated by removing excess THF in a rotary evaporator and subjected to vacuum distillation using a modified D-1160 procedure, which is described elsewhere.[6] The methods for calculating material balances are included in the previous descriptions. In the following discussion, coal conversion equals 100 minus the yield of THF-insoluble organic material (IOM). Resid conversions are calculated as shown below, while coal conversion is derived from the net yield of IOM.

$$Resid\ Conv = 100\ [\ 1 - \frac{[IOM + 524°C^{+}\ Resid\ (maf)]_{Products}}{[Coal\ (maf) + IOM + 524°C^{+}\ Resid\ (maf)]_{Feed}}]$$

RESULTS AND DISCUSSION

The objective of our program is to identify catalysts that warrant further testing in a continuous recycle bench-scale operation. The criteria for a screening test are to simulate, as closely as possible, actual process conditions that would exist under recycle operation. For that reason, solvents were used in the test that were actually generated from Wyodak Black Thunder coal in the Wilsonville plant. In our previous laboratory studies, the Mo catalyst contained in the Run 262E recycle solvent was found to be the most active of any catalyst we had tested. In our microautoclave reactors, we reported that the 565 °C+ (1050 °F+) resid conversion of Black Thunder Wyodak coal after 22 min at 440 °C was 32%.[5] This essentially replicated the conversion observed in the 1st-stage reactor in both Wilsonville Runs 262E and 263J, which were essentially identical. The purpose for the catalyst screening test that is being developed in this program is to identify catalysts that can match the resid conversion that was obtained after the 2nd-stage of the Wilsonville operation with the Mo catalyst contained in the Run 262E recycle solvent.

Because of the complications associated with solids contained in the recycle solvents used in the Wilsonville plant, our intention was to devise a reformulated solids-free solvent containing a significant residual fraction but free of either mineral matter or accumulated catalysts. A solvent composition was chosen comprising a 565 °C- (1050 °F-) distillate material and a 565 °C+ (1050 °F+) solids-free resid, both taken from Wilsonville Run 258. The resid component was a solids-free 565 °C+ (1050 °F+) material produced by the ROSE-SR unit, which made up only about 7% of the total plant recycle solvent. The other major component in the Wilsonville recycle solvent was an ashy resid recycled from the vacuum distillation tower. In the screening test, the distillate and deashed resid components are blended with feed coal in a way to give a resid/maf coal ratio of approximately 1.1, which is similar to that contained in the feed in Run 263J. The composition of the reaction mixture in the catalyst screening test, as determined from distillations on the feed solvent in our laboratory, is shown in Table 2.

The reaction temperature of the catalyst screening test of 440 °C is the same as used in the Phase I test, however, the sulfiding agent was changed from dimethyl disulfide to 2% H_2S in H_2

with an initial starting pressure of 1350 psig. This provides a hydrogen to feed coal ratio of about 18 wt % on dry coal. Total pressure at operating temperature was approximately 2500 psig. The reaction time was selected from a series of experiments that were used to determine the time necessary to provide the same 565 °C+ resid conversion of Wyodak coal as observed in Run 263J. The microautoclave runs in our laboratory were made by adding 30 wt% dry Wyodak BT coal to Run 262E Mo-containing solvent, at a Mo concentration of 300 ppm on dry coal. The 565 °C+ resid conversion after 22, 30, 60 and 90 min were determined to be 32, 44, 47 and 52%, respectively (see Table 3). The source of the 22 min data was above. The corresponding resid conversions on an maf coal basis in these tests were quite high indicating a conversion even higher than observed at Wilsonville. In a plot of log unconverted resid versus reaction time, the 60 and 90 min conversions depart significantly from a plot of the 22 and 30 min reaction results, as shown in Figure 1. Since the resid conversions observed in Run 263J at Wilsonville was about 38%, a 30 min residence time was chosen for the test, since it most closely replicated those results.

To verify the validity of the catalyst test procedure for identifying active catalysts, samples of the catalyst dispersed in the Run 262E recycle solvent were isolated and evaluated in the screening test. This entailed isolating the catalyst-rich solids from the ashy resid portion of the solvent. One sample was prepared using a Soxhlet extraction technique with THF as the extracting solvent. Another sample was prepared by separating the solids from a THF-ashy resid slurry by filtration at ambient temperature. Both materials were dried overnight at 40 °C at 125 mm Hg. The filter cake obtained from the THF slurry was found to contain 740 mg Mo/kg, which provides a Mo/dry coal ratio of 300 ppmw in the test mixture.

In the catalyst screening test, both of these materials added to the reaction mixture at a Mo level of 300 ppmw on dry coal gave 524 °C+ resid conversions of 23-24%, which were significantly lower than the 40+% expected. Although the activities were less than expected, both samples showed activity that was well above the resid conversion activity of coal in the absence of any catalyst, i.e., 19%. By contrast, the coal conversion to THF solubles for the Mo-catalyst runs were much more in line with expected values, i.e., 99-101%.

As a check to determine if the unusually high 565 °C- distillate fraction in the Run 258 deashed resid or the composition of this fraction could be causing an unexpected result, a full range recycle solvent from Run 258, i.e., Wilsonville designation V-131B, was filtered and used as solvent in the screening test. Distillation indicated this material contained 50.2% 524 °C- distillate, 44.3% 524 °C+ resid, and 5.5% THF insolubles. The 524 °C+ resid conversion for Wyodak coal in this solvent, to which was added filter cake to a level of 300 ppm Mo on dry coal, was 26%, as shown in Table 4. This result is comparable to the result when using the deashed resid. For comparison, the 18% resid conversion in the absence of any added catalyst was essentially the same as when deashed resid was used as solvent.

Progress in developing this catalyst screening test will be discussed as well as possible reasons for this difference in activity for catalyst that was isolated from the reaction slurry versus catalyst that remained suspended in the solvent. In addition, results for various dispersed catalysts in this screening tests will be presented.

REFERENCES

1. Technical Progress Report, "Run 263 with Black Thunder Mine Subbituminous Coal and Dispersed Molybdenum Catalyst", DOE/PC/90033-23, Dec. 1992.
2. Final Technical Report for "Advanced Coal Liquefaction Concepts for PETC Generic Units", DOE/PC/91040-55, March 1995.
3. Anderson, R. K.; Derbyshire, F. J.; Givens, E. N. Prep. Pap.-Am. Chem. Soc., Div. Fuel Chem. 1994, 39(4), 1108.
4. Quarterly Technical Report for "Advanced Coal Liquefaction Concepts for PETC Generic Units", DOE/PC/91040-21, February 1993, p.74ff.
5. Anderson, R. K.; Lim, S. C.; Ni, H.; Derbyshire, F. J.; Givens, E. N. Fuel Process. Tech. 1995, 45, 109-122.
6. See Reference 1, p. 1-1.

Table 1. Black Thunder Coal Analysis					
Proximate Analysis	wt%	Ultimate Analysis	wt%	Sulfur Types	wt%
Moisture	21.2	Carbon	68.68	Total	0.39
Ash	5.15	Hydrogen	4.76	Pyritic	0.07
Volatile Matter	34.4	Nitrogen	1.21	Sulfate	0.09
Fixed Carbon	39.3	Sulfur	0.56	Organic	0.23
		Oxygen (diff)	18.25		
		Ash	6.54		
		Ash, SO_3-free	5.42		

Table 2. Composition of Feed in Catalyst Screening Test		
	Dry coal basis, wt %	
Cut point, °C	565	524
Dry coal	35	35
Distillate, wt% at cut point	21.5	26.6
Deashed Resid, wt% at cut point	43.5	38.4

Table 3. Liquefaction of Wyodak Black Thunder Coal in Wilsonville Run 262 Recycle Solvent 440 °C, 30 min, 1350 psig, 2 vol% H_2S/H_2			
Run No.	I	II	III
Feed Composition			
Coal, mf, wt%	30.0		
565 °C- Heavy Distillate, wt%	30.5		
565 °C+ Ashy Resid, wt%	39.5		
Added Catalyst, wt%	none		
Mo Concentration, mg/kg mf coal	380		
Reaction Results			
THF Coal Conv	106	106	107
Gas Yield	22	32	32
565 °C+ Resid Conv	44	47	52
565 °C+ Resid Conv (on maf coal)	92	98	110
H_2 consumption, wt%	4.6	5.4	5.9

Table 4. Catalyst Screening Test Results with Added Wilsonville Run 262E Mo-Containing Solids 440 °C, 30 min, 1350 psig, 2 vol% H_2S/H_2					
Run No.	IV	V	VI	VII	VIII
Source of Run 262E extract	none	filtered	Soxhlet	none	filtered
Feed Composition					
Run 262E extract, wt%	none	12.4	12.6	none	12.4
Mo Concentration, mg/kg mf coal	none	295	300	none	300
Coal, mf, wt%	35	31	31	35	30
Run 258 565 °C- Distillate, wt%	21.5	18.8	22.4	-	-
Run 258 565 °C+ Deashed Resid, wt%	43.6	38.1	35.3	-	-
Run 258 Filtered Recycle Solvent, wt%	-	-	-	65	57.6
Reaction Results					
THF Coal Conv	68	99	101	77	111
Gas Yield	21	21	19	20	20
524 °C+ Resid Conv	19	23	24	18	26
524 °C+ Resid Conv (on maf coal)	41	57	59	35	58
H_2 consumption, wt%	1.7	4.2	3.9	1.9	4.3

Figure 1

Resid Conversion in 262E Recycle Solvent

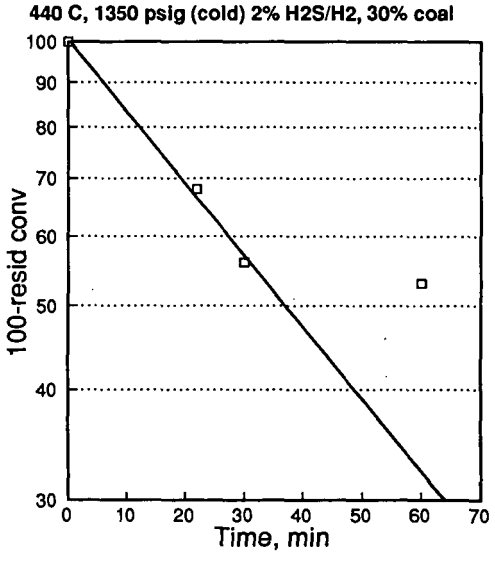

EVALUATION OF FINE-PARTICLE SIZE CATALYSTS USING BITUMINOUS AND SUBBITUMINOUS COALS

Frances V. Stohl, Kathleen V. Diegert, David C. Goodnow
Process Research Dept. 6212
Sandia National Laboratories
P.O. Box 5800
Albuquerque, NM 87185-0709

Keywords: Coal liquefaction; Fine-particle size catalysts; Catalyst test procedures

ABSTRACT

The objectives of Sandia's fine-particle size catalyst testing project are to evaluate and compare the activities of fine-particle size catalysts being developed in DOE/PETC's Advanced Research Coal Liquefaction Program by using Sandia's standard coal liquefaction test procedures. The first test procedure uses bituminous coal (DECS-17 Blind Canyon coal), phenanthrene as the reaction solvent, and a factorial experimental design that is used to evaluate catalysts over ranges of temperature, time, and catalyst loading. The best catalyst evaluated to date is West Virginia University's iron catalyst that was impregnated onto the coal. Current work is aimed at developing a standard test procedure using subbituminous Wyodak coal. This test is being developed using Pacific Northwest Laboratories' 6-line ferrihydrite catalyst and coal samples impregnated with either molybdenum or iron at Argonne National Laboratories. Results of testing catalysts with bituminous coal will be summarized and the development of the subbituminous coal test procedure will be presented.

INTRODUCTION

There are several potential advantages of using cheap, unsupported, fine-particle size (<40 nm) catalysts in direct coal liquefaction. Among these are improved coal/catalyst contact due to good dispersion[1] of the catalyst, and the potential for using low quantities of catalyst (<0.5% based on the weight of coal) because of their very high surface areas. These catalysts could be combined with the coal as either active catalysts or catalyst precursors that would be activated in situ. Research efforts to develop fine-particle size, unsupported catalysts for direct coal liquefaction[2,3] indicate that the use of these catalysts could result in significant process improvements, such as enhanced yields of desired products, less usage of supported catalyst, and possibly lower reaction severities. Realization of these improvements would result in decreased costs for coal liquefaction products.

The goal of Sandia's project is to evaluate and compare the activities/selectivities of fine-particle size catalysts being developed in the DOE/PETC Advanced Research (AR) Liquefaction Program by using standard coal liquefaction activity test procedures. Since bituminous and subbituminous coals have significantly different properties, it is feasible that catalysts may perform differently with these coal types. Because all previous testing has been done with the DECS-17 Blind Canyon bituminous coal, it is important to develop the capability of evaluating catalysts using a subbituminous coal. Wyodak coal from the Argonne Premium Coal Sample Program[4] was chosen for development of this test primarily because there has been significant research work done with Argonne's premium coals and because using existing well characterized samples eliminates the need to collect, prepare, and characterize another coal. The purpose of the current work is to develop a test using the Wyodak subbituminous coal.

EXPERIMENTAL SECTION

Materials. Two coals are being used in this project. DECS-17 Blind Canyon bituminous coal was obtained from The Penn State Coal Sample Bank[5]. It's a high volatile A bituminous coal with 3.74% moisture, 0.36% iron, 0.02% pyritic sulfur, and 7.34% mineral matter (on a dry basis). The particle size is -60 mesh. Subbituminous Wyodak coal was obtained from the Argonne Premium Coal Sample Program. It has 28.09% moisture, 0.17% dry pyritic sulfur, and 9.82% mineral matter (on a dry basis using the Parr formula). Phenanthrene is used as the reaction solvent. Elemental sulfur was added to the reactors to sulfide catalyst precursors.

Microautoclave Reactors. Testing is performed using batch microautoclaves made of type 316 stainless steel components. The total volume of a reactor is 43 cm^3 with a liquid capacity of 8 cm^3. The reactors are loaded with 1.67g coal and 3.34g phenanthrene. If the reaction is catalytic, the catalyst loading is either 0.5 wt% or 1.0 wt% of the amount of coal loaded into the reactor. The amount of sulfur addition (if needed) is specified by the catalyst developer. Reactors are charged to 800 psig H_2 (cold charge) and heated to reaction temperatures in fluidized-sand baths. Temperatures, pressures and times are recorded with a digital data acquisition system every 30 seconds during the course of the reactions. Following the heating period, the reactors are rapidly cooled to ambient temperature in a water bath and a gas sample is collected. The reaction data is analyzed to determine the actual reaction time and the averages and standard deviations for reaction temperature and pressure. Heat-up times and cooling times are also determined.

Product Workup Procedures. The reaction products are rinsed out of the reactors with tetrahydrofuran (THF). THF and heptane solvent solubilities are measured using a Millipore 142 mm diameter pressure filtration device with air pressurization and Duropore (0.45 micron) filter paper. The filter cakes are rinsed twice with THF or heptane as appropriate. After the filtrations are complete, the filter papers are dried under vacuum at 70°C, cooled to room temperature, and weighed to determine the insoluble portions. The THF soluble material is quantitatively sampled for gas chromatographic (GC) analysis, which is used to determine the reaction solvent recovery and final composition. THF is removed from the solubles by rotary evaporation prior to determining heptane conversion. The quantity of gases (CO, CO_2, CH_4, C_2H_6) produced in a reaction is calculated using the post-reaction vessel temperature and pressure with the ideal gas law and the mole percents in the gas sample as determined using a Carle GC and standard gas mixtures.

Factorial Experimental Design and Analysis. The factorial experimental design (Figure 1) evaluates the effects of three variables at two levels: temperature (350 and 400°C), time (20 and 60 minutes), and catalyst loading of either 0.0 wt% or 1.0 wt% of the amount of coal loaded into the reactor. With this full factorial experimental design, the experimental results are evaluated for all combinations of levels of the three variables so that 2^3 evaluations are required. Additional reactions are performed at the center point of this cubic design. An Analysis of Variance (ANOVA) is performed to estimate the effects of the experimental variables and to statistically test their significance. Replication of the experiments is used to estimate measurement error and to reduce its effect on the estimated effects of the variables. Models are constructed using the estimates of the effects of the variables to calculate the expected experimental results for specified sets of reaction conditions[6]. The controlled faetors used in the ANOVA are the measured average reaction temperature, measured reaction time, and the actual weight of catalyst used.

Catalyst. The catalyst chosen for development of the subbituminous coal test was a 6-line ferrihydrite catalyst precursor supplied by J. Linehan of Pacific Northwest National Laboratories (PNNL). This catalyst had been evaluated previously using Sandia's standard test procedure with Blind Canyon coal. It was the best catalyst in the form of a powder found to date. No pretreatment is required. Testing of this material used a 1:1 sulfur to catalyst precursor ratio on a weight basis. All reactions including thermal reactions had the same amount of added sulfur.

RESULTS AND DISCUSSION

Procedure for Comparing the Wyodak Coal with the DECS-17 Blind Canyon Coal

Testing of fine-particle size catalysts at Sandia has been based on a test using DECS-17 Blind Canyon coal, a bituminous coal. Since bituminous and subbituminous coals have significantly different properties, it is feasible that some catalysts may perform better with one coal type than with the other coal type. Therefore, it is important to have the capability of evaluating catalysts using a subbituminous coal. Wyodak coal from the Argonne Premium Coal Sample Program was chosen for development of this test primarily because there has been significant researeh work done with Argonne's premium coals and because using available samples eliminates the need to collect, prepare and store another coal.

One aspect of developing a test with Wyodak coal entails determining how results will be compared to those obtained with Blind Canyon coal. To do this comparison, we decided to evaluate Wyodak coal with PNL's 6-line ferrihydrite catalyst that had been evaluated previously at Sandia using the Blind Canyon coal. This is the best catalyst in the form of a powder evaluated to date at Sandia. The same factorial experimental design that is being used in the Blind Canyon coal test will be used with Wyodak coal. This decision was made because it was felt that the ranges of the three variables were broad cnough to also apply to the Wyodak coal. One of the many significant differences between Blind Canyon coal and Wyodak coal is the moisture content: Blind Canyon coal has 3.74% water and Wyodak has 28.09% water. To ensure that good comparisons could be made, the Wyodak coal was dried to about 6% water. This amount was chosen because it was close to the value for Blind Canyon coal and was also close to the water contents of several coal samples that had been impregnated with either Mo or Fe by Karl Vorres at Argonne National Laboratory. The Fe impregnated sample had 6.79% water and the Mo impregnated sample had 6.19% water. These impregnated coals will be evaluated after the subbituminous coal test is finalized. The dry sulfur contents of the Wyodak coal and the DECS-17 Blind Canyon coal are 0.63% and 0.44% respectively. The dry mineral matter is 10.01% for Wyodak coal (based on the modified Parr formula) and 7.49% for the DECS-17 coal.

Experimental Test Procedure

The testing used 1.67g Wyodak coal, 3.34g phenanthrene, and 1 wt % sulfur for all reactions. Catalyst loadings were either 0%, 0.5%, or 1.0 wt % based on thc experimental design. Sulfur was added to all reactions because previous studies with Blind Canyon coal showed that Fe in the mineral ankerite was converted to pyrrhotite during reaction thus yielding a catalytic effect. The impact of sulfur addition on Wyodak coal conversion will be quantified by comparing results to reactions of Wyodak coal without sulfur addition. Figure 1 shows the factorial experimental design used in the testing.

Testing Results for PNL's 6-Line Ferrihydrite Catalyst with Wyodak Coal

Results for THF conversion (%), heptane conversion (%), 9,10-dihydrophenanthrene (DHP (%)) in the reaction product, and gas yield (mol%) from this testing are shown in Figures 2-5. The values in

parentheses for each reaction condition are the average measured values obtained using PNL's catalyst with the Blind Canyon coal. The following discussion is based on these measured results. A statistical analysis of this data is currently being performed and will include a comparison of the Blind Canyon coal results and the Wyodak coal results.

Results for THF conversion (Figure 2) suggest that at low severity conditions (350°C, no catalyst), THF conversions are about 7.5% (absolute) lower for Blind Canyon coal. However, for all other conditions THF conversions are higher for Blind Canyon coal. At the most severe reaction condition (400°C, 60 minutes, 1% catalyst), Blind Canyon coal yielded 89.6 % conversion whereas Wyodak coal gave about 75.5%.

Results for heptane conversion (Figure 3) suggest that Wyodak coal may give higher heptane conversions for most if not all reaction conditions. Results at the lowest severity condition (350°C, 20 minutes, 0% catalyst) show a small negative conversion (-3.0%) for Blind Canyon coal, but an average conversion of 9.9% was obtained for Wyodak coal. Results at the highest severity condition (400°C, 60 minutes, 1% catalyst), gave an average 34.3% conversion for Wyodak coal but only 26.8% for Blind Canyon coal. Results at 400°C without catalyst show some overlap of results from the two coals. The statistical analysis will determine what differences are statistically significant.

Figure 4 shows the weight % of DHP (based on GC analyses of phenanthrene and DHP in the reaction product) after completion of the run. Results suggest that the Blind Canyon coal yields more DHP at all reaction conditions. At 400°C, 60 minutes, 1% catalyst, there is almost double the amount of DHP in the reaction product with Blind Canyon coal. The lower DHP in the product of the Wyodak reactions may be due to several causes. One possibility is that some of the hydrogen in the DHP is transferred to additional light reaction products as evidenced by higher heptane conversions with Wyodak coal. This could be due to Wyodak's lower coal rank. Another possibility is that Blind Canyon coal may yield higher DHP because some of the ankerite in the coal may get converted to pyrrhotite during the reaction and thus yield extra hydrogenation catalyst.

Figure 5 shows the total amount of gases (CO, CO_2, CH_4, C_2H_4) produced at each reaction condition. Results suggest that there are significantly more gases present with the Wyodak coal. For Blind Canyon coal, the total amount of gases ranges from about 0.30 to 1.86 mol% whereas for Wyodak coal the total amount ranges from about 1.90 to 4.35 mol%. In all cases, CO_2 is by far the biggest contributer to the gas yield, which was also observed with Blind Canyon coal.

CONCLUSIONS

Initial efforts towards developing a subbituminous coal test are aimed at comparing the reactivities of the Wyodak subbituminous coal and the Blind Canyon bituminous coal. Therefore, the same factorial experimental design was used with the Wyodak coal as was used previously with the Blind Canyon coal. In addition, PNL's 6-line ferrihydrite catalyst precursor was used in the development of the Wyodak coal test procedure because this catalyst is the best powder catalyst found to date in Sandia's tests with Blind Canyon coal. Results show that Blind Canyon coal yields higher DHP amounts in the reaction products and higher tetrahydrofuran (THF) conversions at the higher severity conditions. Wyodak coal gives higher heptane conversions and higher gas yields for all conditions tested.

FUTURE WORK

Future work on developing the catalyst test with Wyodak coal will include performing the statistical analyses of the results obtained from the experiments with PNL's 6-line ferrihydrite catalyst. Results from this study with Wyodak coal will be statistically compared to previous results obtained from Blind Canyon coal with PNL's catalyst.

Acknowledgment: This work was supported by the U.S. Department of Energy at Sandia National Laboratories under contract DE-AC04-94-AL85000.

REFERENCES

1. Huffman, G. P.; Ganguly, B.; Zhao, J.; Rao, K. R. P. M.; Shah, N.; Feng, Z.; Huggins, F. E.; Taghiei, M. M.; Lu, F.; Wender, I.; Pradhan, V. R.; Tierney, J. W.; Seehra, M. S.; Ibrahim, M. M.; Shabtai, J.; Eyring, E. M., Energy Fuels 1993, 7, 285-296.
2. Pradhan, V. R.; Tierney, J. W.; Wender, I. Energy Fuels 1991, 5, 497-507.
3. Stohl, F. V.; Diegert, K. V. Energy & Fuels 1994, 8, 117-123.
4. Users Handbook for the Argonne Premium Coal Sample Program, K. S. Vorres, Argonne National Laboratory, Argonne, Illinois, October 1993.
5. The Department of Energy Coal Sample Bank, DECS-Series Data Printouts, The Pennsylvania State University, August 1995.
6. John, P. W. M., Statistical Design and Analyses of Experiments; MacMillan Co., 1971.

FIGURE 1.

FACTORIAL EXPERIMENTAL DESIGN

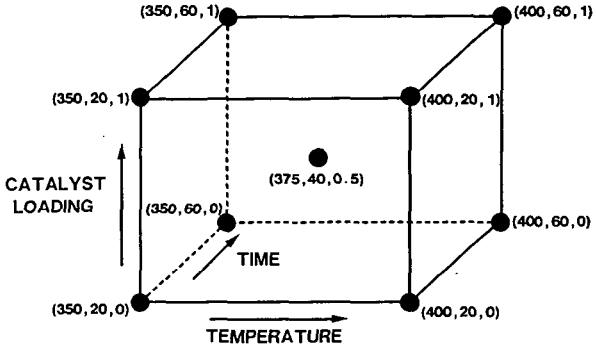

(TEMPERATURE = °C; TIME = MINUTES; CATALYST LOADING = WT % AR COAL)

FIGURE 2.

MEASURED THF CONVERSIONS
(PNL'S 6-LINE FERRIHYDRITE + WYODAK COAL)

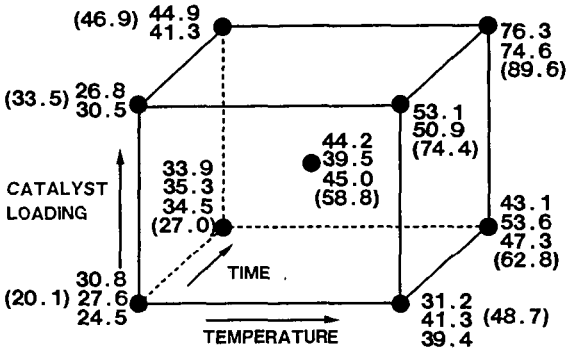

PARENTHESES = AVERAGE MEASURED VALUES FROM BLIND CANYON COAL

FIGURE 3.

MEASURED HEPTANE CONVERSIONS
(PNL'S 6-LINE FERRIHYDRITE + WYODAK COAL)

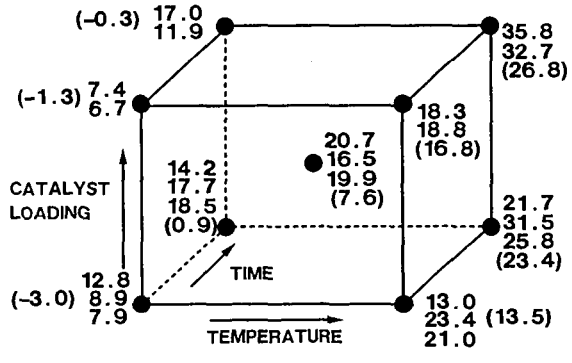

PARENTHESES = AVERAGE MEASURED VALUES FROM BLIND CANYON COAL

FIGURE 4.

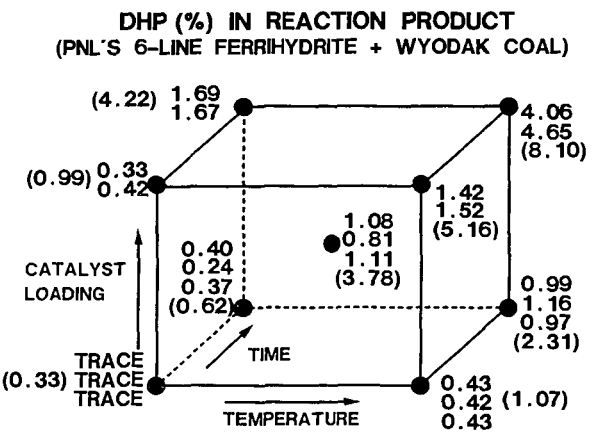

FIGURE 5.

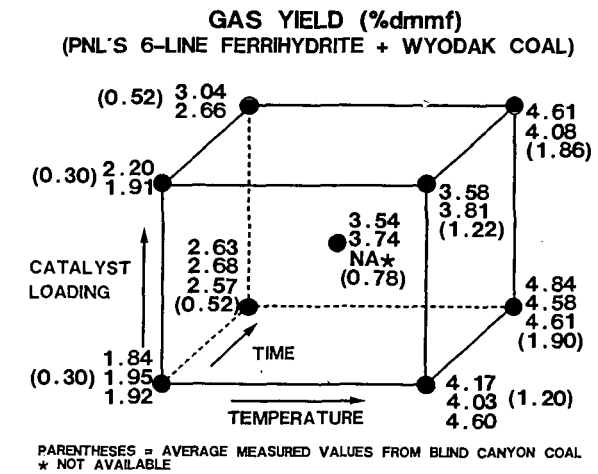

MÖSSBAUER INVESTIGATION OF MATERIALS USED IN SANDIA'S DCL CATALYST TESTING PROGRAM

K. R. P. M. Rao, Frank E. Huggins, G. P. Huffman
CFFLS, University of Kentucky, Lexington KY 40506-0043

and Frances V. Stohl
Sandia National Laboratories, Albuquerque, NM 87185

Keywords: Mössbauer spectroscopy, DCL catalysts, pyrrhotite

ABSTRACT

Mössbauer spectroscopy has been used to determine the iron-bearing phases in the coal, catalysts, and IOM products used and generated in the Direct Coal Liquefaction (DCL) catalyst testing program at Sandia National Laboratories, New Mexico. DCL experiments were conducted with a Blind Canyon, Utah, coal both thermally and with three different iron-based catalysts: (i) a sulfated hematite catalyst (Fe_2O_3/SO_4^{2-}), (ii) a 6-line ferrihydrite catalyst, and (iii) iron-oxide impregnated directly into coal. The catalysts were added to the coal at both a 0.5 and a 1.0 wt% level and sufficient sulfur was added to ensure complete sulfidation of the iron. The Mössbauer spectrum of the Blind Canyon coal revealed that the major iron-bearing mineral present was ankerite, $Ca(Fe,Mg)(CO_3)_2$, which converts first to γ-Fe (austenitic iron) before undergoing partial sulfidation to pyrrhotite in the thermal runs. The percentages of pyrrhotite formed in the catalytic runs were higher than those in the thermal runs indicating that sulfidation of the added iron occurs more rapidly than with the ankerite. Mössbauer data on the amount of pyrrhotite present does not correlate well with THF and heptane conversion percentages, indicating that other parameters like catalyst dispersion must also be considered.

INTRODUCTION

It is well recognized that iron-based materials represent the best option for development of a low-cost, disposable catalyst for direct coal liquefaction (DCL) [1]. As a result, much effort has been recently directed towards the development of iron-oxide-based catalysts for DCL by many groups [2]. However, owing to differences in DCL testing procedures at different laboratories, it has not always been possible to compare directly the conversion and cost effectiveness of different catalyst formulations. The DCL catalyst testing program at Sandia National Laboratories was designed to resolve such uncertainties by providing a facility for the DCL research community where the effectiveness of different catalysts could be directly compared [3]. Each catalyst would be subjected to the same matrix of tests on the same coal (Blind Canyon, UT, DECS-17) under identical conditions and the analysis of the DCL products would also be standardized.

In the current study, Mössbauer spectroscopy has been used to characterize the iron in various starting materials and products from the Sandia DCL program in order to provide additional baseline information for the program. Mössbauer investigations have been carried out on the following materials:

A. (1) Blind Canyon Coal (DECS-17)

(2) A sulfated hematite catalyst, Fe_2O_3/SO_4^{2-}, from the University of Pittsburgh

(3) A 6-line ferrihydrite catalyst from Pacific Northwest Laboratories

(4) An iron-oxide based catalyst impregnated into Blind Canyon Coal from West Virginia University

B. THF-insoluble residues generated in thermal liquefaction runs at 350°C for 20 min and at 400°C for 60 min.

C. THF-insoluble residues generated in liquefaction runs with the sulfated hematite catalyst at:

350°C	20 min	1.0 wt% catalyst loading and 1 wt% sulfur
375°C	40 min	0.5 wt% catalyst loading and 1 wt% sulfur
400°C	60 min	1.0 wt% catalyst loading and 1 wt% sulfur

D. THF-insoluble residues generated in liquefaction runs with the ferrihydrite catalyst at:

350°C	20 min	1.0 wt% catalyst loading and 1 wt% sulfur
375°C	40 min	0.5 wt% catalyst loading and 1 wt% sulfur
400°C	60 min	1.0 wt% catalyst loading and 1 wt% sulfur
400°C	60 min	1.0 wt% catalyst loading and 2 wt% sulfur

E. THF-insoluble residues generated in liquefaction runs with the iron-oxide catalyst impregnated in Blind Canyon Coal at:

350°C	20 min	1.0 wt% catalyst loading and 1 wt% sulfur
400°C	60 min	1.0 wt% catalyst loading and 1 wt% sulfur

EXPERIMENTAL

The thermal and catalytic DCL experiments were carried out under 800 psig H_2 in microreactors at Sandia National Laboratories with the above catalysts and sufficient sulfur to ensure complete sulfidation of the iron [3]. Oil and total conversions, defined as the percentages of the sample after DCL that were soluble in heptane and tetrahydrofuran, respectively, were also determined at Sandia [3]. Samples of the residues and starting materials were shipped to the University of Kentucky for Mössbauer analysis. Mössbauer analysis was carried out using a Halder, GmbH, Mössbauer drive operating in the symmetric saw-tooth mode. A calibration spectrum of metallic iron was obtained at the opposite end of the drive at the same time as the unknown spectrum was being acquired. Each spectrum was acquired over 512 channels representing a velocity range of between ±8 and ±12 mm/s using Canberra/Nuclear Data multichannel scaling units located in 286DX personal computer. Spectra were obtained from all samples at room temperature and from a few samples at cryogenic temperatures as low as 13 K. Analysis of the Mössbauer spectra was conducted in the manner described previously [4,5]. Spectra were fit by means of a least-squares fitting routine as a combination of 6-line magnetic spectra, 2-line quadrupole doublets and single lorentzian-shaped peaks. Identification of the iron-bearing phases present in the samples was based solely on the values obtained for the isomer shift, quadrupole splitting, and magnetic hyperfine splitting of the individual components in the fits. The relative percentages of iron present in the different phases were derived from the areas under the individual components. Mössbauer results for the thermal and catalytic residues from the DCL tests are summarized in Tables I - III for the three different catalysts.

RESULTS AND DISCUSSION

The Mössbauer spectrum of Blind Canyon (DECS-17) coal is shown as Figure 1. The spectrum consists of one major doublet from which the principal iron-bearing mineral in the coal is identified as ankerite, $Ca(Fe,Mg)(CO_3)_2$. It has the same isomer shift (1.23±0.01 mm/s), but a significantly smaller quadrupole splitting (1.67±0.02 mm/s) than that reported [4] for siderite (1.80±0.02 mm/s). Although no positive evidence was established for the presence of pyrite in this coal, it is possible that as much as 5% of the iron could be present as FeS_2. This minor contribution cannot be resolved owing to the overlap of the low-velocity ankerite peak with the pyrite peaks coupled with the relatively poor signal/noise ratio as a result of the low iron content of this particular coal.

Essentially the same results were obtained with the three thermal runs at the two different temperatures. In the thermal residues prepared at 350°C, ankerite, and austenitic or γ-iron were observed; at 400°C (q.v. Figure 2), significant pyrrhotite ($Fe_{1-x}S$), in addition to ankerite (with a smaller quadrupole splitting, 1.52 mm/s, than was found at 350°C) and γ-Fe, was also observed. These observations imply that ankerite in the coal reduces partially to γ-Fe, which then reacts with sulfur to form pyrrhotite.

The Mössbauer spectra of the sulfated hematite consisted of a magnetic component attributed to hematite and a poorly resolved doublet that represents the sulfated surface of the hematite particles and/or superparamagnetic (spm) iron oxide particles of small size (less than about 10 nm [5]). The other two catalysts exhibited only a broad doublet in their Mössbauer spectra; such spectra are consistent with ferrihydrite, either as a separate phase [6,7] or formed by impregnation directly on the coal [7].

The Mössbauer spectra of the catalytic residues (e.g. Figure 3) were similar to each other for the most part. However, the residues from the ferrihydrite and impregnated catalysts did show the persistence of a doublet attributed to unreacted spm iron oxides that was not apparent with the sulfated hematite catalyst. The relative amount of pyrrhotite

Table I

Mössbauer analysis of iron-bearing phases in
THF insolubles from thermal and catalytic reactions
with a sulfated hematite catalyst and Blind Canyon Coal

Sample	Gamma-Fe	Ankerite	Pyrrhotite
350, 20 min, thermal	14	86	
350, 20 min, 1 wt%	26	33	41
375, 40 min, 0.5 wt%	16	33	51
400, 60min, thermal	20	37	43
400, 60 min, 1 wt%	10	21	69

Table II

Mössbauer analysis of iron-bearing phases in
THF insolubles from thermal and catalytic reactions of
with a 6-line ferrihydrite catalyst and Blind Canyon Coal

Sample	γ-Fe	Ankerite	Pyrrhotite	FeOOH/Oxide
As received 6-line ferrihydrite				100 FeOOH
350, 20 min, thermal	13	87		
350, 20 min, 1 wt%	6	28	42	24
375, 40 min, 0.5 wt%	8	25	57	10
400, 60 min, thermal	18	36	46	
400, 60 min, 1 wt%	1	13	68	18
400, 60 min, 1 wt% 2 wt% added sulfur	10	18	67	5

Table III

Mössbauer analysis of iron-bearing phases in
THF insolubles from thermal and catalytic reactions
with iron-oxide impregnated Blind Canyon Coal

Sample	γ-Fe	Ankerite	Pyrrhotite	FeOOH/Oxide
Coal impregnated with iron and sulfur compounds		31		69
350, 20 min, thermal	23	77		
350, 20 min, 1 wt% catalyst in coal	25	25	31	19
400, 60 min, thermal	15	36	49	
400, 60 min, 1 wt% catalyst in coal	5	16	51	28

formation in all three catalytic runs was greater than that in the corresponding thermal run at the same temperature indicating that the iron-based catalyst undergoes sulfidation much more rapidly than the ankerite in the original coal.

The THF conversions for the catalytic runs at 400°C, 60 min, with 1% loading for the sulfated hematite, 6-line ferrihydrite, and impregnated iron-oxide catalysts were 82.3%, 89.4% and 93.2%, respectively. These values do not show a direct correlation with %Fe as pyrrhotite listed in Tables I - III, but do correlate with %Fe remaining as spm oxide.

CONCLUSIONS

Iron in Blind Canyon coal (DECS-17) is present principally in the form of ankerite, $Ca(Fe,Mg)(CO_3)_2$, which is converted during thermal tests, first to γ-Fe and then to pyrrhotite. The conversion is not complete even after 60 mins at 400°C. In contrast, sulfidation of the catalyst materials is more rapid and is essentially complete in the case of the sulfated hematite catalyst at 350°C and nearly so in the case of the 6-line ferrihydrite and impregnated iron-oxide catalysts. With the latter two catalyst materials, a small fraction (up to 25%) of the catalyst persists as spm iron-oxide even to the most severe conditions employed for DCL (400°C, 60 min). It is this fraction of iron present as remnant spm iron-oxide, and not as pyrrhotite, that appears to show a direct correlation with the total DCL conversion percentages. This observation implies that there are significant differences in the ease of sulfidation of the iron-oxides to form pyrrhotite among the three catalysts that are also reflected in the dispersion and size of the pyrrhotite particles. It is these parameters that may have the most influence on the activity of the sulfided iron catalyst during the DCL process.

REFERENCES

1. Huffman, G. P., et al. *Energy & Fuels*, **1993**, *7(2)*, 285-296.
2. Proceedings of an ACS Division of Fuel Chemistry Symposium on Iron-based Catalysts for Coal Liquefaction, (M. Farcasiu, G. P. Huffman, and I. Wender, Eds.) *Energy & Fuels*, **1994**, *8(1)*, 2-123.
3. Stohl, F. V., and Diegert, K. V., *Energy & Fuels*, **1994**, *8(1)*, 117-123.
4. Huggins, F. E., and Huffman, G. P. in *Analytical Methods for Coal and Coal Products*, (C. Karr, Jr., Ed.), Volume III, Academic Press, NY, 1979, 371-423.
5. Ganguly, B., Huggins, F. E., Rao, K. R. P. M., and Huffman, G. P. *J. Catalysis*, **1993**, *142*, 552-560.
6. Schwertmann, U., and Cornell, R. M. *Iron Oxides in the Laboratory*, VCH, Weinheim, Germany, 1991.
7. Zhao., J., Feng, Z., Huggins, F. E., and Huffman, G. P. *Energy & Fuels*, **1996**, *10(1)*, 250-253.

ACKNOWLEDGEMENTS

This work was supported by the research program of the Consortium for Fossil Fuel Liquefaction Science (CFFLS) under contract with the U.S. Department of Energy and the Commonwealth of Kentucky. We also express our gratitude to Drs. Malvina Farcasiu and V.U.S. Rao of the Pittsburgh Energy Technology Center for their interest in and initiation of the work described here.

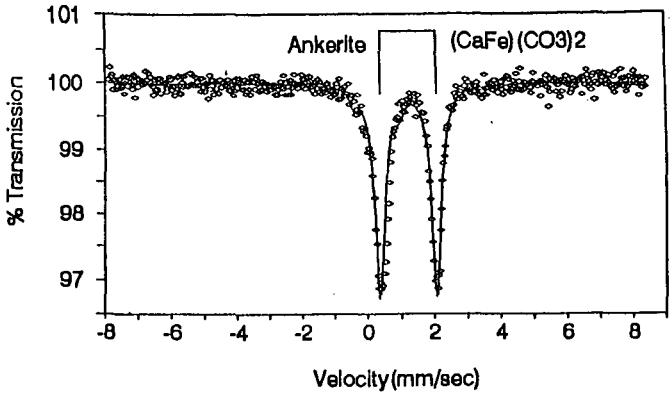

Fig.1 Mossbauer spectrum of Blind Canyon Coal

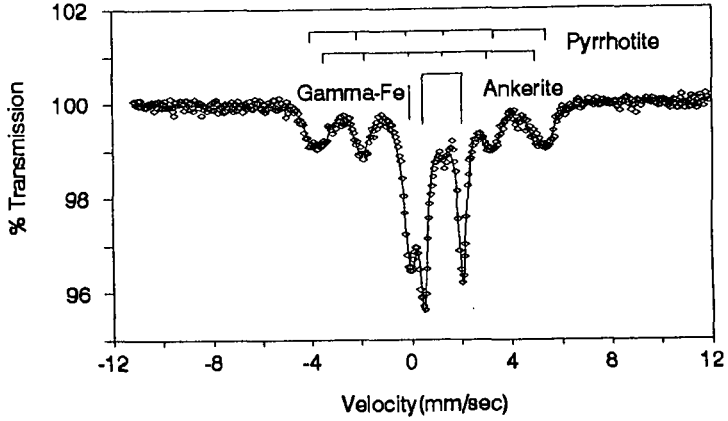

Fig.2 Mossbauer spectrum of THF insoluble from the run at 400C, 60min, without any catalyst (thermal)

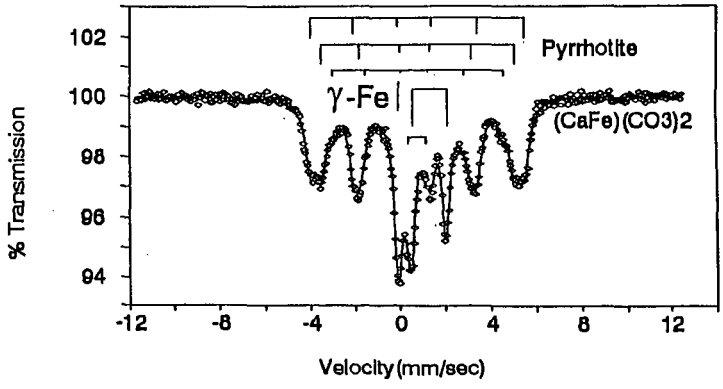

Fig.3 Mossbauer spectrum of THF insoluble from the run at 400C, 60min with Wender's 1% catalyst

SUPPORT CHEMISTRY, SURFACE AREA, AND PREPARATION EFFECTS ON SULFIDED NiMo CATALYST ACTIVITY

Timothy J. Gardner, Linda I. McLaughlin, and Ronald S. Sandoval
Sandia National Laboratories
Process Research Department, Mail Stop 0709
P.O. Box 5800
Albuquerque, NM 87185-0709

Keywords: oxide supports, hydrotreating catalysts, hydrous titanium oxide

INTRODUCTION

Hydrous Metal Oxides (HMOs) are chemically synthesized materials which contain a homogeneous distribution of ion exchangeable alkali cations that provide charge compensation to the metal-oxygen framework. In terms of the major types of inorganic ion exchangers defined by Clearfield,[1] these amorphous HMO materials are similar to both hydrous oxides and layered oxide ion exchangers (e.g., alkali metal titanates). For catalyst applications, the HMO material serves as an ion exchangeable support which facilitates the uniform incorporation of catalyst precursor species. Following catalyst precursor incorporation, an activation step is required to convert the catalyst precursor to the desired active phase.

Considerable process development activities at Sandia National Laboratories related to HMO materials have resulted in bulk hydrous titanium oxide (HTO)- and silica-doped hydrous titanium oxide (HTO:Si)-supported NiMo catalysts that are more active in model reactions which simulate direct coal liquefaction (e.g., pyrene hydrogenation) than commercial γ-Al_2O_3-supported NiMo catalysts.[2-7] However, a fundamental explanation does not exist for the enhanced activity of these novel catalyst materials; possible reasons include fundamental differences in support chemistry relative to commercial oxides, high surface area, or catalyst preparation effects (ion exchange vs. incipient wetness impregnation techniques). The goals of this paper are to identify the key factors which control sulfided NiMo catalyst activity, including those characteristics of HTO- and HTO:Si-supported NiMo catalysts which uniquely set them apart from conventional oxide supports.

EXPERIMENTAL PROCEDURE

Support chemistry effects were examined using both commercially-available oxide supports and HTO/HTO:Si supports. Commercial oxide supports studied included γ-Al_2O_3 (in extrudate form, 1/16 in. diameter) and various commercial forms of TiO_2. In order to fairly evaluate the effect of support chemistry between the commercial oxide and HTO/HTO:Si supports, it was necessary to normalize the Mo loadings per unit surface area. This approach has been previously used with success to differentiate support chemistry effects for hydrodesulfurization reactions.[8] Because it is well known that the surface area of oxide support materials can change significantly with processing (Mo loading, calcination, etc.), it was necessary to select a specific processing state to use as a reference point for catalyst support surface area. We used the support surface area after a standard calcination treatment in air at 500°C for 1 h as a reference point, since this would effectively represent the amount of support surface area available to disperse the molybdenum oxide phase which formed during the calcination procedure.

Table 1 shows the differences between the various supports evaluated in this study in terms of the method of preparation and their surface area, both as-received and after a standard calcination procedure. The surface area of the γ-Al_2O_3 extrudate is fairly typical of γ-Al_2O_3 catalyst supports, and was relatively unchanged after the calcination treatment. The titania supports exhibited different thermal stabilities depending on the preparation method, with the calcined surface area values correlating well with the crystallographic phase evolution of TiO_2. The Degussa P25 TiO_2, prepared by a high temperature flame hydrolysis procedure, showed only a slight decrease in surface area as a result of the calcination procedure. This moderate surface area material consisted of a mixture of anatase and rutile phases of TiO_2. The Tioxide TiO_2 material is prepared via a precipitation process using sulfate precursors followed by low temperature heat treatment to produce a high surface area anatase material. Further heat treatment of this material via calcination

resulted in significant surface area reduction and partial conversion of anatase to rutile. The HTO and HTO:Si supports were evaluated in acidified form following complete H^+/Na^+ exchange. In their as-prepared forms, these materials exhibit very high surface areas (~400 m^2/g). These acidified forms are generally representative of the final HTO or HTO:Si support material which remains following ion exchange (IE) processing. Calcination of these as-prepared materials results in significant surface area reduction. However, SiO_2 additions to HTO materials act to stabilize support surface area at high temperature ($\geq$ 500°C) without significantly altering ion exchange properties.[6,7,9] The improved thermal stability of the HTO:Si supports is due to the retardation of the anatase to rutile phase transformation by the SiO_2 dopant, which has been extensively documented in the literature.[10-13]

Table 1
Oxide Support Characteristics

Support Material	Preparation Technique	As-Received Surface Area (m^2/g)	Calcined Surface Area (m^2/g)*
Degussa P25 TiO_2	Flame Hydrolysis	52	47
Tioxide TiO_2	Precipitation	183	120
H^+/HTO	Sol-Gel + IE	417	63
H^+/HTO:Si	Sol-Gel + IE	390	184
γ-Al_2O_3 Extrudate	Precipitation + Extrusion	235	227

* Calcination procedure: 500°C/1h/air. Surface area was measured by the BET method.

HTO and HTO:Si ion exchangeable supports (Na:Ti and Si:Ti molar ratios = 0.5 and 0.2, respectively) were fabricated using the standard multiple step sol-gel chemistry procedure which has been described in detail elsewhere.[3,6,7,14] HTO- and HTO:Si-supported NiMo catalyst preparation was performed using a two step procedure featuring Mo anion ($[Mo_7O_{24}]^{-6}$) exchange/adsorption followed by incipient wetness impregnation using $Ni(NO_3)_2{\cdot}6H_2O$. For the commercial oxide-supported NiMo catalysts, only incipient wetness impregnation techniques were used; two separate impregnation steps were used, first with ammonium heptamolybdate ($(NH_4)_6Mo_7O_{24}{\cdot}4H_2O$), and next with nickel nitrate ($Ni(NO_3)_2{\cdot}6H_2O$) precursors. Supported Mo and NiMo catalysts with Mo loadings ranging from 0.6 to 25 Mo atoms/nm^2 support surface area were fabricated as part of this study. This range of Mo loadings corresponded to a wide overall range of Mo weight loadings, 0.1 to 25 wt.% (calcined basis), on the various supports. Regardless of the Mo loading level in the catalyst, a constant ratio of moles Ni/(moles Ni + moles Mo) = 0.35 was used to determine the Ni loading for each supported NiMo catalyst.

The final catalyst precursors were activated by first calcining in air at 500°C for 1 h and then sulfiding in 10% H_2S in H_2 at 420°C for 2 h. All TiO_2 (including HTO and HTO:Si)-supported catalysts were pelletized and granulated to -10/+20 mesh prior to activation, and all catalysts were ground and sieved to -200 mesh prior to testing. Catalyst activity was evaluated using two different model reactions representative of hydrotreating reactions: pyrene hydrogenation and dibenzothiophene hydrodesulfurization. For the pyrene hydrogenation tests, pyrene (0.1 g), hexadecane (1 g), and catalyst (0.010 g) were loaded into a batch microautoclave reactor and tested at 300°C under 500 psig H_2 for 10 min. For the dibenzothiophene hydrodesulfurization tests, dibenzothiophene (0.1 g), hexadecane (1 g), and catalyst (0.050 g) were loaded into a batch microautoclave reactor and tested at 350°C under 1200 psig H_2 for 10 min. Reversible first-order kinetics were used to model the pyrene hydrogenation test results,[15] while irreversible first-order kinetics were used to model the dibenzothiophene hydrodesulfurization test results.[16]

RESULTS AND DISCUSSION

Figure 1 summarizes the catalyst activity trends observed for the pyrene hydrogenation testing of the sulfided NiMo catalysts. This type of figure, plotting the intrinsic pyrene hydrogenation activity (rate per g total active metal [Ni+Mo]) vs. specific Mo loading (in Mo atoms/nm^2 calcined support surface area) is used to

normalize surface area differences among the various supports examined in this study. For NiMo/γ-Al_2O_3 catalysts, the intrinsic pyrene hydrogenation activity is stable at low specific Mo loadings, but decreases with increasing specific Mo loading. This behavior is in contrast to that observed for TiO_2-supported catalysts (including HTO and HTO:Si supports), where we find that a maximum in intrinsic pyrene hydrogenation activity is observed as specific Mo loading is increased. Very similar trends, including the location and value of the maximum in the intrinsic pyrene hydrogenation activity, were observed for all of the commercial TiO_2 materials evaluated: Degussa P25 TiO_2, Tioxide TiO_2, and a low surface area (10 m^2/g) rutile form of TiO_2. The characteristic behavior of sulfided NiMo catalysts supported on these commercial TiO_2 support materials is illustrated in Figure 1 by the data shown for the Degussa P25 TiO_2-supported NiMo catalysts.

However, as shown in Figure 1, the location of the maximum in the intrinsic pyrene hydrogenation activity is different for the commercial TiO_2 supports with respect to the HTO or HTO:Si supports. Since the data shown in Figure 1 has been normalized to remove support surface area effects, the differences in behavior for the HTO and HTO:Si supports must be attributable to other fundamental differences in support chemistry or catalyst preparation effects. The HTO-supported NiMo catalysts show a broad range of relatively high activity with the maximum in activity shifted to higher specific Mo loadings. This behavior shows a distinct advantage over typical commercial catalysts since it accommodates higher overall catalyst activities at high weight loading. The controlled addition of SiO_2 to the HTO support produces significant changes in this behavior. The peak intrinsic pyrene hydrogenation activity shifts to very low specific Mo loadings (lower than those observed for the commercial titanias) and is significantly increased in magnitude. This result indicates an important role of the SiO_2 dopant, which might be well dispersed on the surface of small anatase crystallites, therefore affecting the dispersion of the catalytic doped MoS_2 phase.

Similar trends to those shown in Figure 1 were also observed for Mo only catalysts, although intrinsic pyrene hydrogenation activities were consistently lower. It should be noted that due to the limited number of data points for some of the curves in Figure 1 (e.g., Degussa P25 TiO_2 and γ-Al_2O_3 supports), we can only speculate on the presence and/or location of the maximum in catalyst activity. Obviously, more data is necessary to make firm conclusions with respect to these trends.

Similar studies have been performed using the dibenzothiophene hydrodesulfurization model reaction. Very different trends are observed for this model compound reaction in terms of the intrinsic catalyst activity vs. specific Mo loading. Thus far, a valid comparison has been made only with the γ-Al_2O_3-, TiO_2-, and HTO-supported Mo catalysts. These results are shown in Figure 2. In one case (P25 TiO_2 support), both Mo- and NiMo-supported catalysts have been tested. As shown in Figure 2, and consistent with a vast quantity of published literature, the addition of Ni results in a significant promotional effect for the dibenzothiophene hydrodesulfurization reaction.[17,18] However, the trends for TiO_2-supported catalysts are very different for dibenzothiophene hydrodesulfurization compared to pyrene hydrogenation (see Figure 1). All TiO_2-supported catalysts examined to date (including HTO supports) exhibit very high intrinsic activity for dibenzothiophene hydrodesulfurization at low specific Mo loadings, with activity sharply decreasing as Mo loading is increased. In contrast to this behavior, γ-Al_2O_3-supported catalysts exhibit behavior very similar to that observed for pyrene hydrogenation. These trends observed for dibenzothiophene hydrodesulfurization with the TiO_2 (including HTO)- and γ-Al_2O_3-supported Mo catalysts are consistent with those observed previously for thiophene hydrodesulfurization.[8] The fact that the intrinsic activity for all of the TiO_2-supported catalysts is higher than that observed for the γ-Al_2O_3-supported catalysts is also consistent with previous work.[8]

These early results indicate that different types of catalysts, in terms of Mo loading, are optimum for hydrogenation vs. hydrodesulfurization reactions. This is consistent with evidence published in the literature suggesting that hydrogenation and hydrodesulfurization reactions take place on different types of active sites.[19,20] These results also show that the HTO-or HTO:Si-based supports may offer more significant advantages for hydrogenation rather than hydrodesulfurization applications.

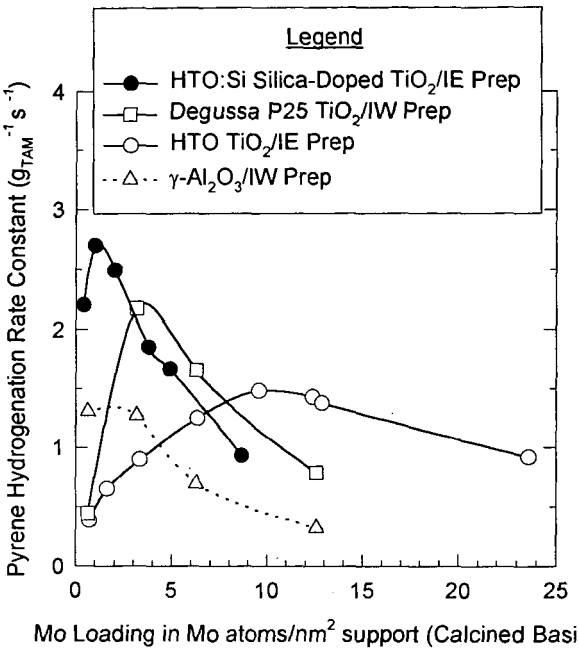

Figure 1. Intrinsic pyrene hydrogenation activity (rate per g total active metal) vs. specific Mo loading (in Mo/nm^2 support) for sulfided NiMo catalysts supported on various oxide supports. The acronyms IW and IE in the legend correspond to incipient wetness impregnation and ion exchange preparation techniques, respectively.

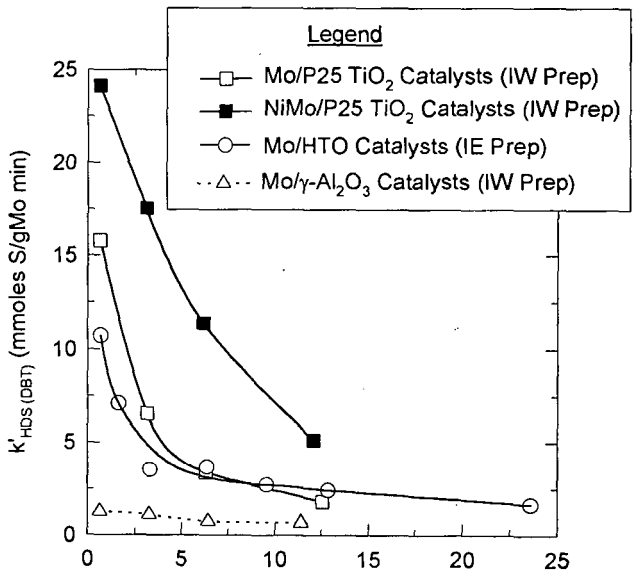

Figure 2. Intrinsic dibenzothiophene hydrodesulfurization activity results vs. specific Mo loading (in Mo atoms/nm^2 support) for selected sulfided Mo- and NiMo-based catalysts. Note that the acronyms shown in the legend were previously defined in the caption for Figure 1.

Additional work is necessary to further investigate the interesting behavior and potential benefits of the HTO- and HTO:Si-based supports. This work will include assessments of changes in MoS_2 dispersion as a function of Mo loading and support chemistry.

SUMMARY

This work has evaluated various catalyst support chemistries with a range of Mo loadings (normalized with respect to surface area) for both pyrene hydrogenation and dibenzothiophene hydrodesulfurization reactions. γ-Al_2O_3-supported Mo and NiMo catalysts were found to behave similarly with respect to both model reactions; intrinsic catalyst activity was relatively constant at low Mo loadings, but slightly decreased with increasing Mo loading. Significant differences were observed for the TiO_2 supports evaluated in this study, both with respect to the γ-Al_2O_3-supported catalyst results and for the different types of TiO_2 supports (including the HTO and HTO:Si materials). For pyrene hydrogenation, all TiO_2-supported catalysts showed a maximum in intrinsic catalyst activity, with the position of the maximum varying with changes in support chemistry and catalyst preparation procedures. In contrast to the pyrene hydrogenation results, all TiO_2-supported Mo catalysts showed a similar trend of significantly decreasing intrinsic catalyst activity with increasing Mo loading for the dibenzothiophene hydrodesulfurization model reaction. These results therefore indicate that HTO-based supports may offer more significant advantages for hydrogenation rather than hydrodesulfurization applications. Experiments are in progress to evaluate changes in MoS_2 dispersion as a function of support chemistry and Mo loading.

This work was performed at Sandia National Laboratories and was supported by the U.S. Department of Energy under contract DE-AC04-94AL85000.

REFERENCES

1. A. Clearfield, Ind. Eng. Chem. Res. **34**, 2865 (1995).
2. H. P. Stephens, R. G. Dosch, and F. V. Stohl, Ind. Eng. Chem. Res. Devel. **24**, 15 (1985).
3. H. P. Stephens and R. G. Dosch, Stud. Surf. Sci. Catal. **31**, 271 (1987).
4. S. E. Lott, T. J. Gardner, L. I. McLaughlin, and J. B. Oelfke, Submitted to Fuel.
5. S. E. Lott, T. J. Gardner, L. I. McLaughlin, and J. B. Oelfke, Prep. of Papers, Fuel Div., Amer. Chem. Soc. **39** 1073 (1994).
6. R. G. Dosch, H. P. Stephens, and F. V. Stohl, Sandia Report, SAND89-2400, Sandia National Laboratories, Albuquerque, NM, 1990.
7. R. G. Dosch and L. I. McLaughlin, Sandia Report, SAND92-0388, Sandia National Laboratories, Albuquerque, NM, 1992.
8. K. C. Pratt, J. V. Sanders, and V. Christov, J. Catal. **124**, 416 (1990).
9. T. J. Gardner and L. I. McLaughlin, Submitted to Mater. Res. Soc. Symp. Proc.
10. Y. Suyama and A. Kato, Yogyo-Kyokai-Shi **86**(3), 119 (1978).
11. C. U. I. Odenbrand, S. L. T. Andersson, L. A. H. Andersson, J. G. M. Brandin, and G. Busca, J. Catal. **125**, 541 (1990)
12. J. R. Sohn, H. J. Jang, M. Y. Park, E. H. Park, and S. E. Park, J. Mol. Catal. **93**, 149 (1994)
13. P. K. Doolin, S. Alerasool, D. J. Zalewski, and J. F. Hoffman, Catal. Lett. **25**, 209 (1994).
14. R. G. Dosch, H. P. Stephens, F. V. Stohl, B. C. Bunker, and C. H. F. Peden, Sandia Report, SAND89-2399, Sandia National Laboratories, Albuquerque, NM, 1990.
15. H. P. Stephens and R. J. Kottenstette, Prep. of Papers, Fuel Div., Amer. Chem. Soc. **30**, 345 (1985).
16. O. Weisser and S. Landa, Sulfide Catalysts, Their Properties and Applications, Pergamon Press, Oxford, 1973.
17. R. R. Chianelli, M. Daage, and M. J. Ledoux, Adv. Catal. **40**, 177 (1994).
18. M. J. Ledoux, S. Hantzer, and J. Guille, Bull. Soc. Chim. Belg. **96**(11-12), 855 (1987).
19. A. Stanislaus and B. H. Cooper, Catal. Rev.-Sci. Eng. **36**(1), 75 (1994).
20. M. Daage and R. R. Chianelli, J. Catal. **149**, 414 (1994).

HINDERED DIFFUSION OF COAL AND PETROLEUM ASPHALTENES IN A SUPPORTED HYDROTREATING CATALYST

Xiaofeng Yang and James A. Guin
Chemical Engineering Department, Auburn University, Auburn, AL 36849

Keywords: Diffusion, Mathematical Model, Asphaltenes

ABSTRACT

In this work, hindered diffusion of one coal and two petroleum asphaltenes was studied by adsorptive uptake in THF from a bath surrounding a commercial $NiMo/Al_2O_3$ catalyst. A mathematical model for the adsorption-diffusion of asphaltenes was developed. The model parameters were obtained by simulating the experimental data with the model solution. Several asphaltene fractions were defined via SEC (size exclusion chromatography), with the molecular weight of each fraction being determined by its elution characteristics using polystyrene standards. It was found that both the coal and petroleum asphaltenes have very broad molecular weight distributions; however, the molecular weights of the coal asphaltenes (50-1000) were much smaller than those of the two petroleum asphaltenes (300-10000 and 300-20000 respectively). The uptake rates for asphaltene fractions with different molecular weights were different, depending on their diffusion rates and adsorption capacities. Simulation results showed that even though the properties of coal and petroleum asphaltenes were quite different, the values of model parameters for the fractions of the three asphaltenes had the same trend; with increasing molecular weight of the fraction, the adsorption constant monotonically increases, and the effective diffusivity decreases. The experimental diffusion data of the three asphaltenes were well represented by similar mathematical models.

INTRODUCTION

Due to comparable sizes of reactant molecules and catalyst pores, hindered diffusion has been widely observed in the hydrotreatment of asphaltenes, heavy oils, coal derived liquids, and other macromolecular feeds. Direct measurements of asphaltene intrapore diffusion in porous catalysts are recent and very few in number. Baltus and Anderson (1983) studied hindered diffusion of petroleum asphaltenes through membranes, in which several fractions were defined by SEC according to their elution characteristics. Mieville et al. (1989) measured the diffusion of petroleum asphaltenes through porous materials by uptake experiments, in which the asphaltenes were treated as monodispersed and a linear adsorption isotherm was obtained.

In this work, hindered diffusion of coal and petroleum asphaltenes in THF was studied by adsorptive uptake experiments from a bath surrounding a commercial $NiMo/Al_2O_3$ catalyst. The asphaltenes were grouped into several fractions via SEC. An adsorption-diffusion model was developed for the uptake process. The objective of this work was to see if the diffusion uptake could be represented by a single mathematical model using reasonable parameter values.

EXPERIMENTAL

Materials. One coal and two petroleum asphaltenes, denoted as C-97500, P-AAK and P-AAG, respectively, were used in the diffusion study. The coal and petroleum asphaltenes, defined as THF(tetrahydrofuran) solubles and n-pentane insolubles, were extracted from a coal resid and petroleum asphalts, respectively. HPLC grade THF was used as solvent in the uptake experiments. Toluene and polystyrenes with narrow molecular weight distributions were used as calibration standards for analysis of asphaltenes on SEC. A commercial unimodal catalyst, Criterion 324, with an average pore diameter of 125 Å, was used in this study. Catalyst samples were crushed to -12+16 mesh size (-1.0+1.4 mm in diameter) and calcined at 673 K for 12 hours prior to use in uptake experiments.

Apparatus and Procedures. Diffusion experiments were performed in a magnetically stirred glass diffusion cell containing a screen wire basket for holding catalyst particles at 308 K. Catalysts were presaturated with THF before diffusion runs, during which the uptake of asphaltenes was monitored periodically by analyzing the concentration of asphaltenes in the bath solution using SEC.

SEC with a UV detector at 262 nm wavelength was used to analyze the concentration of asphaltenes in THF. Four μ-styragel columns, with nominal pore sizes of 1000, 1000, 500 and 500 Å respectively, were used in series for the SEC. A computer data acquisition system was employed to record the UV absorbance vs. elution time of the effluents. HPLC grade THF was used as mobile phase at 1 cm^3/min.

HINDERED DIFFUSION MODEL FOR ASPHALTENES

A mathematical model was utilized to describe the behavior of hindered diffusion of asphaltenes in porous catalyst particles. The asphaltenes are grouped into different fractions according to their molecular weights ascertained from SEC analysis. The porous catalyst particles were immersed in a well-stirred bath containing asphaltenes and solvent. The asphaltene molecules diffuse into the porous particle where they are adsorbed onto the solid catalyst surface. As a result of this diffusion-adsorption process, the concentration of asphaltenes in the surrounding bath is depleted. However, due to the difference in adsorption capacity and diffusion rate of each asphaltene fraction, the depletion rates for different asphaltene fractions will be different.

The hindered diffusion model developed here assumes negligible solute transport by surface diffusion, spherical catalyst particle geometry, uniform pore size distribution along the particle radius, negligible external fluid solid mass transfer resistance, and local adsorption equilibrium inside the particle pores (Yang and Guin, 1996a, 1996b). It is also assumed that the adsorption isotherm is linear for each fraction, and the properties of each fraction, e.g., molecular size, diffusivity, and adsorption capacity, are independent of every other fraction during the adsorption-diffusion process. With the above assumptions, the adsorption-diffusion mathematical model can be developed and solved analytically (Bird et al., 1960), with the dimensionless bath concentration of asphaltene fraction j being expressed as a function of dimensionless time by,

$$\theta_{bj} = \frac{B_j}{1+B_j} + 6B_j \sum_{k=1}^{\infty} \frac{\exp(-b_k^2 t_j^*)}{B_j^2 b_k^2 + 9(1+B_j)} \tag{1}$$

where, the b_k's are the non-zero roots of

$$\tan(b_k) = \frac{3b_k}{3+B_j b_k^2} \tag{2}$$

and

$$\theta_{bj} = \frac{C_{bj}}{C_{bj0}}, \qquad B_j = \frac{V_b}{V_p} \frac{1}{K_{pj}\epsilon + \rho_p K_j}, \qquad t_j^* = \frac{D_{ej}}{R^2} \frac{1}{K_{pj}\epsilon + \rho_b K_j} t \tag{3}$$

In the above equations, D_{ej} is the effective diffusivity expressed as,

$$D_{ej} = \frac{K_{pj} K_{rj} \epsilon}{\tau} D_{\infty j} \tag{4}$$

in which K_{pj} and K_{rj} factors are hindered diffusion parameters due to stearic and hydrodynamic effects, respectively, being estimated by,

$$K_{pj} = (1-\lambda_j)^2 \tag{5}$$

$$K_{rj} = 1 - 2.104\lambda_j + 2.089\lambda_j^3 - 0.948\lambda_j^5 \tag{6}$$

For a hydrodynamic diffusion solute, the molecular diffusivity $D_{\infty j}$ is related to the solute size by the Stokes-Einstein equation,

$$D_{\infty j} = \frac{kT}{6\pi\eta_0 r_{mj}} \tag{7}$$

For a typical adsorptive diffusion system, the values for most parameters in the model are known except those for K_j (or B_j) and D_{ej}. The values of these two parameters can be obtained by fitting the mathematical model to the experimental asphaltene uptake data.

RESULTS AND DISCUSSION

1. Asphaltene Molecular Weights

SEC analysis of asphaltenes requires the use of calibration standards to determine the average molecular weights of the fractions from elution volumes. Several investigators have used polystyrenes as calibration standards to obtain the equivalent molecular weight distributions of heavy oils and asphaltenes (Song et al., 1991; Baltus and Anderson, 1983; Sanchez et al., 1984; Dark and McGough, 1978). By comparing the molecular weights of prefractionated heavy oil fractions obtained from VPO

(vapor pressure osmometry) and polystyrene calibrated SEC, some studies showed that both measurements agreed well at least in some range (Brule, 1981; Bartle et al., 1984; Baltisberger et al., 1984;). However, others stated that there were differences between these two methods (Kiet et al., 1977; Wong and Gladstone, 1983). It might appear that the VPO method would give more accurate molecular weights; however, Nali and Manclossi (1995) stated that VPO molecular weight measurement failed when strong interactions among single molecules, e.g., highly aromatic compounds, were present. Mieville et al. (1989) showed that different asphaltenes with the same VPO molecular weights could elute at different volumes on SEC, inferring the absence of a universal relationship between SEC and VPO molecular weights for different asphaltenes. In the absence of any clear correlation between VPO and SEC molecular wights, we have used polystyrenes as SEC standards to calibrate the molecular weight distribution of our coal and petroleum asphaltenes.

Toluene and polystyrene standards with weight average molecular weights ranging from 92 to 14000 were first dissolved in THF. These solutions were analyzed via SEC, and the logarithm of molecular weights of the standards vs. elution volumes is shown in Figure 1, resulting a good linear fit being expressed as,

$$\log(M_W) = -0.125V_R + 7.261 \qquad (8)$$

Figure 2 shows SEC chromatograms of the coal and petroleum asphaltenes in THF. There are two x-axes in this figure, one is the elution volume, the other is the equivalent polystyrene/toluene molecular weight calculated from equation (8). It is observed that the equivalent molecular weights of the coal asphaltenes, 50-1000, are much smaller than those of the petroleum asphaltenes (300-20000 for P-AAK and 300-10000 for P-AAG). In the simulation of experimental asphaltene diffusion data, several fractions of the asphaltenes will be defined in terms of the equivalent eluted polystyrene/toluene molecular weights.

2. Effective Diffusivities and Adsorption Constants of Asphaltene Fractions

As seen in the model development section, to perform the model simulation for uptake of each asphaltene fraction, the effective diffusivity De_j and the adsorption parameter K_j are required. One method for determination of the molecular diffusivities of asphaltene fractions is to assume that they are the same as those of the polystyrene standards with same elution volumes. However, Baltus and Anderson (1983) showed that these two values are different, with the molecular diffusivities of polystyrenes being roughly two times of those of petroleum asphaltene fractions. Viewed in another way, if we know the size r_{mj} of each asphaltene fraction, the molecular diffusivity can be calculated from equation (7). Nortz et al. (1990) measured hydrodynamic properties of prefractionated heavy oils in THF and obtained the following relationship between the molecular radius in Å and VPO molecular weight,

$$r_m = 0.36\, M_W^{0.50} \qquad (9)$$

In equation (9) the molecule radius was calculated from the Stokes-Einstein equation using the molecular diffusivity experimentally determined by Taylor dispersion measurements. We have assumed that the above equation is applicable to our coal and petroleum asphaltenes, and that the molecular weights from VPO can be represented by those from SEC. With these assumptions, the molecular diffusivity of any asphaltene fraction eluted in SEC can be estimated through equation (7). The results for some asphaltene fractions are shown in Table 1. Comparison of the molecular weight ranges in Figure 2 with Table 1 shows that the effective diffusivities for the coal asphaltenes are in the range of 3-30 x 10^{-7}; while the ranges for the two petroleum asphaltenes P-AAK and P-AAG are 5-10000 x 10^{-10} and 6-1000 x 10^{-9} cm^2/s, respectively.

Due to the instability of asphaltenes in THF solvent, it is difficult to obtain the adsorption constants K_j from equilibrium experiments; however, this value can be ascertained by fitting the experimental diffusional uptake data with the model solution given by equation (1).

3. Simulation of Asphaltene Diffusion into Porous Catalyst

In our diffusion study, one coal and two petroleum asphaltenes were used as solutes. Figures 3, 4 and 5 (points) show the uptake data for the three asphaltenes in THF on Criterion 324 catalyst, respectively. It is seen from these figures that as diffusion time increases, the UV absorbances or concentrations of the coal asphaltenes fractions and most petroleum asphaltene fractions in the bath solution decrease. However, the rates of decrease for asphaltene fractions with different molecular weights are different, depending on their diffusion rates and adsorption capacities. It is interesting that for the two petroleum asphaltenes, as shown in Figures 4 and 5, respectively, some cross-overs of the SEC data were observed at higher molecular weights (approximately greater than 10000). In other words, the molecular weight distribution shifted to higher molecular weights during the uptake process, resulting in increasing bath concentrations for these fractions. A possible reason for this unusual phenomena might be the agglomeration of smaller molecules into larger ones. This aspect of the work needs further investigation.

For the numerical simulation of the experimental uptake results for the three asphaltenes, we first group the SEC data into several fractions, each with an elution volume of 0.5 cm^3. Some of the estimated effective diffusivities for these fractions are shown in Table 1. For each fraction, the dimensionless bath concentration θ_{bj} can be obtained by the ratio of the area under SEC curve at time t to that at time t=0. The adsorption constant K_j can be obtained by fitting the experimental (θ_{bj}, t) data with the model solution for each fraction. Figure 6 shows the values of adsorption constant K_j for different asphaltene fractions. It is seen that even though the properties of the three asphaltenes are quite different, as shown in Figure 2, the values of adsorption parameters for the fractions of these asphaltenes have the same trend; with increasing the molecular weight, the adsorption constant monotonically increases. It has also been observed (Takahashi et al., 1980; Dimino, 1994) that adsorption of polymers in porous materials increased as the molecular weights increased. Best fits of adsorption constant vs. molecular weight for the fractions of the three asphaltenes can be obtained with power regression from the data points in Figure 6, being expressed as,

$$\begin{aligned} C\text{-}97500: &\quad K_j = 3.352\, M_{wj}^{0.530} \\ P\text{-}AAK: &\quad K_j = 0.0239\, M_{wj}^{1.246} \\ P\text{-}AAG: &\quad K_j = 0.105\, M_{wj}^{1.151} \end{aligned} \tag{10}$$

It should be pointed out that for the two petroleum asphaltenes P-AAK and P-AAG in the above equations, we used fractions of molecular weights less than 10000. Beyond this value some of the experimental bath concentrations increased as discussed above and could not be fitted by the uptake model. In the simulation of the experimental uptake data with the model solution, adsorption constants K_j for fractions of molecular weights larger than 10000 were instead obtained by extrapolation of the above equations.

As long as the relationship between the adsorption constant K_j and the molecular weight is determined, the diffusion equation (1) can be solved for any asphaltene fraction eluted from SEC. The simulated model solution for the three asphaltenes are also shown in Figures 3, 4 and 5 (lines), respectively. It is observed that for the coal asphaltenes, the model fits experimental data quite well, as seen from Figure 3. For the two petroleum asphaltenes, the model fits the experimental data fairly well in smaller molecular weight regions, as shown in Figures 4 and 5 respectively; however, in the larger molecular weight regions, some departures were observed due to the cross-overs of the experimental uptake data, particularly at longer diffusion times.

CONCLUSION

Both the coal and petroleum asphaltenes used in this study have very broad molecular weight distributions, with the molecular weights of the coal asphaltenes (50-1000) being much smaller than those of the petroleum asphaltenes (300-20000 for P-AAK and 300-10000 for P-AAG). The coal asphaltene fractions have estimated effective diffusivities which span 1 order of magnitude, whereas these spans are more than 2 orders for the fractions of the two petroleum asphaltenes. The uptake rates for asphaltene fractions with different molecular weights are different, depending on their diffusion rates and adsorption capacities. Even though the properties of the asphaltenes used are quite different, the values of model parameters for the fractions of the three asphaltenes have the same trend; with increasing molecular weight of the fraction, the adsorption constant increases and the effective diffusivity decreases monotonically. The experimental diffusion data for the three asphaltenes can be represented fairly well in most molecular weight regions by the same mathematical model using appropriate parameter values.

Acknowledgment

This work was supported by the US Department of Energy under Grant No. DE-FG22-91PC1311.

Nomenclatures

B	dimensionless model constant
C_b	bath concentration
C_{b0}	initial bath concentration
D_m	molecular diffusivity, cm^2/s
D_e	effective diffusivity, cm^2/s
k	Boltzmann's constant, 1.38×10^{-6} erg/ °K
K	linear adsorption constant, cm^3-solution/g-catalyst
K_p	partition factor
K_r	restriction factor

M_w molecular weight, g/mol
r_m molecule radius, Å
R radius of catalyst particle, cm
t time, h
t^* dimensionless time
T temperature, °K
V_b bath volume, cm^3
V_p catalyst pore volume, cm^3
V_R elution volume on SEC
ϵ catalyst porosity
η_o solvent viscosity, g/cm-s
θ_b dimensionless concentration in bath
λ ratio of solute molecule diameter to catalyst pore diameter
ρ_p catalyst particle density, g/cm^3
τ catalyst tortuosity factor

Subscript

j jth asphaltene fraction defined on SEC

References

Baltisberger, R. J., S. E. Wagner, S. P. Rao, J. F. Schwan, and M. B. Jones, ACS Preprints, Fuel Chem, Div., 29(1), 186(1984).

Baltus, R. E., and J. L. Anderson, Chem. Eng. Sci., 38, 1959(1983).

Bartle, K. D., M. J. Mulligan, N. Taylor, T. G. Martin, and C. E. Snape, Fuel, 63, 1556(1984).

Bird, R. B., W. E. Stewart, and E. N. Lightfoot, "Transport Phenomena", John Wiley & Sons, Inc., p357, 1960.

Brule, B., ACS Preprints, 26(2), 28(1981).

Dark, W. A., and R. R. McGough, J Chrom. Science, 16, 610(1978).

Dimino, S. P., M. S. Thesis, Auburn University, 1994.

Kiet, H. H., L. Ph. Blanchard, and S. L. Malhotra, Separation Sci., 12(6), 607(1977).

Mieville, R. L., D. M. Trauth, and K. K. Robinson, ACS Preprints, Div. Petr. Chem., 34, 635(1989).

Nali, M., and A. Manclossi, Fuel Sci. And Technl. Int'l., 13(10), 1251(1995).

Nortz, R. L., R. E. Baltus, and P. Rahimi, Ind. Eng. Chem. Res., 29, 1968(1990).

Reid, R. C, J. M. Prausnitz, and B. E. Poling, Properties of Gases and Liquids, 4th ed., McGraw-Hill, New York, 599(1987).

Sanchez, V., E. Murgia, and J. A. Lubkowitz, Fuel, 63, 12(1984).

Sane, R. C., T. T. Tsotsis, I. A. Webster and V. S. Ravi-Kumar, Chem. Eng. Sci., 47, 2683(1992).

Song, C., T. Nihonmatsu, and M. Nomura, Ind. Eng. Chem. Res., 30, 1726(1991).

Takahashi, A., M. Kawaguchi, H. Hirota, and T. Kato, Macromolecules, 13, 884(1980).

Wong, J. L., and C. M. Gladstone, Fuel, 62, 871(1983).

Yang, X., and J. A. Guin, Applied Catalysis, in press, 1996a.

Yang, X., and J. A. Guin, Chem. Eng. Comm., in press, 1996b.

Table 1. Estimated effective diffusivities and other parameters at 35 °C

elution vol., cm^3	M_w[a] g/mol	r_m[b] Å	D_∞[c] cm^2/s	D_e[d] cm^2/s
23	24322.0	56.1	7.9E-07	1.3E-10
25	13677.3	42.1	1.1E-06	2.2E-09
27	7691.3	31.6	1.4E-06	1.3E-08
29	4325.1	23.7	1.9E-06	4.9E-08
31	2432.2	17.8	2.5E-06	1.3E-07
33	1367.7	13.3	3.3E-06	2.6E-07
35	769.1	10.0	4.5E-06	4.6E-07
37	432.5	7.5	5.9E-06	7.6E-07
39	243.2	5.6	7.9E-06	1.2E-06
41	136.8	4.2	1.1E-05	1.7E-06
43	76.9	3.2	1.4E-05	2.5E-06
45	43.3	2.4	1.9E-05	3.5E-06
47	24.3	1.8	2.5E-05	4.9E-06

a. Determined by equation (8).

b. Estimated from equation (9).

c. Calculated from equation (7) with THF viscosity of $4.42*10^{-3}$ g/cm-s (Reid et al., 1987).

d. Determined by equation (4) with ϵ=0.66 and τ=3.0.

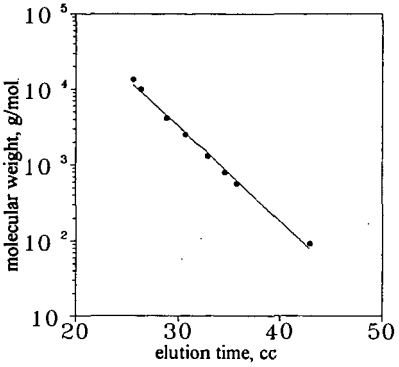

Figure 1. Calibration of SEC columns by toluene and polystyrenes.

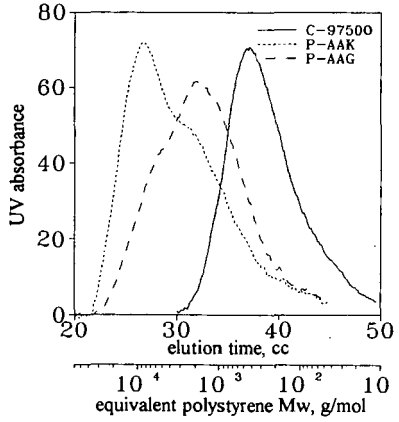

Figure 2. Comparison of SEC Mw distributions in THF for coal and petroleum asphaltenes.

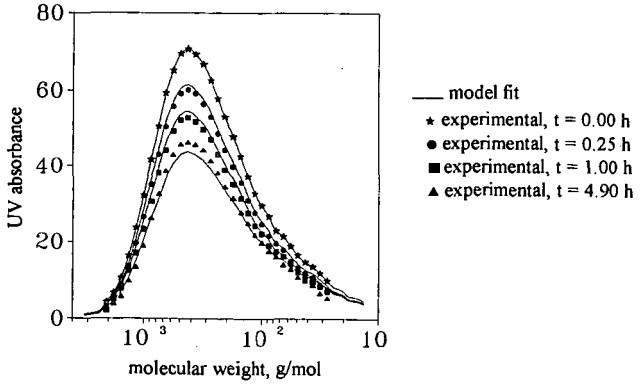

Figure 3. Simulation of experimental uptake data with math model for diffusion of coal asphaltenes in THF into Criterion 324 catalyst at 35 °C.

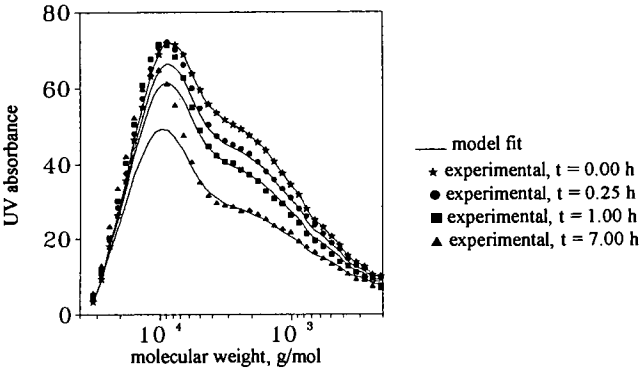

Figure 4. Simulation of experimental uptake data with math model for diffusion of P-AAK asphaltenes in THF into Criterion 324 catalyst at 35 °C.

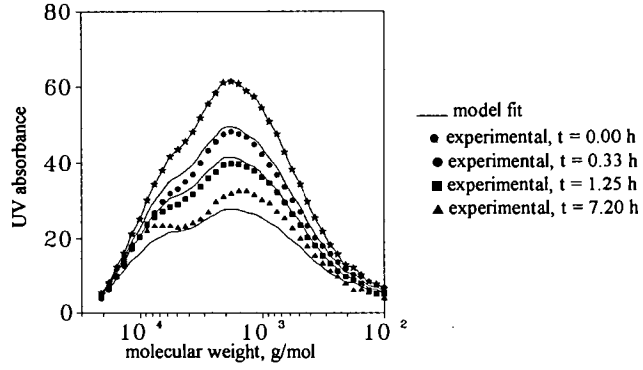

Figure 5. Simulation of experimental uptake data with math model for diffusion of P-AAG asphaltenes in THF into Criterion 324 catalyst at 35 °C.

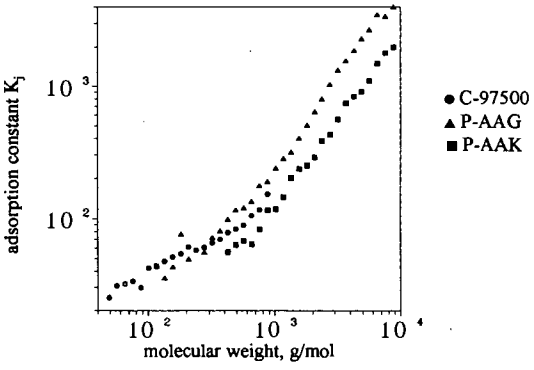

Figure 6. Relationship between molecular weight and adsorption constant for coal and petroleum asphaltenes.

Paper Presented before the ACS Division of Fuel Chemistry
212th American Chemical Society National Meeting, Orlando, FL, August 25-29, 1996

Shape-Selective Catalysis for Synthesis of High-Value Chemicals from Aromatics in Coal Liquids

Chunshan Song and Harold H. Schobert

Department of Material Science & Engineering and Laboratory for Hydrocarbon Process Chemistry
209 Academic Projects Building, Pennsylvania State University, University Park, PA 16802

Keywords: Catalysis, Chemicals, Aromatics, Coal, Coal Liquids, Anthracites, Graphites

INTRODUCTION

Liquids derived from coals contain numerous aromatic compounds. Many of the one- to four-ring aromatic and polar compounds can be converted into valuable chemicals. Economic analysis of the viability of liquefaction (and related conversion processes) may well produce a different result if some of the aromatics and phenolics are used for making high-value chemicals and some of the liquids for making high-quality fuels such as thermally stable aviation fuels. To make effective use of aromatics in coal liquids, we are studying shape-selective catalytic conversion of multi-ring compounds. The products of such reactions are intermediates for making value-added chemicals, monomers of advanced polymer materials, or components of advanced jet fuels (Song and Schobert, 1993, 1995).

Two broad strategic approaches can be used for making chemicals and materials from coals (Schobert, 1984, 1990, 1995). The first is the indirect approach: conversion of coals to liquids, followed by transformation of compounds in the liquids into value-added products. The second is direct conversion of coals to materials and chemicals. Both approaches are being explored in this laboratory (Song and Schobert, 1993, 1996).

In this paper, we will give an account of our recent work on 1) shape-selective catalysis which demonstrates that high-value chemicals can be obtained from aromatic compounds by catalytic conversion over certain zeolites; and 2) catalytic graphitization of anthracites, which reveals that using some metal compounds promotes graphitization at lower temperatures and may lead to a more efficient process for making graphites from coals.

POLYMER MATERIALS FROM AROMATIC MONOMERS

Recent years have witnessed significant growth of existing aromatic polymer materials and rapid development of advanced aromatic polymer materials such as engineering plastics, polyester fibers, polyimides, and liquid crystalline polymers (LCPs) (Beland, 1991, Song and Schobert, 1993). Consequently, there is greater demand for monomers based on aromatic and phenolic compounds. Such compounds can be made from coal-derived liquids and some refinery streams such as light cycle oils.

Scheme 1 shows the structures of some polyester materials, including thermoplastic polyethylene terephthalate (PET), polyethylene naphthalate (PEN), polybutylene terephthalate (PBT), polybutylene naphthalate (PBN), polycarbonate (PC), polyphenylene oxide (PPO), and thermotropic LCPs. PET has found widespread applications in bottles, films, and tapes. PET consumption in the United States reached 1.4 Mt in 1994, with over half being used for soft-drink or custom bottles (MP-News, 1995). Compared to PET, PEN provides five times better oxygen barrier and four times better moisture barrier, as well as 50% greater modulus and 29°C higher thermal resistance temperature. PBT is one of the major engineering plastics. PBN outperforms PBT in chemical and thermal resistance as well as tensile strength (Teijin, 1992). PEN and PBN show great commercial potential. Their markets are expected to grow rapidly. Polycarbonates have found wide-spread applications and are the second most widely used engineering plastics. PPO has an exceptionally high softening point (210°C) and is used for automotive parts, appliance, business machines, computer and electrical equipments. Of all the resins, thermoplastic polyesters grew fastest in 1994 (C&EN-News, 1993, 1994, 1995a).

Among the LCPs, Celanese's Vectra is made from three monomers: 6-hydroxy-2-naphthoic acid, 4-hydroxybenzoic acid, and terephthalic acid. Vectra's tensile strength is about ten-fold greater than regular engineering plastics such as PC. Its heat deflection temperature is also fairly high, up to 240°C. Moreover, Vectra's linear expansion is similar to that of metal. Amoco's Xydar is synthesized from *p,p´*-biphenol (or 4,4´-biphenol), *p*-hydroxybenzoic acid, and terephthalic acid (NRC, 1990). Xydar's heat deflection temperature is the highest among all the thermoplastic engineering plastics, about 350°C. Its heat-resistance is comparable to high-temperature heat-resistant polyimides. Xydar was originally developed for use in cookware; it can be used at 240°C for one hundred thousand hours (LCP-News, 1988). The global market for LCPs is about 4,500 t, about half in the Asia-Pacific market, 40% in the U.S., and 10% in Europe (MP-News, 1995). Despite their cost, LCPs are enjoying 25% annual growth worldwide and are forecast to maintain that level through the decade. Growth is 20% in the U.S. and Europe, 30% in Asia. Most LCPs are made from naphthalene-based and biphenyl-based monomers, as shown in Scheme 1. More information on these materials may be found elsewhere (Seymour, 1987; Beland, 1991; Allcock and Lampe, 1990; NRC, 1990; Song and Schobert, 1993; Relles, 1994).

Scheme 1. **Structures of Some Important Aromatic Polymer Materials**

Thermoplastic Polyesters

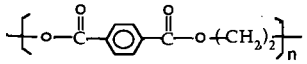

Polyethylene Terephthalate (PET) / Dacron, Mylar

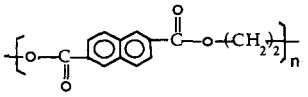

Polyethylene Naphthalate (PEN) / Teijin, Amoco

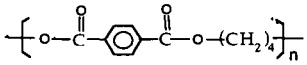

Polybutylene Terephthalate (PBT) / Valox, Celanex

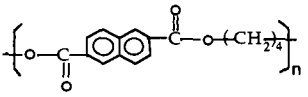

Polybutylene Naphthalate (PBN) / Teijin's PBN Resin

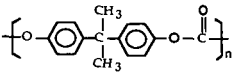

Polycarbonate (PC) /GE's Lexan, Dow's Calibre

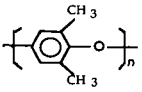

Polyphenylene Oxide (PPO) / GE's PPO, Noryl

Thermotropic Polyester LCPs

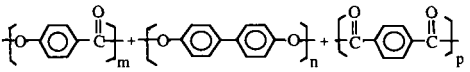

LCP / Amoco's Xydar; Sumitomo's Ekonc

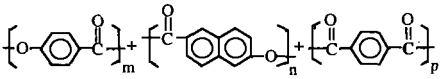

LCP / Hoechst Celanese's Vectra

High-Temp Heat-Resistant Polymers

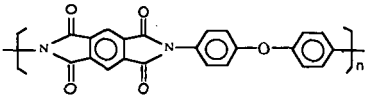

Polyimide / Du Pont's Kapton

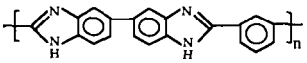

Polybenzimidazole / Celanese's Celazole

AROMATIC AND PHENOLIC CHEMICALS FROM COAL LIQUIDS

Detailed analysis of liquids from several pilot plants of coal liquefaction has clearly shown that phenol, naphthalene, phenanthrene, pyrene, biphenyl, BTX (benzene, toluene, xylene) and their derivatives are present in relatively high concentrations in various fractions (Wright et al., 1986; Lai et al., 1992). Analysis of liquefaction and pyrolysis products in the laboratory indicates the same trends (Caroline et al., 1993; Huang et al., 1993; Song et al., 1993) Many of the one- to four-ring aromatic and polar compounds in coal-derived liquids can be converted into valuable chemicals.

Phenolic Compounds from Coal Liquids. Phenol can be separated from coal liquids by liquid-phase extraction. Phenol is one of the top twenty organic chemicals and is commercially produced in a multi-step process involving benzene isopropylation, oxidation of isopropylbenzene, and separation of phenol. Phenol can be used as-is for making phenol resins or converted to monomers such as bisphenol A and 2,6-xylenol for making aromatic polymers and engineering plastics. Phenol can also be converted to ε-caprolactam, which ranks third in phenol utilization in USA and Western Europe (Weissermel and Arpe, 1993). Production of synthetic phenol has increased significantly in the past decade in USA, from 1311 to 1838 kt during 1984-1994 (C&EN-News, 1995a). The amounts of phenol produced from coal tar and waste water in USA were 20 and 21 kt in 1972 and 1989, respectively, and they are much smaller compared to synthetic phenol. Synthetic phenol production in Japan is also increasing rapidly, from 308 to 670 kt during 1987–94 (Weissermel and Arpe, 1993; C&EN-News, 1995b). Western Europe produced 1488 kt in 1991, with 98.1% synthetic phenol and 1.9% phenol from coal tar and waste water (Weissermel and Arpe, 1993). It appears that the market for phenol is large enough for considering the phenolic compounds from coal liquefaction.

Naptha fractions of coal liquefaction products generally contain 1.5–3.5 wt% oxygen, due to the presence of mainly phenolic compounds (Yoshida et al., 1991). Phenols are more abundant in the oils from coal hydrogenation using dispersed Mo catalyst and water (Saini and Song, 1994; Song and Saini, 1995). Separation of phenolics from coal-derived oils can not only produce useful chemicals, but also eliminate the need for down-stream hydrodeoxygenation which consumes the costly hydrogen to produce useless water byproduct. Therefore, such an operation also contributes to improving the economics of coal liquefaction. According to the recent reports by Yoshida and co-workers at Hokkaido National Industrial Research Institute in Japan and by Kodera and Ukegawa of National Institute for Resources and Environment in Japan, phenolic compounds (mainly phenol and cresols) can be obtained from naphtha distillates of coal liquefaction products by surfactant-mediated (Yoshida et al., 1991) or methanol-mediated (Kodera et al., 1990, 1993) aqueous extraction.

Catechol from Coal Liquids. Catechol (1,2-dihydroxybenzene) has some industrial applications such as therapeutic agent, tanning agent, anticorrosion agent, anti-UV agent, antioxidant for rubber, polyolefins and polyurethanes, intermediate for synthesis of agrochemicals, and intermediate for perfumes, cosmetics, and aromas (Phone-Poulenc, 1991). A new synthetic process developed in Italy produces 10,000 t/y of catechol and hydroquinone by hydroxylation of phenol with H_2O_2 using titanium silicate catalyst (Notari, 1991). On the other hand, catechol is one of the major products detected in flash pyrolysis-GC-MS of subbituminous coals and lignites (Song et al., 1992; 1993; Saini et al., 1992). It may be possible to obtain catechol-rich liquids from low-rank coals through some new processing methods.

Aromatic Compounds from Coal Liquids. The use of aromatics in coal liquids for making value-added chemicals requires the starting material to be reasonably pure. This requirement adds a challenge for chemists and engineers, since coal liquids contain dozens or even hundreds of components. Dealkylation or dehydrogenation of oils from coal can significantly simplify the composition, leading to simple separation of individual components by distillation.

Nomura and co-workers at Osaka University in Japan have reported making aromatic chemicals from coal through catalytic dehydrogenation and dealkylation of liquefaction products (Ida et al., 1991; Nomura et al., 1995). In particular, dehydrogenation can simplify the liquid composition, because two or more isomers (e.g., 2- and 6-methyltetralin) become one compound (e.g., 2-methylnaphthalene) upon dehydrogenation In the presence of a carbon-supported palladium catalyst, dehydrogenation of heavy naphtha (bp ca. 200-220°C) and light oil (bp ca. 220-240°C) from several coal-derived liquids is effective for producing naphthalene and methylnaphthalene, respectively (Nomura et al., 1995). Sato and co-workers at National Institute for Resources and Environment reported that non-catalytic hydrodealkylation of middle distillates (bp 180-450°C) from coal liquefaction produces mainly unsubstituted and methylsubstituted 1- to 3-ring aromatic chemicals including benzene, toluene, indene, naphthalene, methylnaphthalene, biphenyl, acenaphthylene, fluorene, and phenanthrene (Sato et al., 1992, 1994). They have also shown that catalytic cracking of the middle distillates (bp 200-260°C) from coal liquefaction produces the oils that consist mainly of alkylnaphthalenes; hydrodealkylation of such oils can produce high-purity naphthalene and methylnaphthalene as chemicals (Sato et al., 1994).

SHAPE-SELECTIVE SYNTHESIS OF HIGH-VALUE CHEMICALS

Our attention on chemicals has focused on shape-selective catalytic synthesis of value-added chemicals from polycyclic aromatic compounds that are rich in coal liquids (and in some refinery streams such as LCO). We are studying ring-shift isomerization of phenanthrene derivatives to anthracene derivatives, shape-selective alkylation of naphthalene, conformational

isomerization of *cis*-decahydronaphthalene, shape-selective hydrogenation of naphthalene, and shape-selective isopropylation of biphenyl, as described below.

Ring-Shift Isomerization. Phenanthrene and its derivatives are rich in various coal-derived liquids, but their industrial use is still very limited (Kurata, 1986, Song and Schobert, 1992). On the other hand, anthracene and its derivatives have found wide industrial applications (Song and Schobert, 1993). Some catalysts selectively promote the transformation of *sym*-octahydrophenanthrene (*sym*-OHP) to *sym*-octahydroanthracene (*sym*-OHAn), which we call ring-shift isomerization (Song and Moffatt, 1993, 1994). This reaction is in distinct contrast to, and mechanistically different from, the well-known ring-contraction isomerization of tetralin (Hooper et al., 1979; Franz and Camaioni, 1980), *sym*-OHP (Cronauer et al., 1979), and *sym*-OHAn (Collin et al., 1985); ring-contraction results in methylindane-type products.

Under mild conditions, some zeolites can afford over 90% selectivity to *sym*-OHAn with high conversion of *sym*-OHP (Song and Moffatt, 1994; Lai et al., 1995). This could provide a cheap route to anthracene and its derivatives, which are valuable chemicals in demand, from phenanthrene, which is rich in liquids from coal. Possible applications of *sym*-OHAn include the manufacturing of anthracene (for dyestuffs), anthraquinone (pulping agent), and pyromellitic dianhydride (the monomer for polyimides such as Du Pont's Kapton) (Song and Schobert, 1993).

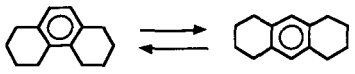

1)

sym-OHP sym-OHAn

Shape-Selective Alkylation of Naphthalene. Naphthalene and its derivatives are rich in oils from bituminous coals. Shape-selective alkylation over some molecular sieve catalysts can produce 2,6-dialkyl substituted naphthalene (2,6-DAN). 2,6-DAN is needed now as the feedstock for monomers for making advanced polyester materials such as polyethylene naphthalate (PEN, Scheme I), polybutylene naphthalate (PBN), and liquid crystalline polymers (LCP). By using some shape-selective catalysts, regioselective alkylation of naphthalene can be achieved with over 65% selectivity to 2,6-DAN by using isopropanol (Song and Kirby, 1993, 1994) or propylene as the alkylating agent (Schmitz and Song, 1994, 1995). Partially dealuminated proton-form mordenite can be used as shape-selective catalyst for isopropylation of naphthalene (Katayama et al., 1991; Schmitz and Song, 1994, 1995). We also found some simple and effective methods for enhancing the shape selectivity (Schmitz and Song, 1994, 1996b).

Shape-selective Alkylation of Biphenyl. Biphenyl and its derivatives are present in coal-derived liquids, although at concentrations lower than those of naphthalene derivatives. Shape-selective alkylation of biphenyl can produce 4,4'-dialkyl substituted biphenyl (4,4-DAB), the starting material for monomer of some LCP materials represented by Xydar (Scheme I). Partially dealuminated proton-form mordenite can be used as shape-selective catalyst for isopropylation of biphenyl (Lee et al., 1989; Sugi et al., 1991, 1994; Schmitz and Song, 1995). Dealumination of some commercial mordenites by acid treatment first increases then decreases their activity, but increases their selectivity toward 4,4-DAB in isopropylation with propylene (Schmitz and Song, 1995). More recently, we have found a simple method using an additive to inhibit deactivation of the partially dealuminated mordenite catalysts without losing activity and selectivity (Schmitz and Song, 1996c).

Conformational Isomerization. Commercial decalins obtained from naphthalene hydrogenation are almost equimolar mixtures of *cis*-decalin and *trans*-decalin. Recently we have found that *cis*-decalin isomerizes to *trans*-decalin, as shown in equation 1, at low temperatures (250°C) over some catalysts (Song and Moffatt, 1993, 1994). This reaction would require a temperature of about 450°C in the absence of a catalyst (Song et al., 1992). It is possible to achieve over 90% conversion with 95% selectivity with some zeolites at 200°C (Lai and Song, 1995). *trans*-Decalin has substantially higher thermal stability at temperatures above 400 °C (Song et al., 1992). Possible applications are high-temperature heat-transfer fluids and advanced thermally stable jet fuels, which can be used both as heat sinks and as fuels for high-Mach aircraft (Coleman et al., 1993; Song et al., 1993, 1994).

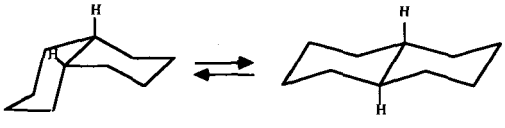

3)

cis-DeHN trans-DeHN

Shape-selective Naphthalene Hydrogenation. Complete hydrogenation of naphthalene in conventional processes produces mixtures of *cis*- and *trans*-decalin. The motivation for selective naphthalene hydrogenation comes from our accidental finding on zeolite-catalyzed isomerization of *cis*-decalin and from the need to tailor the formation of desired isomers from two-ring compounds (Song and Moffatt, 1994). In our previous studies on naphthalene hydrogenation, certain catalysts show higher selectivity towards *cis*-decalin or *trans*-decalin (Song and Grainne, 1993; Lin and Song, 1995; Schmitz et al., 1995; Reddy and Song, 1995). More recently, we found that zeolite-supported catalysts selectively promote the formation of *cis*-decalin or *trans*-decalin (Schmitz et al., 1995, 1996), as shown below.

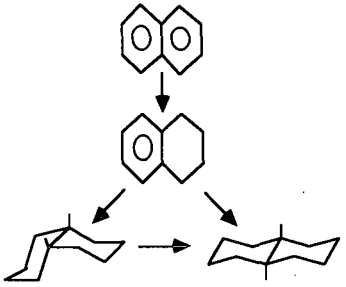

Now we can produce *cis*-decalin, with over 80% selectivity (or over 80% trans-decalin) at 100% conversion by using some zeolite-supported catalysts at 200°C (Schmitz et al., 1995, 1996). *cis*-Decalin may have potential industrial application as the starting material for making sebacic acid. Sebacic acid can be used for manufacturing Nylon 6,10 and softeners (Weissermel and Arpe, 1993).

There is also an industrial need for selective production of tetralin, a hydrogen-donor solvent, from naphthalene. Partial passivation of some zeolite-supported noble metal catalysts by sulfur can make them highly selective for the production of tetralin during metal-catalyzed hydrogenation of naphthalene at low temperatures (Song and Schmitz, 1996).

CATALYTIC GRAPHITIZATION OF ANTHRACITES

We are also exploring the direct synthesis of high-value carbon materials—graphites—from coals. Both non-catalytic and catalytic graphitization of anthracites has been studied. The main objectives of catalytic graphitization are to further improve the quality of the graphitic product, and to reduce the temperature of graphitization. A reduction in graphitization temperature from typical present-day practice (≈2900°C) to, say, 2000°C could translate into enormous energy savings for the graphite industry. The product quality parameter of interest is the apparent crystalline height, L_c, which is the thickness of the "stack" of aromatic planes.

Four Pennsylvania anthracites are being evaluated as feedstocks. The catalysts under investigation are iron, cobalt, and nickel naphthenates, used at various loadings. Preliminary results demonstrate that using some metal compounds significantly promotes the graphitization at lower temperatures. For example, West Cameron anthracite graphitized at 2000°C with added nickel naphthenate shows an interlayer spacing (d-spacing) of 0.3365 nm, approaching the value of 0.3354 nm characteristic of perfectly crystalline graphite. An unanticipated finding is that, for most anthracites and graphitization reaction conditions, the nature of the metal in the naphthenate salt is relatively unimportant in terms of improved d-spacings or L_c values. Often when a family of compounds is evaluated for catalytic activity there is a progressive change in activity among the family, depending on the metallic element in the catalyst. The metal naphthenate catalyzed graphitization of anthracites is unusual in this respect. We have not yet elucidated the reasons, but it appears that metal carbides may be intermediates. The carbides decompose at the extreme temperatures of graphitization. We hypothesize that the thermal decomposition of the carbides liberates carbon in a highly reactive form, this reactive carbon then interacting with non-graphitic carbon or with heteroatoms in the anthracite to facilitate the graphitization.

Catalytic graphitization is presently being tested by standard industrial procedures for the production of molded graphite articles. Two anthracites, one which graphitizes well without added catalyst and a second which shows significant benefit of catalyst, are being tested. Control experiments with sponge coke are being run in parallel. Nickel naphthenate is the catalyst; experiments without added catalyst will also be run. The anthracites and the petroleum coke were mixed with coal tar pitch and isostatically molded into test billets, using standard industrial mixing and molding methods. At the time of writing, the molded billets are in the baking cycle in an industrial car bottom furnace. Upon completion of baking, half the samples will be graphitized in an induction furnace at a standard industrial temperature (2850–2900°) and the other half will be graphitized at ≈2500°C. The full range of industrial characterization tests, such as density, electrical resistivity, and coefficient of thermal expansion, will be run on all graphitized samples, and the results will be compared with standard commercial products.

CONCLUDING REMARKS

Shape-selective catalysis is an effective approach for making high-value chemicals from aromatic components in coal liquids and some refinery streams such as light cycle oils (LCO). Catalytic graphitization is promising for producing graphites from anthracites at substantially lower temperatures compared to current practice. Expansion of the non-fuel uses of hydrocarbon resources, particularly coals, is desirable, because coal will also become more important as source of both energy and chemical feedstocks in the next century. From the viewpoints of the resource conservation and effective utilization, many of the components in coals as well as in petroleum should be converted to, or used as value-added chemicals, polymers, and carbon materials.

ACKNOWLEDGMENTS

Helpful discussions with Drs. F. Rusinko, W.-C. Lai, A. Schmitz, and S. Zeng of PSU, and D. Struble and W. Nystrom of Carbone of America are gratefully acknowledged. Various portions of our research were supported through funding or donations of special samples from the U.S. Department of Energy, Pittsburgh Energy Technology Center, the Pennsylvania Energy Development Authority, Air Products and Chemicals Inc., PQ Co, and Duracell Co.

REFERENCES

Allcock, H. R. and Lampe, F. W., Contemporary Polymer Chemistry. Prentice Hall, Englewood Cliffs, NJ., 1990.

NRC. Liquid Crystalline Polymers. National Academy Press, 1990, 106 pp.

Beland, S. High Performance Thermoplastic Resins and Their Composites. Noyes Data Corporation: Park Ridge, New Jersey, 1991, 177 pp.

Burgess, C. E., K. Wenzel, C. Song, P. G. Hatcher, and H. H. Schobert. Structural Correlation of Coal Liquefaction Oils with Flash Pyrolysis Products. Proc. 7th Internat. Conf. Coal Sci., Banff, Canada, Sept. 12-17, 1993, Vol. I, pp.311-314.

C&EN-News. *Chem. Eng. News*, 1993, June 28.

C&EN-News. *Chem. Eng. News*, 1994, July 4.

C&EN-News. Chem. Eng. News, 1995a, June 26.

C&EN-News. Chem. Eng. News, 1995b, December 11.

Coleman, M. M., H. H. Schobert and C. Song. Chemistry in Britain, 1993, 29 (9), 760-763.

Collin, P. J., and H. Rottendorf. Proc. 1985 Int. Coal Sci. Conf., Sydney, Oct. 28-31, 1985, pp..710-713.

Cronauer, D. C., D. M. Jewell, Y. T. Shah, R. J. Modi and K. S. Seshadri. Ind. Eng. Chem. Fundam., 1979, 18, 368-376.

Franz, J. A. and D. M. Camaioni. Fuel, 1980, 59, 803-805.

Hirota, T., M. Nomura, and C. Song. A Method for Manufacture of Aromatic Chemicals from Coals. Japan Patent, 1-279990 (Assigned to Osaka Gas Company, Japan), November 10, 1989 (in Japanese).

Hooper, R. J., H. A. J. Battaerd, and D. G. Evans. Fuel, 1979, 58, 132-1348.

Huang, L., C. Song, and H. H. Schobert. Liquefaction of Low-Rank Coals as a Potential Source of Specialty Chemicals. Am. Chem. Soc. Div. Fuel Chem. Prepr., 1994, 39 (2), 591-595.

Ida, T., Kikukawa, T., Matsubayashi, K., Miyake, M, and Nomura, M. Catalytic Hydrodealkylation of SRC Fractions. Sekkiyu Gakkaishi, 1991, 34 (1), 44-51.

Kurata, N. Kagaku To Kogyo, 1986, 60 (7). 274-280.

Lai, W.-C., C. Song, H. H. Schobert., and R. Arumugam. Pyrolytic Degradation of Coal- and Petroleum-Derived Aviation Jet Fuels and Middle Distillates. Am. Chem. Soc. Div. Fuel Chem. Prepr., 1992, 37 (4), 1671-1680.

Lai W.-C. and C. Song. Am. Chem. Soc. Div. Fuel Chem. Prepr., 1995, 40 (4), 1018-1023.

Lai W.-C., C. Song, A. van Duin, and J. W. de Leeuw. Am. Chem. Soc. Div. Fuel Chem. Prepr., 1995, 40 (4), 1007-1012.

Lai, W.-C. and C. Song. Temperature-Programmed Retention Indices for GC and GC-MS Analysis of Coal- and Petroleum-derived Liquid Fuels. Fuel, 1995, 74, 1436-1451.

LCP-News. Speciality Chemicals, 1988, 12 (8), 17-22.

Lee, G.S., J.J. Maj, S.C. Rocke, and J.M. Garces, Shape Selective Alkylation of Polynuclear Aromatics with Mordenite-Type Catalysts: A High Yield Synthesis of 4,4'-Diisopropylbiphenyl. Catal. Lett., 1989, 2, 243-248.

Lin, S.-D. and Song, C. Am. Chem. Soc. Div. Fuel Chem. Prepr., 1995, 40 (4), 962-967.

MP-News Modern Plastics, 1995, January, p.54-66.

Nomura, M.; Moritaka, S.; Miura, M. Catalytic Dehydrogenation of Coal Liquefied Products: An Alternative Route to Produce Naphthalenes from Coal. Energy & Fuels, 1995, 9 (5), 936-937.

Relles, H. H. Engineering Plastics. Technomic Publishing Company: Lancaster, PA, 1994.

Saini, A.K., C. Song, P.G. Hatcher, and H.H. Schobert. Prepr. Pap.-Am. Chem. Soc., Div. Fuel Chem., 1992, 37 (3), 1235-1242.

Sato, Y., Yamamoto, Y., and Miki, K. Thermal Hydrodealkylation of Coal Liquids and Related Model Compounds. Sekkiyu Gakkaishi, 1992, 35 (3), 274-281.

Sato, Y., Yamamoto, Y., Kamo, T., and Miki, K. Fluid Catalytic Cracking of Coal Liquids (Part 4). Production of Fuel and Chemicals from Coal Liquids. Sekkiyu Gakkaishi, 1994, 37 (1), 58-63.

Schmitz, A., G. Bowers, and C. Song. Am. Chem. Soc. Div. Fuel Chem. Prepr., 1995, 40 (4), 930-934.
Schmitz, A., and C. Song. Shape-Selective Isopropylation of Naphthalene over Dealuminated Mordenite. Am. Chem. Soc. Div. Fuel Chem. Prepr., 1994, 39 (4), 986-991.
Schmitz, A., and C. Song. Am. Chem. Soc. Div. Fuel Chem. Prepr., 1995, 40 (4), 918-924.
Schmitz, A., and C. Song. Catalysis Today, 1996a, in press.
Schmitz, A., and C. Song. Catalysis Letters, 1996b, in press.
Schmitz, A., and C. Song. 1996c, unpublished results.
Schobert, H.H., In: W.R. Kube, E.A. Sondreal, and C.D. Rao (Eds.), Technology and Utilization of Low-rank Coals. U.S. Dept. of Energy Report DOE/METC/84-13; 1984, pp. 83-103.
Schobert, H.H. The Chemistry of Hydrocarbon Fuels. Butterworths, London, 1990, Chapter 14.
Schobert, H.H. Lignites of North America. Elsevier, Amsterdam, 1995, Chapter 12.
Seymour, R. B. Polymers for Engineering Applications. ASM Int., Metals Park, OH, 1987, 198pp.
Song, C. and Bowers, G., 1993, unpublished results.
Song, C., K. Hanaoka, and M. Nomura. Short-Contact-Time Pyrolytic Liquefaction of Wandoan Subbituminous Coal and Catalytic Upgrading of SCT-SRC. Fuel, 1989, 68 (3), 287-292.
Song, C., L. Hou, A. K. Saini, P.G. Hatcher, and H. H. Schobert. CPMAS ^{13}C NMR and Pyrolysis-GC-MS Studies of Structure and Liquefaction Reactions of Montana Subbituminous Coal. Fuel Processing Technol., 1993, 34 (3), 249-276.
Song, C. and S. Kirby. Shape-Selective Alkylation of Naphthalene over Molecular Sieve Catalysts. Am. Chem. Soc. Div. Petrol. Chem. Prepr., 1993, 38 (4), 784-787.
Song, C. and S. Kirby. Shape-Selective Alkylation of Naphthalene with Isopropanol over Mordenite Catalysts. Microporous Materials, Elsevier, 1994, 2 (5), 467-476.
Song, C., W.-C. Lai, and H. H. Schobert. Hydrogen-Transferring Pyrolysis of Long-Chain Alkanes and Thermal Stability Improvement of Jet Fuels by Hydrogen Donors. Ind. Eng. Chem. Res., 1994, 33 (3), 548-557.
Song, C. and K. Moffatt. Zeolite-Catalyzed Ring-Shift and Conformational Isomerization Reactions of Polycyclic Hydrocarbons. Am. Chem. Soc. Div. Petrol. Chem. Prepr., 1993, 38 (4), 779-783.
Song, C. and K. Moffatt. Zeolite-Catalyzed Ring-Shift Isomerization of sym-Octahydrophenanthrene and Conformational Isomerization of cis-Decahydronaphthalene. Microporous Materials, Elsevier, 1994, 2 (5), 459-466.
Song, C., and A. K. Saini. Using Water and Dispersed MoS_2 Catalyst for Coal Conversion into Fuels and Chemicals. Am. Chem. Soc. Div. Fuel Chem. Prepr., 1994, 39 (4), 1103-1107.
Song, C., and A. K. Saini. Strong Synergistic Effect between Dispersed Mo Catalyst and H_2O for Low-Severity Coal Hydroliquefaction. Energy & Fuels, 1995, 9 (1), 188-189.
Song, C. and H. H. Schobert. Specialty Chemicals and Advanced Materials from Coals: Research Needs and Opportunities. Am. Chem. Soc. Div. Fuel Chem. Prepr., 1992, 37 (2), 524-532.
Song, C. and H. H. Schobert. Opportunities for Developing Specialty Chemicals and Advanced Materials from Coals. Fuel Processing Technol., 1993, 34 (2), 157-196.
Song, C. and H. H. Schobert. Aromatic Polymer Precursors from Coals: A New Direction in Coal Chemistry. Proc. 10th Ann. Internat. Pittsburgh Coal Conf., University of Pittsburgh, Pittsburgh, Sept. 20-24, pp.384-389, 1993.
Song, C. and H. H. Schobert. Non-fuel Uses of Coals and Synthesis of Chemicals and Materials. Fuel, 1996, 75, in press.
Song, C., H. H. Schobert and P.G. Hatcher. Energy & Fuels, 1992, 6, 326-328.
Song, C., H.H. Schobert, and A.W. Scaroni. Current Status of U.S. Coal Utilization Technologies and Prospects. Energy & Resources (Japanese), 1994, 15 (2), 142-153.
Sugi, Y., Matsuzaki, T., Hanaoka, T., Takeuchi, K., Tokoro, T., and Takeuchi, G. Alkylation of Biphenyl Catalyzed by Zeolites. Proc. of International Symposium on Chemistry of Microporous Crystals, Tokyo, June 26-29, 1990, 303-340.
Sugi, Y., Matsuzaki, T., Hanaoka, T., Kubota, Y., Kim, J.-H. Shape-Selective Alkylation of Biphenyl over Mordenites: Effects of Dealumination on Shape-Selectivity and Coke Deposition. Catal. Lett., 1994, 26, 181-187.
Teijin. Teijin PBN Resins-Introduction, 1992.
Weiss, R.A. and C. K. Ober (Eds.), Liquid-Crystalline Polymers. Am. Chem. Sym. Ser., 1990, No. 435, 32 chapters, ACS: Washington, D.C., 510 pp.
Weissermel, K. and H.-J. Arpe. Industrial Organic Chemistry. VCH: Weinheim, 1993, 457 pp.
Wright, C. W., D. L. Stewart, D. D. Mahlum, E. K. Chess, and B. W. Wilson. Am. Chem. Soc. Div. Fuel Chem., 1986, 31 (4), 233-239.

THEORETICAL MODELING OF COLIQUEFACTION REACTIONS OF COAL AND POLYMERS

H.F. Ades and K.R. Subbaswamy,
Department of Physics and Astronomy,
University of Kentucky, Lexington KY 40506-0055

Keywords: coliquefaction, quantum chemical modeling

Differences in the behavior of coliquefaction reactions involving polyethylene/coal and polypropylene/coal have been reported. For instance, conversion and oil yields are higher with the polypropylene/coal system while preasphaltene and asphaltene products are higher in the presence of polyethylene. Also, differences have been observed in the coliquefaction of polystyrene and polyisoprene with coal in the absence of a catalyst, with coal conversion increasing from 38% to 60% with polystyrene and to 80% with polyisoprene. Synergism was observed in the polyisoprene/coal system. In an attempt to explain the differences in coliquefaction behavior of these polymers we have begun quantum chemical studies of these systems, using the Gaussian, MOPAC and TBMD suite of programs, to investigate possible differences in cracking of the polymers, in hydrogen transfer behavior and in addition reactions between polymer fragments and coal. Reaction barrier heights for the possible reaction pathways are being calculated and will be compared in order to build a kinetic model.

I. Introduction

Coliquefaction studies of coal with waste products has focused on certain basic questions: (1) what waste products and in what combinations are the best ones to use in coliquefaction processes; (2) what catalysts are good for coliquefaction and how do they act; and (3) is there synergism involved in coliquefaction? Given the complexity of the systems involved, answering these questions will require a combination of empirical and analytical approaches.

In this report on our preliminary modeling studies pertinent to the coliquefaction of coal and waste polymers we specifically address some of the available experimental results of Huffman, et al. [1] and Curtis, et al. [2]

II. Calculations

A. Polyethylene and Polypropylene

Huffman and coworkers[1] found large differences in the coliquefaction behavior of polyethylene (PE) and polypropylene (PPE) with Black Thunder (BT) coal in the presence of a zeolite catalyst (HZSM-5) and tetralin solvent. The oil yields of PPE with BT coal are higher (71%) than with PE and BT coal (41%). The preasphaltene and asphaltene yields are higher with PE and BT coal (28%) than with PPE and BT (18%). The total conversion for PPE and BT is 93%, while for PE and BT it is 72%. In the presence of the HZSM-5 catalyst and in the absence of the coal, PE and PPE essentially undergo 100% conversion at 430°C. However, with no catalyst present PE undergoes a 65% conversion at 430°C and PPE 88% at 420°C.

In an earlier study we[3] addressed the experimental results of Huffman, et al.[1] by considering several factors that might explain the differences in the coliquefaction of the two polymers with coal, namely: (i) the ease of cracking of PE vs. PPE, (ii) hydrogen transfer reactions from coal fragments to PE+ and PPE+ fragments , and (iii) addition reactions similar to the methylation of benzene found by He et al.[4]

Zeolites are known to be cracking catalysts of hydrocarbons and these cracking reactions are thought to proceed through carbocation ion intermediates.[5]

Therefore, our starting point was to assume that the zeolite catalyst reacted with the neutral polymer to generate carbocation ions. We then looked at reactions of toluene with PE+ and with PPE+ in order to try to address the factors listed above. We used the MOPAC 5.0 program of Stewart[6] and the Tight Binding Molecular Dynamics (TBMD) program developed by Menon and Subbaswamy.[7] The TBMD method is based on parametrized Hamiltonian band structure methods of solid state physics and ideas from the extended Hückel method. Orbitals are not explicitly introduced at all, and no integrals need be computed. Hence, the method can be used for computing forces for performing molecular dynamics simulations on large systems. Results for structure are at least comparable to the commonly used semi-empirical methods such as MNDO. [6]

We calculated the bond dissociation energies (BDE) for the process

Long [PE+ or PPE+] fragment → Short [PE+ or PPE+] fragment + neutral alkene

using the MOPAC suite of programs and found the BDE for the break up of PE+ to be 2.10 eV, while that for PPE+ is 1.52 eV. The difference in BDE, indicating that PPE+ should be easier to crack than PE+ is an intrinsic factor that could contribute to the higher coliquefaction yield with PPE than with PE. Our finding is consistent with the observation of Feng, et al.,[1] who find that PPE is more easily liquefied than PE at lower temperatures, with or without a catalyst.

To investigate possible reactions with coal-derived fragments, we considered the interaction of PE and PPE carbocation ion fragments with toluene and with Model I, 4-(1-naphthylmethyl)bibenzyl, using the tight-binding molecular dynamics (TBMD) method. The method gives results similar to MOPAC, but can be used to study the "real time" dynamics of processes involving large numbers of atoms. We investigated potential H transfer from the methyl group of toluene to the carbocation ion site of the polymer and found that the H transfer occurs much more readily to PE+ than to PPE+, suggesting a higher barrier in the latter. In fact, we never observed a complete transfer of the methyl H of toluene to PPE+. Such hydrogen transfer processes might provide another pathway for subsequent break-up of the coal fragment. We also investigated the possible transfer of the ring hydrogen from the para position in toluene, since it is known that the methyl group activates the para hydrogen in electrophilic reactions. However, we found no transfer in either PE+ or PPE+.

Within the TBMD calculation we also investigated the possibility of an electrophilic addition reaction in which the PE+ or PPE+ carbocation ion fragment adds to the toluene molecule (leading to carbon-carbon bond formation). This addition reaction was found to occur from an initial C-C distance of 2.5 Å with both PE+ and PPE+. The hydrogen transfer reaction should compete with this addition reaction in the case of PE+. However, we find the addition reaction to be lower in energy than the hydrogen transfer reaction and so the addition reaction should be favored. This latter reaction would lead to higher molecular weight products, *i.e.*, a retrograde process.

In trying to explain why in the PPE coliquefaction scheme there are fewer preasphaltenes and asphaltenes than with PE, we noted the following qualitative differences in the reactions and reaction products in our simulations.

1. We find that with TBMD the C-C bond of the addition product is longer in PPE+ than in PE+. In general the longer the bond, the smaller the overlap between the orbitals of the atoms in the bond, which thus leads to weaker bonds. Therefore, the addition product formed with PPE+ should have a weaker bond compared to the PE+ addition product and the reaction could be relatively more reversible under liquefaction conditions.

2. Primary carbocation ions are much higher in energy than secondary, which are higher in energy than tertiary. Therefore, the primary carbocation should

be much more reactive and undergo faster reactions. Using the MOPAC 5.0/PM3 computational scheme, we find with PE+ that the addition products are more stable than the starting reactants by 2.2 eV; for PPE+ the corresponding stabilization energy is only 1.2 eV. Therefore, the PE+ addition is more exothermic than PPE+. In an attempt to quantify the energy differences between PE+and PPE+ for the addition reaction we compared the MOPAC calculated energies of the starting MOPAC minimized toluene and PE+ or PPE+ to the configuration that the toluene, PE+ and PPE+ took after addition but with removing the other species (a 1-SCF calculation) and found it takes 1.4 eV for PE+ to move to the configuration after addition and 1.65 eV for PPE+ to move. Including the rearrangement of the toluene, a first approximation to the "barrier" for molecular adjustment is 3.28 eV for PE+ and 3.43 eV for PPE+. Therefore, it appears that the PPE+ reaction has a higher activation energy for addition and is, therefore, slower than the PE+ addition reaction.

In our latest series of calculations we have been investigating possible hydrogen transfer reactions from solvent to the two polymeric cation fragments. It has also been found that good hydrogen donor solvents, such as tetralin, the solvent used by Huffman, et al.[1], act as chain terminators in the chain depolymerization schemes of polymers. This, in turn, will lead to lower conversion.[8] Therefore, we investigated potential hydrogen transfer from tetralin to PE+ and PPE+ using the TBMD method. (See Figure 1.) We have found that hydrogen transfer readily occurs from tetralin to PE+ at PE+— (H-tetralin) distances up to 2.5 Å . The transfer from tetralin to PPE+ was found to occur only when the PPE+ — (H-tetralin) distance was 1.9 Å . Therefore, the depolymerization of PE+ is much more readily terminated in the tetralin solvent than the depolymerization of PPE+., which would lead to lower conversions for PE. We are now quantifying the barriers for the H transfer from tetralin and for H transfer from the aliphatic carbon atoms of Model I to the two polymers, as well as the barrier for C bond formation in order to construction an overall kinetic scheme.

B. Polystyrene and Polyisoprene

Curtis, et al.,[2] have observed differences in the coliquefaction behavior of polystyrene (PS) and polyisoprene(PI) with Illinois No.6 coal. When liquefied alone, polystyrene and polyisoprene liquefied readily, while coal underwent a 38% conversion. No solvent or catalyst was used. In coliquefaction with coal, and in the absence of either catalyst or solvent, conversion increased to 60% with coal/polystyrene and 80% with coal/polyisoprene. A synergistic effect was observed in the coal/isoprene system. The experiments were carried out at 400°C.

Synergism was also observed for the PI/coal system when a Mo naphthenate plus sulfur or Fe naphthenate plus sulfur catalyst was used. However, for the PS/coal system a slight synergism was observed with the Mo naphthenate plus sulfur catalyst but not with the Fe naphthenate plus sulfur catalyst.

We have begun our modeling of the PI /coal and PS /coal systems by considering the experiments in which there were no catalysts or solvents present. We are using the PM3 option in the MOPAC computational scheme and, in the absence of any catalyst, we are assuming that free radical decomposition of the two polymers would occur. By comparing the energies of the two free radicals formed on bond cleavage to the energy of the whole polymer fragment, we calculate the BDE of PS to be 2.54 eV while that of PI is 2.42 eV. For comparison, the PM3 BDE of the bibenzyl bond of Model I is 2.96 eV. Therefore, PI should be slightly easier to liquefy than PS and both decompose more readily than Model I .

We are now investigating hydrogen transfer barriers for transfer of hydrogen between toluene (our initial model for coal derived fragments) and the two free radical fragments formed in the thermal decomposition of PI and PS.(See Figure 2.) A lower hydrogen transfer barrier in the PI/coal system, which would aid in the decomposition of coal, than in the PS/coal system might explain the synergism observed in one system and not the other. We will also consider radical hydrogen

transfer reactions and hope to extend our studies to the catalyst systems in the future.

Acknowledgements: This research was supported by USDOE contract DE-FC22-93PC93053 to the Consortium on Fossil Fuel Liquefaction Science.

References

1. Feng, Z.; Zhao, J.; Rockwell, J.; Bailey, D.; Huffman, G. *Prepr., Div. Fuel Chem., Am. Chem. Soc.*, **1995**, *40*, 34.;*Fuel Proc Tech*, **1996**, in press.
2. Curtis,C.; Tang, Y.; Luo,M. Presented at 8th Annual Technical Meeting, CFFLS, **1994**.
3. Ades, H.F.; Subbaswamy. K.R. *Fuel Proc Tech*, **1996**, in press.
4. He, S.J.X.; Long, M.A.; Wilson, M.A.; Gorbaty, M.L.; Maa, P.S. *Energy Fuels*, **1995**, 9, 616.
5. Bhatia, S. *Zeolite Catalysis: Principles and Applications*; CRC Press, **1990**.
6. Dewar, M.J.S.; Stewart, J.J.P. *Quantum Chemistry Program Exchange No. 58 vers. 5.0*, Indiana University (Bloomington).
7. Menon, M.; Subbaswamy, K.R. *Phys. Rev. Lett.*, **1991**, *67*, 3487; Menon.M.; Richter. E.; Subbaswamy, K.R. *J.Chem.Phys.* **1996**,*104*, 5875.
8. Sato,S.; Murakata, T.; Baba, S.; Saito, Y.; Watanabe, S. *J. Appl. Polym. Sci.*, **1990**, *40*, 2065.

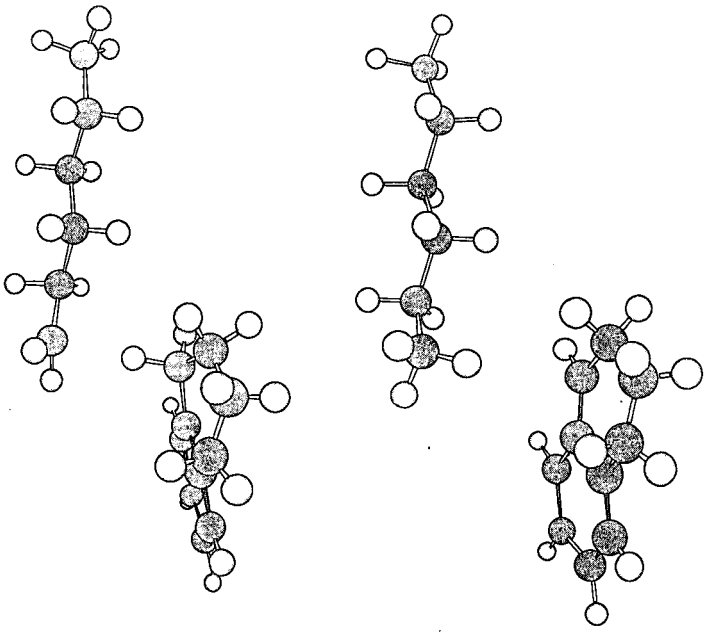

Fig. 1. Tetralin-PE^{+} before and after H transfer from tetralin to PE^{+}.

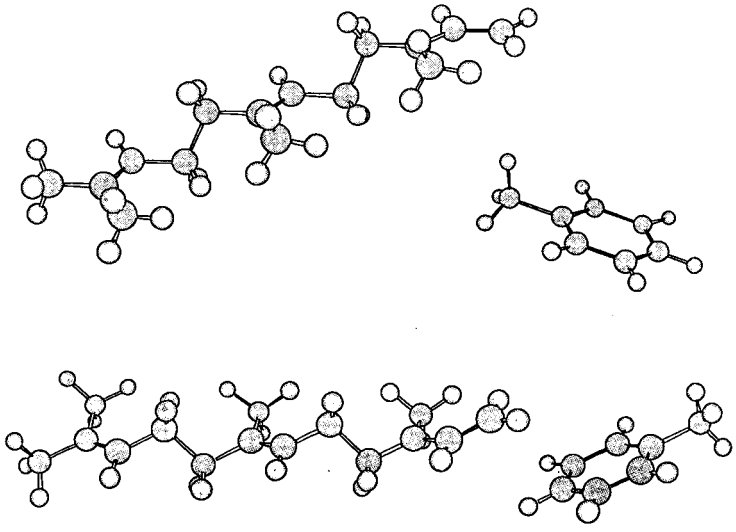

Fig. 2. Typical initial configurations considered for H atom transfer from toluene to a PI free radical fragment.

CATALYTIC TWO STAGE COPROCESSING OF WASTE PLASTICS AND COAL

Mingsheng Luo and Christine W. Curtis
Chemical Engineering Department
Auburn University, Al 36849-5127

Keywords: two stage, coprocessing, waste plastics, coal

INTRODUCTION

The disposal of post-consumer plastics has become an increasingly serious environmental problem throughout the world as well as in the United States. Because of its ever increasing volume, disposal of waste plastics by landfilling is an undesirable option, particularly in densely populated areas. Recycling of plastics is a direct way of reusing the hydrocarbon content in the plastics. (Leaversuch, 1991). However, primary recycling of plastics into the monomer is only accomplished in approximately 2% of the cases (Smith, 1995) and requires that the recycled plastic be separated from the mixed waste. Recycling the mixed plastics wastes to liquid or gases provides a means for reutilizing the hydrocarbons as fuels or chemical feedstock and abstracting the energy or chemical value from the waste material. Pyrolysis and liquefaction of waste plastics as well as liquefaction of waste plastics with coal have been explored by a number of researchers. (Taghiei et al., 1994; Anderson and Tuntawiroon, 1993; Ng, 1995a; Ng, 1995b; Palmer et al., 1995; Huffman et al., 1995)

The supply of waste plastics is limited; even if all of the waste plastics were recycled to transportation fuels, only one month's supply of would be available on annual basis (DOE, 1995). The feasibility of tertiary waste plastics recycling is limited by the availability of waste plastics and the constancy of the supply. Hence, waste plastics liquefaction can provide a valuable addition to our energy supply but will not substantially affect self-sufficiency. Utilization of a native natural resource such as coal in conjunction with waste plastics will not only provide sufficient hydrocarbon resources and a constant feedstock supply but will also provide more self-sufficiency in our energy supply.

In a previous research study, waste plastics were coprocessed directly with coal using commercial hydrotreating catalysts, slurry phase catalysts, zeolite catalysts, and fluid catalytic cracking (FCC) catalysts (Luo and Curtis, 1996 a and b). Since the reactants are composed of chemically different materials, coal being aromatic and most common plastics in the waste stream being polyolefins and aliphatic, these two materials are basically chemically incompatible. The efficacy of the conversion of coprocessed coal and waste plastics to THF soluble material depended upon the plastics composition, efficacy of the catalyst used for the reactant composition, and use of a solvent as well as type of solvent. Coliquefaction reactions of mixtures of waste plastics as well as coprocessing reactions of those mixtures with coal evinced that reaction parameters must be tailored to the waste plastics stream to achieve maximal plastics conversion to liquids. Those reaction parameters were often in conflict with the most efficacious reaction conditions for coal. Typical coal liquefaction catalysts were not sufficiently active to hydrocrack the polyolefins while hydrocracking catalysts were easily and rapidly deactivated in the presence of liquefying coal because of the heavy hydrocarbons and heteroatoms present. Hence, simultaneously coprocessing coal and waste plastics when they are initially both solid reactants does not usually produce an optimal product from either material.

To circumvent the problems associated with simultaneously reacting materials that are inherently so different, two stage processing was investigated. The two stage process was composed of a first stage in which the waste plastics mixture was liquefied and of a second stage where coal was liquefied with the hexane soluble product from the first stage. The reaction conditions and catalysts for each stage were optimized to yield the highest conversion of the reactants to THF soluble and hexane soluble materials in each stage.

EXPERIMENTAL

Materials. The model plastics used in this research were high density polyethylene (HDPE), polyethylene terephthalate (PET), and polystyrene (PS), all of which were obtained from Aldrich. A mixture consisting of 50% HDPE, 30% PET, and 20% PS was used as a base plastics mixture in single and two stage reactions. The solvents used in this study were tetralin and hexadecane, obtained from Aldrich and Fisher Scientific, respectively. The plastics and the solvents were used as received. Illinois No. 6 coal, obtained from the Argonne Premium Coal Sample Bank, was used as received. The catalysts used in this study were fluid catalytic cracking catalysts, Low Alumina and Super Nova-D, which were supplied by Davison Chemical Division of W. R. Grace and Company. A zeolite HZSM-5, obtained from United Catalysts, was also used. The catalysts used for the second stage coal reactions included the slurry phase hydrogenation catalyst precursors, molybdenum naphthenate (6% Mo; MoNaph) and iron naphthenate (6% Fe; FeNaph), obtained from Shepherd Chemical. Both of the slurry phase catalysts were reacted in the presence of excess elemental sulfur, which was obtained from Aldrich.

First Stage Reaction. In the first stage reaction, a waste plastics mixture was liquefied in order to obtain a liquid solvent to be used as the solvent in the second stage coprocessing reaction. The plastics mixture was liquefied in ~50 cm^2 stainless steel microtubular reactors at 713 K (440 °C)

for 60 min under an initial H_2 pressure of 2.8 MPa introduced at ambient temperature. The reactors were agitated vertically at 450 rpm. Ten grams of plastics mixture were charged to the reactor. The loading for the catalytic reactions using FCC and HZSM-5 catalysts was 10 wt % on a plastics charge basis. Both HZSM-5 and the FCC catalysts were pretreated prior to being used in the reaction by heating the catalysts for 2 hr at 477 K (400 °F) followed by 2 additional hours at 811 K (1000 °F). After the reaction was completed, the reactor was quenched in ambient water. The amount of gaseous products was weighed and the gaseous products were removed. The liquid products were extracted with hexane and the soluble amount determined. The hexane solvent was evaporated from the liquid product which was then used as a coal liquefaction solvent in the second stage reaction.

Second Stage Reaction. The second stage coprocessing reaction was performed with 2 g of coal and 2 g of first stage solvent in 20 cm^2 stainless steel microtubular reactors at 713 K (440 °C) for 30 min. The reactors were charged with 5.6 MPa of H_2 introduced at ambient temperature and were agitated at 435 rpm during the reaction. Slurry phase MoNaph and FeNaph catalysts at 1000 ppm of active metal and elemental sulfur at 6000 ppm were charged on a total reactant basis. In some reactions, a loading of 500 ppm of MoNaph and 500 ppm of FeNaph was used.

Product Analysis. The liquid products for the second stage reaction were analyzed by solvent fractionation using hexane as the initial solvent followed by THF. Any solid residue left in the reactor after extraction was carefully scraped from the reactor walls. The amount of hexane and THF soluble materials was determined as well as the amount of THF insoluble material or IOM (insoluble organic matter which is ash free). The hexane soluble fraction produced in the first stage was used as the solvent in the second stage reaction.

The recoveries obtained in the reactions were calculated by

$$\text{Recovery} = (\text{g Recovered} / \text{g Charged}) \times 100\%$$

as are given in the tables. The conversion of the solid reactants to THF soluble material was determined on a solvent, moisture, and ash free basis using the equation

$$\text{Solid Conversion} = 100\% - \text{IOM}\%$$

where IOM is produced from reactions of either coal or plastics or both.

RESULTS AND DISCUSSION

Two stage coprocessing of coal and waste plastics was investigated to determine if higher conversion to THF soluble material and higher production of hexane soluble material could be obtained than with single stage coprocessing. Two sets of experiments were performed. The first set of reactions consisted a first stage catalytic reaction using the base plastic mixture. Then coal was placed in the reactor and reacted with the liquefied plastics as well as the unconverted material. The second set of reactions consisted also of two stage processing, but in these reactions the hexane soluble material produced in the first reaction of the base plastics mixture was used as the solvent for second stage coal reaction. The reaction products from each stage were analyzed using solvent fractionation and a determination of the conversion of the solids to THF soluble products.

Two Stage Coprocessing. The first set of the two stage reactions is presented in Table 1. The first stage reaction involved the base plastics mixture consisting of 50% HDPE, 30% PET, and 20% PS that was reacted at 440 °C and 30 min using Low Alumina and HZSM-5 catalysts. Both catalysts promoted plastics conversion to THF solubles of more than 85% and hexane soluble yields 69.8% and 61.5%, respectively. The second stage reaction was performed with coal at 400 °C for 30 min and 5.5 MPa of initial H_2 pressure. The coal was placed in the reactor with the entire reacted base plastics mixture as well as the first stage catalyst. The products obtained from the second stage reaction were similar regardless of the first stage reaction. These second stage reactions produced high levels of gas make of 32.5 and 29.7%, respectively, for the first stage Low Alumina and HZSM-5 catalysts. The conversions from the second stage reactor were similar and low, 57.5 and 54.9%, respectively, for Low Alumina and HZSM-5 first stage catalysts. The second stage hexane solubles were also similar and low, yielding 22.8 and 23.5%, respectively.

Two Stage Coprocessing using First Stage Hexane Solubles as Solvent. The disadvantage of the first set of two stage reactions was the presence of unconverted and difficult to convert plastics in the second stage reaction. In addition, the catalyst from the first stage was present during the coal reaction. These hydrocracking catalysts promoted high gas production during the second stage. Consequently, the reaction sequence was changed to eliminate the presence of both the unconverted material and the hydrocracking catalyst in the second stage. In both stages the reaction conditions were tailored so as to promote the desired reactions during that stage and to minimize the undesirable reactions.

The first stage reaction was performed at 440 °C and 60 min with each of the three hydrocracking catalysts, Low Alumina, HZSM-5, and Super Nova-D, and the base plastics mixture. High conversions to THF soluble materials were obtained with all three reactions yielding 88.4 , 94.5, and 95.1, respectively, as shown in Table 2. The majority of the product produced was hexane

soluble material that was extracted for use as the solvent in the second stage. Although gas yields ranged from 14.9 to 17.9%, these products did not affect the second stage reaction and could presumably be used as a fuel.

The second stage reaction employed coal at reaction conditions of 400 °C and 30 min with 5.6 MPa H_2 introduced at ambient temperature (Table 3). Two reactions were performed at a higher temperature of 440 °C. The slurry phase catalysts, MoNaph and FeNaph with excess sulfur, were used individually and as a mixture. Three different solvents, each produced with one of the three different first stage catalysts, were employed in the second stage reaction.

Catalyst type strongly affected the conversion and product distribution of the second stage reaction. The reactions that contained only MoNaph as the catalyst resulted in higher conversions than the reactions with either FeNaph or the combination of the two catalysts. The highest conversions were achieved with the HZSM-5 produced solvent and MoNaph, yielding 93.7%. The next highest conversion, 88.2%, occurred using the Low Alumina produced solvent and with MoNaph. The MoNaph catalyst also gave the highest production of hexane soluble materials, yielding 42.5% in the HZSM-5 produced solvent and 39.9% in Low Alumina produced solvent. Since half of the material that was introduced into the reactor was the hexane soluble fraction of the plastics mixture and since the hexane soluble materials present after reaction was less than half of the material that was charged, the plastics mixture converted to other fractions during reaction. The most likely products produced from the reaction of these plastics oils was gas; however, in the case of Low Alumina produced solvent, the sum of gas produced and the hexane solubles was greater than 50% of the product, indicating that some of these products were produced from coal.

Comparison of the two second stage catalysts showed that regardless of the first stage solvent used, less conversion of coal to THF soluble material was achieved with FeNaph and excess S than with MoNaph and excess S. The largest difference was observed with the solvent produced with HZSM-5 which produced a conversion of 66.6% compared to 93.7% with MoNaph. The hexane soluble yields were also less with FeNaph with all of the first stage solvents than with MoNaph. Combining MoNaph and FeNaph in the second stage resulted in nearly equivalent conversion to MoNaph with the Low Alumina solvent and somewhat less conversion with the HZSM-5 solvent. The most notable difference observed between the combined and single catalysts was the product distribution. The combined catalyst produced an extremely high yield of THF soluble materials indicating that although the reactants were converted from solids to THF soluble material, little upgrading to hexane solubles occurred. In fact, both the hexane solubles yield and the gas make were low with the combined catalyst compared to either individual catalyst.

Comparison of One-Step and Two Step Coprocessing. Comparisons of one stage and two stage coprocessing of coal and base plastics mixture are given in Figures 1 to 3. In each of these figures a comparison of the product distributions, in terms of gas, hexane solubles, THF solubles and IOM, are given for four reactions. The reactions are (1) a single stage reaction of waste plastics and coal without a solvent; (2) a single stage reaction of waste plastics and coal with 30% tetralin in hexadecane solvent; (3) a two stage reaction using first stage solvent with coal and FeNaph in the second stage; and (4) a two stage reaction using first stage solvent with coal and MoNaph in the second stage. The product distributions from the two stage reactions given in the figures are the combined product distributions from both stages.

The two stage reactions produced an improved overall product slate for the coprocessing reactions than the single stage reactions reacted with or without solvent. The two stage reaction with either FeNaph or MoNaph as the catalyst produced more hexane soluble and THF soluble yields and less IOM for two of the first stage solvents (HZSM-5 and Low Alumina) than the single stage reactions. For the Super Nova-D solvent, more hexane solubles and less IOM were produced with the two stage reactions while more gas and THF solubles were produced with the single stage reaction.

CONCLUSIONS

Increased conversion and hexane soluble yields with the two stage reactions clearly point to the advantage of two stage processing of coal and waste plastics. The predissolution of the waste plastic prior to contacting coal and the ability to tailor the catalysts and the reaction conditions specifically to the materials being reacted enhanced the reactivity of the system and promoted the desired end products.

REFERENCES

1. Anderson, L.; Tuntawiroon, W. *ACS Fuel Chem. Div. Prepr. 30(4),* 816, 1993.
2. Huffman, G.P.; Feng, Z.; Mahajan, V.; Sivakumar, P.; Jung, H.; Tierney, J.W.; Wender, I. *ACS Fuel Chem Div. Prepr. 40(1),* 35, 1995.
3. Leaversuch, R. *Modern Plastics,* July, 40, 1991.
4. Luo, M.; Curtis, C. W. *Fuel Process. Techno.* in press, 1996 a.
5. Luo, M.; Curtis, C. W. *Fuel Process. Techno.* in press, 1996 b.
6. Ng, S.H. *Energy Fuels, 9,* 216, 1995.
7. Ng, S.H. *Energy Fuels, 9,* 735, 1995.

8. Palmer, S.R.; Hippo, E.J.; Tardon, D.; Blankenship, M. *ACS Fuel Chem. Div. Prepr. 40(1),* 29, 1995.
9. Department of Energy, Technical News Release on Coprocessing of Coal with Waste Plastics, 1995
10. Smith, R. Presentation at the Consortium for Fossil Fuel Liquefaction Science, Ninth Annual Meeting, Pipestem, WV August, 1995.
11. Taghiei, M.M.; Feng, Z.; Huggins, F.E.; Huffman, G.P. *Energy Fuels, 8,* 1228, 1994.

Table 1. Product Distribution from Two-Stage Plastics and Coal Liquefaction Reactions

Stage Number and Conditions	Product Distribution (%)		
	Catalyst	HZSM-5	Low Alumin
Stage 1[a,b] Base Plastic Mixture	Gas	15.4±0.7	17.9±0.1
	Hexane Solubles	75.3±0.2	66.4±0.3
	THF Solubles	4.4±0.5	4.1±0.0
	IOM[c]	4.9±0.1	11.6±0.2
	Conversion (%)	95.1±0.1	88.4±0.2
Stage 2[d] Coal Added to reacted Base Plastic Mixture	Gas	32.5±0.5	29.7±0.2
	Hexane Solubles	22.8±0.2	23.5±1.0
	THF Solubles	2.2±0.7	1.1±1.7
	IOM	42.5±0.4	45.1±1.4
	Conversion (%)	57.5±0.4	54.9±1.4
	Recovery (%)	71.4	74.8

a. Stage 1 reaction conditions and charge: 440°C, 2.8 MPa of H_2 and 30 min, 2 g of base plastic mixture and 10% catalyst based on plastic charge.
b. *Base plastic mixture:* 50% HDPE, 30% PET and 20% PS.
c. IOM: insoluble organic matter, that is ash- and moisture-free
d. Second stage reaction conditions and charge: 2 g of coal at 400°C, 5.6 MPa initial H_2 pressure for 30 min.

Table 2. Product Distribution from Catalytic Liquefaction of Base Plastics Mixture[a,b]

Catalyst	Catalyst		
	Low Alumina	Super Nova-D	HZSM-5
Gas	17.9±0.1	14.9±0.1	15.2±0.7
Hexane Solubles	66.4±0.3	75.1±0.4	75.5±0.2
THF Solubles	4.1±0.0	4.5±0.5	4.4±0.5
IOM[c]	11.6±0.2	5.5±0.8	4.9±0.1
Conversion (%)	88.4±0.2	94.5±0.8	95.1±0.1
Recovery (%)	73.9	70.8	71.8

a. Reaction Conditions: 440°C, 60 min and 2.8 MPa of H_2 introduced at ambient. 2 g of base plastic mixture and 10% catalyst based on plastic charge; no additional solvent was added.
b. *Base plastic mixture:* 50% HDPE, 30% PET and 20% PS.
c. IOM: insoluble organic matter.

Table 3. Product Distribution from Second Stage Coal Liquefaction Reactions using Hexane Soluble Plastic Oil as Solvent[a,b]

Reaction Temperature	First Stage Catalyst and Charge	Second Stage Catalyst[c]	Product Distribution, %				Conversion (%)	Recovery (%)
			Gas	Hexane Solubles	THF Solubles	IOM		
400°C	HZSM-5+Base Plastics	1000 ppm Mo	8.0±0.3	42.5±0.5	43.2±1.0	6.3±0.2	93.7±0.2	81.7±3.7
400°C	HZSM-5+Base Plastics	1000 ppm Fe	9.5±0.8	32.8±0.4	24.3±3.2	33.4±2.8	66.6±2.8	81.4±2.2
400°C	HZSM-5+Base Plastics	500 ppm+Mo 500 ppm Fe	3.8±0.1	29.2±1.1	54.2±2.4	12.9±3.6	87.1±3.6	88.7±1.3
400°C	Low Alumina+ Base Plastics	1000 ppm Mo	19.9±0.6	39.9±1.1	28.3±0.6	11.8±0.0	88.2±0.0	72.2±1.5
400°C	Low Alumina+Base Plastics	1000 ppm Fe	23.0±0.0	29.6±0.9	19.3±0.1	28.1±0.7	71.9±0.7	74.6±2.4
400°C	Low Alumina+Base Plastics	500 ppm+Mo 500 ppm Fe	3.6±0.7	19.2±2.6	64.6±0.1	12.6±1.9	87.4±1.9	92.6±2.0
440°C	Low Alumina+Base Plastics	1000 ppm Mo	49.7±1.2	8.4±5.2	6.1±1.2	35.9±2.7	64.1±2.7	75.9±1.2
440°C	Low Alumina+Base Plastics	1000 ppm Fe	46.9±0.1	0.5±1.4	4.0±0.8	48.7±0.7	51.3±0.7	81.8±1.3
400°C	Super Nova-D+ BasePlastics	1000 ppm Mo	35.7±0.1	27.2±0.0	10.0±0.1	27.1±0.3	72.9±0.3	67.5±0.6
400°C	Super Nova-D+Base Plastics	1000 ppm Fe	33.5±0.1	18.5±0.5	5.3±0.5	42.8±0.9	57.2±0.9	69.1±0.3

a. Reaction Conditions: 400 °C, 30 min, 5.6 MPa H_2 introduced at ambient temperature, and 2 g of coal and 2 g of plastic oil were added to the reactor.
b. Solvent was from base plastic mixture (HDPE:PET:PS=50:30:20), which was liquefied at 440 °C, 2.8 MPa of H_2 for 60 min.
c. Catalyst contained 1000 ppm Mo or Fe naphthenate plus 6000 ppm S. When combined catalysts were used, 500 ppm Fe and 500 ppm Mo plus 6000 ppm S were added to the reactor.

Figure 1. Comparison of One-Stage and Two-Stage Coprocessing of Coal and Base Plastic Mixture Using HZSM-5

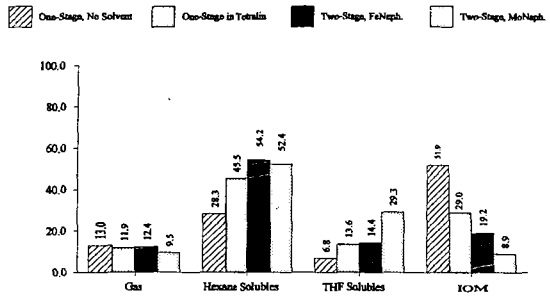

a. One-stage coprocessing: coal + base plastic mixture at 440°C.
b. Two-stage coprocessing: coal + base plastic oil at 400°C.

Figure 2. Comparison of One-Stage and Two-Stage Coprocessing of Coal and Base Plastic Mixture Using Low Alumina

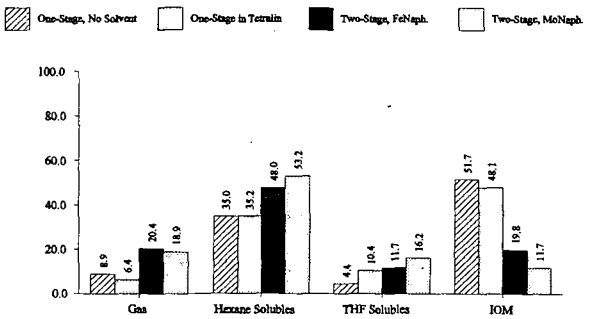

a. One-stage coprocessing: coal + base plastic mixture at 440°C.
b. Two-stage coprocessing: coal + base plastic oil at 400°C.

Figure 3. Comparison of One-Stage and Two-Stage Coprocessing of Coal and Base Plastic Mixture Using Super Nova-D

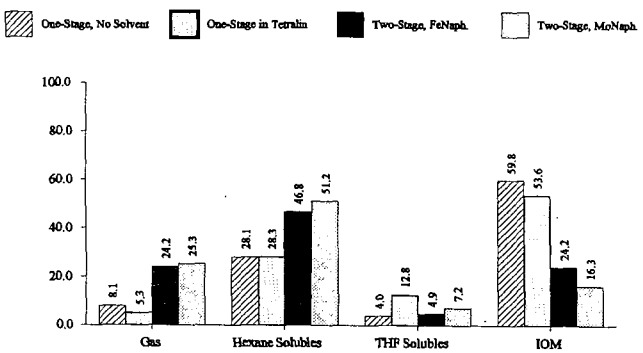

a. One-step coprocessing: coal + base plastic mixture at 440°C.
b. Two-step coprocessing: coal + base plastic oil at 400°C.

TWO-STAGE COPROCESSING OF WASTE PLASTICS WITH COAL

Weibing Ding, Jing Liang and Larry L. Anderson
3290 MEB
Department of Chemical and Fuels Engineering
University of Utah
Salt Lake City, UT 84112

Keywords: two-stage coprocessing, waste plastics, synthetic fuel

INTRODUCTION

Commingled post-consumer plastic waste (CP#2) or high density polyethylene (HDPE) was found to be thermally degraded only at temperatures higher than 430°C, while typical coal liquefaction temperatures are about 400°C. This causes difficulty for coprocessing coal with waste plastic in single stage at appropriate reaction conditions. Moreover, it is hard to find a catalyst which is effective for depolymerization of both coal and HDPE or CP#2. In this study, two-stage coprocessing was developed to produce liquid fuels. In the first stage, CP#2 or HDPE was liquefied in an 150-cm^3 autoclave reactor at 435°C, 1 hr, with stirring speed of 800 rpm, under N_2 or H_2 with and without catalyst (HZSM-5). The resulting liquid products (yields of 78-88 wt%) were utilized as solvents for liquefaction of DECS-6 coal or Fe loaded DECS-6 coal in tubing reactors at 400°C, 1 hr, 160 rpm, ~2000 psig H_2.

The conversion of coal to liquids is generally perceived to proceed via free-radical mechanisms. Reactive radical fragments are formed by thermally rupturing scissile bonds and by hydrogenolysis [1]. Once formed, fragments are either stabilized by hydrogen addition or recombined to form regressive, polymeric products. Two external sources of hydrogen are available to meet these demands. These are donor hydrogen in the solvent and gaseous molecular hydrogen. Therefore, solvent quality plays a significant role in determining which reaction path is taken during coal liquefaction. The solvents investigated were mostly hydroaromatics (tetralin, isotetralin), aromatics (naphthalene, anthracene oil, phenathrene, pyrene), naphthenics (decalin), and their combinations [2-6]. Recently, phenolic compounds (phenol, cresol) were also used as coal liquefaction solvents [7]. These solvents are relatively expensive, therefore we chose Plastic-Derived-Liquids (PDL) as a solvent for coal liquefaction.

For coal liquefaction, iron-based catalysts, because of obvious economic and environmental benefits, have been widely studied recently [8-13]. Yuen [8] investigated the effects of various iron precursors on liquefaction of DECS-6 and DECS-17 coals in absence of solvent. As an iron precursor, ammonium iron (III) sulfate dodecahydrate was found to be very effective in increasing the liquid yields of catalytic hydroliquefaction of Blind Canyon coal. Derbyshire [14] also reported that in the presence of solvent, there are the advantages of adding the precursor by impregnation over its addition in the form of particulates. Thus, a DECS-6 coal, impregnated with Fe catalyst, was selected for liquefaction studies in the second stage. Noncatalytic reactions were also examined for comparison.

EXPERIMENTAL

High-volatile bituminous Blind Canyon DECS-6 coal, obtained from the Penn. State Coal Sample Bank, was ground to pass through a 100 mesh Tyler series screen using a ball mill grinder under nitrogen. Ground coals were dried under vacuum at 100°C for six hours, kept overnight at room temperature, stored in glass bottles sealed with nitrogen, and then put in a refrigerator for future use. Iron loaded DECS-6 coal was prepared by incipient wetness impregnation. Ammonium iron (III) sulfate dodecahydrate (AFS(III)), obtained from Aldrich Chemical Company, was used as precursor of iron. After impregnation, the resulting coal was dried at the same conditions as mentioned above. The weight ratio of iron to moisture-free coal was 1.12:100.

HDPE (M.W.=125,000) in bead form was purchased from Aldrich Chemical Company. Commingled post-consumer plastic (CP#2), obtained from the American Plastics Council, was ground to -25 mesh. Detailed analyses of DECS-6 coal and CP#2 are listed elsewhere [15]. Synthesized according to U.S. Patent 4,250,345 [16], HZSM-5 catalyst contains 35 wt% Al_2O_3 binder. HZSM-5, with a Si/Al mole ratio of 35, was pulverized to -100 mesh and calcined in air at 500°C for 3 hours before use.

Depolymerization of HDPE or CP#2 was carried out in a 150-cm^3 stainless steel autoclave (Autoclave Engineers). A mixture of HDPE or CP#2 (20.0000 g) and catalyst (0.4000 g HZSM-5) were charged into the reactor. For reaction under N_2, the reactor was purged with N_2 5 times

and then closed with a zero pressure gauge value. For reactions with H_2, the reactor was pressurized with 1000 psig H_2 after being purged with N_2 at room temperature. The fixed reaction conditions were: 435°C, 60 minutes, 800 rpm. When the reaction was finished and the reactor cooled to room temperature, the gases were collected. The detailed procedure is described elsewhere [15]. Liquid and solid products were separated by filtration at room temperature. The solid portion was washed with excess pentane and then dried at 60°C under vacuum overnight. The solid yield is defined as (weight of solid)x100/(weight of feed), while oil yield is defined as {100 - gas yield - solid yield}. This oil (Plastic-Derived-Liquids) was utilized as solvent in the next stage. The weight of feed refers to weight of HDPE or CP#2. All experiments were performed in duplicate; repeatability of the results was $\pm$1.5% for oil yield.

In the 2nd stage, solvent (Plastic-Derived-Liquids , tetralin, or waste oil) and dried or iron loaded DECS-6 coal were fed into the 27-cm^3 tubing reactors with a ratio of 2:1 (solvent : dry coal, by weight). The reaction parameters were 400°C, ~2000 psig H_2, 60 minutes, 160 rpm. The reaction procedure was identical to that described in reference 15. As gaseous products came from both coal and solvent, it was difficult to determine how much gas was from coal depolymerization. Therefore, the reaction products were lumped as oil+gas, asphaltenes+preasphaltenes, and THF insolubles. The total conversion is defined as {100x[1-(weight of THF insoluble)/(weight of maf coal)]} and the asphaltenes+preasphaltenes yield as {(weight of THF soluble but pentane insoluble)x100/(weight of maf coal)}. The oil+gas yield is {100x[1-(weight of pentane insoluble)/(weight of maf coal)]}.

The gases obtained from the first stage were analyzed by a flame ionization detector on gas chromatography (HP-5890II) using a column packed with HayeSep Q. The liquid products were analyzed by GC/MS using a 30-m long DB-5 capillary column. The boiling point distribution of the liquid products from the second stage of two-stage processing were determined by modified simulated distillation according to ASTM D 2887-89 and D5307-92. The analysis was performed on HP-5890 series II gas chromatograph, using a Petrocol B column (6 inches long and 0.125 inches outside diameter).

RESULTS AND DISCUSSION

Degradation of HDPE and CP#2 to Obtain Plastic-Derived-Liquids. For degradation of HDPE, the maximum oil yield, 87.2%, was obtained under N_2 without catalyst, while the maximum gas yield, 21.2%, was produced over HZSM-5 under hydrogen (Table 1). For non-catalytic decomposition of HDPE, the solid yield obtained by reaction under nitrogen was 5.5%, while the same yield obtained under hydrogen it was 15.1%. Thermal depolymerization of HDPE was favored in N_2. Since hydrogen is a kinetic chain transfer agent; it might saturate the thermally cracked radicals and prevent them from cracking further. Catalytic reaction over HZSM-5 with hydrogen (Table 1) gave the highest gas yield (21.2%) and lowest solid yield (1.1%). The hydrogenation ability of HZSM-5 was also demonstrated by conversion of ethene [17].

Thermal degradation of CP#2 under N_2 gave the highest oil yield, 86.2%, while catalytic reaction over HZSM-5 under H_2 led to the highest gas yield, 17.6%. The cracking or hydrocracking ability of HZSM-5 is reflected in the resulting lower solid yields and higher gas yields, compared with those from thermal reactions (Table 1). Compared with degradation of CP#2 under nitrogen, the non-catalytic reaction under hydrogen gave higher solid yield and less gas and oil yields (Table 1). This means that hydrogen also inhibited thermal decomposition of CP#2 to some extent.

Upon detailed GC/MS analyses, the oil products were categorized into five groups: 1-olefins, n-paraffins, aromatics, naphthenes, and others (Figure 1), where "others" included mainly iso-paraffins, cyclic-olefins, branched and normal internal olefins. For HDPE, compared with oil products from the thermal reaction under N_2, the oil obtained from non-catalytic reaction under H_2 contained higher n-paraffins and 1-olefins, with lower naphthenes, aromatics and others. Compared with the thermal runs, catalytic reactions over HZSM-5 under both N_2 and H_2 produced oil products with large amounts of aromatics, naphthenes, and others at the expense of 1-olefins and n-paraffins (Figure 1). This is consistent with a similar observation reported previously [18]. Therefore, shape selective zeolite, HZSM-5, had not only high cracking (or hydrocracking) ability, but also had cyclization and aromatization functions.

For degradation of CP#2 under nitrogen, like HDPE degradation under N_2, the same change in oil composition was observed when HZSM-5 was added, i.e., more aromatics and naphthenes, less 1-olefins and n-paraffins. Obviously, HZSM-5 had a stronger effect on HDPE than on CP#2. This may be due to a negative effect of the heteroatoms and trace metals contained

in CP#2. For degradation of CP#2 under hydrogen, the general trends of non-catalytic and catalytic reactions were like those under nitrogen (Table 1, Figure 1).

Plastic-Derived-Liquids Used as Solvents for Coal Liquefaction. Table 2 shows the effects of different solvents on liquefaction of DECS-6 coal at 400°C, 2000 psig H_2, for 60 minutes. Compared with the non-solvent reaction, reactions in the presence of A-1, A-2, A-7, and A-8 oil gave higher total conversions and gas+oil yields. However, A-4, A-5, A-10, and A-11 oil, which were derived from degradation of CP#2, had slightly negative effects on total conversion although increased gas+oil yields. In the presence of waste oil, total conversion increased to some extent, with slightly increasing gas+oil yield. The positive effect of waste oil may be due to a higher content of metals, which may behave as catalysts at reaction conditions [19]. Tetralin, an excellent hydrogen donor solvent, gave the highest conversion and gas+oil yield. The difference in conversion corresponding to different solvents is significant, with 81.4% for tetralin, 57.1% for waste oil, 39.9-48.4% for Plastic-Derived-Liquids, and 44.0% for the non-solvent reaction.

In Table 3, the catalytic results, using PDL as solvents, are compared with those when tetralin and waste oil were used, and when no solvent was used. Compared with thermal reactions (Table 2), the trend of the effects of solvents on conversion and yields for catalytic runs is the same. A-1, A-2, A-7, and A-8 oil were active for catalytic coal liquefaction, increasing both total conversion and yields, while A-4, A-5, and A-11 oil (obtained from CP#2), decreased total conversion slightly, although enhanced the gas+oil yields greatly. Compared with thermal reactions, the difference in conversion corresponding to different solvents decreased in the presence of catalyst. From Tables 1 and 2, at a catalyst loading of 1.12%, the difference in coal conversions between tetralin and PDL is only about 2-10 percentage points, while the difference in thermal conversions for these solvents is about 33-41 percentage points. This implies that PDL can be used with this Fe catalyst, and results obtained are nearly the same as those obtained from tetralin, an expensive hydrogen donor for coal liquefaction. Compared with the thermal reactions, the total conversions and yields were higher in the presence of iron catalyst for each solvent used. This shows that the Fe catalyst was active for the reaction system at conditions used.

For thermal reactions (Table 4), compared with oil from the non-solvent run, the oil products obtained from the reactions with PDL as solvent contained higher amounts of lower-boiling fractions (gasoline, kerosene, and gas oil), except for A-7 oil, which was produced from degradation of HDPE under hydrogen. It is notable that A-7 oil gave highest conversion and oil+gas yield among PDL (Table 2). The lightest oil was from reaction with A-2 oil as solvent, with 92.1% lower-boiling fractions (b.p. up to 325°C). The quality of oil products obtained from reaction with waste oil as solvent was very poor, although the total conversion was increased to some extent. The lower-boiling fractions (b.p. up to 325°C) was only 14.0%. This indicated that further severe upgrading of the oil products would be required.

For catalytic reactions (Table 5), addition of each PDL improved the quality of oil products, producing more lighter components in oil fractions. The oil product with best quality was obtained with A-8 oil, produced from decomposition of HDPE using HZSM-5 as catalyst under hydrogen. This oil contains 59.6% gasoline fraction (<200°C), 24.3% kerosene fraction (200-275°C), and 7.9% gas oil fraction (275-325°C).

Compared with the corresponding thermal reactions, catalytic reactions gave heavier oil products except for the reaction using A-8 oil as solvent. For example, for the non-solvent reaction, the oil products contain 67.5% and 48.1% lower-boiling fractions (b.p. up to 325°C) for thermal and catalytic reactions, respectively. The same numbers for the reaction with A-1 oil as solvent were 78.4% and 70.3% for thermal and catalytic reactions, respectively. This indicated that the total conversion and gas+oil yield increased for catalytic reactions at the expense of oil quality, although the quality just slightly decreased and conversion greatly improved.

Taking into consideration conversion, oil quality, process economics, and process safety, a reasonable senario is: in the first stage, HDPE or CP#2 is degraded under nitrogen; in the second stage, oil products obtained from the first stage (A-1 oil from HDPE and A-4 oil from CP#2) are used as solvents for liquefaction of iron loaded DECS-6 coal. With A-1 oil as solvent, the total conversion of coal was 85.0%, and oil products contained 26.9% gasoline (<200°C), 27.5% kerosene (200-275°C), 15.9% gas oil (275-325°C), 16.6% gas heavy gas oil (325-400°C), and 13.1% vacuum gas oil (400-538°C). The coal conversion was 77.9% in the presence of A-4 oil, and oil products contained 72.0% lower-boiling fractions (b.p. up to 325°C).

CONCLUSIONS

- HDPE and CP#2 can be thermally or catalytically depolymerized under either nitrogen or hydrogen at 435°C. Thermal reactions gave better results with nitrogen than with hydrogen, while catalytic reactions (HZSM-5 used as catalyst) produced oil products with higher quality under hydrogen than under nitrogen.

- The oil from degradation of HDPE or CP#2 can be used as coal liquefaction solvents. In the presence of the impregnated iron catalyst, the Plastic-Derived-Liquids (oil obtained from decomposition of HDPE at 435°C, 0 psig initial nitrogen pressure, 1 hour) produced similar gas+oil yield and total conversion as did tetralin. The resulting oil contained 70.3% lower boiling fractions (b.p. up to 325°C).

- The bench-scale experiments showed that two-stage coprocessing is a feasible and promising method for utilization of plastic waste. In the first stage, plastics can be degraded alone under nitrogen at 435°C; the resulting liquids can be utilized as solvent for liquefaction of Fe loaded coal at 400°C in the second stage.

ACKNOWLEDGMENT

The authors gratefully acknowledge the funding support from the U.S. Department of Energy through the Consortium for Fossil Fuel Liquefaction Science.

REFERENCES

1. Vernon, L.W. (1980), Fuel, **59**(2), 102.
2. Clarke, J.W., Rantell, T.D., Snape, C.E. (1984), Fuel, **63**, 1476.
3. Mochida, I., Takayama, A., Sakata, R., Sakanishi, K. (1990), Energy and Fuels, **4**, 398.
4. Bedell, M.W. and Curtis, C.W. (1991), *ibid*, **5**, 469.
5. Tagaya, H., Takahashi, K., Hashimoto, K., Chiba, K. (1989), *ibid*, **3**, 345.
6. Takemura, Y., Saito, Y., Okada, K., Koinuma, Y. (1989), *ibid*, **3**, 342.
7. Winschel, R.A., Robbins, G.A., Burke, F.P. (1986), Fuel, **65**, 526.
8. Yuen, W.H. (1994), Dissertation, University of Utah.
9. Okamoto, S., Kitajima, A., Taniguchi, H., Ikenaga, N., Suzuki, T. (1994), Energy and Fuels, **8**, 1077.
10. Anderson, R.K., Armstrong, B.T., Givens, E.N., Derbyshire, F.J. (1994), Preprints of ACS, Div. Fuel Chem., **39**(4), 1093.
11. Huffman, G.P., Ganguly, B., Zhao, J., Rao, K.R.P.M., Shah, N., Feng, Z., Huggins, F.E., Taghiei, M.M., Lu, F., Wender, I., Pradhan, V.R., Tierney, J.W., Seehra, F.E., Ibrahim, M.M., Shabtai, J., Eyring, E.M. (1993), Energy and Fuels, 7, 285.
12. Pradhan, V.R., Hu, J., Tierney, J.W., Wender, I. (1993), Energy and Fuels, 7, 446.
13. Eklund, P.C., Stencel, J.M., Bi, X.X., Keogh, R.A., Derbyshire, F.J. (1991), Preprints of ACS, Div. Fuel Chem., **36**(2), 551.
14. Derbyshire, F.J. (1988), in Catalysis in Coal Liquefaction, IEACR/08, IEA Coal Research: London, UK, p69.
15. Ding, W., Tuntawiroon, W., Liang, J. and Anderson, L.L. (1996), Fuel Proc. Tech., in press.
16. U.S. Patent 4,250,345.
17. Kanai, J., Martens, J.A. and Jacobs, P.A. (1992), J. of Catalysis, 133:527.
18. Anders, G., Burkhardt, I., Illgen, U., Schulz, I.W. and Scheve, J. (1990), Applied Catalysis, 62:272.
19. Tarrer, A.R., Kuo, C.H., Mulgaonkar, M.S., Parkash, K.R., Wimberly, J.D. (1994), Proceedings of Contractors' Review Conference, Coal Liquefaction and Gas Conversion (Pittsburgh), p539.

Table 1. Yields of Products Obtained from Thermal and Catalytic Degradation of HDPE or CP#2 in a 150-cm^3 Autoclave at 435°C, 60 Minutes, 800 rpm (0.4 g HZSM-5 was used as catalyst for 20.0 g HDPE or CP#2)

Initial Pressure	Run Number	Reaction System	Gas Yield, wt%	Oil Yield, wt%	Solid Yield, wt%
0 psig N_2					
	A-1	HDPE	7.3	87.2	5.5
	A-2	HDPE+2% HZSM-5	16.5	82.1	1.4
	A-4	CP#2	9.3	86.2	4.5
	A-5	CP#2+2% HZSM-5	12.5	83.4	4.1
1000 psig H_2					
	A-7	HDPE	3.1	81.8	15.1
	A-8	HDPE+2% HZSM-5	21.2	77.8	1.1
	A-10	CP#2	7.5	83.7	8.8
	A-11	CP#2+2% HZSM-5	17.6	76.2	6.2

Table 2. Yields (refer to coal alone) of Products Obtained from Liquefaction of DECS-6 Coal with Plastic-Derived-Liquids as Solvents in a 27-cm^3 Tubing Reactor at 400°C, ~2000 psig H_2, 60 Minutes, 160 rpm (solvent : dry coal = 1:1, weight)

Solvent	Gas+Oil Yield, wt%	Asphaltenes+ Preasphaltenes Yield, wt%	Conversion, wt%
None	24.4	19.5	43.9
Tetralin	40.2	41.2	81.4
Waste Oil	26.6	30.5	57.1
A-1 Oil (1st stage: HDPE, N_2)	28.9	18.6	47.5
A-2 Oil (1st stage: HDPE+2% HZSM-5, N_2)	31.2	17.2	48.4
A-4 Oil (1st stage: CP#2, N_2)	30.5	9.4	39.9
A-5 Oil (1st stage: CP#2+2% HZSM-5, N_2)	27.5	13.9	41.4
A-7 Oil (1st stage: HDPE, H_2)	34.1	14.3	48.4
A-8 Oil (1st stage: HDPE+2% HZSM-5, H_2)	28.5	18.6	47.1
A-10 Oil (1st stage: CP#2, H_2)	28.4	13.2	41.6
A-11 Oil (1st stage: CP#2+2% HZSM-5, H_2)	25.8	17.0	42.8

Table 3. Yields (refer to coal alone) of Products Obtained from Liquefaction of Fe Loaded DECS-6 Coal (Fe:dry coal =1.12:100, in weight) with Plastic-Derived-Liquids as Solvents in a 27-cm^3 Tubing Reactor at 400°C, ~2000 psig H_2, 60 Min., 160 rpm (solvent : dry coal = 1:1, weight)

Solvent	Gas+Oil Yield, wt%	Asphaltenes+ Preasphaltenes Yield, wt%	Conversion, wt%
None	29.6	49.6	79.2
Tetralin	41.8	45.1	86.9
Waste Oil	37.9	42.1	80.0
A-1 Oil (1st stage: HDPE, N_2)	39.1	45.9	85.0
A-2 Oil (1st stage: HDPE+2% HZSM-5, N_2)	36.1	48.6	84.7
A-4 Oil (1st stage: CP#2, N_2)	42.5	35.4	77.9
A-5 Oil (1st stage: CP#2+2% HZSM-5, N_2)	36.5	41.1	77.6
A-7 Oil (1st stage: HDPE, H_2)	39.8	42.7	82.5
A-8 Oil (1st stage: HDPE+2% HZSM-5, H_2)	42.3	38.4	80.7
A-10 Oil (1st stage: CP#2, H_2)	37.9	42.0	79.9
A-11 Oil (1st stage: CP#2+2% HZSM-5, H_2)	35.2	41.1	76.3

Table 4. Boiling Point Distribution (numbers in weight percent) of Final Oil Products Obtained from Two-Stage Coliquefaction of DECS-6 Coal with HDPE or CP#2 (in the first stage, HDPE or CP#2 was degraded in a 150-cm^3 autoclave at 435°C, 1 hour, 800 rpm, under N_2 or H_2; in the second stage, DECS-6 coal was liquefied with Plastic-Derived-Liquids obtained from the 1st stage as solvents in 27-cm^3 tubing reactors at 400°C, ~2000 psig H_2, 60 minutes, 160 rpm (solvent : dry coal = 2:1, weight ratio))

Solvent	Gasoline (<200°C)	Kerosene (200-275°C)	Gas Oil (275-325°C)	Heavy Gas Oil (325-400°C)	Vacuum Gas Oil (400-538°C)	Vacuum Residue (>538°C)
None	12.6	33.2	21.7	17.0	15.4	0.1
Waste Oil	2.9	5.0	6.1	23.0	47.2	15.8
A-1 Oil	29.6	31.5	17.3	14.6	7.0	0.0
A-2 Oil	49.4	31.4	11.3	6.0	1.9	0.0
A-4 Oil	36.9	31.4	15.5	11.6	4.6	0.0
A-5 Oil	39.4	25.2	12.7	13.5	9.2	0.0
A-7 Oil	24.0	22.6	16.0	16.9	17.3	3.2
A-8 Oil	54.1	23.7	9.1	8.4	4.7	0.0
A-10 Oil	32.7	30.1	16.7	14.0	6.5	0.0
A-11 Oil	46.6	31.2	12.0	7.9	2.3	0.0

Table 5. Boiling Point Distribution (numbers in weight percent) of Final Oil Products Obtained from Two-Stage Coliquefaction of Fe Loaded DECS-6 Coal (Fe: dry coal = 1.12:100, weight ratio) with HDPE or CP#2 (in the first stage, HDPE or CP#2 was degraded in a 150-cm^3 autoclave at 435°C, 1 hour, 800 rpm, under N_2 or H_2; in the second stage, DECS-6 coal was liquefied with Plastic-Derived-Liquids obtained from the 1st stage as solvents in a 27-cm^3 tubing reactor at 400°C, ~2000 psig H_2, 60 minutes, 160 rpm (solvent : dry coal = 2:1, weight ratio))

Solvent	Gasoline (<200°C)	Kerosene (200-275°C)	Gas Oil (275-325°C)	Heavy Gas Oil (325-400°C)	Vacuum Gas Oil (400-538°C)	Vacuum Residue (>538°C)
None	8.2	24.0	15.9	19.7	30.7	1.5
Waste Oil	3.0	5.3	5.7	22.7	47.0	16.3
A-1 Oil	26.9	27.5	15.9	16.6	13.1	0.0
A-2 Oil	42.6	28.0	12.3	11.4	5.7	0.0
A-4 Oil	31.3	26.0	14.7	16.1	11.9	0.0
A-5 Oil	35.0	27.1	14.1	14.1	9.7	0.0
A-7 Oil	22.3	22.6	14.2	17.5	16.9	6.5
A-8 Oil	59.6	24.3	7.9	5.6	2.6	0.0
A-10 Oil	26.5	22.3	13.8	17.8	18.0	1.6
A-11 Oil	38.0	25.2	12.8	13.7	10.3	0.0

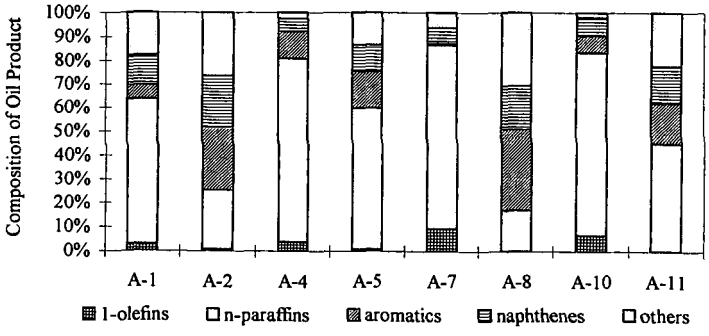

Figure 1. Effects of Catalyst (HZSM-5) and Reaction Atmosphere (N_2 or H_2) on Composition of Oil Products Obtained from Degradation of HDPE or CP#2 in a 150-cm^3 Autoclave at 435°C, 800 rpm, for a Reaction Time of 60 Minutes

LIQUEFACTION OF COMMINGLED WASTE PLASTICS CONTAINING PVC

G.P. Huffman, Zhen Feng, Dan Bailey, Jeff Rockwell, Jianmin Zhao, and F.E. Huggins, CFFLS, 533 S. Limestone St., Room 111, University of Kentucky, Lexington, KY 40506

ABSTRACT

Direct liquefaction studies were conducted on a washed, commingled waste plastic(CWP), as received from the American Plastics Council and after addition of 5 wt.% of polyvinyl chloride (PVC). Both non-catalytic and catalytic experiments were performed; the catalytic experiments utilized 1 wt.% of HZSM-5. The experiments on the CWP-PVC mixture were conducted with and without the addition of 5 wt.% of calcium hydroxide. The effect of PVC on product yields was evaluated. Oil quality was examined by GC simulated distillation. The forms of occurrence of chlorine in the liquefaction products were determined by x-ray absorption fine structure(XAFS) spectroscopy utilizing the X-ray absorption near edge structure(XANES).

INTRODUCTION

Previous research[1-11] has demonstrated that direct liquefaction of waste plastics is a very promising recycling option as well as a significant potential new oil resource. As discussed elsewhere, waste plastics can be liquefied at low hydrogen pressure[5,8] and no solvent is needed,[5-11] although waste automotive oil and petroleum resid[9,10] can serve as excellent solvents, if desired. Solid acid catalysts, such as HZSM-5[3-5,8] and sulfated zirconia[7] are very active for plastic liquefaction and metal-promoted solid acid catalysts have been demonstrated to improve the oil product substantially.[7,11] The coliquefaction or coprocessing of coal with plastics also looks promising.

An aspect of plastics liquefaction that has not been adequately studied is the liquefaction of plastics containing realistic amounts of polyvinyl chloride (PVC). Several groups, including our own, have worked with a washed commingled waste plastic(CWP) provided by the American Plastic Council (APC) that contains very little chlorine, due to the fact that PVC has a higher specific gravity than most other resins and separates out during washing. In the current study, we have investigated the liquefaction of the APC CWP with and without the addition of PVC, calcium hydroxide, and HZSM-5.

EXPERIMENTAL

Liquefaction: The liquefaction experiments were conducted in "tubing bomb" reactors with a volume of 50 ml, which were heated in a fluidized sand bath for 60 minutes while being shaken at a rate of 400 rpm. The reactors were charged with 10 g of plastic, with all combinations of additions of 5 wt.% of PVC and $Ca(OH)_2$ and 1 wt.% of HZSM-5. No solvent was used and hydrogen gas was added at low pressure (200 psig, cold). The HZSM-5 was a commercial catalyst[12] with average particle sizes of 40-50 Å and a Si/Al = 4.[8]

At the end of each run, the reactor was cooled rapidly to room temperature in a second sand bath. Gas products were then collected and analyzed by gas chromatography. The other products were removed from the reactor with tetrahydrofuran (THF) and extracted in a Soxtech apparatus for 2 hours. Total THF conversion was determined from the amount of insoluble material that remained (residue). All insoluble materials were dried at 80°C overnight before weighing. Any added catalyst was subtracted from the residue sample weight. The THF solubles were subsequently separated into pentane soluble (oils) and pentane insoluble (preashpaltenes + ashpaltenes(PA + AS)) fractions. The experimental errors for total conversion and oil yield are approximately ±3%.

The oil fraction was analyzed by GC - simulated distillation. The GC operating parameters were as follows: column - Petrocol B, 20" x 1/8" packed column; temperature - 0 - 360 °C with 10 °C/min ramp; detector - FID at 380 °C; flowrate - 35 ml/min He. The simulated distillation method is described in ASTM D-2887. The oil product was categorized into three fractions: gasoline (B.P. < 200 °C); kerosene (B.P. - 200-275 °C); and heavy oil (B.P. - 275 - 550 °C).

Cl XAFS Spectroscopy: XAFS spectroscopy was carried out at beamline X-19A at the National Synchrotron Light Source at Brookhaven National Laboratory. Spectra were obtained at the chlorine K absorption edge (at ca. 2825 eV) from the oils, asphaltenes + pre-asphaltenes, and IOM residues separated from the products of the liquefaction runs. Some of the fractions were also examined at the calcium K absorption edge (at ca. 4038 eV). The samples were suspended in the X-ray beam in ultrathin polypropylene bags in a Lytle fluorescent detector.[13] The x-ray beam path

was flushed with helium to minimize x-ray absorption by air. Spectra were collected from 75 eV below the chlorine edge to about 300 eV above the chlorine edge, at which point the K absorption edge arising from argon at 3107 eV was encountered. Over the near-edge or XANES region (from about 10 eV below the edge to 50 eV above the edge), the spectra were acquired with a step width of only 0.2 eV/point. The maximum in the derivative of the Cl XAFS spectrum of NaCl was taken as the zero point of energy for the Cl XAFS spectra and all spectra were calibrated with respect to this point. Most samples were sufficiently rich in chlorine to obtain an adequate spectrum with a counting time of 1 sec/point; however, multiple spectra were run and summed to give a single spectrum with improved signal/noise ratio if the chlorine content was relatively low.

XAFS spectral analysis consisted of (i) calibration of the XAFS spectrum relative to the NaCl standard spectrum, (ii) subtraction of the pre-edge slope from the XAFS spectrum, and (iii) division of the spectrum into two distinct regions for the X-ray absorption near-edge structure (XANES) and the extended X-ray absorption fine structure (EXAFS). In this report, only the XANES data will be described.

RESULTS AND DISCUSSION

Liquefaction results: The liquefaction results are briefly summarized in Figures 1 and 2. Chemical compositions of the feedstock (CWP + PVC), the IOM samples and the oil products are given in Table 1. Two points should be noted regarding Figure 1. First, the yields are given as oil + gas, as the gas yields of all experiments was not determined. However, for most of the samples the gas yield was determined and found to be ≤5%. Second, the yields indicated for the CWP alone and the CWP + 1% HZSM-5 are for experiments that utilized a cold hydrogen pressure of 800 psig rather than 200 psig. It is seen that neither the oil + gas yields nor the total conversion were much affeeted by the presence of either PVC or HZSM-5 at 445 °C. Furthermore, the oil quality as reflected by the relative fractions of gasoline, kerosene and heavy oil does not vary dramatically. In general, there is some increase in both the quantity and quality of the oil produced with the addition of HZSM-5; at this relatively high temperature, however, the results of the thermal runs are almost as good as those of the catalytic runs. Perhaps the most significant result is the fact that the presence of 5% PVC does not appear to have any significant damaging effect on either oil yields or quality.

The distribution of the most critical elements(C, H, Ca, and Cl) in the IOM and oil samples is given in Table 1. It is seen that the addition of calcium hydroxide increased the amount of Cl retained in the IOM significantly, and somewhat more for the case where 1% HZSM-5 was added than for the thermal run. Similarly, the oil samples exhibited a decrease in Cl content when Ca was present. However, the decrease was larger for the thermal run than for the catalytic run. It should be emphasized that *none* of the oils would be acceptable in most refineries because of their relatively high Cl contents.

Cl XANES spectra: As shown in Figure 3, quite different chlorine XANES spectra were obtained from the oil and IOM fractions. Strong chlorine XANES spectra were also obtained from the AS+PA fractions, but they were closely similar to the IOM spectra obtained from the baseline situation (no catalyst, no Ca additive). The Ca additive appears to have little effect on the appearance of the Cl XANES spectra of the oil and AS+PA fractions; these spectra show relatively little variation. However, the Ca additive clearly did affect the appearance of the Cl XANES spectra of the IOM fractions. As shown in Figure 3, the sharp peak at -4.8 eV is much reduced in intensity when the Ca additive is present. The presence or absence of the HZSM-5 catalyst had relatively little effect on the appearance of the spectra.

The chlorine spectrum of the oil clearly arises from organochlorine species. The peak position of the first prominent sharp peak at -1.45 eV is consistent with data in the literature for organic chlorides[14], with the possible exception of aryl chlorides, which tend to have a more positive peak position in the range -1.0 to -0.5 eV. Furthermore, a similar sequence of three increasingly broader and weaker peaks at about -1.5 eV, 4 eV, and 12 eV is observed in a number of organochlorine compounds. In contrast, the chlorine spectrum of the IOM with the Ca additive is largely consistent with inorganic occurrences of chloride anions, and we have observed similar spectra from hydrated calcium chlorides. The prominent sharp peak observed at -4.8 eV observed in the spectra of all of the AS+PA fractions and of the two IOM fractions without Ca additive, however, is difficult to explain at this time and indicates a complication that cannot be explained by a simple separation of the PVC-derived chlorine into organic and inorganic chlorides. The width of the peak is narrow and

very similar to that observed for the organochlorine occurrence in the oil, but the remainder of the spectrum appears to be more like that of an inorganic chloride. Possibly, a chlorine occurrence based on the hypochlorite molecular anion (OCl^-) may offer an explanation for this peak.

It is also worth comparing the results obtained here with data obtained earlier[15] on coliquefaction of PVC-doped waste plastics with a North Dakota lignite. In those experiments, no organochlorine compounds were found in the oil; rather the chlorine XANES spectrum obtained from the oil was consistent with a hydrochloride adduct attached to presumably a quaternary nitrogen functionality in the oil derived from the coal. In the present coal-absent system, there is virtually no nitrogen to form such HCl adducts. Also, the Cl XANES indicated the formation of significant NaCl in the lignite/waste plastics/PVC experiments, suggesting that sodium may be a better sink for chlorine than calcium.

Acknowledgment

This research was supported by the U.S. Department of Energy through DOE contract No. DE-FC22-93-PC93053 as part of the research program of the Consortium for Fossil Fuel Liquefaction Science. We are grateful to Richard Anderson of the University of Kentucky Center for Applied Energy Research for assistance with liquefaction experiments and to Fulong Lu of the CFFLS for assistance with the XAFS experience.

References

1. B.O. Strobel and K-D. Dohms, *Proc. Int. Conf. Coal Sci, II*, 536-539(1993).
2. L.L. Anderson and W. Tuntawiroon, *Prepr.Pap.-Am. Chem. Soc., Div. Fuel Chem., **38(4)**,* 816-822(1993).
3. M.M. Taghiei, F.E. Huggins, and G.P. Huffman, *Prepr.Pap-Am. Chem. Soc., Div. Fuel Chem., **38(4)**,* 810-815(1993).
4. M.M. Taghiei, Zhen Feng, F.E. Huggins, and G.P. Huffman, *Energy & Fuels,* 1228-1232(1994).
5. G.P. Huffman, Zhen Feng, V. Mahajan, P. Sivakumar, H. Jung, J.W. Tierney, and I. Wender, *Prepr.Pap.-Am. Chem. Soc., Div. Fuel Chem.*, **40(1)**, 34-37(1995).
6. E.C. Orr, W. Tuntawiroon, W.B. Ding, E. Bolat, S. Rumpel, E.M. Eyring, and L.L. Anderson, *Prepr.Pap.-Am. Chem. Soc., Div. Fuel Chem.*, **40(1)**, 44-50(1995).
7. X. Xiao, W. Zmierczak, and J. Shabtai, *Prepr.Pap.-Am. Chem. Soc., Div. Fuel Chem.,* **40(1)**, 4-8(1995).
8. Z. Feng, J. Zhao, J. Rockwell, D. Bailey, and G.P. Huffman, "Direct Liquefaction of Waste Plastics and Coliquefaction of Coal-Plastic Mixtures," to be published in *Fuel Processing Technology.*
9. H.K. Loo and C.W. Curtis, "Catalytic Coprocessing of Plastics with Coal and Petroleum Resid using $NiMo/Al_2O_3$," to be published in *Energy & Fuels.*
10. M.S. Luo and C.W. Curtis, "Thermal and Catalytic Coprocessing of Illinois No. 6 Coal with Model and Commingled Waste Plastics," to be published in *Fuel Processing Technology.*
11. W.B. Ding, W. Tuntawiroon, J. Liang and L.L. Anderson, "Depolymerization of Waste Plastics with Coal over Metal-Loaded Silica-Alumina Catalysts," to be published in *Fuel Processing Technology.*
12. United Catalysts Inc., Post Office Box 32370, Louisville, KY 40232.
13. F. W. Lytle, R. B. Greegor, D. R. Sandstrom, E. C. Marques, Joe Wong, C. L. Spiro, G. P. Huffman, and F. E. Huggins, Nuclear Instruments & Methods, 226, 542-8 (1984).
14. F.E. Huggins and G.P. Huffman, *Fuel*, **1995**, *74*, 556-569.
15. F.E. Huggins, M.M. Taghiei, and G.P. Huffman, *Proceedings, Emerging Technologies in Hazardous Waste Management VI (Atlanta, GA)*, D.W. Tedder, Ed., American Chemical Society, Washington D.C., **1994**; pp. 993-996.

Table 1. Chemical composition of oils and IOM samples (wt. %).

IOM Samples	C	Ca	Cl
CWP-PVC	63	1.2	3.4
CWP-PVC-Ca	51	31	5.5
CWP-PVC, HZSM-5	45	0.7	3.9
CWP-PVC-Ca, HZSM-5	39	32	7.0
Oil Samples	C	H	Cl
CWP-PVC Feedstock	83	14	2.8
CWP-PVC	82	13	0.07
CWP-PVC-Ca	82	13	0.4
CWP-PVC, HZSM-5	84	12	0.1
CWP-PVC-Ca, HZSM-5	87	12	0.08

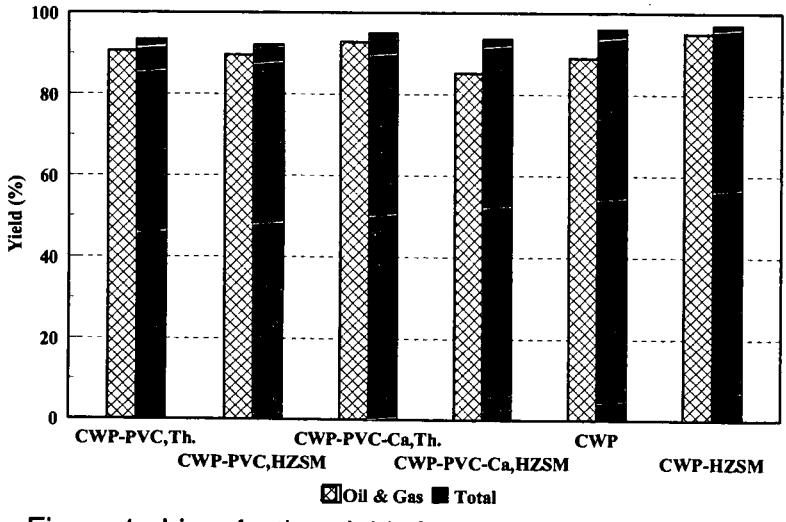

Figure 1. Liquefaction yields for the commingled waste plastic with and withoutadditions of PVC(5%), calcium hydroxide(5%), and HZSM-5(1%).

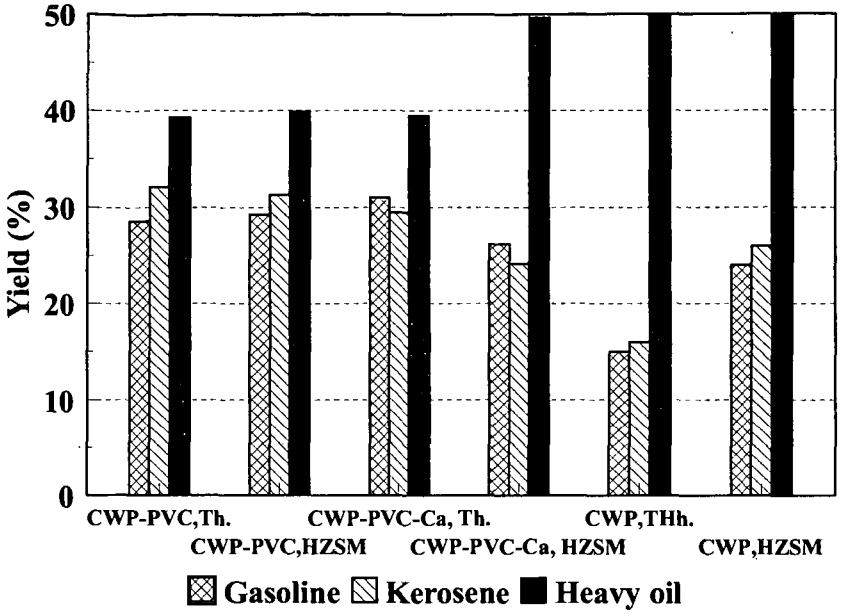

Figure 2. Simulated distillation analysis of the oil product from liquefaction of CWP with and without addition of PVC, calcium hydroxide, and HZSM-5.

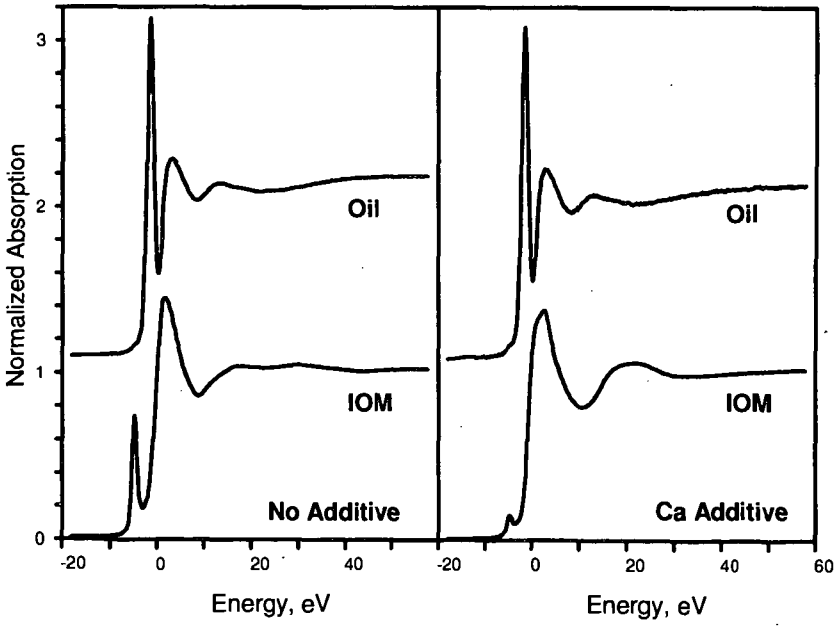

Figure 3. Chlorine K-edge XANES spectra of IOM and oil samples with and without calcium hydroxide additive.

COPROCESSING OF WASTE PLASTICS WITH COAL AND PETROLEUM RESID USING DIFFERENT CATALYSTS

Hyun Ku Joo and Christine W. Curtis
Chemical Engineering Department
Auburn University, AL 36849

Keywords: Coprocessing, petroleum resid, coal, waste plastics

INTRODUCTION

Waste plastics are a source of hydrocarbons that are currently not being used effectively. Only ~2% of the plastics are being recycled (Smith, 1995), and the remainder is being disposed of in landfills. Waste plastics are produced from petroleum and are composed primarily of hydrocarbons but also contain some antioxidants and colorants (Leidner, 1981). A number of problems are associated with the recycling effort, including convincing consumer households of the necessity to recycle, separating the waste plastics effectively for primary recycling of the plastic back to the monomer, and having sufficient waste plastic for processing, particularly in areas a far distance from the population centers. Tertiary recycling that results in the production of fuels and chemical feedstocks from waste plastics will provide an additional source of hydrocarbon fuels and chemical feedstocks. The addition of other hydrocarbon sources such as our most abundant U.S. hydrocarbon resource, coal, will provide a constancy of supply as well as an additional source of hydrocarbon fuels and feedstocks.

The direct coprocessing of coal and waste plastics is difficult because of chemical and processing incompatibility of the two materials (Luo and Curtis, 1996 a, 1996 b; Joo and Curtis, 1995, 1996). Typical household plastics waste consists of ~ 63% polyolefins (high and low density polyethylene (HDPE, LDPE)), 11% polypropylene, ~11%polystyrene, ~7% PET and 7% (Erwin and Henley, 1990), causing the wastes to be highly aliphatic. By contrast, coal is ~70% aromatic. These differences in chemistry result in the two materials being incompatible. Joo and Curtis (1996) have shown that heavy petroleum resid acts as an effective bridging solvent that when added to coal and waste plastics provides a medium for their mutual dissolution (Joo and Curtis, 1995, 1996).

The current research evaluated the effect of three different catalysts on the conversion and product distributions obtained from the coprocessing of coal, heavy petroleum resid, and waste plastics. The plastic used in this study was LDPE since it and its higher density form has been shown to be especially difficult to coprocess with coal (Luo and Curtis, 1996a). A hydrogenation catalyst with some hydrocracking activity is needed to convert coal and upgrade coal liquids and petroleum resid and a hydrocracking catalyst is required to break apart the bonds and make shorter chains of LDPE. Therefore, three different catalysts having these selectivities were employed in this study: presulfided $NiMo/Al_2O_3$, presulfided NiMo/zeolite, and Zeolyst Z-753, a hydrocracking catalyst. The addition of 10 wt % hydrocracking catalyst Z-732 to presulfided $NiMo/Al_2O_3$ was also examined to determine if adding some hydrocracking capacity to the system would increase the conversion and hexane soluble production of the plastics.

EXPERIMENTAL

Materials. The model plastic, low density polyethylene (LDPE), was obtained from Aldrich Chemical Co. and used as received. Blind Canyon DECS-17 bituminous coal was used in the study and obtained from the Penn State Coal Sample Bank. The proximate analysis of the coal is 45% fixed carbon, 45% volatile matter, 6.3% ash and 3.7% moisture. The ultimate analysis of the coal is 82.1% C, 6.2% H, 0.4% S, 1.4% N, and 0.12% Cl. The resid used was Manji obtained from Amoco. The analysis of the Manji resid is 85.1% C, 10.8% H, 0.7% N, 2.6% S, 231 ppm V, 220 ppm Ni and 23 ppm Fe. The solvents used for fractionation of the reaction products were HPLC grade hexane, toluene, and tetrahydrofuran (THF) from Fisher Scientific. Hexane solubles (HXs) were dissolved in carbon disulfide (CS_2) for simulated distillation.

The catalysts tested in this study were $NiMo/Al_2O_3$, NiMo/zeolite, and Zeolyst Z-753. The $NiMo/Al_2O_3$ catalyst from Shell was composed of 2.72 wt % Ni and 13.16 wt % Mo while the NiMo/Zeolite from Akzo was <25 wt % of molybdenum oxide and 1-10 wt % of nickel oxide with ultrastable zeolite. The Zeolyst Z-753 from Shell was composed of <60 wt % of amorphous silica, <15 wt % of tungsten oxide, <5 wt % of nickel oxide, <1 wt % of sodium oxide, and balanced alumina.

Reactions and Procedures. The reaction systems, LDPE, coal plus LDPE, and coal plus Manji plus LDPE, were studied to evaluate the activity of selected catalysts in coprocessing. Two sets of reactions were conducted: one set was performed with each of the two individual catalysts except $NiMo/Al_2O_3$ (Table 1) and the other with combined catalysts of $NiMo/Al_2O_3$ and Z-753. Reactions using a single catalyst and the same charging method as ones with combined catalyst were also performed for LDPE, coal/LDPE, and coal/Manji/LDPE systems to evaluate the effect of the catalyst combination (Table 2). For all reactions, reactants were charged at 1.0 g each for coal and polymer and 1.5 g for resid, giving resid to polymer and resid to coal ratios of 3:2 in the binary

systems and coal to resid to polymer ratios of 2:3:2 in the ternary systems. All reactions were performed using 1 wt % of powdered, presulfided $NiMo/Al_2O_3$ and NiMo/zeolite, and pretreated Z-753 on a total charge basis.

All reactions were performed in ~20 cm^3 stainless steel tubular microreactors at 400 °C or 430 °C for 30 or 60 min with 8.3 MPa of H_2 introduced at ambient temperature. The microreactors were agitated horizontally at 450 rpm in a fluidized sand bath and were immediately quenched in water after reaction. The coal was stored in a vacuum desiccator before being used.

The procedure for presulfiding $NiMo/Al_2O_3$ and NiMo/zeolite began with predrying $NiMo/Al_2O_3$ with N_2 for one hr at 300 °C. Then, 10 vol % H_2S/H_2 gas mixture was flowed over the catalyst at 225 °C for one hr, at 315 °C for one hr, and 370 °C for two hr. In the final step N_2 was flowed N_2 at 370 °C over $NiMo/Al_2O_3$ for one hr and turning off the furnace to room temperature. The pretreatment procedure for Z-753 involved heating the catalyst for two hr at 204 °C, and then increasing the temperature to 538 °C for two hr. After this, it was cooled down to room temperature. During the entire procedure, the catalyst was kept under a flow of N_2. All catalysts were stored in vacuum desiccator prior to use.

The reaction products were determined by using solvent fractionation and by weighing the gaseous products. The liquid products were fractionated using a series of solvents into hexane soluble materials (HXs); toluene soluble, hexane insoluble material (TOLs); and THF soluble, toluene insoluble material (THFs), and THF insoluble material or IOM which is defined as insoluble organic matter that is moisture and ash-free. The definition for conversion used in this study is the conversion of the reactant to THF soluble material.

$$\% \text{ conversion} = \left[1 - \frac{g\ IOM}{g\ maf\ total\ reactant} \right] \times 100 .$$

The coal is a solid at room temperature and is essentially insoluble in THF; LDPE is solid at room temperature and has limited solubility in THF (3.1%), while resid is a semi-solid at room temperature and are totally soluble in THF. The boiling point distribution of HXs were analyzed using ASTM D-2887 method. Detailed procedure can be referred to in the previous work (Joo and Curtis, 1996).

RESULTS AND DISCUSSION

The investigation of coprocessing waste plastics with coal and heavy petroleum resid was performed using two different sets of reactions: a set of reactions was performed in which LDPE was reacted at four different reaction conditions with presulfided NiMo/zeolite and Z-753 catalysts, and a second set was performed in which coal, resid, and LDPE were coprocessed with the two above mentioned catalysts and presulfided $NiMo/Al_2O_3$, as well as with a combination of 10 wt % Z-753 with presulfided $NiMo/Al_2O_3$. The measures that were used to evaluate the efficacy of the catalysts were conversion of the solids to THF solubles, product distribution in terms of HXs and THFs. The boiling point distributions of the products obtained in the HXs fractions were also determined and compared for the different catalytic systems.

Individual Reaction Systems. The conversion and product distributions of LDPE reactions with the two catalysts are given in Table 1 for Z-753 and presulfided NiMo/zeolite catalysts. The reaction conditions used were 430 °C, 60 min; 430 °C, 30 min; 400 °C, 60 min; and 400 °C, 30 min. A composite of the conversion and product distribution data for the two sets of catalytic LDPE reactions is given in Figure 1. Increased reaction time and temperature resulted in higher conversions for LDPE for both the Z-753 and presulfided NiMo/zeolite catalysts. For example, with Z-753 a conversion of 35.7% was achieved at 400 °C and 30 min but increased to 94.2% when 430 °C and 60 min was used. The highest production of hexane solubles yielding 69.7% also occurred at 430 °C and 60 min. Similar LDPE reaction behavior was observed for presulfided NiMo/zeolite catalyst, although its hydrocracking activity was higher than Z-753 as evidenced by the higher conversion to gases at all reaction conditions. LDPE conversion and hexane soluble production decreased somewhat with longer reaction time at the lower temperature for both catalysts, although the gas make remained fairly constant. Recoveries were low at the highest severity condition of 430 °C which was caused by the high volatility of the reaction products.

An experimental design analysis of a 2^k factorial which involved 3 factors (temperature, time, and catalyst) with each two levels (400 °C and 430 °C, 30 min and 60 min, Z-753 and NiMo/zeolite), respectively, was performed for this set of experiments to determine the factor that most affected the product distribution obtained (Table 2). For production of gas, the catalyst and reaction temperature were equally strong-effect factors. The yield of hexane solubles from LDPE as well as the conversion to THF solubles, was affected by temperature as the predominant effect factor but was also affected by a two-factor interaction of reaction temperature and time. This analysis clearly demonstrated the importance in selecting reaction temperature with proper catalyst and reaction time to obtain maximum amount of desirable product from LDPE liquefaction.

Coprocessing Reactions. Individual reactions of LDPE and coprocessing reactions with coal/LDPE and coal/Manji/LDPE were performed with the three previously described catalysts and with the combination of presulfided $NiMo/Al_2O_3$ with 10 wt % Z-753. The conversions and product

distributions for these systems at reaction conditions of 430 °C and 60 min are given in Table 3. These high severity conditions were selected on the basis of the LDPE liquefaction results from Table 1 and of the results previous reactions containing both coal and LDPE and in some cases resid which indicated that this severity was necessary to coprocess all three materials simultaneously (Joo and Curtis, 1995, 1996; Luo and Curtis, 1996 a, b).

The catalysts directly influenced the reactivity of the LDPE liquefaction and coprocessing systems although the composition of the systems also had a strong influence on both conversion and hexane soluble yield. The LDPE conversions and product distributions obtained were directly related to the hydrocracking propensity of the catalysts. The conversions increased from 69.6% for $NiMo/Al_2O_3$ to 76.2% with the 10 wt% Z-753 hydrocracking catalyst present. When hydrocracking catalysts were used exclusively, the reactions with Z-753 and NiMo/zeolite produced 94.2 and 93.1% conversion, respectively. Similarly, gas production increased with hydrocracking activity with the NiMo/zeolite yielding the highest amount. The Z-753 catalyst produced the highest hexane soluble yields and conversion while the stronger hydrocracking catalyst NiMo/zeolite produced more gas and less hexane solubles.

By contrast, the coal/LDPE reactions were not influenced by catalyst type. All of the catalysts gave very similar conversions, ranging from 41.3% to 43.5%. Similarly, the amount of gas produced and hexane soluble yields were similar for all of the catalysts. The catalysts appeared to be ineffectual in the system; however, results in our laboratory have indicated that increasing the time of the LDPE/coal reaction has a significant effect on the both conversion and product distribution (Joo, 1996). Extended reaction time experiments are currently being performed to determine the effect of these catalysts on this system.

Coprocessing reactions of coal/Manji/ LDPE were influenced by the catalyst type during the 60 min reaction time as was the LDPE system. The conversion increased from 61.7% for $NiMo/Al_2O_3$ to 69% for 10 wt% for Z-753 in $NiMo/Al_2O_3$ while 100% Z-753 gave a similar conversion of 68%. The highest conversion of 74.9% obtained was with NiMo/zeolite. The results from using the NiMo/zeolite catalyst showed the advantage of having the hydrocracking selectivity from the zeolite and the hydrogenation activity from the NiMo. The different catalysts did not have any differential effect on production of the hexane solubles from the three component coprocessing reactions. All of the catalysts with hydrocracking activity resulted in similar amounts. Only slight differences were observed in the gas production.

Simulated distillation of the hexane soluble fraction from each of these reactions was performed to determine the boiling point distribution of the products produced. The fractions that were determined were gasoline (~180 °C), naphtha (170 to 290 °C), heavy oil (260 to 350 °C), and lubricant (~300 to 370 °C) as shown in Table 4. The reaction of LDPE alone produced the largest amount of material boiling less than 370 °C while the reactions with LDPE and coal produced the lowest weight percent. The type of catalyst employed affected the weight percent of material boiling less than 370 °C for LDPE with the hydrocracking catalysts yielding the highest amounts, but catalyst type had little effect on the products produced from the other two types of reactions.

CONCLUSIONS

The coprocessing of LDPE with coal and petroleum resid was affected by catalyst type. The presence of hydrocracking selectivities during reaction increased conversion and production of hexane soluble materials in the LDPE reaction. Reaction temperature also strongly affected the conversion and the product slate in the LDPE reactions. None of the catalysts affected either the conversion or product distribution from the coal/ LDPE system at the reaction conditions used. Longer reaction time experiments are currently underway to determine if these catalysts influence the two component reaction to any appreciable extent. Simultaneous reactions of LDPE/resid and coal also responded to the different selectivities of the different catalysts. At reaction conditions of 60 min and 430 °C, catalysts with substantial hydrocracking activity yielded higher levels of conversion and hexane soluble material than did the reaction with $NiMo/Al_2O_3$. Catalysts, like NiMo/zeolite and the 10% Z-753 in $NiMo/Al_2O_3$, with combined hydrogenation and hydrocracking selectivities, affected the three component system most positively, producing the highest yields of hexane solubles and conversion to THF soluble materials.

REFERENCES

1. Erwin, L.; Healy, L.H., Jr. "Packing and Solid Waste Management Strategy" American Management Association, New York, 1990.
2. Joo, H. K., personal communication, 1996.
3. Joo, H. K.; Curtis, C. W. *Energy and Fuels*, in press, 1996.
4. Joo, H. K.; Curtis, C.W. *ACS Fuel Chem. Div. Prep.* 1995.
5. Leidner, J. "Plastics Waste," Marcel Dekker, Inc. 1981
6. Luo, M; Curtis, C. W. *Fuel Process. Techno.*, in press, 1996a.
7. Luo, M; Curtis, C. W. *Fuel Process. Techno.*, in press, 1996b.
8. Smith, R. Presentation at the Consortium for Fossil Fuel Liquefaction Science, Ninth Annual Meeting, Pipestem, WV, August 1995.

Table 1. Effect of Reaction Temperature and Time on Reactions with Different Catalysts[a]

Catalyst[b]	Product Distribution (%)					Conversion (%)	Recovery (%)
	gas[c]	HXs	TOLs	THFs	IOM		
430 °C, 60 min							
LDPE with Z	24.5±1.3	69.7±1.2	-	-	5.8±2.1	94.2±2.1	55.6±2.3
LDPE with NZ	37.1±1.2	56.0±1.3	-	-	6.9±2.6	93.1±2.6	54.9±2.8
430 °C, 30 min							
LDPE with Z	19.6±1.1	22.6±1.4	-	-	57.8±1.9	42.2±1.9	91.5±1.9
LDPE with NZ	28.5±0.8	23.7±1.6	-	-	47.9±1.8	52.1±1.8	84.6±0.7
400 °C, 60 min							
LDPE with Z	20.2±0.4	5.1±1.4	-	-	74.6±1.1	25.4±1.1	94.2±1.5
LDPE with NZ	22.1±0.7	6.5±0.9	-	-	71.5±2.0	28.5±2.0	92.1±1.7
400 °C, 30 min							
LDPE with Z	19.2±2.1	16.5±0.7	-	-	64.3±0.7	35.7±0.7	89.7±1.1
LDPE with NZ	22.7±1.7	9.4±1.1	-	-	67.9±1.4	32.1±1.4	94.1±2.4

[a] Reaction conditions : 8.3 MPa H_2 1g of reactant. 1 wt% catalyst of total feedstock.
[b] Z = Zeolyst 753 catalyst, NZ = NiMo/zeolite
[c] gas = gaseous products; HXs = hexane solubles; TOLs = toluene solubles; THFs = THF solubles; IOM = insoluble organic matter which is calculated on an ash-free basis.

Table 2. Factorial Design Analysis for LDPE Reaction with Two Different Catalysts

		A[a]	B	C	AB	AC	BC
gas	0	84.2	90.0	83.5	103.5	105.0	98.0
	1	109.7	103.9	110.4	90.4	88.9	95.9
	delta[b]	25.5	13.9	26.9	13.1	16.1	2.1
HX	0	37.5	72.2	113.9	151.6	101.3	101.6
	1	172.0	137.3	95.6	57.9	108.2	107.9
	delta	134.5	65.1	18.3	93.7	6.9	6.3
Conversion	0	121.7	162.1	197.5	255.1	206.3	199.5
	1	281.6	241.2	205.8	148.2	197.0	203.8
	delta	159.9	79.1	8.3	106.9	9.3	4.3

[a] A=temperature, B= time, and C=catalyst.
[b] The higher the **delta** is, the stronger effect that factor has.

Table 3. Effect of Catalyst Combination on Selected Coprocessing[a] Systems

Reaction Combination	Catalyst N, Z, or NZ[b]	Product Distribution (%)					Conversion (%)	Recovery (%)
		gas[c]	HXs	TOLs	THFs	IOM		
430 °C, 60 min								
LDPE	N	19.1±1.0	50.5±2.2	-	-	30.4±1.6	69.6±1.6	93.9±3.3
	10% Z in N	21.0±0.9	55.3±1.8	-	-	23.7±2.0	76.2±2.0	82.6±2.5
	Z	24.5±1.3	69.7±1.2	-	-	5.8±2.1	94.2±2.1	55.6±2.3
	NZ	37.1±1.2	56.0±1.3	-	-	6.9±2.6	93.1±2.6	54.9±2.8
Coal/LDPE	N	9.8±0.8	25.3±0.6	3.4±0.3	4.3±1.5	57.1±1.3	42.9±1.3	96.3±1.2
	10% Z in N	9.7±1.5	23.7±0.9	4.2±1.1	3.7±1.1	58.7±1.4	41.3±1.4	98.3±2.2
	Z	9.8±1.1	24.5±1.1	4.2±0.7	5.0±0.4	56.5±0.6	43.5±0.6	97.4±1.0
	NZ	10.7±1.9	23.9±0.8	3.5±0.6	4.2±0.5	57.7±2.8	42.3±2.8	97.7±1.1
Coal/Manji/LDPE	N	7.4±1.2	38.3±0.8	8.9±2.1	7.1±1.1	38.3±2.2	61.7±2.2	98.4±0.9
	10% Z in N	7.7±1.7	45.3±0.3	8.3±1.3	7.6±0.3	31.0±0.9	69.0±0.9	96.5±1.1
	Z	8.5±0.8	43.7±0.4	8.7±2.2	7.1±1.1	32.0±1.1	68.0±1.1	97.7±1.2
	NZ	8.4±0.4	45.2±2.1	9.5±1.1	11.8±0.9	25.1±2.3	74.9±2.3	96.5±2.4

[a] Reaction Conditions : 430 °C, 60min, and 8.3 MPa H_2 introduced at ambient temperature. Reactant loading : 1g of coal (Blind Canyon DECS-17), 1g LDPE, 1.5 g resid (Manji).
[b] N = Presulfided $NiMo/Al_2O_3$, Z = Pretreated Z-753, NZ=NiMo/Zeolite. 1 wt% catalyst loading on total charge basis.
[c] gas = gaseous products; HXs = hexane solubles; TOLs = toluene solubles; THFs = THF solubles; IOM = insoluble organic matter which is calculated on an ash-free basis.

Table 4. Simulated Distillation of Hexane Solubles from Coprocessing Reactions[a]

Catalyst[b]		Weight %					
		SIMREC[c]	Gasoline[d]	Naphtha	Heavy oil	Lubricant	Total with gas
LDPE	N	73.7	1.7±0.9	6.8±1.3	7.9±1.4	6.8±1.3	42.3±1.4
	10% Z in N	74.3	2.5±1.0	7.1±1.4	8.7±1.6	7.4±1.4	46.7±1.6
	Z	65.3	2.4±1.1	8.7±1.7	13.1±2.0	10.0±1.8	58.7±2.0
	NZ	52.5	2.1±0.8	5.4±1.2	7.6±1.4	5.6±1.2	57.8±1.4
Coal/ LDPE	N	51.4	0.9±0.4	2.1±0.6	3.0±0.7	2.3±0.6	18.1±3.0
	10% Z in N	59.9	0.8±0.4	2.3±0.6	3.5±0.8	2.7±0.7	19.0±3.5
	Z	57.8	0.9±0.4	2.6±0.6	3.4±0.7	2.6±0.6	19.2±0.7
	NZ	64.1	0.7±0.4	3.2±0.7	3.8±0.8	2.9±0.7	21.3±0.8
Coal/ LDPE/ Manji	N	63.8	1.2±0.6	5.1±1.0	5.7±1.1	4.6±1.0	24.0±1.1
	10% Z in N	65.0	1.7±0.8	5.7±1.2	6.5±1.2	5.4±1.1	27.1±1.2
	Z	65.5	1.2±0.7	6.1±1.2	7.0±1.3	5.6±1.1	28.3±1.3
	NZ	70.3	1.4±0.8	6.1±1.2	7.7±1.4	6.2±1.2	29.7±1.4

[a] 430 °C, 60 min. 8.3 MPa H_2. 1 wt % catalyst loading on the total charge basis. Reactant roading : 1g of coal (Blind Canyon DECS-17), 1g of LDPE, and 1.5g of Manji resid.
[b] N = NiMo/Al_2O_3, Z = Z-753, NZ = NiMo/Zeolite.
[c] SIMREC = Simulated distillation recovery.
[d] Gasoline ~180 °C, 170 °C < Naphtha < 290 °C, 260 °C < Heavy oil < 350 °C, 300 °C < Lubricant < 370 °C.

Figure 1. Product Distribution Trends for LDPE Reaction

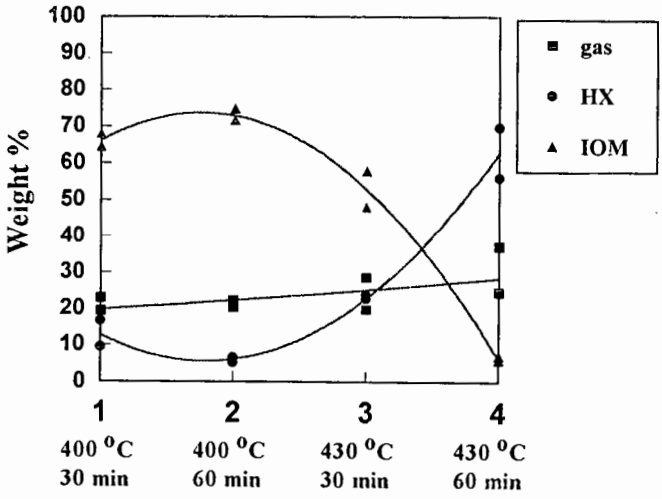

A KINETIC MODEL FOR CO-PROCESSING OF COAL AND WASTE TIRE

Dady B. Dadyburjor, Ramesh K. Sharma, J. Yang and John W. Zondlo
Department of Chemical Engineering
West Virginia University
P.O. Box 6102, Morgantown WV 26506-6102

Keywords: Kinetics, coal liquefaction, co-liquefaction.

ABSTRACT
Liquefaction of waste (recycled) tire and coal was studied both separately and using mixtures with different tire-to-coal ratios. Temperatures from 350-425°C were used. The data were analyzed using a model with a second-order consecutive reaction scheme (liquefaction to asphaltenes to oil and gas) for coal; a second-order conversion of tire to oil and gas; and an additional synergism reaction forming asphaltenes, first order in both coal and tire, when both are present. The agreement between the model and experiment was good.

INTRODUCTION

Disposal of used tires is a major environmental problem. Liquefaction of such tires in conjunction with coal has been suggested as an alternative to their disposal [1-3]. Farcasiu and Smith [1] studied the co-liquefaction of tire and Illinois #6 coal at 425°C and observed a synergistic effect of tire on coal conversion. Similar results were obtained at 400°C by Liu et al. [2] for the liquefaction of DECS-6 coal with a tire sample prepared from an used Goodyear Invicta tire. In all these studies a complete conversion of the volatile matter of the tire was obtained.

In this work, co-liquefaction of DECS-6 coal and a waste tire sample was studied at 350-425°C. Runs were made with tire and coal separately as well as by using mixtures with tire/coal ratios of 0-4. The hydrogen pressure was kept at 1000 psi (cold). The data were analyzed using a second-order consecutive reaction scheme for the liquefaction of coal to asphaltenes and then to oil and gas.

EXPERIMENTAL

The coal used was DECS-6 which is a high-volatile-A bituminous coal from the Blind Canyon seam in Utah. The tire sample was obtained from the University of Utah Tire Bank and represented mixed recycled tires ground to -30 mesh. The proximate and ultimate analyses showed that the coal contained 49% volatile matter (on a dry, ash-free basis) and 51 wt% fixed carbon. The amounts of volatile matter and fixed carbon in tire were 71 wt% and 29 wt%, respectively. The fixed carbon essentially represents the content of carbon black in the tire.

The details of the experimental equipment, run procedures and analytical techniques have been described earlier [4]. A stainless-steel tubing bomb reactor with a volume of 27 ml was used for the liquefaction. The reactor was loaded with the feed, purged and pressurized with H_2 to 1000 psi (cold). The feed consisted of tire or coal or a mixture of the two in different ratios. The gaseous products were collected and analyzed by gas chromatography. The solid and liquid products in the reactor were washed and extracted with tetrahydrofuran (THF) for 24h. The THF-insoluble material (TI) was separated by filtration. The conversion is calculated from the amount of THF-insoluble material. After the removal of THF by rotary evaporation, the THF-solubles were extracted with hexane for 2h. The extract was separated into hexane-insoluble (HI) and hexane-soluble (HS) fractions by filtration. The THF-soluble/ hexane-insoluble fraction, i.e. the HI fraction, represents asphaltenes. The HS fraction was the 'oil'. The oil yield was obtained by difference. In many cases, the combined oil + gas yield was calculated by difference. Most runs were made in duplicate and the experimental error was ±2.5%.

In the co-liquefaction runs, the overall conversion and the yields of asphaltenes and oil + gas fractions were calculated as above. However, in order to get a better insight, the results were also analyzed in terms of incremental conversion and yields, based on coal, which were calculated as follows;

$$X_{cm} = (X_{ov} - w_t X_t)/w_c \qquad (1)$$

where X_{ov} is the total conversion and w_t and w_c are the weight fractions of tire and coal in the feed, respectively. In equation (1), X_{cm} is the conversion of the mixture on a coal-alone basis and X_t is the conversion of tire alone under the same conditions. The yield of asphaltenes on a coal-alone basis was calculated similarly. The oil+gas yield from coal was calculated by difference.

RESULTS AND DISCUSSION

Effect of R_{TC} and Temperature

Figure 1 shows the effect of tire-to-coal ratio (R_{TC}) on conversion and oil+gas yield at 375°C. The results are presented on a coal-alone basis, i.e., the contribution of the tire has been subtracted. The conversion increases from 30% (at R_{TC}=0) to about 40% at R_{TC}=4. This indicates that the addition of tire has a synergistic effect on coal conversion. The synergistic effect is mainly towards the asphaltenes since the oil+gas yield is essentially unaffected by the addition of the tire.

The results at 400°C, presented in Figure 2, indicate a significant effect of R_{TC} on conversion, especially at low values of R_{TC}. The conversion of coal alone increases from 35% (without tire) to 49% when R_{TC}=1. At higher R_{TC} values, the addition of tire has only a small effect on coal conversion. There seems to be slight maximum in the conversion at R_{TC}~3, where the conversion is 54%. The decrease in conversion at high R_{TC} may be due to a low concentration of coal in the reaction mixture. The oil+gas yield decreases more-or-less linearly with increase in R_{TC}.

Similar observation are made from the results obtained at 425°C (Figure 3). In this case, the maximum conversion is over 70% at R_{TC}=1. The oil+gas yields at 425°C are also higher than those at 400°C.

Data Analysis

Since oil and gas are the major products of tire liquefaction, the liquefaction of tire (TR) is essentially represented by:

$$TR \xrightarrow{k_{tr}} OG \qquad (2)$$

For coal liquefaction, the experimental data suggest a predominantly consecutive reaction scheme with liquefaction of coal (C) to asphaltenes (A) and oil+gas (OG).

$$C \xrightarrow{k_t} A \xrightarrow{k_a} OG \qquad (3)$$

In the presence of the tire (TR), the conversions increase due to the synergism by the free-radical reactions between coal and tire. The synergism is mainly towards asphaltenes and is represented by:

$$C + TR \xrightarrow{k_s} A \qquad (4)$$

Now, the rates of conversion of tire (r_{tr}) and coal (r_c), and the rate of asphaltenes formation (r_a) are:

$$r_{tr} = k_{tr}C_{tr}^2 + k_sC_{tr}C_c \qquad (5)$$

$$r_c = k_tC_c^2 + k_sC_{tr}C_c \qquad (6)$$

$$r_a = k_tC_c^2 + k_sC_{tr}C_c - k_aC_a^2 \qquad (7)$$

where C_{tr}, C_c and C_a are the mass fractions of tire, coal and asphaltenes, respectively. In order to minimize the correlation between the activation energy and the pre-exponential factor, the rate constants were reparametrized to the form:

$$k = k(M)\ \exp[E\{1/T(M)-1/T\}/R] \qquad (8)$$

with k and k(M) being the values of the rate constant at T and T(M); E and R represent the activation energy and universal gas constant. The results are presented in Table 1. The rate constant for the liquefaction of tire (k_{tr}) is higher than that for the coal (k_t), as expected. The activation energies for both the liquefaction of coal and tire are low indicating a possible pore diffusion effect. The activation energy (E_a) for k_a was found to be not significantly different from zero indicating that the rate of asphaltene-to-oil+gas reaction is not dependent on temperature.

The experimental values of the overall conversion (of coal+tire) and overall yield (of oil+gas) are compared in Figure 4 with values calculated from the parameters of Table 1. The comparison seems satisfactory, considering the complexity of coal/tire co-liquefaction.
The model shows that the synergistic effect of tire is strongly dependent on the process conditions. Both the observed and predicted conversions decrease above 400°C when R_{TC} is 2. The oil+gas yields are governed mainly by the concentration of asphaltenes, increasing with an increase in asphaltene concentration.

CONCLUSIONS

1. The conversion and product yields from coal and tire are strongly dependent on temperature.
2. The co-liquefaction of tire with coal has a considerable synergistic effect on the conversion and asphaltene yield from coal. The synergism increases with an increase in tire/coal ratio, at least up to a tire/coal ratio of 1.
3. A consecutive reaction scheme for the conversion of coal to asphaltenes and oil+gas represents the data reasonably well at various temperatures and tire/coal ratios. The model uses second-order kinetics for the separate liquefaction of coal and tire and an overall second-order rate expression for the co-liquefaction (synergism reaction).

ACKNOWLEDGEMENT. This work was conducted under U.S. Department of Energy Contract No. DE-FC22-90PC90029 under the cooperative Agreement to the Consortium for Fossil Fuel Liquefaction Science.

REFERENCES

1. Farcasiu, M. and Smith, C.M. Prepr. Pap.- Am. Chem. Soc., Div. Fuel Chem. 1992, 37(1), 472.
2. Liu, Z., Zondlo, J.W. and Dadyburjor, D.B. Energy & Fuels 1994, 8(3), 607.
3. Tang, Y. and Curtis, C.W. Fuel Process Technol. 1996, 46, 195.
4. Sharma, R.K., Yang, J., Zondlo, J.W. and Dadyburjor, D.B. Fuel submitted.

Table 1. Summary of Kinetic Results[a]

Rate Constant	k(M)* [Min^{-1}]	Activation Energy [kJ.mole^{-1}]
k_{tr}	4.0±1.1	24.4±6.9
k_t	1.0±0.4	35.7±7.2
k_a	6.8±1.8	0
k_s	3.6±0.6	83.8±27.4

[a]±represents 95% confidence limits; *k at 673K.

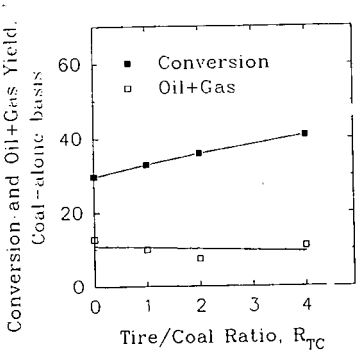

Figure 1. Effect of R_{TC} on co-processing of coal and waste tire at 375°C. Other conditions: 30 min, 1000 psi H_2 (cold).

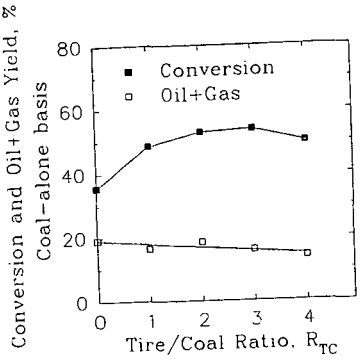

Figure 2. Effect of R_{TC} on co-processing of coal and waste tire at 400°C. Other conditions same as in Figure 1.

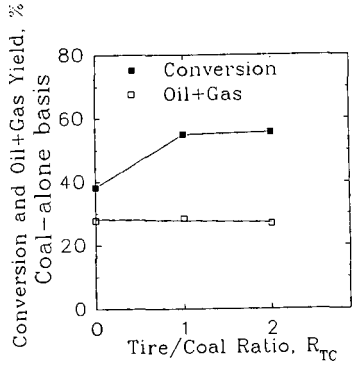

Figure 3. Effect of R_{TC} on co-processing of coal and waste tire at 425°C. Other conditions same as in Figure 1.

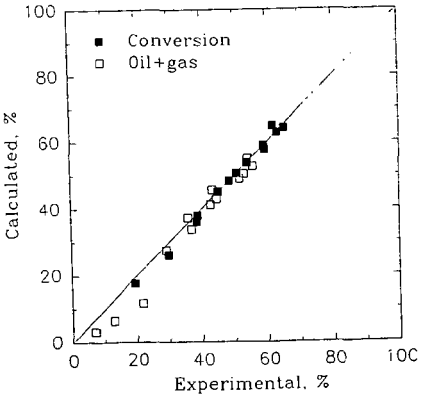

Figure 4. Comparison of the experimental and calculated values of the conversions and oil+gas yields from coal/tire co-processing

TWO STAGE COPROCESSING OF WASTE TIRES AND COAL

Ying Tang and Christine W. Curtis
Chemical Engineering Department
Auburn University, AL 36849-5127

Keywords: waste tires, coal, coliquefaction, coprocessing

INTRODUCTION

Waste tires present an insidious waste disposal problem since piles of waste tires often attract rodents and other varmints and frequently burn. Recent use of ground waste tires as a fill material for roads has resulted in oil being released from the tire after weathering and the tire fill erupting into flames. Therefore, safe and healthy disposal of waste tires is necessary and needs immediate attention since the Department of Energy has reported that 350 million waste tires are disposed of each year in the United States. A number of safe and useful waste tire processing technologies have been developed as alternatives to disposing in landfills. Waste tires have been used as fuel to generate electricity [1], as filler in asphalt road pavement,[2] and as raw material for secondary product production. [3] Waste tire pyrolysis [4-6] and liquefaction [7-12] are two technologies that can be applied to waste tires to produce fuels and chemical feedstock, thereby recycling the hydrocarbon base.

Several pyrolysis methods are being developed at pilot or industrial scale.[4] Cypres et al. [4] investigated the effect of pyrolysis conditions on the liquid product and found an increase of naphthalene and benzene with a decrease of the liquid fraction as the residence time increased. Merchant et al. [5] recovered solid material, primarily consisting of carbon black, from waste tire pyrolysis, activated the material, and used it for waste water treatment. Recently, Conesa et al.[6] examined gas production from scrap tires pyrolysis in a fluidized sand bed reactor. The yield of total gas was reported to increase in the range of 600-800 °C from 6.3 to 37.1%.

Waste tire liquefaction has been actively investigated in recent years. Farcasiu et al.[7] indicated that coprocessing waste tire with coal was beneficial for enhancing coal conversion. Liu et al.[8] investigated the liquefaction of coal and waste tire individually and compared the results to that of simultaneously coprocessing the two materials. The conversion obtained from the coprocessing reactions was greater than that achieved from combining the individual reactions. Orr et al. [9] also observed synergism in reactions where there was a 10 to 30% loading of waste tires to coal and the reaction occurred at 350 °C and in reactions at 430 °C at almost all loadings levels of waste tires. Tang and Curtis [10] performed thermal and catalytic coprocessing of waste tires and coal using waste tires from two sources and coals of three different ranks. The bituminous coals yielded higher conversions than either subituminous coal or lignite when coprocessed with waste tire. Catalytic coprocessing of waste tires with coal using slurry phase hydrogenation catalysts increased conversion of the total system and the coal within the system compared to the conversions obtained in thermal reactions. Orr et al. [11] coprocessed Blind Canyon coal with ground waste tire particles and vacuum pyrolyzed tire oil (PTO), respectively. Coprocessing of coal with PTO yielded higher coal conversion than coprocessing with ground waste tire particles. Badger et al. [12] evaluated hydrogen transfer in coal/oil coprocessing by coprocessing coal with heavy oil (petroleum) distillates (HOD) and pyrolyzed tire oil (PTO). HOD, being highly aliphatic, did not show any H-donation capability. By contrast, PTO, being highly aromatic and containing substantial phenanthrenes and substituted phenanthrenes but very little hydroaromatic compounds, could be induced to transfer hydrogen by hydrogen shuttling. PTO was more effective for dissolving coal after being prehydrogenated and, thereby, containing more hydroaromatic compounds.

The objective of the current research was to investigate the effect of two stage processing of waste tires and coal. The first stage served as a reaction medium by which waste tires were converted to liquids and the solids and where carbon black and other minerals can be removed from the system. In the second stage, the liquefied waste tire served as a solvent for coal and was coprocessed with coal under reaction conditions that were favorable for liquefying of coal and upgrading of coal liquids. Reaction conditions for producing high quality products from both reactions were examined. Both slurry phase and supported catalysts were used.

EXPERIMENTAL

Materials. Two stage reactions were performed by dissolving waste tires in waste oil in the first stage. The carbon black was removed from the liquid by filtration. The waste tire/oil liquid was used as the solvent for coal in the second stage. The waste tire used was supplied by Rouse Rubber industries, Vicksburg, MS. The waste oil was provided by Auburn Waste Oil Reprocessing Lab. The two coals utilized in this research were Beulah Zap lignite and Wyodak Anderson subituminous coal, both of which were obtained from the Argonne Premium Coal Sample Bank.

Catalytic reactions were performed using slurry phase hydrotreating catalyst, molybdenum naphthenate (MoNaph)(6% Mo), obtained from Shepherd Chemical. Elemental sulfur obtained from Aldrich was added to the catalytic reactions with MoNaph. A supported hydrotreating catalyst, $NiMo/Al_2O_3$ (SNiMo), supplied by Shell, was also used in this research. The catalyst was presulfided

prior to reaction by purging the catalyst with N_2 at 300 °C for 1 hr, then subjecting the catalyst to 10.1% H_2S/H_2 with a flow rate of 60 ml/min at 225 °C for 1 hr, followed by 315 °C for two hr, and then 370 °C for 1 hr.

Reaction Procedures. The first stage coliquefaction reactions of waste tires with waste oil were performed in approximately 60 cm^3 stainless steel tubular microreactors at 400 °C for 30 min. H_2 or N_2 was introduced at 6.9 MPa at ambient temperature. The total charge to the reactor was 12 g with the waste tire to waste oil ratio being 5:1 or 1:1. In the first stage catalytic coliquefaction reactions, MoNaph was charged at 1000 ppm of active metal per total reactor charge. Elemental sulfur was added to the catalytic reaction with MoNaph in a 3 to 1 stoichiometric ratio of sulfur to metal using the assumption that MoS_2 was formed. For the reactions with SNiMo, the catalyst loading was at 1.5 wt% of SNiMo powder on a total charge basis.

The second stage coprocessing reactions of coal with THF solubles obtained from the first stage reactions were conducted in approximately 20 cm^3 stainless steel microreactors at 400 °C for 30 min. The total charge to the reactor was 5 g with a solvent to moisture and ash free (maf) coal ratio being 1 to 1. In the second stage catalytic coprocessing reactions, the type and loading of the catalysts were the same as the first stage catalytic coliquefaction reactions.

Several reactions were performed by combining waste tire, waste oil, and coal in a single stage reaction at 400 °C for 30 min with initial H_2 pressure at 6.9 MPa. Rouse waste tire and waste oil were added to the reactor with tire to oil ratio at 5 to 1 or 1 to 1 in an amount that would produce 2 g THF solubles when the tire and oil were coliquefied without coal. In catalytic one stage reactions, SNiMo was charged to the reactor together with waste tire, waste oil, and coal at 1.5 wt% of the catalyst on a total charge basis.

Analysis. After reaction, gaseous products were determined by weighing the tubular microreactor before and after releasing gaseous products. The liquid and solid products were analyzed by solvent fractionation using sequential extractions of hexane and THF. The organic material that was not soluble in THF was defined as insoluble organic matter or IOM which was ash free.

RESULTS AND DISCUSSION

Two stage coprocessing of coal and waste tires was investigated to determine if more coal conversion and hexane soluble products could be produced if the waste tire was liquefied prior to contact with coal and the carbon black was removed. The first stage was a coliquefaction of waste tires with waste oil, the waste oil providing a dissolving medium for the tires. Two ratios of waste tires to waste oil, 5:1 and 1:1, were used. At the reaction conditions of 400 °C for 30 min, high conversions to THF soluble materials of the convertible material were obtained regardless of whether the atmosphere was H_2 or N_2. After reaction, the unconverted material, including carbon black and other mineral constituents in the tire, were removed. The THF soluble liquid was then used as the solvent for the second stage coal reaction.

Thermal Coprocessing Reactions Using First Stage Liquids as Solvents. Thermal reactions of Beulah Zap lignite and Wyodak subbituminous coal were performed with first stage liquids as well as waste oil, waste tire, and two hydroaromatic solvents, including tetralin and dihydroanthracene (DHA) as given in Table 2. The reactions with waste tire and/or waste oil were performed in H_2 while the reactions with tetralin and DHA were performed in N_2. The product distributions and the conversion of the materials were the measure by which the effectiveness of the solvent for liquefaction was determined. The total product distribution and total conversion measured the reactivity of the total system both the solvent and coal. By contrast, the product distribution on a coal basis and the coal conversion removed the effect of the solvent on these two measures, thereby describing how the coal itself reacted in the solvent.

The total conversions obtained for Beulah Zap lignite and Wyodak coal second stage reactions with first stage waste tire and oil solvents were similar and ranged from 64.2 to 67.3% for Beulah Zap and 63.9 to 69.2% for Wyodak. The total conversions with DHA and tetralin as solvents were somewhat higher but also similar and gave values of 74.6 and 72.8%, respectively. The total product distribution yields for gases, hexane solubles, and THF solubles were also similar for all of the reactions with waste tire and waste oil first stage liquids. However, tetralin yielded the highest hexane solubles, while DHA yielded the lowest. The reaction with DHA gave the largest amount of THF solubles of any of the reactions.

Coal conversions and, particularly, product distributions based on coal with the solvent effect removed showed more variability than those from the total values. Factors that affected coal conversion included type of coal used, atmosphere used in the first stage reaction, and ratio of waste tires to waste oil used in the first stage. The amount of hexane soluble and THF soluble material produced was also dependent on these factors. For lignite, coal conversion with solvents consisting of 5:1 ratio of waste tires to waste oil was greater than the 1:1 ratio regardless of the type of atmosphere used in the first stage reaction. Coal conversion was also higher when a H_2 atmosphere was used in the first stage rather than a N_2 atmosphere regardless of ratio. The coal conversion ranged from 34.2% for a 5:1 tires to oil ratio in the first stage reacted in H_2 to a low of 25.7% when a 1:1 ratio was reacted in a N_2 atmosphere. The ratio of waste tire to waste oil also strongly affected

the amounts of hexane solubles and THF solubles obtained with a given atmosphere. The higher ratio resulted in less hexane solubles and more THF solubles.

The factors that affected the second stage lignite thermal reaction also affected the Wyodak second stage reaction. Higher conversion was observed with first stage having a 5:1 ratio and when reacted in H_2. Reactions were performed with the individual reactants as well. Waste tires as a solvent gave a Wyodak conversion of 40.2 % while waste oil yielded 34.1%. The hexane solubles based on coal were higher with the higher ratio of 5:1 and a H_2 atmosphere in the first stage reaction.

Hydrogen donation to coal by solvents derived from waste tires during liquefaction is feasible since these solvents contain aromatic oil that can be hydrogenated to form hydroaromatics during coprocessing. Badger et al. (1994) evaluated H-donation to coal using solvent produced from the pyrolysis of waste tires. The pyrolyzed oil itself was ineffectual in converting coal even in a H_2 environment. Prehydrogenating the waste tire liquids was effectual for H-donation if the extent of prehydrogenation was not too great, since too much hydrogenation decreases the hydrogen donor capability of the solvent. (Badger et al., 1994; Curtis et al., 1981) In the current study, hydrogen donation from liquefied waste tires to coal was evaluated by comparing the coal conversion obtained in a liquefied waste tire/waste oil solvent to that obtained with tetralin and DHA in a N_2 atmosphere. The highest coal conversions, 48.7 and 44.5%, respectively, were achieved with these hydrogen donors, thereby indicating that the waste tire/waste oil solvents were much inferior hydrogen donors.

Catalytic Two Stage Coprocessing. The low total and coal conversions obtained from thermal two stage coprocessing clearly showed the need for introducing catalysts into one of the stages. Table 3 presents the conversions and product distributions from two stage reactions with catalysts being introduced separately in the first and second stage. Sulfided $NiMo/Al_2O_3$ and MoNaph plus excess S catalysts were each added to the second stage of the two stage reaction using Wyodak coal. The total conversion for the SNiMo catalyst ranged from 79.7 to 86.5% while higher total conversions were observed for the second stages with MoNaph + S, ranging from 94.5 to 95.2%. The coal conversion using SNiMo catalysts resulted in higher conversion, which ranged from 61.5 to 73.1%, than the thermal reaction which ranged from 25.6 to 40.5%. The MoNaph was even more effective since reactions with MoNaph + S and coal resulted in coal conversion which ranged from 89.8 to 91.2%. Reactions performed with solvents of the 5:1 ratio of waste tires to waste oil that had been liquefied in a H_2 atmosphere yielded the highest conversions with each catalyst. However, when either catalyst was added to the first stage, neither was effectual resulting in low total conversions of ~68% and coal conversion of ~40 to 41 %. These low two stage conversions showed that adding the catalyst to the first stage resulted in conversion values that were similar to thermal reactions. These results strongly indicated that the catalysts were deactivated by contact with the waste tires while they were being liquefied.

Comparison of One and Two Stage Coprocessing. A comparison of one and two stage coprocessing reactions is given in Table 4 where thermal and catalytic reactions of Wyodak coal performed under equivalent conditions but using different staging are given. The catalyst used in the comparison is SNiMo. The separation of the tire liquefaction reaction from the coal liquefaction reaction dramatically improved the efficacy of the catalyst. At a 5:1 ratio of waste tire to waste oil, the thermal conversion was higher in the single stage reaction than in the two stage reaction. However, the addition of the catalyst in the single stage reaction resulted in only minimal improvement of less than 2% conversion, while a substantial increase in conversion (32.6%) was observed when the catalyst was added to second stage of the two stage reaction. In addition, the observation can be made that the less contact between liquefying waste tire and catalyst, the better the overall conversion obtained. The single stage conversions with the catalyst with a waste tire to waste oil ratio of 1:1 were higher than the reactions with ratios of 5:1. These results emphasize the detrimental effect on catalytic activity that resulted from direct contact between the liquefying waste tire and the hydrotreating catalysts.

SUMMARY AND CONCLUSIONS

The advantage of two stage coprocessing of waste tires with coal was most apparent when a catalyst was used. The introduction of a hydrotreating catalyst in the second stage resulted in improved overall conversion and coal conversion. The slurry phase Mo naphthenate catalyst was more effective than the supported $NiMo/Al_2O_3$ catalyst when added to the second stage. In the second stage, the catalyst contacted waste tire that had been already liquefied and whose carbon black and mineral constituents had been removed, and, hence, the catalyst suffered less deactivation.

The waste tire itself was a reasonably effective solvent for coal dissolution but did not provide much H-donor capability. The result was clearly observed when the conversions obtained with liquefied waste tires were benchmarked against these obtained with known H-donors. Increased reactivity of the waste tire solvent for coal dissolution may be possible by pyrolyzing and prehydrogenating the waste tire. This research is currently underway.

REFERENCES

1. Tesla, M.R., *Power Engineering*, 1994, May, 43-44.
2. *Paul J. Kirk-Othmer Encyclopedia of Chemical Technology*, Wiley, New York, 1982, Vol198, 1002-1010.
3. Orgasawara, S.; Kuroda, M.; and Wakao, N., *Ind. Eng. Chem. Res., 26*, 1987, 2552-2556.
4. Cypres, R.: Bettems, B. in Pyrolysis and Gasification, Ferrero, G.L.; Maniatis, K.; Buekens, A.; Bridgwater, A.V., Editors, Elsevier Applied Science, London, 1989, p 209.
5. Merchant, A.A.; Petrich, M.A., AICHE J. 1993, 39(8), 1370.
6. Conesa, J. A.; Font, R.; Morcilla, A., *Energy and Fuels*, 1996, 10, 134-140.
7. Farcasiu, M.; Smith, C.M., *ACS Fuel Chem Div Prepr., 37,1,* 1992, 472-479.
8. Liu, Z.; Zondlo, J.W.; Dadyburjor, D.B., Energy Fuels, 8(3), 1994, 607-12.
9. Orr E.C.; Tuntawiroon, W.: Anderson, L.L., Eyring, E.M., *ACS Fuel Chem Div Prepr.,39,* 1994, 1065-1072.
10. Tang, Y., Curtis, C. W., *Fuel Processing Technology, 46,* 1996, 195-215.
11. Orr, E.C.; Burghard, J. A.; Tuntawiroon, W.; Anderson, L. L.; Eyring E. M., *Fuel Processing Technology,* 1996, in press.
12. Badger, M.W.; Harrison, G.; Ross, A.B., Presentation at 208th National Meeting, ACS, Washington, D.C.,1994, August 21-26.
13. Curtis, C.W.; Guin, J.A.; Jeng, J.F.; Tarrer, A.R. *Fuel, 60,* 677-783, 1981.

Table 1. Thermal Coliquefaction of Waste Tires with Waste Oil[a]

Reactants	Ratio (wt)	THF Solubles (wt%)		Conversion (wt%)	
		Total	Tire	Total	Tire
6.9 MPa of H_2 at ambient temperature					
RWT/WO[b]	5:1	94.2±1.2	93.1±1.6	96.2±1.3	95.7±1.4
RWT/WO	1:1	95.5±0.4	92.4±0.5	97.5±0.8	93.5±0.9
6.9 MPa of N_2 at ambient temperature					
RWT/WO	5:1	93.0±1.4	91.5±1.8	95.5±1.5	93.9±1.9
RWT/WO	1:1	94.7±0.9	90.2±1.2	96.6±1.0	91.3±1.0

[a] Coliquefaction reaction conditions: 400°C, at 6.9 MPa H_2 and N_2, for 30 min, total charge 12 gram with ratio of waste tire to waste oil being 5 to 1 and 1 to 1.
[b] RWT=Rouse waste tire provided by Rouse Company, WO=waste motor oil provided by Auburn Waste Oil Reprocessing Lab.

Table 2. Thermal Coprocessing Reactions of Coals with the Liquids Obtained by First Stage Coliquefaction of Waste Tire and Waste Oil[a]

Liquid Source	Coal	Product Distribution (wt%)						Conversion (%)	
		Total			Coal				
		GAS	HEXS[b]	THFS[b]	GAS	HEXS	THFS	Total	Coal
WO[b]	BZ[b]	3.9±0.3	51.1±1.0	12.3±1.1	5.3±0.6	4.8±2.9	24.6±2.7	67.3±2.2	34.7±1.3
RWT/WO 5/1 H_2[c]		4.9±0.5	44.0±0.8	16.6±1.0	6.9±0.9	3.2±2.3	24.1±2.5	65.5±2.0	34.2±1.1
RWT/WO 1/1 H_2		4.3±0.2	50.1±1.1	10.1±1.3	6.0±0.5	11.3±3.0	13.0±3.2	64.5±2.5	30.3±1.4
RWT/WO 5/1 N_2		4.6±0.4	47.3±0.6	13.2±0.9	6.6±0.8	5.8±1.8	18.1±2.3	65.1±1.7	30.5±0.9
RWT/WO 1/1 N_2[c]		4.8±0.6	54.0±1.3	5.4±0.6	7.2±1.1	15.1±3.4	3.4±1.5	64.2±1.9	25.7±1.6
Tetralin with N_2	WY[b]	2.1±0.4	63.1±1.6	9.2±0.9	2.3±0.4	28.0±2.0	18.4±1.7	74.6±2.7	48.7±3.4
DHA with N_2		3.0±0.6	45.4±1.4	24.4±1.1	4.2±1.1	37.6±1.8	2.7±1.3	72.8±2.9	44.5±3.2
RWT		3.2±0.2	51.1±1.0	14.3±0.9	3.8±0.4	16.7±2.3	19.7±1.8	68.6±1.8	40.2±1.9
WO		3.5±0.4	54.9±1.4	8.1±0.8	4.4±0.8	13.8±1.5	15.9±2.0	66.5±2.4	34.1±2.0
RWT/WO 5/1 H_2		3.4±0.2	54.0±0.7	11.8±0.3	4.1±0.5	21.4±0.9	15.0±0.5	69.2±1.0	40.5±1.4
RWT/WO 1/1 H_2		3.8±0.3	52.1±1.0	8.4±1.0	5.0±0.5	15.4±1.0	9.5±1.9	64.3±2.0	29.9±2.9
RWT/WO 5/1 N_2		3.0±0.2	52.5±0.8	11.7±0.8	3.4±0.5	19.7±1.3	14.7±0.9	67.2±1.9	37.8±2.0
RWT/WO 1/1 N_2		3.6±0.5	52.5±1.2	7.8±0.8	4.6±0.8	12.5±1.1	8.5±1.5	63.9±1.6	25.6±2.5

[a] Reaction conditions: 400°C, 30 min, 6.9 MPa H_2 at ambient temperature, 2 g maf coal, maf coal:solvent=1:1.
[b] HEXS=hexane solubles; THFS= THF soluble and Hexane insolubles;
BZ=Beulah-Zap lignite; WY=Wyodak subbituminous coal; RWT= Rouse waste tire provided by Rouse Company;
WO= waste motor oil supplied by Auburn Waste Oil Reprocessing Lab.
[c] RWT/WO 5/1 H_2 = the liquid(THF solubles) obtained by first stage coliquefaction of Rouse waste tire and waste oil at 400 °C, in 6.9 MPa initial H_2, at waste tire:waste oil=5:1, for 30 min, then extracting the product with THF;
RWT/WO 1/1 N_2 = the liquid(THF solubles) obtained by first stage coliquefaction of Rouse waste tire and waste oil at 400 °C, in 6.9 MPa initial N_2 at waste tire:waste oil=1:1, for 30 min, then extracting the product with THF.

Table 3. Coprocessing Reactions of Wyodak Coal with the Liquids Obtained by Coliquefying Waste Tires and Waste Oils Thermally and Catalytically[a]

Liquid Source	Catalyst	Product Distribution (wt%)						Conversion (%)	
		Total			Coal				
		GAS	HEXS[b]	THFS[b]	GAS	HEXS	THFS	Total	Coal
Catalyst added in the second stage but not in the first stage									
RWT/WO 5/1 H_2[c]	SNiMo	4.8±0.8	50.0±1.7	31.7±1.2	7.0±1.6	11.3±3.2	54.8±2.3	86.5±2.8	73.1±3.3
RWT/WO 5/1 N_2		2.7±0.3	52.7±1.6	24.3±0.6	2.9±0.6	20.1±1.8	38.5±0.8	79.7±1.8	61.5±2.6
RWT/WO 1/1 H_2		3.9±0.7	52.0±1.6	26.0±1.1	5.1±1.3	18.1±2.8	42.6±2.1	81.9±2.6	65.8±2.9
RWT/WO 5/1 H_2	MoNaph+S	4.0±0.6	48.6±1.3	42.6±0.9	5.0±1.0	14.6±2.4	71.6±1.7	95.2±2.1	91.2±2.5
RWT/WO 5/1 N_2		2.6±0.4	53.7±1.9	38.2±1.1	2.8±0.7	23.1±3.4	63.9±1.9	94.5±3.0	89.8±3.4
RWT/WO 1/1 H_2		3.5±0.7	55.1±1.5	36.3±1.0	4.3±1.3	22.0±2.8	63.8±1.8	94.9±2.6	90.1±3.0
Catalyst added in the first stage but not in the second stage									
RWT/WO 5/1 H_2	SNiMo	3.2±0.3	52.1±1.2	12.8±1.0	3.6±0.7	20.0±2.3	16.6±1.8	68.1±2.2	40.3±3.0
RWT/WO 5/1 H_2	MoNaph+S	3.4±0.7	50.5±0.9	15.0±0.7	4.1±1.2	17.0±1.7	20.7±1.5	68.9±1.6	41.8±2.8

[a] Coprocessing Reaction conditions: 400°C, 30 min, 6.9 MPa H_2 and N_2 at ambient temperature, 2 g maf Wyodak coal, maf coal:solvent = 1:1, SNiMo 1.5wt%; MoNaph 1000 ppm Mo, S:Mo=6:1.

[b] HEXS=hexane solubles; THFS= THF soluble and hexane insolubles.
RWT= Rouse waste tire provided by Rouse Company.
WO=waste motor oil supplied by Auburn Waste Oil Reprocessing Lab.

[c] RWT/WO1 5/1 in H_2=the liquid(THFS) obtained by coliquefying Rouse waste tire and waste oil at 400 °C, in 6.9 MPa initial H_2, at waste tire:waste oil=5:1, for 30 min, then extracting the product with THF. For catalytic coliquefaction, SNiMo(1.5 wt%) and MoNaph+S(1000 ppm, S:Mo=6:1).

Table 4. Comparison of Single and Two Stage Thermal and Catalytic Coprocessing Reactions of Wyodak Coal with Waste Tire and Waste Oil[a]

Reactants	Catalyst	Product Distribution (wt%)						Conversion (%)	
		Total			Coal				
		GAS	HEXS[b]	THFS[b]	GAS	HEXS	THFS	Total	Coal
Two Stage Reaction									
WY+(RWT/WO 5/1/H_2)[c]	None	3.4±0.2	54.0±0.7	11.8±0.3	4.1±0.5	21.4±0.9	15.0±0.5	69.2±1.0	40.5±1.4
WY+(RWT/WO 5/1/H_2)	SNiMo	4.8±0.8	50.0±1.7	31.7±1.2	7.0±1.6	11.3±3.2	54.8±2.3	86.5±2.8	73.1±3.3
WY+(RWT/WO 1/1/H_2)	None	3.8±0.3	52.1±1.0	8.4±1.0	5.0±0.5	15.4±1.9	9.5±1.9	64.3±2.0	29.9±2.9
WY+(RWT/WO 1/1/H_2)	SNiMo	3.9±0.7	52.0±1.6	26.0±1.1	5.1±1.3	18.1±2.8	42.6±2.1	81.9±2.6	65.8±2.9
One Stage Reaction									
WY+RT+WO(T/O 5/1)[c]	None	5.8±0.5	41.0±1.1	24.0±1.2	5.5±0.6	1.4±0.3	40.9±2.4	70.7±1.3	47.8±2.0
WY+RT+WO(T/O 5/1)	SNiMo	6.7±0.6	44.7±1.7	22.1±1.4	7.1±1.0	2.4±0.4	39.9±2.1	73.5±1.7	49.5±1.9
WY+RT+WO(T/O 1/1)	None	5.5±0.2	42.4±1.5	25.5±1.8	5.0±0.8	6.0±0.5	44.6±2.7	73.3±1.9	50.2±2.8
WY+RT+WO(T/O 1/1)	SNiMo	6.2±0.4	48.0±1.8	22.8±1.5	6.5±1.2	4.6±0.4	42.5±2.1	77.0±2.0	53.6±2.7

[a] Reaction conditions: 400°C, 30 min, 6.9 MPa H_2 at ambient temperature, 2 g maf Wyodak coal, maf coal:solvent(THF solubles) = 1:1.

[b] WY=wyodak coal;
RWT=Rouse waste tire;
WO=waste oil from Auburn Waste Oil Reprocessing Lab;
HEXS=hexane solubles;
THFS= THF solubles;
SNiMo= presulfided $NiMo/Al_2O_3$

[c] For two stage reactions, (RT/WO 5/1 H_2)= THF Solubles obtained from the first stage reaction with Rouse waste tire to waste oil ratio of 5 to 1 in H_2; For one stage reactions, RT+WO(T/O 5/1)= Rouse waste tire with waste oil at tire to oil ratio of 5 to 1 in an amount that would produce 2 g THF solubles.

POLYETHYLENE DEGRADATION IN A COAL LIQUEFACTION ENVIRONMENT

Kurt S. Rothenberger, Anthony V. Cugini, and Robert L. Thompson
U.S. Department of Energy, Pittsburgh Energy Technology Center,
P.O. Box 10940, Pittsburgh, PA 15236

KEYWORDS: polyethylene, liquefaction, waste coprocessing.

INTRODUCTION

The coprocessing of coal with waste materials such as plastic has shown promise as an economical means to recover the inherent value of the wastes while producing useful products. Polyethylene (PE) is one of the dominant plastic materials; recent statistics indicate that low- and high-density PE together make up about half of all municipal plastic waste.[1] The degradation of PE in a pyrolysis environment has been well studied,[2] and pyrolysis-based methods for the conversion of PE to fuels have been published.[3] However, recent studies have shown that PE is among the most difficult plastics to convert in the traditional liquefaction environment, particularly in the presence of coal and/or donor solvents.[4] The coal liquefaction environment is quite different than that encountered during thermal or catalytic pyrolysis. Understanding the degradation behavior of PE in the liquefaction environment is important to development of a successful scheme for coprocessing coal with plastics.

In this paper, a novel analytical method has been developed to recover incompletely reacted PE from coprocessing product streams. Once separated from the coal-derived material, gel permeation chromatography, a conventional polymer characterization technique, was applied to the recovered material to ascertain the nature of the changes that occurred to the PE upon processing in a bench-scale continuous liquefaction unit. In a separate phase of the project, 1-L semi-batch reactions were performed to investigate the reactivity of PE and coal-PE mixtures as a function of temperature.

EXPERIMENTAL SECTION

Materials. Liquefaction experiments were conducted using -200 mesh Black Thunder mine coal (Wyodak-Anderson seam, Campbell County, WY). High-density polyethylene (PE; T_m = 135 °C, d = 0.96 g/mL) was supplied by Solvay Polymers. Polystyrene (PS; T_m = 95 °C, d = 1.0 g/mL) was supplied by BASF. Polypropylene (PP; T_m = 176 °C, d = 0.94 g/mL) was supplied by Amco Plastics. The same plastics were used in both the semi-batch experiments and the bench-scale continuous run. All plastics were supplied as 3.2 mm (0.125 in) extruded pellets. A mildly hydrogenated petroleum-derived oil, containing small amounts of coal derived liquid, was used as a solvent in the semi-batch coprocessing tests. The bench scale continuous unit run was started up on a similar solvent but then operated in a recycle mode. An aged Ni-Mo catalyst supported on alumina in the form of 1/16" extrudates (AO-60) was supplied by Akzo and used in the semi-batch tests. Both molybdenum and iron based catalysts were used in the bench-scale continuous run. Tetrahydrofuran (THF) and dichloromethane (CH_2Cl_2) solvents used in work up and/or extraction procedures were obtained in bulk grade and used without further purification. Decane fraction (bp 171-177°C), used in the PE recovery procedure, was obtained from Fluka Chemie AG and used without further purification.

Reactions. Semi-batch tests were performed in a 1-L stirred-tank reactor system.[5] Sample work-up and feed conversions were calculated by a procedure described previously.[6] Samples were obtained from a bench scale continuous mode run performed on a close-coupled, two-stage, catalytic reactor system, and operating as part of the U.S. Department of Energy's coal liquefaction program. A simplified schematic diagram of the continuous unit configuration is shown in Figure 1. Samples were obtained from the following points, identified in Figure 1: (1) feed slurry, (2) first reactor, (3) second reactor, (4) atmospheric still bottoms, (5a) vacuum still overhead, and (6a) vacuum still bottoms, or (5b) pressure filter liquid, and (6b) pressure filter solids. Samples were taken during three different coprocessing run conditions, identified by the feed type: (1) coal mixed plastics in a 2:1 ratio (67% coal, 13% PE, 11% PP, 9% PS), (2) coal:PE in a 2:1 ratio, and (3) coal:plastics in a 1:1 ratio (50% coal, 20% PE, 16.5% PP, 13.5% PS).

Extraction of Incompletely Reacted PE from Bench Scale Continuous Unit Process Streams. In order to more thoroughly investigate the behavior of PE in a coal liquefaction system, a general method was devised to recover incompletely reacted PE

from coal liquefaction process streams. The method is diagrammed in Figure 2. The first step involved a cold THF wash to remove as much soluble coal-derived material as possible without affecting the incompletely reacted PE. In fact, this step alone was sufficient to isolate PE from a tarry stream that contained no insoluble coal matter (e.g., a non-ashy recycle stream).[7] The THF insolubles were then subjected to a hot decane extraction; the decane fraction dissolved the incompletely reacted PE, but left the coal derived solids behind. After the hot decane was filtered and concentrated, a dichloromethane wash was used to remove any remaining coal derived materials and aid in formation of an beige, powdery solid. The method also removes other polyolefins, such as PP. The method was applicable to a wide range of process streams including tars, solids, and multi-phase mixtures.

The process samples containing unreacted PE existed either as solids or as viscous tars. If solid, the sample was crushed in a mortar and pestle prior to the extraction procedure. If tar, the sample was heated in an oven at low temperature (<100°C) and poured into a reaction flask. The procedure began by digesting the solid co-processing residue in THF. The sample (5-25 g) was placed into a Whatman cellulose Soxhlet thimble (25 mm od x 100 mm), submerged in THF (ca. 250 mL) within a beaker and sonicated for about 1 hr at ambient temperature. At this point the THF solution had turned dark brown with soluble coal-derived material. After the THF was removed, the thimble was placed in a Soxhlet extraction apparatus and exhaustively extracted with another 500 mL of fresh THF. This extraction typically required 24 hr before the washings become colorless.

The THF insoluble material (at this point typically 1-10 g) were vacuum dried inside the extraction thimble in an oven at 50°C to evaporate any residual THF, then transferred to a 500 mL flask along with ca. 300 mL decane fraction (bp 171-177°C), used as received from Fluka Chemie AG. The mixture was refluxed under flowing nitrogen (preventing atmospheric oxygen from coming into contact with the hot decane solution) for 1 to 2 days to digest the PE. The *boiling hot* decane solution was then filtered through a fresh cellulose Soxhlet thimble (43 mm od x 125 mm) to give a black solid and a viscous yellow filtrate containing the incompletely reacted PE. The decane was evaporated under reduced pressure on a rotary evaporator at 70°C to yield a yellow to yellow-brown filmy residue which adhered to the walls of the flask.

After addition of ca. 300 mL CH_2Cl_2, the residue was then scraped from the walls of the flask and sonicated at ambient temperature for 1 hr. After sonication the CH_2Cl_2 had become yellow and the residue had formed flocculent particles and flakes. The mixture was filtered through a medium-porosity glass frit to give a light beige to tan solid and yellow CH_2Cl_2 filtrate. The beige incompletely reacted PE product was vacuum dried in an oven at 50°C until constant weight.

Gel Permeation Chromatography (GPC). GPC of the recovered PE samples was performed by Jordi Associates, Inc., of Bellingham, MA. Samples were dissolved in trichlorobenzene at 145°C, and analyzed on a Waters 150C high pressure liquid chromatograph, equipped with a mixed bed linear column (prepared at Jordi) and refractive index detector. Calibration was done with polystyrene standards. Molecular weight distribution parameters M_n, the number average molecular weight, and M_w, the weight average molecular weight, were provided by the data acquisition and handling software at Jordi. For convenience in interpreting samples with bimodal molecular weight distributions, the maximum points in the distribution curves (i.e., the most frequently occurring molecular weight values) were calculated at PETC.

RESULTS AND DISCUSSION

The efficacy of a coal liquefaction procedure is generally measured in terms of conversion, usually defined in terms of solubility in a given solvent or distillation at or below a given endpoint. Although this is a functional way of evaluating a set of processing parameters, it reveals little about the chemical nature of the species involved in the reactions. The ability to isolate and recover unconverted PE from a coal-plastics coprocessing stream affords the ability to characterize it withour the complexity of the coal and coal derived products. This yields a significant opportunity to understand the degradation of PE in the coal liquefaction environment.

The PE recovery method was developed at PETC according to the procedure diagrammed in Figure 2 and described in the Experimental Section. The method was

tested on a sample of virgin PE (M_n = 15,000; M_w = 100,000) of the same source as was used as feed in the semi-batch and bench-scale continuous runs. The percentage of original PE recovered, and the GPC data for the virgin PE before and after the extraction procedure is shown in the first two lines of Table I. None of the initial PE was left behind; the recovery of 86% represents losses that occurred upon the filtration step due to rapid cooling of the decane solution. A better hot filtration method is currently being implemented to improve quantitation of the technique. The slightly higher molecular weight values of the PE obtained after extraction may indicate the occurrence of condensation reactions during extraction; this observation is currently being investigated.

The PE extraction technique was also tested by examining a coprocessing sample (containing both coal and PE) before and after PE extraction, using solid state nuclear magnetic resonance (NMR) spectroscopy done by Ronald Pugmire and Mark Solum at the University of Utah.[9] Before extraction, the aliphatic portion of the spectrum consisted of a single sharp peak in the CH_2 region superimposed on a broader signal due to coal-derived material. After extraction, the recovered PE yielded only the sharp CH_2 signal; the coal-derived residue materials showed only the broader signal.[9] Thus it is reasonable to assume that, except for filtration losses, the method removes essentially all of the incompletely reacted PE and no coal derived material.

The extraction technique was used to recover PE from a series of sampling streams during three different feed conditions of a coprocessing operation on a bench scale continuous unit. The percentage of each sample stream recovered, as well as the molecular weight distribution parameters obtained from GPC of the recovered material, are listed in Table I. Molecular weight distribution curves, obtained from GPC data for the 2:1 coal:PE feed condition, are shown in Figure 3a-e. For comparison, a GPC trace of the unreacted PE after extraction is shown in Figure 3f.

The most dramatic observation from Figure 3 is the presence of two peaks in the samples taken from the feed slurry (Figure 3a) and first reactor (Figure 3b). The two peak maxima occur at molecular weight values of approximately 2,000 and 50,000 amu. The larger maximum in Figure 3a (and 3b) strongly resembles the unreacted, extracted PE in Figure 3f. Therefore, the larger, or higher molecular weight peak in Figure 3a (and 3b) can be assigned to fresh PE feed. The smaller, or lower molecular weight peak in Figure 3a (and 3b) resembles the PE recovered from the sampling points downstream in the process (Figure 3d,e). In particular, the PE-containing pressure filter liquid stream (Figure 3e) constituted the recycle vehicle during the 2:1 coal:PE operating condition of the continuous unit. Therefore the peak at about 2,000 amu in Figure 3a (and 3b) can be attributed to PE that had been recycled back to the feed slurry after having been through the process. In the other two feed conditions listed in Table I, the sample from the feed slurry (and first reactor) also exhibits bimodal distributions. The feed slurry and first reactor samples also contain unreacted PP, but the same conclusions are valid. This is the first time that a method exists to unambiguously distinguish PE that has been recycled through the process to that has been freshly added to the feed.

Downstream of the feed slurry, the distribution of recovered PE remains bimodal into the first reactor (Figure 3b, Table I). However, by the sampling point for the second reactor (Figure 3c), the bimodal distribution is gone. The GPC molecular weight distribution shows only a single peak, with a maximum and an M_n value approaching that found in the downstream samples (Figure 3d, Table I). This observation confirms that most of the PE breakdown occurs in the reactor zones, i.e., between the sampling points for the first and second reactors. A gradual narrowing of the lineshape from the second reactor (Figure 3c) to the atmospheric still bottoms sample (Figure 3d) and pressure filter liquid (Figure 3E) with accompanying reduction in molecular weight seen in Table I is indicative that some PE breakdown continues past the reactor section of the unit. The same argument can be made for the 2:1 coal:plastics and 1:1 coal:plastics feed conditions (Table I). Thus, it appears that most, but not all, of the PE degradation takes place in the reactor zone.

An important point that should not be overlooked in this finding is that virtually all of the PE feed material *has* undergone some degree of reaction. Because conventional solubility tests or distillation procedures in coprocessing experiments have indicated that PE is difficult to convert, it is easy to make the erroneous assumption that the unconverted PE is also unreacted. These experiments show conclusively that such is not the case. The molecular weight of the PE feed has been reduced by a factor of 10 to 30, depending on what parameter is used to characterize the molecular weight

distribution. The recovered PE has simply not reacted sufficiently to be considered to be converted by traditional coal liquefaction measures.

Two different methods of solids separation were used on the atmospheric still bottoms stream during the continuous run. During the 2:1 coal:plastics feed condition, vacuum distillation was employed. In this configuration no PE was found in the vacuum still overhead material; it all went with the solids. Therefore, a recycle stream produced from only vacuum distilled material would be free of incompletely reacted PE. (In actuality, the recycle stream during the 2:1 coal:plastics condition was a combination of vacuum still overhead and atmospheric still bottoms; hence the PE in the recycle stream.) During the 2:1 coal:PE and 1:1 coal:plastics feed conditions, pressure filtration was employed on the atmospheric still bottoms. In this configuration, most of the unconverted PE went with the filtrate; only a small, approximately constant amount was recovered with the solids. The pressure filtration was done at a temperature above the melting point of PE so most of the PE passed through the filter as liquid or in solution; a small amount became entrained and trapped in the filter cake. Therefore, a recycle stream produced from pressure filtered material would be high in incompletely reacted PE. In this way, the method of solids separation could be tailored to retain or exclude incompletely reacted PE from the recycle stream.

In a separate aspect of the project, 1-L semi-batch reactions were performed to investigate methods for optimizing PE conversion and overall feed conversion in coal-plastics coprocessing. The effect of temperature on the conversion three different feed mixtures to <850°C distillable products is illustrated in Figure 4. The results from a 1:1 ratio of coal:mixed plastics, a 1:1 ratio of coal:PE, and PE feed alone are compared at 430°C, 445°C, and 460°C. The conversion of 1:1 coal:mixed plastics increases from 430°C to 445°C, then levels out from 445°C to 460°C. The conversion of 1:1 coal:PE increases fairly steadily across the entire temperature range. The conversion of the PE only feed shows the most significant increase between 445°C and 460°C. Although the conversion of all three feed mixtures increase with temperature, the PE, at least when used without coal or other plastics, seems to be influenced most by increasing the temperature from 430°C to 460°C. The results suggest that temperature is an important parameter in processing of PE under coal liquefaction conditions. This study will be continued by applying the PE extraction method discussed earlier to the incompletely reacted PE from these semi-batch runs, in order to determine how the temperature or feed composition influences the nature of the PE left unconverted.

Summary. A novel method has been developed to isolate and recover incompletely reacted PE from coal-plastics coprocessing product streams. The method has been applied to samples obtained from a bench scale continuous unit and the recovered material has been characterized by gel permeation chromatography. The method has conclusively established that virtually all PE undergoes some reaction in the coal liquefaction environment, with an average reduction in molecular weight distribution for the "unconverted" material of 10 to 30. The method can definitively distinguish between fresh (feed) and recycled PE in the process stream, and has established that most of the PE degradation occurs in the reactor zone. Vacuum distillation and pressure filtration have dissimilar effects on the incompletely reacted PE present in the atmospheric still bottoms process stream. Finally, semi-batch studies demonstrate the influence of temperature on the distillate conversion of various coal and plastics feed combinations.

Acknowledgements. The authors acknowledge Dr. Gary Robbins of Consol, Inc., and Dr. Vivek Pradhan of Hydrocarbon Technologies, Inc., whose information that PE could be isolated from a deashed coprocessing recycle stream on the basis of THF insolubility led us to develop the generalized PE recovery method reported here. The authors acknowledge Professor Ron Pugmire and Dr. Mark Solum at the University of Utah for solid state NMR to confirm the efficacy of the extraction method. The work of one of the authors (RLT) was performed under an appointment to the U.S. Department of Energy Postgraduate Research Training Program at the Pittsburgh Energy Technology Center administered by the Oak Ridge Institute for Science and Engineering.

DISCLAIMER

REFERENCES

1. Smith, R.A. "Overview of Feedstock Recycling of Commingled Waste Materials," Ninth Annual Technical Meeting, Consortium for Fossil Fuel Liquefaction Science, Pipestem, WV, August 15-18, 1995.
2. Madorsky, S.L. "Thermal Degradation of Organic Polymers," Polymer Reviews Volume 7, Mark, H.F., Immergut, E.H., Eds.; Wiley-Interscience: New York, 1964; pp 93-129.
3. Ng, S.H. Fuel, **1995**, 9, 735-742.
4. (a) Palmer, S.R.; Hippo, E.J.; Tandon, D.; Blankenship, M. Prepr. Pap. - Am. Chem. Soc., Div. Fuel Chem., **1995**, 40(1), 29-33. (b) Huffman, G.P.; Feng, Z.; Mahajan, V.; Sivakumar, P.; Jung, H.; Tierney, J.W.; Wender, I. Prepr. Pap. - Am. Chem. Soc., Div. Fuel Chem., **1995**, 40(1), 34-37.
5. Cugini, A.V.; Krastman, D.; Lett R.G.; Balsone, V.D. Catal. Today, **1994**, 19(3), 395-408.
6. Cugini, A.V.; Rothenberger, K.S.; Ciocco, M.V.; McCreary, C. In Coal Science, Proceedings of the Eighth International Conference on Coal Science, Volume II, Pajares, J.A.; Tascon, J.M.D., Eds.; Coal Science and Technology Series, Volume 24; Elsevier: Amsterdam; 1995; pp 1299-1302.
7. Robbins, G.; Pradhan, V., personal communication
8. Pugmire, R.; Solum, M., personal communication

Figure 1: Simplified diagram of continuous unit configuration.

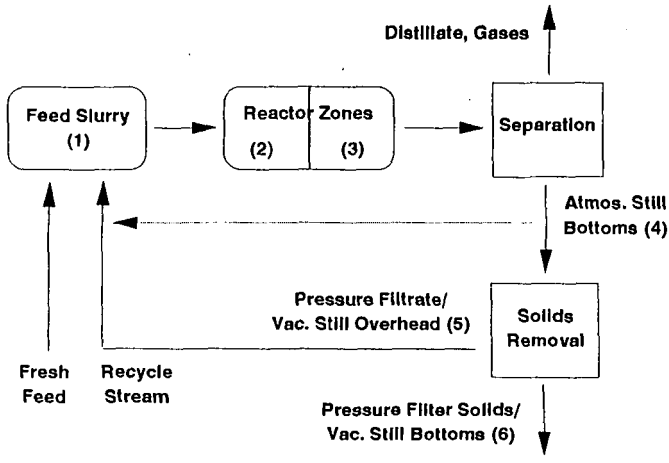

Figure 2: Scheme for recovery of incompletely reacted PE.

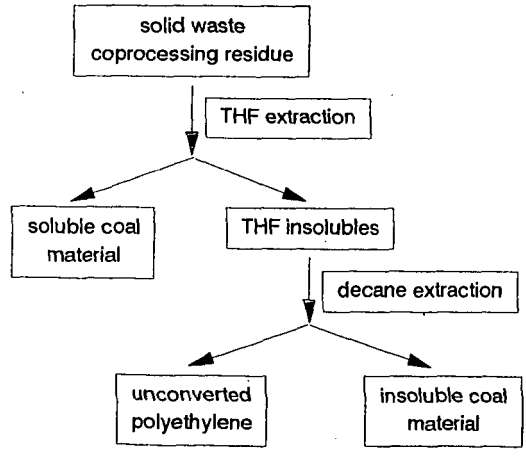

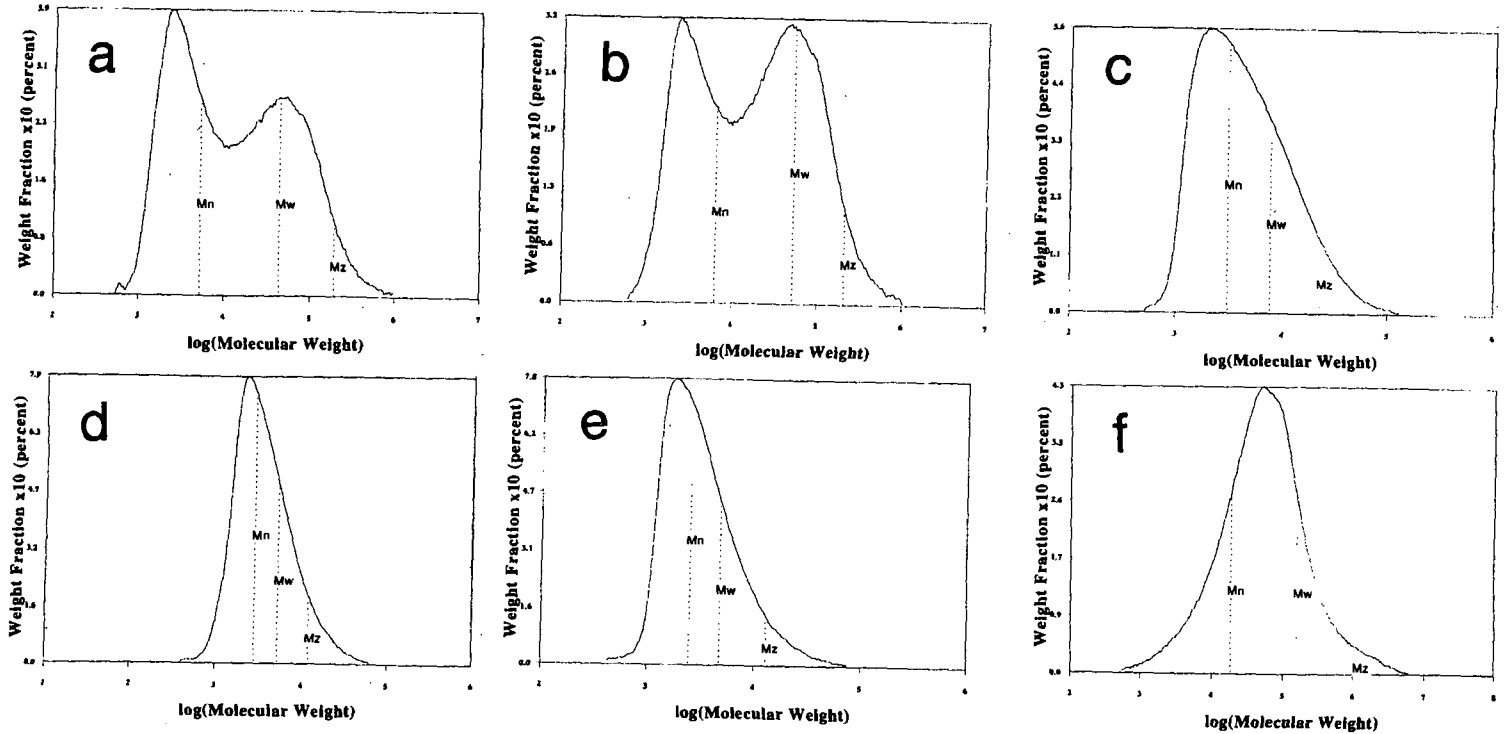

Figure 3: GPC data for 2:1 coal:PE feed condition. (a) feed slurry [sample stream **1**], (b) first reactor **[2]**, (c) second reactor **[3]**, (d) atmospheric still bottoms **[4]**, (e) pressure filter liquid **[5b]**, (f) unreacted, extracted PE.

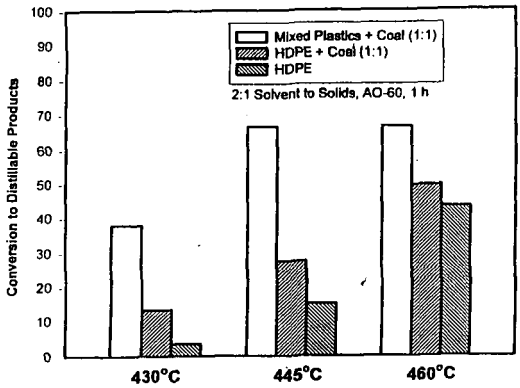

Figure 4: Effect of Temperature on Conversion to Distillable Products (Semi-Batch Studies)

Table I. GPC Results for PE Recovered from Continuous Bench Scale Unit.

Sample Description	PE yield[a]	Max[b]	M_n[b]	M_w[b]
Unreacted Polyethylene (PE)				
PE before extraction	----	46,000	15,000	100,000
PE after extraction	86 %	54,000	19,000	150,000
2:1 coal:plastics condition				
(1) feed slurry	8 %	2,500; 85,000	9,700[c]	230,000[c]
(2) reactor #1	8 %	1,900; 96,000	8,000[c]	200,000[c]
(3) reactor #2	3 %	2,400	3,400	8,000
(4) atmospheric still bottoms	3 %	2,000	2,500	4,100
(5a) vacuum still overhead	0 %	-----	-----	-----
(6a) vacuum still bottoms	12 %	1,500	1,900	3,100
2:1 coal:PE condition				
(1) feed slurry	11 %	2,500; 47,000	5,000[c]	42,000[c]
(2) reactor #1	14 %	2,500; 50,000	6,200[c]	51,000[c]
(3) reactor #2	12 %	2,200	3,000	7,500
(4) atmospheric still bottoms	12 %	2,500	2,800	5,100
(5b) pressure filter liquid	18 %	1,800	2,400	4,800
(6b) pressure filter solids	2 %	1,400	1,900	3,500
1:1 coal:plastics condition				
(1) feed slurry	16 %	2,600; 76,000	3,000[c]	160,000[c]
(2) reactor #1	17 %	2,200; 80,000	2,700[c]	120,000[c]
(3) reactor #2	NA	NA	NA	NA
(4) atmospheric still bottoms	9 %	2,000	2,300	4,100
(5b) pressure filter liquid	10 %	1,300	1,300	1,500
(6b) pressure filter solids	2 %	1,300	1,700	2,900

a. This value represents the amount of PE reclaimed based on the total mass of the sample, not on the amount of PE originally located in the sample.
b. All data points except unreacted PE represent an average of two determinations. Unreacted PE value is based on a single determination.
c. Single M_n and M_w values were calculated by the GPC software based on the composite bimodal lineshape. Maxima were determined for each individual peak when more than one peak was present.

DETERMINATION OF UNCONVERTED HDPE IN COAL/PLASTICS CO-LIQUEFACTION STREAM SAMPLES

Gary A. Robbins, Richard A. Winschel, and Francis P. Burke

CONSOL Inc.
Research & Development
4000 Brownsville Road
Library, PA 15129

KEYWORDS: coal liquefaction, coal/waste coprocessing, analysis

INTRODUCTION

In several coal/plastics liquefaction runs performed by Hydrocarbon Technologies, Inc. (HTI), a substantial amount of incompletely converted high-density polyethylene (HDPE) was present in ash-free recycle resid streams when either the ROSE-SR unit was used in Run POC-2, or the pressure filter unit was used in Runs CMSL-8 and CMSL-9. This indicates that the HDPE is less reactive than coal at the liquefaction conditions used.[1-4] In these ash-free streams, there is no solid organic or inorganic material arising from the coal, and the incompletely converted HDPE can be recovered by extraction and filtration with tetrahydrofuran (THF) at room temperature. The HDPE (or HDPE-like material, which could also consist of heavy waxes) is THF insoluble. However, in ashy streams, there are both inorganic ("ash") and organic (unconverted coal) components present from liquefaction of the coal, that interfere with an easy and clean separation of the HDPE from the coal/plastics liquefaction stream sample. Therefore, CONSOL developed an analytical procedure for HDPE in the ashy stream samples based on extraction of HDPE from the sample using hot (150 °C) decalin (decahydronaphthalene), in which the HDPE is soluble. The decalin extraction is both preceded and succeeded by extractions and washes with THF at room temperature, to remove the coal-derived components from the sample.

EXPERIMENTAL

HDPE Solubility and Filtration Tests. The first tests were performed to identify a suitable solvent and temperature for dissolution and recovery of the HDPE feedstock used in several HTI liquefaction runs. These experiments were conducted by heating beakers containing HDPE/solvent mixtures on a hot plate. The virgin HDPE, consisting of clear pellets, was supplied to HTI by Amco plastics, manufactured by BASF, mp 135 °C, and density 0.96 g/cc.[5] It is essentially devoid of ash, sulfur, nitrogen, and oxygen.[1] The decahydronaphthalene (decalin) was obtained from Aldrich Chemical Co., as anhydrous, 99+% purity, consisting of a mixture of cis- and trans- isomers, and with bp 189-191 °C.

In mixed cresol at ≈150 °C, HDPE (2 g/25 mL cresol) melted, but did not dissolve. The HDPE readily dissolved in decalin at 125 °C (2 g HDPE/50 mL decalin), forming a colorless solution. The HDPE-decalin solution at 125 °C was pressure-filtered (about 7 psig nitrogen) through a Whatman no. 42 paper in a filtration apparatus which was heated to 145 °C. Hot decalin was used to rinse the beaker and filter paper, but some precipitated HDPE adhered to the beaker. The filtrate was cooled to room temperature. It then was pressure-filtered through Whatman no. 42 paper and washed with fresh, cool decalin. The filtrate was clear, and slightly yellow in color. The filter cake was dried in a vacuum oven at 60 °C. After drying, it still had a faint decalin odor. 91.6% of the original HDPE was recovered as a hard white solid.

Tests of Extraction Sequence. It was expected that a THF wash would be needed to distinguish HDPE from other materials that may be extracted in hot decalin, since HDPE is completely insoluble in THF at room temperature. However, it was uncertain whether or not the decalin extraction step also should be preceded by THF-extraction to remove distillate and coal-derived residual components. A test was conducted in which aliquots of one sample were extracted using both test sequences. In the decalin-first procedure: 1) the sample was extracted and filtered with hot decalin, 2) the decalin extract was cooled to room temperature, 3) the precipitated solid HDPE was filtered and dried, 4) the tan-colored filter cake was washed with THF, and 5) all fractions were dried in the vacuum oven to remove solvent. In the THF-first procedure, the sample was extracted and filtered with THF at room temperature, and then steps 1 through 5 were followed. In this sequence, both the THF-soluble fractions obtained prior to and after decalin extraction were combined before solvent removal. Results of the extraction sequence tests are described below.

RESULTS AND DISCUSSION

Method Development and Validation. The solubility and filtration tests demonstrated that unreacted feed HDPE could be dissolved, filtered, and recovered in high yield (>90% recovery). The results obtained using the two extraction sequences are quite similar (Table 1). Yields of the fractions were 34 to 39 wt % HDPE (decalin-soluble, THF-insoluble), 58 to 62 wt % THF solubles, and 3 wt % THF and decalin insolubles. The similarity of the results provided overall validation of the method, and indicated that either method was probably adequate for routine analysis. HDPE products from both extractions had a similar tan color and coarse powdery appearance. However, the THF-first procedure minimizes the possibility of interferences, and the HDPE product was cleaner in appearance. FTIR spectra (not shown) indicated that the recovered HDPE fractions obtained by

the two extraction sequences are similar to each other, and to the feed HDPE. Thus, these recovered decalin solubles appear to be essentially pure HDPE (or heavy n-paraffins, which may be indistinguishable from HDPE). The THF-first procedure requires an additional extraction step, but the total time required for the extraction steps is only about four hours. It was adopted as the routine method, a flow chart for which is shown in Figure 1. Solvent removal steps are not shown in the flow chart. This method was found to be easy to perform in a routine manner. Combined recoveries of the three fractions (THF solubles, HDPE, and THF/decalin insolubles) ranged from 98% to 105%, averaging 102% in 19 tests using the method (this includes the decalin-first test described above). It is presumed that recoveries are biased high because of the difficulty in removing solvents (THF or decalin) from the recovered fractions. For routine use, the fraction percentages are reported on a normalized basis. Additional validation information was developed in conjunction with application of the extraction method to authentic samples from HTI Runs CMSL-8 and CMSL-9, and is described in sections to follow.

Application to Runs CMSL-8 and CMSL-9. The HDPE extraction method was applied to selected samples from HTI Runs CMSL-8 and CMSL-9 to characterize the samples and determine the fate of HDPE.[2-4] The data were used for four purposes: 1) determine the amount of HDPE in the pressure filter cake (PFC) samples from periods in which coal and plastics were fed, 2) determine the degree of analytical interference from HDPE-like material produced from the coal, 3) determine the HDPE conversion for each of the periods of coal/plastics operation, and 4) develop a HDPE material balance around the solids separation unit (vacuum still or pressure filter, depending on run and operating period).[2,4] The conditions in Runs CMSL-8 and CMSL-9 relevant to this discussion are given in Table 2. Solids separation operations in the HTI bench unit are conducted using either pressure filtration or vacuum distillation; characteristics of the bottoms and overhead streams from these two operations differ greatly. Sample streams relevant to this discussion are: 1) continuous atmospheric still bottoms (CASB), the flashed bottoms product of liquefaction and the feed to the solids separation device in use; 2) pressure filter liquid (PFL), the solids-free recycle stream; 3) pressure filter cake (PFC), the corresponding filter solids containing rejected insolubles; 4) vacuum still overheads (VSOH), the 524 °C$^-$ distillate; and 5) vacuum still bottoms (VSB), the rejected 524 °C$^+$ resid and ash.

The extraction results (not shown) for Conditions 8-1 and 9-6 (coal feed only) show that little coal-derived material reports as "HDPE" using this method. In samples of resid from CASB and of PFC from Condition 8-1 and 9-6, only 0.06 to 0.32 wt % of each sample reported as "HDPE".[2,4] Extraction results from the coal/plastics operating periods show that with pressure filtration, little HDPE goes out in the PFC stream; instead, most of the HDPE is recycled in the PFL stream. During coal/plastics periods of Run CMSL-8 there was about 5 wt % HDPE in the PFC stream, and 16 to 37 wt % HDPE in the PFL stream. During coal/plastics periods of Run CMSL-9 there was about 2 wt % HDPE in the PFC stream, and about 23 wt % HDPE in the PFL stream.[4] CASB 454 °C$^+$ resids from Conditions 8-2 through 8-5 were found to contain 15 to 62 wt % HDPE; those from Conditions 9-7 through 9-9 were found to contain 9 to 35 wt % HDPE. In Condition 9-7, there was 11 wt % HDPE in the VSB sample (it is presumed that none is in the corresponding VSOH sample).

Material balances (based on a combination of CONSOL analytical results with HTI material balance data) for HDPE around the solids separation operations gave generally poor results (not shown, results ranged from 32% to 374% in Runs CMSL-8 and CMSL-9). Corresponding ash balances based on CONSOL analytical data from the same samples ranged from 102% to 1264%, i.e., more than twelve-fold over recovery. The poor ash balances indicated that the problem was not an analytical problem with the HDPE method, per se. We had observed that some CASB samples from Runs CMSL-8 and CMSL-9 were inordinately low in ash, and the sample integrity was suspect. We examined the percent total THF insolubles (THFI) obtained from two extraction procedures on two CASB sample types (whole or resid). Assuming robust extraction procedures, the THFI contents determined by different extraction procedures on the same sample should agree well. Using Method 1, (the decalin extraction method), the THFI content is the sum of THF/DI (THF and decalin insolubles) and HDPE fraction weight percentages. Using Method 2 (the THF extraction procedure that is our normal work-up procedure for liquefaction samples), the THFI content is the sum of unconverted coal and ash component weight percentages. As shown in Figure 2, the amount of THFI obtained by the two methods on two sample types (CASB 454 °C$^+$ resid and whole CASB), shows considerable scatter for samples representing a particular run condition. These data thus confirm that a major problem may lie in obtaining good data from the CASB samples from coal/plastics operations at HTI. In contrast, we find that percent THF insolubles obtained by the decalin extraction method of VSB and PFC are very similar to those obtained by THF extraction of the same samples (Figure 3). These results indicate that there may be little problem with use of the decalin extraction data obtained from the VSB and PFC samples.

HDPE Conversion During Runs CMSL-8 and CMSL-9. Our original procedure for estimating HDPE conversions during Run CMSL-8 employed the simplifying assumption that the PFC contained no unconverted HDPE.[2,3] At the time, we had no way of measuring the concentration of unconverted HDPE in solids-containing streams. We can now make these measurements directly with the hot decalin extraction procedure. The HDPE extraction results described above for samples from Runs CMSL-8 and CMSL-9 generally validate the original assumption that the PFCs contain no HDPE, because little HDPE (1 to 6 wt %) was found in the PFC samples.

Both overall and single-pass conversions of HDPE are given by:

Conversion = [Mass of HDPE In - Mass of HDPE Out] x 100 / [Mass of HDPE In],

where the masses of HDPE in and out are defined differently for overall conversion than for single-pass conversion. For overall conversion, the "mass of HDPE in" is the HDPE in the fresh feed, and the "mass of HDPE out" is summed from HDPE in any net product streams, such as PFL and PFC or VSB. For single-pass conversion, the "mass of HDPE in" is the sum of HDPE in the fresh feed and all recycle streams (such as CASB, PFL, and PFC or VSB), and the "mass of HDPE out" is the sum of HDPE in all of the gross product streams (such as CASB, PFL, and PFC or VSB). The results presented here for Run CMSL-8 differ from those given previously,[2,3] in that HDPE can be accounted for in more streams, whereas previously it could only be accounted in the fresh feed and PFL streams. Note that CASB can be accounted directly (if the HDPE content of CASB is measured), or it can be accounted as both PFL and PFC (or as VSB). Thus, it is possible to measure single-pass HDPE conversion with CASB as a recycle or product stream, even if the HDPE content of the CASB is not measured directly. Problems described above with use of the CASB data suggests that it may be better to use the PFL/PFC accounting approach, since the HDPE concentrations of PFC samples seem to be more reliable than those of CASB samples.

In Figure 4, the overall and single-pass conversions of HDPE in each period of Runs CMSL-8 and 9 that were evaluated are compared. The overall conversion of HDPE ranged from 69-86% during Run CMSL-9, comparable to those obtained for periods Conditions 8-2, 8-4, and 8-5. This was accomplished in spite of operation at a higher space velocity and without benefit of supported catalyst, but at higher liquefaction temperatures in Run CMSL-9. A high space velocity led to operating problems and low HDPE conversion in Condition 8-3. Higher conversion of HDPE in Condition 9-7, in which vacuum distillation and ashy recycle were used, relative to Conditions 9-8 and 9-9, in which pressure filtration and ash-free recycle were used, suggests that use of ashy recycle may increase HDPE conversion. In Figure 5, the overall HDPE conversions based on this direct measurement method for Run CMSL-9 periods are compared with those estimated by HTI[6] based on measured total feed conversions, and assumed fixed conversions of 88% for the coal, and 100% for all of the non-HDPE plastics. These two sets of results show fair to good overall agreement, for the overall run and for individual periods. HTI's model assumptions thus appear to apply to the combination of coal and plastics tested in Run CMSL-9.

CONCLUSIONS

A HDPE extraction method was developed that can be routinely applied to ashy coal/plastics co-liquefaction stream samples. The method requires about four hours of operator and extraction time, with several hours of additional time needed for solvent removal from recovered fractions. The HDPE extraction method shows little interference from coal-derived material. Results from the HDPE extraction method show that during coal/plastics operations with pressure filtration, little HDPE goes out in the PFC stream; instead, most of the HDPE is recycled in the pressure-filter liquid (PFL) stream. HDPE extraction results were combined with material balance data to calculate HDPE balances and conversions during Runs CMSL-8 and CMSL-9. HDPE extraction results obtained from PFC and VSB samples appear to be reliable, but those from CASB samples are generally poor, either from sampling or analytical inconsistencies. The overall conversion of HDPE ranged from 69-86% during Run CMSL-9, comparable to those obtained for most periods of Run CMSL-8. Run CMSL-9 results suggest that ashy recycle may increase HDPE conversion. Overall HDPE conversions determined by CONSOL are consistent with those estimated by HTI for Run CMSL-9.

FUTURE WORK

The HDPE concentration data provided by this method can provide a basis for consideration of kinetics of HDPE conversion, and in development of improved processing strategies. In runs following CMSL-9, HTI's feedstocks for co-liquefaction have included municipal solid waste (MSW) plastics and petroleum resid, in various combinations with and without coal. The HDPE extraction method provides a potential means to determine HDPE concentration in mixed MSW feeds. A potential difficulty for the method is interference from petroleum resid. Since heavy waxes may behave like HDPE in terms of solubilities in decalin and THF, it may be more difficult to distinguish petroleum resid and HDPE than to distinguish coal-derived material and HDPE. We will continue to apply this characterization method to samples from appropriate streams in subsequent runs in which HDPE was fed.

ACKNOWLEDGMENTS

Samples and other information were provided by Dr. Vivek Pradhan of HTI. This work was sponsored by the U.S. Department of Energy under contract no. DE-AC22-94PC93054.

REFERENCES

1. Robbins, G. A.; Brandes, S. D.; Winschel, R. A.; Burke, F. P. "A Characterization and Evaluation of Coal Liquefaction Process Streams, Quarterly Technical Progress Report October 1 through December 31, 1994", DOE/PC 93054-10, May 1995.

2. Robbins, G. A.; Brandes, S. D.; Winschel, R. A.; Burke, F. P. "A Characterization and Evaluation of Coal Liquefaction Process Streams, Quarterly Technical Progress Report April 1 through June 30, 1995", DOE/PC 93054-18, September 1995.

3. Robbins, G. A.; Brandes, S. D.; Winschel, R. A.; Burke, F. P. "Characteristics of Process Oils from HTI Coal/Plastics Co-Liquefaction Runs", Proceedings of the DOE Coal Liquefaction and Gas Conversion Contractors Review Conference, August 29-31, 1995, Pittsburgh, PA.

4. Robbins, G. A.; Brandes, S. D.; Winschel, R. A.; Burke, F. P. "A Characterization and Evaluation of Coal Liquefaction Process Streams, Quarterly Technical Progress Report October 1 through December 31, 1995", DOE/PC 93054-25, May 1996.

5. Comolli, A. G. "Results of Recent POC Run at HRI on Waste/Coal Coprocessing", Proceedings of the PETC/DOE Workshop "Waste/Coal Coprocessing", Pittsburgh, PA, September 9, 1994.

6. V. R. Pradhan, personal communication, and HTI reports covering Runs CMSL-8 and CMSL-9 under DOE Contract No. DE-AC22-93PC92147.

TABLE 1. TEST OF THF AND DECALIN EXTRACTION SEQUENCE IN A TEST SAMPLE

Fraction	Fraction Wt % of Sample (454 °C⁺ Resid from CAS Bottoms Sample, Period 38 of Run CMSL-9)	
	Decalin Extraction First - Unnormalized (Normalized)	THF Extraction First - Unnormalized (Normalized)
THF/Decalin Insolubles	2.91 (2.77)	3.59 (3.46)
THF Solubles	61.0 (58.2)	64.3 (62.1)
Decalin Solubles/THF Insolubles (HDPE)	40.9 (39.0)	35.7 (34.4)
Recovery	104.8 (100.0)	103.6 (100.0)

TABLE 2. SUMMARY OF CONDITIONS FROM COAL AND COAL/PLASTICS OPERATIONS IN HTI RUNS CMSL-8 AND CMSL-9

Run and Condition Number	Run Period	% Plastics in Fresh Feed (Remainder is Coal)	% HDPE in Fresh Feed	Recycle/Solids Separation Methods
CMSL-8 (227-85) Coal: Crown II Mine, Ill. 6 Seam Mixed Plastics: HDPE, PS, PET Catalysts: Shell 317/1st Reactor, Dispersed Mo (100-200 ppm) and Fe (10000 ppm) Temperatures: T_1/T_1 + ca. 15 °C in 1st/2nd Liquefaction Reactors				
8-1	6	0	0.0	Ash-Free/Pres. Filt.
8-2	11	25 (mixed)	12.5	Ash-Free/Pres. Filt.
8-3	16	25 (mixed)	12.5	Ash-Free/Pres. Filt.
8-4	20	33 (mixed)	16.5	Ash-Free/Pres. Filt.
8-5	22/23	33 (HDPE)	33.0	Ash-Free/Pres. Filt.
CMSL-9 (227-87) Coal: Black Thunder Mine, Wyodak & Anderson Seams Mixed Plastics: HDPE, PP, PS Catalysts: Dispersed-Only, Mo (100-300 ppm) and Fe (10000 ppm) Temperatures: T_2/T_2 + ca. 10 °C in 1st/2nd Liquefaction Reactors, $T_2 > T_1$ in CMSL-8				
9-6	29	0	0	Ashy/Vac. Still
9-7	34	33 (mixed)	13	Ashy/Vac. Still
9-8	38	33 (HDPE)	33	Ash-Free/Pres. Filt.
9-9	41	50 (mixed)	20	Ash-Free/Pres. Filt.

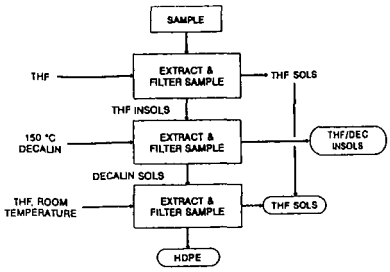

Figure 1. Flow Chart of Hot Decalin Extraction Method to Recover HDPE from Coal/Plastics Co-Liquefaction Samples.

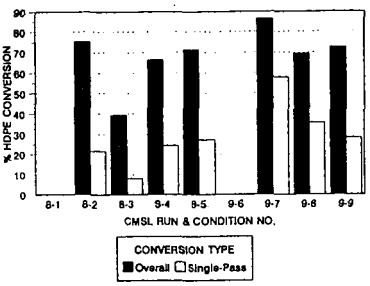

Figure 4. Overall and Single-Pass Conversion of HDPE in HTI Runs CMSL-8 and CMSL-9.

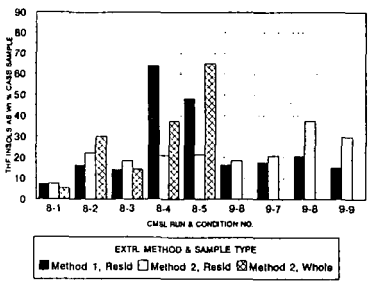

Figure 2. THF Insolubles Concentration in CASB Samples from HTI Runs CMSL-8 and CMSL-9 as Measured by Two Extraction Procedures, Showing Poor Agreement.

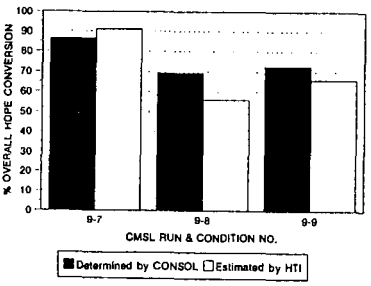

Figure 5. A Comparison of CONSOL (Determined) and HTI (Estimated) Overall Conversion of HDPE in HTI Run CMSL-9.

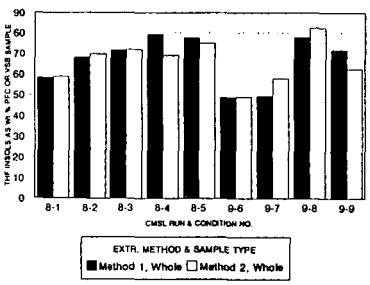

Figure 3. THF Insolubles Concentration in PFC and VSB Samples from HTI Runs CMSL-8 and CMSL-9 as Measured by Two Extraction Procedures, Showing Good Agreement.

CONVERTING NATURAL AND METHANE GASES DIRECTLY INTO LIQUIDS

: Quentin J. Adams
Earth Resources Technology Services
3208 N. 37th St. #9, Phoenix, AZ 85018-6333

Keywords: liquefaction, Coal-bed Methane Gas Feeedstock, Synthetic Fuels

INTRODUCTION

The recent increase in Crude 0il, gasoline and natural gas prices, dried-up reserves and the petroleum industry's reluctance in increasing petroleum production and drilling any new wells have brought **ECONOMICS** back as a major player in the development of synthetic (alternate) fuels.

Petroleum experts state that there are approximately 30 to 40 years of crude oil and natural gas left, after all of the enhanced recovery technologies have been utilized. **There are about 200 years of coal left.** This time line can be increased if we drill into and remove the coalbed methane gas instead of mining the coal.

DOE's Clean Coals Technology Programs has spent **$7 Billion** to date for joint venture industry/government investment in a new generation of clean coal technology. Plus millions of dollars have gone into DOE's programs for improving the technologies for coal liquefaction and gas conversion. Some of the programs included revising and modifying versions of the classical Fisher-Tropsch process developed just prior to Word War II and used by the Germans to provide Synthetic Diesel fuel for their Panzer Tanks..

Sasol Ltd. of South Africa and Haldor Topsoe AS of Lyngby, Denmark, have signed a technology cooperation agreement to promote Sasol's Slurry Phase Distillate technology together with Topsoe's natural gas conversion technology for the production of high quality diesel fuels from natural gas.

It is anticipated that this combination will allow the economic conversion of natural gas from any viable source world-wide to high quality environmentally friendly diesel fuels, with the additional potential to produce petrochemicals.

U.S. DOE's Pittsburgh Energy Technology Center's (PETC) let a contract with the Bechtel Group for a Baseline Design/Economics using Advanced Fisher-Tropsch Technology. The plant design includes all process equipment necessary to convert coal to gas and gas to the desired transportation fuels (i.e., gasoline and diesel fuel). In addition, Bechtel has developed an aspen process simulation model to perform additional process sensitivity studies in the future.

DOE/PETC has also issued an amendment to the above study that includes modifying the design model and that the modifications should include the development of an enhanced computer model that incorporates **coalbed methane and natural gas feedstocks.**

A Synfuels plant provides owners of Coalbeds producing **methane** Gas.(**40%** of the gas produced in Alabama that goes into the Interstate Gas Pipeline is Coalbed Methane Gas) plus natural gas reserves, City and County Landfills, Sewer Treatment plants with Digestors and any thing that can produce methane gas, provides an opportunity to capitalize on previously unprofitable resources

As stated in the abstract t"The development of synthetic (alternate) fuels was motivated by the 1990 Clean Air Act Amendment. .

The mission for Synfuels is from the Office of Mobile sources, Motor vehicles and Urban buses (extracts from Pages 4 and 5)..

1994 - Truck and buses must meet stringent diesel particulate emission standards, equivalent to 5% of the uncontrolled level. All buses in service in cities with populations of 750,000 or more, to be operated on clean alternate fuels.

1996 - Establishes a new program, initially in California and required in 1996, to require the sale of 150,000 ultra-clean vehicles in the state, increasing in 1999 to 300,000 annually.

Clean Fuels, An Overview, What are Clean Fuels?, The most familiar transportation fuels in this county are gasoline and diesel fuel, but any number of energy sources are capable of powering motor vehicles. These include grain, wood and coal alcohol, electricity, natural and methane gases (including coalbed methane) and propane. Some vehicle fuels because of physical or chemical properties, create less pollution than do to days gasoline. These are called "clean fuels".

Synthetic diesel fuels derived from methane gas emits, at a minimum, 18% less particulate, 15% less hydrocarbons, and 14% less carbon monoxide than No. 2 diesel fuel. Environmentally friendly synthetic fuels, lubricants and waxes. Synthetic diesel fuel are the cleanest fuel available, and unlike other alternate fuels, does not require any special equipment or engine alterations.

A number of process technologies that convert coal-derived syngas into liquid fuels have been demonstrated at DOE's Alternate Fuels Development Unit (AFDU), located in LaPorte, Texas. U.S. DOE's Pittsburgh Energy Technology Center's (PETC) is presently managing a number of programs for improving the technologies for coal liquefaction and gas conversion.

Gas-to-Liquids Conversion Technologies

Coupling of two methane molecules to higher hydrocarbons is not thermodynamically feasible because the energy of formation is not favorable. However, in the presence of a co-reactant, such as oxygen, the reaction path can be altered, and methane conversion reactions can be successfully carried out. Natural gas (primarily methane) can be upgraded to higher hydrocarbons either by direct conversion routes (single-step or staged), or via synthesis gas (a mixture of carbon monoxide and hydrogen). The important process considerations for commercially viable natural gas upgrading operations are methane conversion rate and selectivity to preferred products.

Based on chemistry, the processes for natural gas upgrading include 1) partial oxidation to oxygenates, such as methanol, 2) oxidative coupling to higher hydrocarbons, such as ethylene, 3) derivatization, such as oxyhydrorochlorination to chlorinated hydrocarbons, which are subsequently converted to higher hydrocarbons, and 4) pyrolysis to aromatic and/or higher hydrocarbons.

In the indirect process, natural gas is first converted to synthesis gas, followed by catalytic hydrocarbon of the carbon monoxide in a synthesis reactor to a variety of higher hydrocarbon fuels. Fisher-Tropsch (FT) synthesis and its variants are important synthesis reactions, involving **low-pressure conversion of synthesis gas to gasoline, diesel fuel, wax, and oxygenates.** The products of reaction depend on the temperature, pressure, and catalyst used in the synthesis reactor.

PETC's Gas-To-Liquids Program

The goals of PETC's Gas-To-Liquids Program can be summarized as follows:

- Discover new chemistry and catalysts for the conversion of methane and other light hydrocarbon gases to value-added, easily transportable fuels and chemicals
- Obtain necessary design and engineering information to develop prototype technologies for demonstration and commercial deployment.
- Pursue cost-shared, risk-shared, industry-driven R&D, demonstration, and technology transfer to ensure pay-off of Federal R&D investments.

- Contribute to energy policy goals by selecting investments consistent with the four major policy thrusts:
  - Energy security
  - Economic growth
  - Environmental quality improvement
  - Enhancing scientific foundations.

Some of the Synfuel development milestones:

1 DOE Contract No. DE-AC-911PC90027 with the Bechtel Group, This Advanced Fisher-Tropsch indirect Liquefaction Study is for the conversion of Coal to gas and the gas into liquids:

The present indirect liquefaction technology is the base for Bechtel's baseline design study, the PFS model, developed for a wide range of plant capabilities and operating parameters, is a research tool for evaluation of future technology advances. This effort was a logical continuation of Bechtel's baseline design study and will provide additional capabilities to the model for future use with the appropriate modifications of the current baseline design and computer mode, any hydrocarbon feedstock can be used.

2 PETC has amended Bechtel Group's contract for the modification of Bechtel's baseline design study to include an economic analysis for natural gas and coalbed methane gas as feedstock.

Capital and operating costs are called for in the contract, this will also include individual plant costs for the alternative cases.

An ASPEN/SP Process Flowsheet (PFS) model and an economic spreadsheet model. Sensitivity studies have been performed to demonstrate the effects of key independent process variables and economic assumptions.

Some Synfuel Plants in Operation

A 14,500 BPD natural gas-to-gasoline plant started operating in New Zealand in 1985 and is on stream producing 87 octane unleaded gasoline. In this process, natural gas was first converted to methanol via synthesis gas, followed by conversion of methanol to gasoline using a novel catalyst developed by Mobil in the 1970s.

In April 1993, Exxon announced its AGC-SA Advanced Gas Conversion Technology for converting natural gas to high quality refinery feedstock. Olefin-based transportation fuels from natural gas is produced in the Mossgas plant in South Africa.

The Shell Middle Distillate Synthesis (SMDS) process is by now well known as Shell's development to broaden the basis of natural gas utilization.

This technology is now being applied by Shell MDS (Malaysia) Sendirian Berhad in a first full scale application of 12,500 bbl/day, which was started in Bintylu, Sarawak in 1993. The plant produces automotive fuels of exceptional quality, and , in addition to this, special chemicals and waxes. Flexibility in the process operation allows for a wide range of product selection, which is a valuable asset in a variable market.

Because of these excellent properties, which are in particular far in excess of the market minimum specifications for smoke point and cetane number, these products make excellent blending components for upgrading of lower quality stock derived from conventional crude oil processing or catalyst and thermal cracking operations e.g. cycle oils The linear blending characteristics of Shell MDS gasoil, shows that the addition of some 35 per cent (35%) of SMDS gasoil to a typical naphthionic gasoil is sufficient to raise the cetane number from 33 to the required specification of 47..

There are other Synfuel Plants, a operating Industrial demonstration plant in Shanxi province, China and a plant by Intevap in Venezuela

Due to the nature of the feedstock, products do not contain any sulfur or nitrogen and conform to the new EPA Clean Air Act regulations with respect to particulate emissions, sulfur and aromic content. Distillates from this process are finding a premium value in the market .

The MITRE Corp., McLean VA, a DOE consultant is analyzing a number of Synfuels plant technologies resulting in lowering plant cost and operating reductions. MITRE Corp. DOE contract is to review the development of any technologies that can reduce the costs in Bechtel's technoeconomic analysis

An extensive report prepared November, 1991 by the MITRE Corp., McLean, VA (under a DOE contract) in the form of a technoeconomic analysis for The Great Plains Synfuels plant in Beulah, North Dakota that is developing a Hybrid Plant Coal Liquefaction Concept for a 2,000 barrel per day Synfuels plant.

The report analyzed a number of liquefaction processes and found that the Rentech, Inc. process is rated one of the best economically. Ref. to Page 50 Figure #8-1 Rentech - 1 Indirect shows 640 BPSD times Incremental Capital = $6.8 Million.

Incremental Capital costs of $6.8MM (Million) to produce 640 Total Liquids (BPSD) - Barrels (26,880 gallons) per day. In the Report's Section 8.2 "Economic Evaluations" shows the varies rates of return. What it does not show is the fact that Synfuel plants can eliminate approximately 60% of the front-end cost of using direct coal liquefaction technologies in their design/build process.

Other products produced by a Synthetic Fuels Plant.

Wal Mart is selling a Biodegradable Motor oil for approximately $3.00 a Quart. (You can buy Regular Motor oil from Auto Zone or Checker for $.85 to $1.25 a quart). Wal-Marts supplier is Synthetic Oil Services International (SOS), McLean, VA. SOS also offers a synthetic low smoke biodegradable motor oil formulated for outboard marine use. .

WAXES

Waxes produced from Synfuels plants are known as Fisher-Tropsch (F-T) waxes, and have the potential to be refined to compete with F-T waxes currently produced in South Africa. They have a very high molecular weight, melting point, and have excellent hardness. F-T waxes are similar to petroleum hydrocarbon waxes with the exception that they have a higher proportion of higher melting, linear molecules.

The United States alone consumes approximately 25 - 30 million pounds of F-T waxes each year. However, until now, no F-T waxes was produced in the United States. About one-half of the waxes consumed in the U.S. are used in hot melt adhesives, 25 - 30 percent in inks and coatings, mainly as micro pulverized materials, and the balance in a large variety of applications as:

* Candles
* Crayons
* Lipsticks
* Textiles
* Resin-wax polish formulations
* Paste and emulsion polishes for floor ,furniture and automobiles
* Anticorrosion coatings
* Internal lubricants and mold-release agents for plastics

NAPHTHA

Naphtha produced by the Synfuels process can be used as a feedstock for chemical processing or refined to be used in the following products:

Varnish maker and paints
Type IV mineral spirits
Petroleum ether
Textile spirits and ink oil

While Liquid Hydrogen is the fuel of choice for a space-launch vehicle that accelerates quickly out of the atmosphere, studies have shown that liquid methane is better for an aircraft cruising at Mach 5 to Mach 7.

Methane (either natural gas or coalbed methane gas) is widely available, provides more energy than jet fuels, and can absorb five times as much heat as kerosene. Compared with liquid hydrogen , it is three times denser and easier to handle. This is the fuel used by the U.S. hypersonic spy plane, Aurora SR-71.

CONCLUSIONS:

As seen in table 1, by converting Natural gas or Coalbed methane Gas extracted from the Coalbeds directly into liquids can save a total of 72% compared to Coal liquefaction.

The environmentally friendly products produced from a Synthetic fuels plant, such as biodegradable motor oil, marine oil, lubricating oils can save millions of dollars now being spent in oil clean-up costs of used motor oils and petroleum based lubricants.

As stated earlier, Synfuels plants provides owners of Coalbeds producing methane Gas plus natural gas reserves, City and County Landfills, Sewer Treatment plants with Digestors and any thing that can produce methane gas, provides an opportunity to capitalize on previously unprofitable resources

REFERENCES

1 Gerald N. Choi, Sheldon J. Kkramer and Samuel S. Tam (Bechtel Corporation San Francisco, CA) Joseph M. Fox III Consultant) "SIMULATION MODELS AND DESIGN FOR ADVANCED FISHER-TROPSCH TECHNOLOGY", DOE CONTRACT NUMBER DE-AC22-DE-AC22-91PC90027

2 Hugh D. Guthrie, Gary J. Stiegel, Rodney D. Malone "Gas-to-Liquids Program Overview" Presented at the 1995 Coal Liquefaction and Gas Conversion Conference August 29-31, 1995

3 Publication - The Shell Middle Distillate Synthesis Plant in Bintulu, Malaysia, 20 Pages, May, 1992

4. Publication - Large-scale Conversion of Natural Gas to Liquid Fuels by, Haldor-Topsoe A/S

5 Jan H. Fourie General Manager Sasol Limited "The Sasol Slurry Phase Distillate Process: An alternative to LNG projects" Presented at the Fourth Annual Middle East Petroleum & Gas Conference, Bahrain, January 1996 .

6 Peter J.A. Tijm, J. M Marriott, H. Hasenack, M.M.G. Senden, Th. Van Herwijnen "The Market for Shell Middle Distillate Synthesis Products", presented at the ALTERNATE ENERGY '95 Vancouver, Canada, May 2-4, 1995

7 David Grey, Glen C. Tomlinson, Abdel ElSawy "Hybrid Plant Coal liquefaction Concept at the Great Plains Synfuels Plant", Report prepared for Basin Cooperative Services November 1991

Table 1. Element of cost - Bechtel Design costs in a indirect coal liquefaction baseline plant where further reductions in costs may be possible.

	%	OMIT
Coal Handling	6	OMIT
Gasification	32	OMIT
Oxygen Plant	14	OMIT
Byproduct Recovery	3	
Fisher-Tropsch Synthesis	7	
Syngas Recycle Loop	12	
Product Refining	6	
Field Cost	20	OMIT
TOTAL	100	

FISCHER-TROPSCH INDIRECT COAL LIQUEFACTION DESIGN/ECONOMICS - MILD HYDROCRACKING VS. FLUID CATALYTIC CRACKING

Gerald N. Choi, Sheldon J. Kramer and Samuel S. Tam
(Bechtel Corporation, San Francisco, CA)
Joseph M. Fox III (Consultant)
William J. Reagan (Amoco Oil Company, Naperville, IL)

Keywords: Fischer-Tropsch, Economics, Fluid Catalytic Cracking

In order to evaluate the economics of Fischer-Tropsch (F-T) indirect coal liquefaction, conceptual plant designs and detailed cost estimates were developed for plants producing environmentally acceptable, high-quality, liquid transportation fuels meeting the Clean Air Act requirements. The designs incorporate the latest developments in coal gasification technology and advanced (F-T) slurry reactor design. In addition, an ASPEN Plus process simulation model was developed to predict plant material and energy balances, utility requirements, operating and capital costs at varying design conditions. This paper compares mild hydrocracking and fluid catalytic cracking as alternative methods for upgrading the F-T wax.

FISCHER-TROPSCH PLANT DESIGN

Plant Configurations

Figure 1 is a block flow diagram showing the overall process configuration for the original design using mild hydrocracking. The plant contains three main processing areas. Area 100 generates a clean syngas from Illinois No. 6 coal from the Burning Star mine. Area 200 is the Fischer-Tropsch (F-T) synthesis area, and Area 300 is the product upgrading and refining area. Areas 100 and 200 are identical for both the mild hydrocracking and fluid catalytic cracking (FCC) cases. Utility plants and storage requirements in the offsites were estimated, but they are not detailed here.

1. Area 100 - Syngas Production -- Synthesis gas is generated in Shell gasifiers from ground, dried coal. Processing of the raw synthesis gas from the gasifiers is conventional, with Wet Scrubbing followed by single-stage COS/HCN Hydrolysis and Cooling, Acid Gas Removal by inhibited amine solution and Sulfur Polishing. Sour Water Stripping and Sulfur Recovery units are included in this area.

2. Area 200 - The Fischer-Tropsch Synthesis Loop -- This area includes the Fischer-Tropsch Synthesis, CO_2 Removal, Recycle Gas Compression and Dehydration, Hydrocarbon Recovery by deep refrigeration, Hydrogen Recovery and Autothermal Reforming. The Hydrocarbon Recovery unit includes deethanization, depentanization, fractionation and an oxygenates wash column. At low H_2/CO ratios, CO_2 is the primary byproduct of the F-T reaction (using a iron based catalyst) so a large CO_2 removal unit is required. The Autothermal Reformer converts the unrecovered light hydrocarbons to additional syngas which is recycled back to the F-T synthesis reactors.

3. Area 300 - Product Upgrading
   Hydrocracking Design -- Figure 2 is a block flow diagram of Area 300 of the mild hydrocracking design. This area contains eight processing steps; 1) wax hydrocracking, 2) distillate hydrotreating, 3) naphtha hydrotreating, 4) naphtha reforming, 5) C4 isomerization, 6) C5/C6 isomerization, 7) C3/C4/C5 alkylation, and 8) saturated gas processing and product blending. The hydrocracked and hydrotreated naphthas are catalytically reformed to produce an aromatic gasoline blending component. The lighter materials are isomerized and alkylated to produce a high quality gasoline blending stock. Purchased butanes are required to alkylate all the available C3/C4/C5 olefins.

   Fluid Catalytic Cracking Cases -- Figure 3 is a block flow diagram of Area 300 for the Fluid Catalytic Cracking (FCC) cases. Two FCC upgrading cases are considered; one uses a beta zeolite cracking catalyst, and the other uses an equilibrium USY cracking catalyst. In these cases, the wax hydrocracker is replaced by a FCC unit, a MTBE (methyl-tertiary-butyl ether) plant, and a NExTAME (mixed C5/C6/C7 ethers) plant. The other seven processing plants are unchanged.

The F-T slurry reactor is a bubble column reactor in which the slurry phase is a mixture of liquid hydrocarbons (molten wax) and catalyst. Synthesis gas provides the agitation necessary for good mixing and mass transfer of the reactants and products between the two phases. The slurry bed reactor design was chosen over a fixed bed reactor design based on an earlier DOE sponsored Bechtel study[1,2]. The reactor design is based on Mobil's two-stage, slurry reactor pilot plant studies[3]. These results were the basis for the yield correlations contained in the F-T slurry bed reactor computer model used in this study[4]. Details concerning the overall design basis, process selection, and costs have been reported[5].

Product and Byproduct Yields

A Fischer-Tropsch liquefaction facility can produce a wide variety of products of various qualities depending on the method used to upgrade the F-T wax.

In the mild hydrocracking case, the facility produces C3 LPG, an upgraded C5-350 °F naphtha and a 350-850 °F distillate. Liquid sulfur also is produced by the syngas production area. The hydrocarbon products have no measurable sulfur or nitrogen contents. Oxygen is removed to less than 30 ppmv. There are virtually no aromatics in the distillate. Both the naphtha and distillate products have low

rcsidual olefin concentrations. The diesel fraction has a very high cetane number. The jet fuel and heavy distillate fractions have low smoke points. The naphtha product is a mixture of C3/C4/C5 alkylate, C5/C6 isomerate and catalytic reformate. It is basically a raw gasoline with a clear (R+M)/2 octane of about 88.

In the FCC upgrading cases, the facility produces a propylene product in addition to those produced in the hydrocracking case. Methanol is purchased and reacted with the tertiary C4, C5, C6 and C7 olefins to produce MTBE and a mixed C5/C6/C7 ethers stream from the NExTAME etherification plant. The ether streams are mixed with the C5-350 °F naphtha to form an oxygenated gasoline blending component which contains significant amounts of olefins and has higher octane numbers than in the mild hydrocaracking case. Except for a lower pour point, the distillate fraction has about the same properties as that produced in the hydrocracking case.

PROCESS SIMULATION MODEL

The ASPEN Plus process flowsheet simulation model predicts the effects of key process variables on the overall material and utility balances, operating requirements and capital costs. It was developed as a planning/rcsearch guidance tool for use by the DOE and its subcontractors to explore, evaluate and define additional promising areas for future research in the production of liquid transportation fuels. The model is not a detailed plant design tool although it contains some design features. The F-T synthesis loop design is modeled in some detail, and Bechtel's slurry bed F-T reactor sizing and yield models have been incorporated into the ASPEN model. For the other plants, only overall yield, utility requirements and capital costs are estimated. Individual plant costs are prorated on capacity using cost-capacity exponents in conjunction with minimum and maximum single train capacity limits.

All plants in the three main processing sections are simulated either by stand-alone user Fortran blocks or a combination of ASPEN Plus process blocks and user Fortran blocks. Material balances, as well as utility consumptions, operating personnel requirements and ISBL costs for each plant are generated. The offsites, engineering and contingency costs are estimated as a percentage of the processing plant costs to generate the total installed cost of the facility. Detailed discussions of the ASPEN model development and simulation results have been presented in three separate papers[6-8]; the last of which discusses the beneficial effect of treating the F-T reactor vapor products in a close-coupled ZSM-5 reactor as an alternative product upgrading scheme.

A linear programming (LP) model of a typical PADD II refinery was developed using Bechtel Corporation's proprietary Process Industry Modeling System (PIMS) to assess the values of the F-T products from the mild hydrocracking case[9]. With the ASPEN and LP model results, a discounted-cash-flow analysis was carried out under a given set of financial assumptions to calculate the cost of F-T production for a 15% return on investment. Results are presented in terms of a Crude Oil Equivalent (COE) price which is defined as the hypothetical break-even crude oil price at which the liquefaction products are competitive with those produced from crude oil. Table 1 summaries the overall simulation model results for the mild hydrocracking case and the two FCC upgrading cases; one of which uses a beta zeolite cracking catalyst, and the other uses an equilibrium USY cracking catalyst.

FLUIDIZED-BED CATALYTIC CRACKING OF F-T WAX

Fischer-Tropsch wax can be readily cracked in a FCC unit under normal petroleum feedstock operating conditions, as demonstrated by the Amoco Oil Company[10]. The product is rich in C4 to C7 reactive olefins which are valuable for oxygenates production. The hydrocracking design and the ASPEN Plus simulation model were modified to use FCC instead of mild hydrocracking for upgrading the F-T wax. In addition, both a MTBE plant and a NExTAME (mixed C5/C6/C7 ethers) plant were included in Area 300. Both ether plants contain an associated selective hydrogenation unit to saturate diolefins in the feed.

Based on the Amoco data, two FCC cases were considered; a beta zeolite catalyst case and an equilibrium USY catalyst case. Although not in widespread commercial use, beta zeolite catalyst was selected for comparison with an equilibrium USY catalyst since it produces more olefins which can be converted to ethers for use as reformulated gasoline blending components. The propylene is purified and sold. The butenes are sent to the MTBE (methyl-tertiary-butyl ether) plant in which the isobutene is converted to MTBE, and the normal butenes are passed through to the alkylation unit. The C5, C6 and C7 olefins are sent to a NExTAME unit which converts most of the C5 olefins, less of the C6 olefins, and still less of the C7 olefins to ethers. This design produces significantly more gasoline blending components at the expense of distillate production than the hydrocracking design.

Amoco found that the F-T wax cracks so easily in a FCC unit that it does not produce enough coke to maintain the unit in heat balance. One solution to this problem is to supply additional fuel, sometimes called torch oil, to the regenerator to heat the regenerated catalyst to a high enough temperature to sustain the cracking operation. In a conventional petroleum refinery whenever torch oil is required, a low-value heavy material is used. However, in this stand-alone situation, no high-boiling low-valued streams are available from sources other than the FCC unit. Therefore, the heaviest portion of the potential distillate product is used as torch oil and burned in the regenerator to maintain the FCC unit heat balance.

Table 1 compares the model results for the wax hydrocracking case with those for the two FCC wax upgrading cases. In the hydrocracking case, approximately 3100 bbls/day of butanes are purchased and

isomerized for alkylation unit feed since the F-T reaction does not produce a sufficient amount to alkylate all the C3/C4/C5 olefins. The two FCC cases produce more olefins for alkylation unit feed, and as a result, still more butanes have to be purchased. Both FCC cases produce significantly more gasoline than the hydrocracking case. This additional gasoline is produced at the expense of distillate production which is reduced by over 60% resulting in gasoline to distillate ratios of over 4/1 compared to a 0.97/1 ratio for the wax hydrocracking case. In addition, the gasoline products are of better quality. They now contain oxygenates and have higher octanes, lower Reid vapor pressures, and contain less aromatics.

ECONOMIC COMPARISON

The predicted installed cost of each case is just under 3 billion dollars in mid-1993. The FCC upgrading cases have somewhat higher capital costs because of a larger alkylation plant, and the cost of the FCC plant and two etherification plants are more than the hydrocracker. These are preliminary cost estimates and have an accuracy range of +/- 30%. Most of the cost is in the syngas preparation and F-T synthesis areas. For the hydrocracking case, the entire product upgrading and refining area accounts for less than 8% of the ISBL cost.

A discounted-cash-flow economic comparison of the three cases was made using the spreadsheet program with previously reported economic assumptions[8]. Inflation projections are those of the Energy Information Administration[11]. Results are reported in terms of a Crude Oil Equivalent (COE) price which is the hypothetical break-even crude oil price at which the F-T liquefaction products are competitive with those produced from crude oil in an average PADD II refinery.

The hydrocracking case has an expected COE price of 35.4 $/bbl. The expected COE prices for the two FCC upgrading cases are the same at 34.5 $/bbl. These COE prices were calculated using the same margins for the gasoline and diesel blending stocks that were calculated for the hydrocracking case at the typical PADD II refinery. The gasoline blending stocks produced in these two FCC upgrading cases are of better quality than those from the hydrocracking case and should be more valuable. However, the COE calculations for the two FCC cases did not account for this expected increased value. Thus, the calculated COE prices for both FCC cases are conservative in the sense that they are somewhat higher than they should be because the products probably are undervalued. In order to accurately evaluate these two FCC upgrading cases, additional refinery LP modeling studies are required to assess the value of these blending stocks properly, and they will be done under another DOE contract.

In addition, there is another significant difference between the beta zeolite and equilibrium USY catalyst cases which can influence the choice between them. Both FCC upgrading cases consume methanol and produce a propylene product; whereas neither component is present in the hydrocracking case. The beta zeolite catalyst case consumes about 54% more methanol and produces about 57% more propylene than the equilibrium USY catalyst case. For 1995, propylene prices have ranged between 350 and 495 $/s-ton, and methanol prices have ranged at least between 0.47 and 1.35 $/gal (141 to 406 $/s-ton)[12]. The above expected COE prices were calculated using the average propylene price of 422.5 $/s-ton and the average methanol price of 0.91 $/gal (273 $/s-ton). The following table shows the effect of these variations in the methanol and propylene prices on the COE price for the two FCC upgrading cases.

	Most Optimistic	Average	Most Pessimistic
Propylene price, $/ton	495	422	350
Methanol price, $/ton	141	273	406
COE Prices, $/bbl			
Beta zeolite catalyst FCC upgrading case	33.2	34.5	35.8
Equilibrium USY catalyst FCC upgrading case	33.7	34.5	35.3

Thus, the COE price for the beta zeolite catalyst FCC upgrading case can vary between 33.2 and 35.8 $/bbl, a range of 2.6 $/bbl. For the equilibrium USY catalyst case, the COE price can vary between 33.7 and 35.3 $/bbl, a smaller range of only 1.6 $/bbl. This leads to the conclusion that with all other factors being the same, the equilibrium USY catalyst FCC upgrading case is less risky based on recent prices since it minimizes the effect of price variations on the expected COE price.

In conclusion, FCC upgrading of the F-T wax appears to be preferable to upgrading it by mild hydrocracking. Recent wide variations in methanol and propylene prices have been shown to cause significant fluctuations in the COE price of the F-T liquefaction products. Additional petroleum refinery modeling studies are needed to determine more accurately the values of the FCC upgraded products and to define a more reliable COE price for both of the FCC indirect F-T liquefaction cases. It is expected that this will improve the economics of upgrading the F-T wax by fluid catalytic cracking.

ACKNOWLEDGMENT

Bechtel, along with Amoco who was the main subcontractor for a major portion of this study, expresses our appreciation to the DOE/Pittsburgh Energy Technology Center for both technical guidance and financial funding under Contract No. DE-AC22-91PC90027

REFERENCES

1. Fox, J. M., "Slurry vs. Fixed-Bed Reactors for Fischer-Tropsch and Methanol", DOE Contract No. DE-AC22-89PC89876, Final Report, June 1990.
2. Fox, J., M., "Fischer-Tropsch Reactor Selection", *Catalysis Letters* 7 (1990) 281-292.
3. Kuo, J. C., "Slurry Fischer-Tropsch/Mobil Two-Stage Process of Converting Syngas to High Octane Gasoline", DOE Contract No., DE-AC22-80PC30022, Final Report, June 1983; and "Two-Stage Process for Conversion of Synthesis Gas to High Quality Transportation Fuels", DOE Contract No. DE-AC22-83PC60019, Final Report, October, 1985.
4. Fox, J. M. and Tam, S. S., "Correlation of Slurry Reactor Fischer-Tropsch Yield Data", *Topics in Catalysis* 2,(1-4), 285-300 (1995).
5. Choi, G. N., Tam, S. S., Fox, J. M., Kramer, S. J. and Marano, J. J., "Baseline Design/ Economics for Advanced Fischer-Tropsch Technology", DOE/Proceedings of The Coal Liquefaction and Gas Conversion Contractors' Review Conference, September 27-29, 1993.
6. Choi, G. N., Tam, S. S., Fox, J. M., Kramer, S. J. and Rogers, S., Process Simulation Model for Indirect Coal Liquefaction using Slurry Reactor Fischer-Tropsch Technology", Symposium on Alternative Routes for the Production of Fuels, ACS National Meeting, Washington, D. C., August 21-26, 1994.
7. Choi, G. N., Tam, S. S., Fox, J. M., Kramer, S. J. and Marano, J. J., "Process Design Simulation Models for Advanced Fischer-Tropsch Technology", DOE/Proceedings of The Coal Liquefaction and Gas Conversion Contractors' Review Conference, September 7-9, 1994.
8. Choi, G. N., Kramer, S. J. Tam, S. S. and Fox, J. M., "Simulation Models and Design for Advanced Fischer-Tropsch Technology", DOE/Proceedings of The Coal Liquefaction and Gas Conversion Contractors' Review Conference, August 29-31, 1995
9. Marano, J. J., Choi, G. N. and Kramer, S. J., "Product Valuation of Fischer-Tropsch Derived Fuels", Symposium on Alternative Routes for the Production of Fuels, ACS National Meeting, Washington, D. C., August 21-26, 1994.
10. Reagan, W. J., Nicholas, J. J., Hughes, R. D., and M. M. Schwartz, "The Selective Catalytic Cracking of Fischer-Tropsch Liquids to High Value Transportation Fuels", DOE Contract No. DE-AC22-91PC90057, Final Report, August 1994.
11. U.S. Department of Energy, Energy Information Administration, "Annual Energy Outlook 1995", January 1995.
12. Propylene prices are from the Chemical Marketing Reporter. Methanol prices are from Hart's Oxy-Fuel News, Vol. VII, No. 6, Sept. 4, 1995

TABLE I

Comparison of Mild Hydrocracking and Fluid Catalytic Cracking Upgrading of Fischer-Tropsch Wax

	Method of Upgrading the F-T Wax		
	Hydrocracking	FCC 1	FCC 2
Wax Upgrading Mode	Hydrocracking	FCC	FCC
FCC Catalyst Type	--	Beta Zeolite	Equilibrium USY
Plant Input:			
ROM Coal, TSD (MF)	18575	18575	18575
Methanol, TSD	0	321	209
Mixed Butanes, BSD	3110	5204	4327
Electric Power, Mwatts	54	58	56
Plant Output:			
Gasoline, BSD	23943	39723	39950
Distillate, BSD	24686	9764	9347
Propylene, BSD	0	5060	3215
Liquid Propane, BSD	1922	1573	1584
Sulfur, TSD	560	560	560
Slag, TSD (MF)	2244	2244	2244
Total Net C5+ Production, BSD	48629	49487	49297
Total Net C4+ Production, BSD	45519	44283	44970
Blended Gasoline Properties:			
Research Octane Number	90.9	96.8	95.8
Motor Octane Number	86.1	88.9	87.8
(R+M)/2 Octane Number	88.5	92.8	91.8
Reid Vapor Pressure, psi	5.0	4.7	4.7
Benzene, wt%	0.3	0.1	0.1
Aromatics, wt%	28.1	11.0	13.9
Olefins, wt%	0.0	12.7	15.5
Oxygen, wt%	0.0	3.3	2.1
Blended Distillate Properties:			
Pour Point, °F	- 28	- 40	- 40
Cetane Index	74	74	74
Installed Plant Cost, MM$ in mid-1993	2964	2987	2978

Figure 1
Indirect Coal Liquefaction Baseline Study
Overall Process Configuration

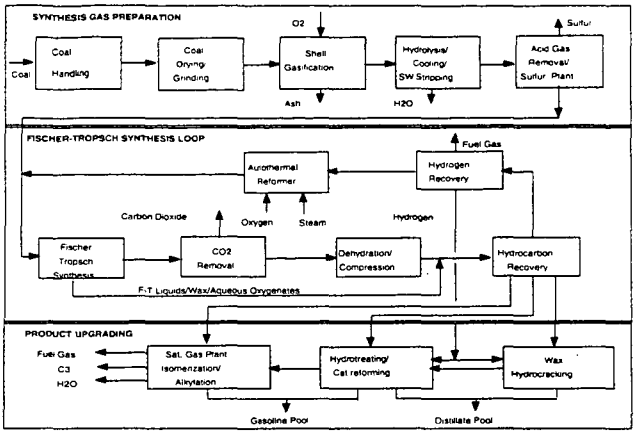

Figure 2
Area 300 Block Flow Diagram - Baseline Design With Wax Hydrocracking

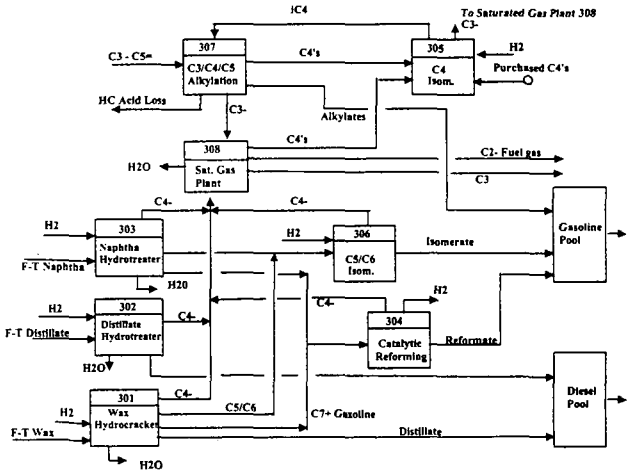

Figure 3
Area 300 Block Flow Diagram - Fluid Catalytic Cracking

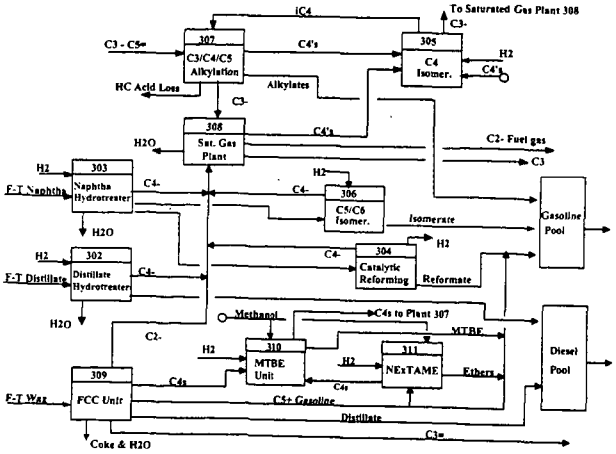

DECARBOXYLATION OF COAL MODEL COMPOUNDS UNDER LIQUEFACTION CONDITIONS: DOES DECARBOXYLATION LEAD TO RETROGRADE REACTIONS?*

Thomas P. Eskay, Phillip F. Britt, and A. C. Buchanan, III
Chemical and Analytical Sciences Division, Oak Ridge National Laboratory
P.O. Box 2008, MS-6197, Oak Ridge, Tennessee 37831-6197

Keywords: Decarboxylation, Liquefaction, Cross-Linking, Model Compounds.

Introduction

In recent years, it has become clear that oxygen functional groups in low-rank coals are major actors in retrograde reactions which inhibit their efficient thermochemical processing. In the pyrolysis and liquefaction of low-rank coals, low-temperature cross-linking reactions have been correlated with the loss of carboxyl groups and the evolution of CO_2 and H_2O [1,2]. Pretreatments such as *methylation, demineralization,* or *ion-exchange* of the inorganic cations reduce cross-linking and CO_2 evolution in pyrolysis [2a,3a]. In pyrolysis and liquefaction, the exchange of Na^+, K^+, Ca^{++}, or Ba^{++} into demineralized coal increases cross-linking and CO_2 evolution [3,4]. Cross-linking reactions also have a deleterious effect on liquefaction yields and the distribution of oils, preasphaltenes and asphaltenes [3,4]. These results suggest that decarboxylation may occur by a pathway that initiates retrograde (cross-linking) reactions in the coal polymer independent of the reaction conditions. However, the decarboxylation pathways in liquefaction and pyrolysis of low-rank coals are not known, and it is not clear how decarboxylation leads to cross-linking. Radical recombination or radical addition reactions have been suggested as being involved in retrograde reactions. However, the involvement of radical pathways in thermal decarboxylation reactions has recently been brought into question. We have presented evidence that in the pyrolysis of several bibenzyls containing aromatic carboxylic acids, radical pathways are not involved in thermal decarboxylation reactions and no cross-linking or coupling products are formed [5]. Further, Manion et al. observed that decarboxylation of benzoic acid derivatives in tetralin yielded only small amounts of aryl-aryl coupling products [6]. To gain a better understanding of the role decarboxylation plays in cross-linking reactions during liquefaction in low-rank coals, we have studied the thermal decomposition of several bibenzyls containing aromatic carboxylic acids, and their salts, in the presence of a hydrogen donor solvent (tetralin) and a nondonor solvent (naphthalene). The structures currently under investigation are 1,2-(3,3'-dicarboxyphenyl)ethane (**1**), 1-(3-carboxyphenyl)-2-(4-biphenyl)ethane (**2**), and the di-potassium salt of 1,2-(4,4'-dicarboxyphenyl)ethane (**3**).

Experimental

1,2-(3,3'-dicarboxyphenyl)ethane (**1**) was synthesized as described previously [5]. The synthesis of 1-(3-carboxyphenyl)-2-(4-biphenyl)ethane (**3**) and di-potassium 1,2-(4,4'-dicarboxyphenyl)ethane (**2**) are described below. Tetralin (Aldrich) was purified by washing with concentrated H_2SO_4 until the acid layer was colorless, washing with dilute aqueous $NaHCO_3$, followed by fractional distillation under reduced pressure (purity 99.4 % by GC). Naphthalene (Aldrich , 99.9 %) was used without further purification. THF (J.T. Baker HPLC Grade) was distilled from K before use. Gas chromatography analysis was performed using a Hewlett-Packard 5890 Series II gas chromatograph equipped with a J&W Scientific 30 m x 0.25 mm id, 0.25 μm film thickness DB-1 column and a flame ionization detector. Mass spectra were obtained at 70 eV on a Hewlett-Packard 5972 GC/MS equipped with a capillary column identical to that used for GC analysis.

Dipotassium 1,2-(4,4'-dicarboxyphenyl)ethane (3). 1,2-(4,4'-dicarboxyphenyl)ethane [7] (0.498 g, 1.85 mmol) was placed in DMF (10 mL) and aqueous KOH (1.0 M) was added dropwise until the solution became homogeneous. Ethanol (175 mL) was added to precipitate the salt, and the salt was collected by vacuum filtration (0.601 g, 94 %) and dried over P_2O_5 in a vacuum.

Diethyl 3-bromobenzylphosphonate. Into an oven-dried 100 mL flask equipped with a reflux

* Research performed at Oak Ridge National Laboratory, managed by Lockheed Martin Energy Research Corp. for the Division of Chemical Sciences, Office of Basic Energy Sciences, U.S. Department of Energy under contract DE-AC05-96OR22464.

condenser was placed 3-bromobenzyl bromide (20.01 g, 80 mmoles) and triethyl phosphite (13.8 mL, 80 mmol). The mixture was heated under argon to 140 °C with stirring for 2 h and then cooled to room temperature. The reflux condenser was replaced with a still head and the mixture was slowly reheated to 170 °C to distill off ethyl bromide and unreacted triethyl phospite. After cooling, the liquid (24.2 g, 99 %) was stored under argon. GC-MS retention time 17.9 min, *m/z* (relative intensity) 308 (M^+, 26), 306 (26), 171 (89), 169 (100), 138 (95).

1-(3-bromophenyl)-2-(4-biphenyl)ethene. Sodium hydride (3.2 g, 60 % mineral oil dispersion, 0.080 moles) was suspended in THF (100 mL) in a 250 mL oven-dried flask under a positive pressure of argon. A solution of diethyl 3-bromobenzylphosphonate (24.5 g, 80 mmol) in THF (100 mL) was transferred to the flask by cannula, and the mixture was stirred for 0.5 h. A solution of 4-biphenylcarboxaldehyde (14.6 g, 80 mmol) in THF (50 mL) was added dropwise over a period of 1 h, and the solution was refluxed for 2 h. The reaction was quenched with H_2O (200 mL) and a white solid was collected by vacuum filtration (19.4 g, 78 %). GC-MS retention time 26 min, *m/z* (relative intensity) 336 (M^+, 98), 334 (100), 255 (21).

1-(3-carboxyphenyl)-2-(4-biphenyl)ethene. 1-(3-bromophenyl)-2-(4-biphenyl)ethene (12.0 g, 35.8 mmol) was weighed into an oven-dried flask under an atmosphere of argon and THF (300 mL) was added. The stirred solution was cooled to -78°C and *n*-BuLi (14.5 mL, 2.5 M solution in hexane, 35.8 mmol) was added over a period of 0.25 h and the solution was stirred for 0.5 h. Carbon dioxide (produced from warming dry ice and passed through a $CaSO_4$ drying tube) was bubbled through the solution for 1.5 h. The solution was warmed to room temperature and quenched with 10 % H_2SO_4 (100 mL) and H_2O (300 mL). The THF layer was collected and the aqueous layer was extracted with THF (2 x 200 mL). The combined organic layers were washed with H_2O (100 mL) and dried over Na_2SO_4 . The THF was removed under reduced pressure to produce 10.1 g (93 %) of a white solid. GC-MS, analyzed as the trimethyl silyl ester, retention time 27.8 min, *m/z* (relative intensity) 372 (M^+,100), 357 (32), 283 (20).

1-(3-carboxyphenyl)-2-(4-biphenyl)ethane (2). Crude 1-(3-carboxyphenyl)-2-(4-biphenyl)ethene (3.02 g, 10.1 mmol), 10 % Pd/C (0.30 g), and EtOH (50 mL) were placed into a Parr hydrogenation bottle and shaken under 50 psi of H_2 until 1-(3-carboxyphenyl)-2-(4-biphenyl)ethene could no longer be detected by GC analysis (72 h). The solution was vacuum filtered and the Pd/C was washed with CH_2Cl_2. The solution was evaporated to dryness producing a white solid (3.10 g, 99%). GC-MS, analyzed as the trimethylsilyl ester, retention time 25.5 min, *m/z* (relative intensity) 374 (M^+, 9), 359 (6), 207 (3), 167 (100). The product was recrystallized 4 times from isopropyl alcohol (GC purity 99.9 %) and dried in vacuum with P_2O_5 prior to use in pyrolysis.

Pyrolyses. Pyrolyses in tetralin were performed by weighing the carboxylic acid and tetralin into a pyrex glass tube. The sample was frozen in liquid N_2, evacuated (10^{-4} Torr), backfilled with argon, and allowed to warm to room temperature. This process was repeated 7 times, the sample was frozen, the tube was evacuated (ca. 10^{-5} Torr), and sealed. Pyrolyses in naphthalene were performed by loading pyrex tubes with the appropriate amounts of carboxylic acid and naphthalene and conducting 3 freeze-pump-thaw cycles prior to sealing the tube at 10^{-5} Torr. The neat acid was pyrolyzed in sealed pyrex tubes (sealed at ca. 10^{-5} Torr). The pyrolyses were performed in a Tecam fluidized sandbath at 400 $\pm$ 1.5 °C. Following the pyrolysis, the samples were quickly removed from the sandbath and cooled in liquid N_2. The tubes were cracked open, and the solid products were removed with a 2:1 mixture of pyridine:N,O-bis(trimethylsilyl)trifluoroacetamide (BSTFA). Internal standards (2-phenylbenzoic acid and 2,4,6-trimethylbenzoic acid for (**1**) or 3,5-dimethylbenzoic acid for (**2**)) were added and the reaction mixtures analyzed by GC and GC-MS. For toluene analysis, the solids from the pyrolysis were extracted with CH_2Cl_2, internal standards (cumene and those mentioned above) were added, and the sample was analyzed by GC. The CH_2Cl_2 was blown off under argon, and the sample was dissolved in BSTFA:pyridine and reanalyzed. The identities of products from the thermolysis of **1** and **2** were determined by GC-MS analysis and were further confirmed by comparison with commercially available or synthesized authentic materials.

Results and Discussion

Thermolysis of 1 and 2 in Tetralin and Naphthalene

Previously, we have studied the pyrolysis of neat **1** at 400 °C [5]. The major products in the pyrolysis are shown in equation 1, and a typical product distribution for a 30 min pyrolysis is given in Table 1, entry 1. Excellent mass balances were observed in these thermolyses (97 % at 67 % conversion) and no coupling or high molecular weight products were observed by GC or HPLC analysis. From these results, we proposed that decarboxylation occurs by an acid-promoted, ionic mechanism as shown in equation 2. We have now extended our study of thermal decomposition of

aromatic carboxylic acids to include "liquefaction" conditions. In this study, a mono-carboxybibenzyl (**2**) was also investigated to provide an additional example of decarboxylation, and to confirm the diacid does not decompose by a unique pathway. Thermolysis of **1** and **2** in tetralin and in naphthalene were conducted at 400 °C in sealed pyrex tubes and the products were analyzed by GC and GC-MS.

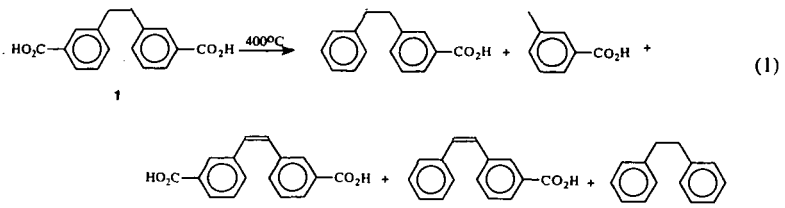

(1)

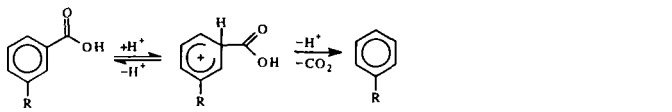

(2)

The major products from the thermolysis of **1** and **2** are shown in equation 1 and 3, respectively, and the product distributions at various time intervals are given in Tables 1 and 2. Several other products

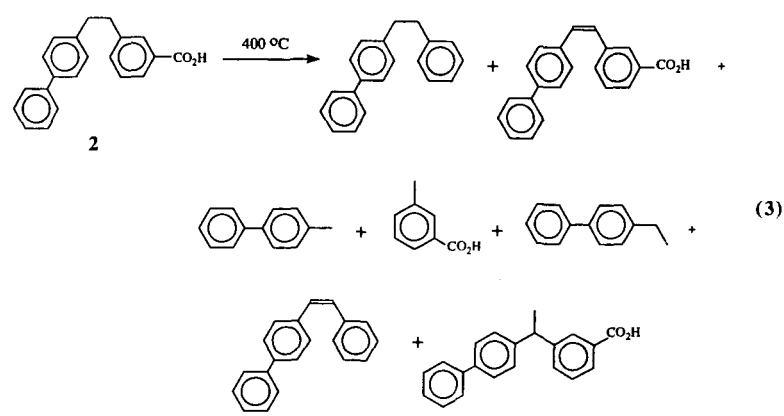

(3)

are formed in the pyrolysis that have not been identified, but based upon the GC peak area and the good mass balance, the amount of these products are small (<5 % mole % at conversions >30 % for **1** and <2 mole % at conversions of 14 % for **2**).

The results of the thermolysis of **1** and **2** in a hydrogen donor and nondonor solvent at 400 °C show that decarboxylation is a major reaction pathway. Despite the large amount of decarboxylation, no cross-linked products are detected. The good mass balances suggest that decarboxylation does not lead to any significant amounts of undetected coupling or cross-linking products. Compared to the pyrolysis of the neat acids, dilution with either a hydrogen donor solvent or a nondonor solvent increases the mole % of toluene products formed and decreases the amount of decarboxylation. This trend is due to a decrease in the rate of decarboxylation with dilution. The rate of unimolecular C-C homolysis, which leads to the toluene products, is unaffected by dilution. On the basis of the similar effect of dilution by a hydrogen donor and nondonor solvent, we propose that decarboxylation is occuring by an acid-promoted, ionic mechanism (eq 2) under "liquefaction" conditions. The source of acid for this decarboxylation is believed to be a second molecule of carboxylic acid and a second-order process is supported by the observation that the rate of decarboxylation decreases when compounds **1** and **2** are diluted in napthalene or tetralin. Additional

investigations into the reaction order for decarboxylation are currently in progress. Furthermore, we have established that a substituent effect is present that supports the mechanism in equation 2. The rate of decarboxylation of 1,2-(4,4'-dicarboxyphenyl)ethane (**5**) is roughly a factor of 2 faster than **1** neat or diluted in diphenyl ether. If the rate-determining step is *ipso*-protonation of the aromatic ring, as shown in equation 2, the *para*-alkyl substituent in **5** would stabilize the carbocation intermediate while the *meta*-alkyl substituent in **1** would not. McMillen has also observed that benzoic acids containing electron donating substituents (-OH and -OMe) decarboxylate faster than benzoic acid at 400 °C in tetralin [6]. This enhanced rate with activated benzoic acids in tetralin provides additional evidence that supports the acid-promoted ionic decarboxylation pathway shown in equation 2.

The results in Tables 1 and 2 also show that in tetralin, the formation of stilbene products is suppressed. The toluic acid and stilbene derivatives are formed by a free-radical reaction analogous to that reported for the thermolysis of bibenzyl [8,9]. Homolysis of **1** produces 2 ($HO_2CPhCH_2\bullet$), which can form toluic acid by hydrogen abstraction from tetralin or **1** to form $HO_2CPhCH_2CH(\bullet)PhCO_2H$ (**4**) (Scheme 1, the same pathway will also occur with **2**). Because

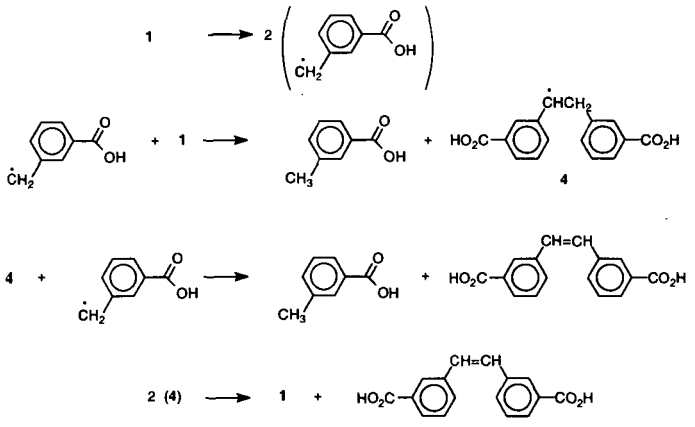

Scheme 1

tetralin is in large excess (10-fold), it quenches most of the free-radicals and any **4** produced will hydrogen abstract from tetralin before undergoing disproportionation to form stilbene. Also, stilbenes have been shown to react with tetralin at 400 °C to produce bibenzyl [10].

Thermolysis of 3 in Tetralin and Naphthalene

The exchange of inorganic cations, such as Na^+, K^+, Ca^{++}, or Ba^{++}, into demineralized low-rank coals can significantly decrease the liquefaction yields. For example, in the liquefaction (400 °C, 30 min, tetralin, H_2) of Zap lignite coal, exchange of potassium cations into an acid demineralized coal increases retrogressive reactions and decreases the liquefaction yields 40 % compared to the demineralized coal [3]. For Wyodak and a North Dakota lignite, ion exchange of potassium cations into the coal decreases the liquefaction yields 25 % compared to an acid demineralized coal [4]. Thermolysis of the dipotassium salt (**3**) was investigated in tetralin and naphthalene at 400°C for 0.5 h. No products were detected in either solvent and **3** was recovered unreacted (>99 % by GC analysis of the reaction mixtures). In addition, we have found that the neat salts are stable at 400 °C for times up to 2 h. The dipotassium salt is relatively stable at 400 °C under the liquefaction and inert solvent conditions and the salt remained solid during the thermolysis. These preliminary results suggest that the salts of aromatic carboxylic acids do not readily undergo decarboxylation that might lead to cross-linking reactions. Further investigation of the decarboxylation of inorganic salts of carboxylic acids is planned using the carboxy salts of **1** and **2** under liquefaction conditions.

Summary and Conclusion

The thermolysis of two aromatic carboxylic acids **1** and **2** and a dipotassium salt of a carboxylic acid (**3**) have been investigated at 400 °C as models of carboxylic acids in low rank coals under liquefaction and inert solvent conditions. Thermolysis of acids **1** and **2** leads to a large amount of decarboxylation products, but no evidence for the occurrence of retrograde reactions associated

with the decarboxylation process. It is proposed that the decarboxylation occurs by an acid-promoted, ionic pathway and further investigation of this reaction mechanism under liquefaction conditions is in progress. The dipotassium carboxy salt, **3**, is relatively stable at 400 °C and decarboxylation is not observed under liquefaction or inert solvent conditions. This preliminary result suggests that formation of carboxy salts in low-rank coals does not contribute to the retrograde chemistry. Overall, the results of both the acids and salt suggest that decarboxylation does not contribute to retrogressive reactions during the thermal processing of low-rank coals under liquefaction conditions. The evolution of CO_2 from low rank coals during thermal processing may well be coincidental with the chemistry occuring that results in cross-linking.

References

1. Suuberg, E.M.; Lee, D.; Larsen, J.W. *Fuel* **1985**, *64*, 1668.
2. (a) Solomon, P.R.; Serio, M.A.; Despande, G.V.; Kroo, E. *Energy and Fuels* **1990**, *4*, 42. (b) Ibarra, J.V.; Moliner, R.; Gavilan, M.P. *Fuel* **1991**, *70*, 408.
3. (a) Serio, M.A.; Kroo, E.; Chapernay, S.; Solomon, P.R. *Prepr. Pap.-Am. Chem. Soc. Div., Fuel Chem.* **1993**, *38(3)*, 1021. (b) Serio, M.A.; Kroo, E.; Teng, H.; Solomon, P.R. *Prepr. Pap.-Am. Chem. Soc., Div. Fuel Chem.* **1993**, *38(2)*, 577.
4. Joseph, J.T.; Forria, T.R. *Fuel* **1992**, *71*, 75.
5. (a) Eskay, T.P; Britt, P.F.; Buchanan, A.C. III *Prepr. Pap.-Am. Chem. Soc., Div. Fuel Chem.* **1996**, *41(2)*, 739. (b) Eskay, T.P; Britt, P.F.; Buchanan, A.C. III, submitted for publication in *Energy and Fuels.*
6. Manion, J.A.; McMillien, D.F.; Malhotra, R. *Prepr. Pap.-Am. Chem. Soc., Div. Fuel Chem.* **1992**, *37(4)*, 1720.
7. Britt, P.F.; Buchanan, A.C., III, Hoenigman, R.L. *Coal Science* Pajares, J.A. and Tascon, J. M. D. Eds.; Coal Science and Technology 24; Elsevier Science B.V.: Amsterdam, Netherlands, 1995, 437.
8. Stein, S.E.; Robaugh, D.A.; Alfieri, A.D.; Miller, R.E. *J. Am. Chem. Soc.* **1982**, *104*, 6567.
9. Poutsma, M. L. *Fuel* **1980**, *59*, 335.
10. King, H-H., Stock, L.M. *Fuel* **1984**, *63*, 810.

Table 1. Product Distributions Observed from the Thermolysis of *m,m*-$HO_2CPhCH_2CH_2PhCO_2H$ Diluted 10:1 (Molar Ratio) with Tetralin or Naphthalene at 400°C for Various Time Intervals.

Entry	1	2	3	4	5	6
Products (mole %)[b]	30 min (neat)	45 min Naph	45 min Tet	90 min Tet	225 min Naph	225 min Tet
$PhCH_3$	0[a]	0[a]	0[a]	0[a]	13.1	12.7
$PhCO_2H$	0.1	0	0	0	0	0
m-CH_3PhCO_2H	8.4	28.2	42	34	20.2	21.4
m-$CH_3CH_2PhCO_2H$	1.5	2.3	0	0	1.1	0.3
$PhCH_2CH_2Ph$	0.2	0	0	0	3.1	3.5
PhCH=CHPh	0	0	0	0	0.1	0
m-$HO_2CPhCH_2CH_2Ph$	77.1	62.5	58	66	55.1	59.7
m-HO_2CPhCH=CHPh	0.5	0.3	0	0	2.2	0
m,m-$HO_2CPhCH_2PhCO_2H$	0	0	0	0	0.3	0
m,m-$HO_2CPhCH(CH_3)PhCO_2H$	4.3	0.6	0	0	1.3	1.8
m,m-HO_2CPhCH=$CHPhCO_2H$	7.7	5.4	0	0	2.9	0
Conversion[b]	9.6	6.6	5.7	14.1	34.0	35.2
Mass Balance	99.1	97.1	99.4	96.2	95.0	93.0

a-Analysis for toluene not performed.
b-Based on products identified.
Tet=Tetralin; Naph=Naphthalene

Table 2. Product Distributions Observed from the Thermolysis of *m*-$HO_2CPhCH_2CH_2Ph$-Ph Diluted 10:1 (Molar Ratio) with Tetralin and Naphthalene at 400°C.

Entry	1	2	3
Product (mole %)[b]	60 min Neat	90 min Tet	90 min Naph
$PhCH_3$	0[a]	5.6	1.1
$PhCO_2H$	1.1	0	0
m-CH_3PhCO_2H	12.9	34.3	28.2
m-$CH_3CH_2PhCO_2H$	0.6	0	0.76
p-Ph-$PhCH_3$	14.6	38.7	30.7
p-Ph-$PhCH_2CH_3$	4.0	0	0
p-Ph-$PhCH(CH_3)Ph$	0.4	0	0.13
p-Ph-$PhCH_2CH_2Ph$	42.4	21.3	24.1
p-Ph-PhCH=CHPh	1.8	0	0
p-Ph-$PhCH_2Ph$-*m*-CO_2H	0.78	0	0.40
p-Ph-$PhCH(CH_3)Ph$-*m*-CO_2H	5.14	0	3.0
p-Ph-PhCH=CHPh-*m*-CO_2H	16.1	0	11.4
Conversion %[b]	14.4	11.6	14.2
Mass Balance	95.3	103	99.5

a-Toluene analysis not performed.
b-Based on products identified.
Tet=Tetralin; Napb=Naphthalene

UNIQUE FRACTIONATION OF BIOMASS TO POLYOLS PROVIDES INEXPENSIVE FEEDSTOCK FOR LIQUID FUELS PROCESS

J. Michael Robinson*, Caroline E. Burgess, Hari D. Mandal,
Chris D. Brasher, Kevin O'Hara, and Preston Holland
Science and Mathematics Department/Chemistry Faculty
The University of Texas of the Permian Basin
4901 E. University Blvd., Odessa, TX 79762

Keywords: biomass fractionation, coal liquefaction, coal hydrolysis

INTRODUCTION

Previous work in this laboratory established a unique process that converts C_5 and C_6 polyols (straight-chain hydrocarbons with a hydroxyl group on each carbon) to hydrocarbons using hydroiodic acid and phosphoric acids.[1] Polyols, such as sorbitol and xylitol, are commercially available from highly purified glucose and xylose but are expensive. To use less costly and renewable biomass resources as feedstock for this process, the biomass must first be fractionated (e.g. by steam explosion [2]) for cellulose and/or hemicellulose recovery; these polysaccharides can then be hydrolyzed and reduced to polyols. We are investigating a one-step Russian method [3] to directly convert raw "biomass-to-polyols" (BTP) to determine more definitive optimum reaction conditions and the economics of this method for comparison to using steam-exploded cellulose. In the Russian method, biomass is subjected to simultaneous dilute acid hydrolysis and catalytic hydrogenation at ~170 °C and ~50 atm H_2 (cold), thus trapping the incipient aldoses as their corresponding, but less reactive, polyols (alditols).

At this point, the main limitation to the effectiveness of the Russian method is the recycle of the catalyst, as using ruthenium/carbon (Ru/C) once-through is costly. In this process, the solid phase by-product lignin remains separate from the solution of polyols as the latter is formed from cellulose/hemicelluloses. The solid, with the catalyst, are simply filtered from solution. A major milestone in our investigation is separation of the lignin from the catalyst either by (1) base-extracting the lignin or (2) reacting it further at higher temperature and pressure in base. As the Russian paper suggests, clean catalyst can be recovered at 280-320 °C and ~50-70 atm H_2 (cold).[3]

As lignite has structural features similar to cellulose and lignin, we anticipated these reaction conditions could also convert a high percentage of coal into smaller moieties. Coal has been converted to liquids using many different solvents, temperatures, catalysts, and gas atmospheres.[4-6] However, few researchers have done acid or base hydrolysis/hydrogenation, particularly at such low severity conditions. Base extraction is used to remove humic acids, typically about 10-20 % of lignite.[7] Some of the original coal liquefaction reactions were done at low temperature by Berthelot where he heated coal with hydroiodic acid in a sealed glass tube to 250°C.[8] The bituminous coal was converted into a semi-liquid material with an oil content of 60 %. However, other research suggests that this conversion to oil would have contained a high iodide content.[9] In more recent work, lignite had high hexane-soluble yield using sodium aluminate and molybdenum/nickel catalysts at ~360°C.[10] Ruthenium catalysts have also been used successfully in coal liquefaction reactions at 400 °C and 50 atm of H_2, with a total conversion of Australian Yallourn brown coal of 96.5 % to THF-solubles/gas and an oil yield of 57.8 %.[11]

We describe in this paper the results for the BTP conversion at our typical reaction conditions, the cleaning of the ruthenium catalyst and how well the clean catalyst performed. We also include some preliminary experiments on a Texas coal at each of the reaction conditions of our BTP, possibly in stages, to see if indeed lignite can be converted under such low severity reaction conditions.

EXPERIMENTAL

Materials

The sawdust used was an oak hardwood. The catalyst was purchased from Aldrich Chem. Co., 5 % ruthenium on carbon (5% Ru/C). Phosphoric acid, sodium hydroxide, and methylene chloride are reagent grade. Lignite coal was obtained from COPL at Pennsylvania State University, sample DECS-1, with an ultimate analysis (dry) of %C - 62.5, %H - 4.8, %N - 1.2, %S - 1.0, %O - 14.7, % ash - 15.8.

Reaction Conditions

The reactions are done in a 3 L stirred autoclave that is heated by electric coils on the outside and cooled by water-cooled coils inside the reactor. The heater is temperature-controlled by computer. The reaction conditions for the BTP process are 180 °C, 2h, 50 atm H_2 (cold). The acid is a 0.8 % solution of phosphoric acid, and enough Ru/C is added for a 0.5% metal loading (~200g sawdust to 20g of 5% Ru/C catalyst). After reaction, the solid material is filtered from the liquid product by vacuum filtration and rinsing with water. The remaining solid is not dried. For the coal reaction, only 50 g (dry) coal and 5g of catalyst are used, the reaction was done twice using 0.8 % solution of phosphoric acid and sulfuric acid each, and the remaining solid after filtration is extracted with methylene chloride by ultrasonicating for 10 min and filtering the remaining solid.

For the sawdust reactions, initial experiments were done to determine if the lignin/catalyst could be run again without separation, but deactivation already occurred. Two methods were tried to remove the lignin from catalyst. The first involved base extraction of the catalyst to remove the lignin at atmospheric conditions. Using a 5 % solution of NaOH, the catalyst/base mixture was heated to 100 °C for 2-6 h, then filtered and rinsed repeatedly with water to remove the base.[2] The second method, described in the Russian literature [3] was to mix the catalyst with a 1.5 % solution of NaOH in the stirred autoclave to a temperature of 235-250 °C, 2 h, 44 atm H_2 (cold), then filtered and rinsed repeatedly with water.

The reaction conditions for a second lignite reaction are 235 °C, 2 h, 44 atm H_2 (cold) while in a 1.5 % solution of NaOH, which is then filtered and rinsed repeatedly with water. Only 50 g (dry) coal and 5g of catalyst are used, and the remaining solid after filtration is extracted with methylene chloride by ultrasonicating for 10 min and filtering the remaining solid. The results of these experiments and the process are explained in the next section.

RESULTS AND DISCUSSION

Figures 1-3 contain schematics of the processes used for these experiments. Figure 1 is a schematic of the entire process, each box representing a key step in our process and each circle representing a small step in our process that must be done in order to make our process economical. As described in previous publications,[1] the first step of our process is to convert either raw biomass or steam exploded biomass to polyols, followed by a second step to reduce the polyols to hydrocarbons using HI/H_3PO_3, and then finally to eliminate iodine from the hydrocarbons by using NaOH to produce hexene. The focus of this paper is Step 1, the BTP method, which is shown in the white box and highlighted in Figures 2 and 3.

BTP Method

As discussed in the introduction, the BTP method is used to convert the raw biomass to polyols using 0.7 % phosphoric acid, Ru/C catalyst at 180 °C, 50 atm H_2 (cold) for 2 h. Several different reaction conditions were tried as the Russian literature explained a range of reaction conditions,[3] but we found with these parameters the greatest yield of polyols, about 70 % of the wood, and about 30% of the remaining wood is lignin, as expected. These results are reproducible. However, in the process of separating the polyols from the lignin and catalyst, the lignin and catalyst are solids that are not easily separated, and without the separation of the lignin and catalyst, the catalyst cannot be recycled as it becomes deactivated. Without being able to recycle the catalyst and the loss of potentially sellable product lignin, the process is not very economical. So a major milestone for using this method is to separate lignin from the Ru/C catalyst.

Separation of Lignin and Catalyst

Two methods to accomplish this separation have been tried. The first method was to extract the lignin using hot sodium hydroxide; this is a well-known method to extract lignin from plants. This facile method has significant potential to remove most if not all of the lignin and has much less severe conditions than the alternative method. After six hours, about 75 % of the lignin is extracted. The yield of polyols in subsequent BTP reactions using the cleaned catalyst was reduced to 58 % upon the first recycle reaction and 51% upon the second recycle reaction indicating some deactivation of the catalyst.

The second method is from the Russian literature.[3] It is claimed that clean catalyst is obtained after reaction of the catalyst/lignin at 280-320 °C, 50-70 atm H_2, and 1.5 % NaOH solution, the product being phenolic compounds. At this time, mechanical problems have kept us from completing these reactions. Another reactor has been acquired to complete this study.

Coal Reactions

As discussed in the introduction, we felt both of these mild reaction conditions could significantly alter the structure of lower rank coal, so we have some preliminary results from these reactions. When reacting the coal at the 180 °C reaction condition in acid, we converted ~40 % of the coal to methylene chloride-solubles with little of the H_2 consumed during the process. When reacting the coal in base at 250 °C (the temperature did reach 250 °C for about 20 min, but fell to about 235 °C over a period of 80 min) and an initial H_2 pressure of 44 atm, we converted ~20 % of the coal to water-solubles; however, as these are intial experiments, we plan to continue to vary these reaction conditions. The pressure profile for this reaction was unusual in comparison to the reactions at lower temperature and could indicate the reaction ran at supercritical conditions.

For low temperature reactions using a hydrogenation catalyst (reactions < 320 °C), usually conversions are quite low, typically < 20 % of the coal reacts.[6, 10, 12] Most researchers believe the controlling mechanism of coal liquefaction is the depolymerization of the coal which does not significantly occur until 350 °C.[6] Exceptions to these data are acid-catalyzed reactions, such as Berthelot using HI [8] and other researchers using $ZnCl_2$ and $SnCl_2$,[6] as these catalysts are known to crack C-C bonds.

REFERENCES

1. (a) Robinson, J.M. *Amer. Chem. Soc. Division of Fuel Chemistry Preprints*, **1995**, *40*(3), 729, (b) U.S. Patent No. 5516960, May, **1996**.
2. Heitz, M., Capek-Menard, E., Koeberle, P.G., Gagne, J., Chornet, E, Overend, R.P., Taylor, J.D., and Yu, E. *Bioresource Tech.*, **1991**, *35*, 23.
3. Sharkov, V.I. *Angew. Chem. I.E.E.*, **1963**, *2*(8), 405.
4. Gorin, E., in *Chemistry of Coal Utilization*, **1981**, M.A. Elliott, Editor. John Wiley & Sons: New York, p1845-1918.
5. Donath, E.E., in *Chemistry of Coal Utilitzation*, **1963**, H.H. Lowry, Editor. John Wiley & Sons: New York, p1041-1080.
6. Derbyshire, F.J., *Catalysis in Coal Liquefaction*, **1988**, IEA Coal Research, London, IEA CR/08.
8. Berthelot, P.E.M., *Bull. Soc. Chim.*, **1869**, *11*, 278.
9. Geerards, J. J. Th. M., van Krevelen, D.W., and Waterman, H.I., Brenn.-Chemie, **1958**, *39*, 11.
10. Hulston, C.J.K., Redlich, P.J., and Marshall, M., *Fuel*, **1995**, *74*, 1870.
11. Suzuki, T., Yamada, H., Yunoki, K., and Yamaguchi, H. *Energy & Fuels*, **1992**, *6*, 352.
12. Redlich, P., Jackson, W.R., and Larkins, F.P. *Fuel*, **1985**, *64*, 1383.

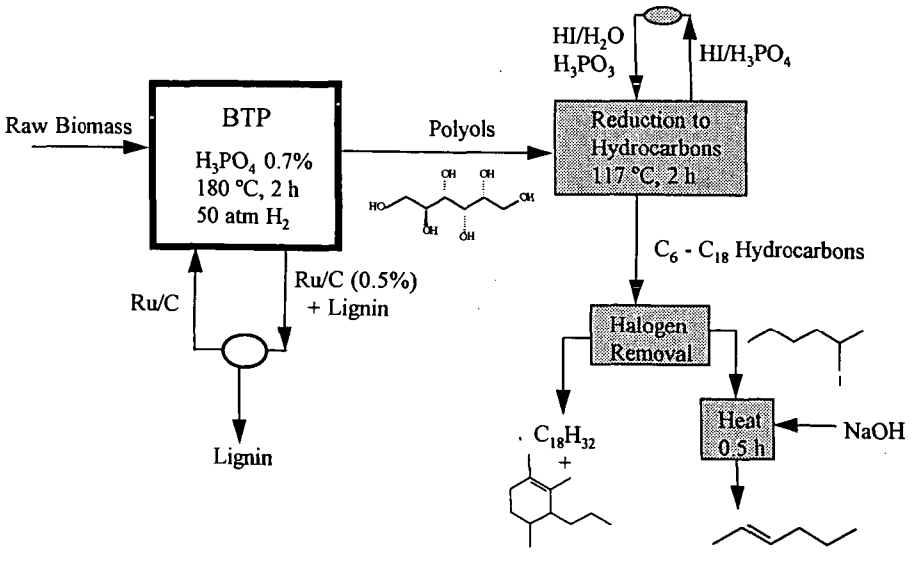

Figure 1: Schematic of Overall Biomass-to-Hydrocarbon Process

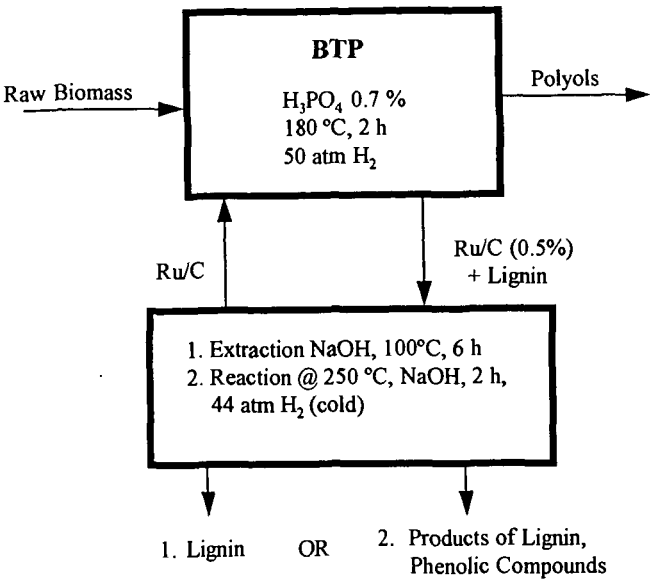

Figure 2: Schematic of BTP Process and Possible Processes to Separate Lignin and Ru/C for Recycle

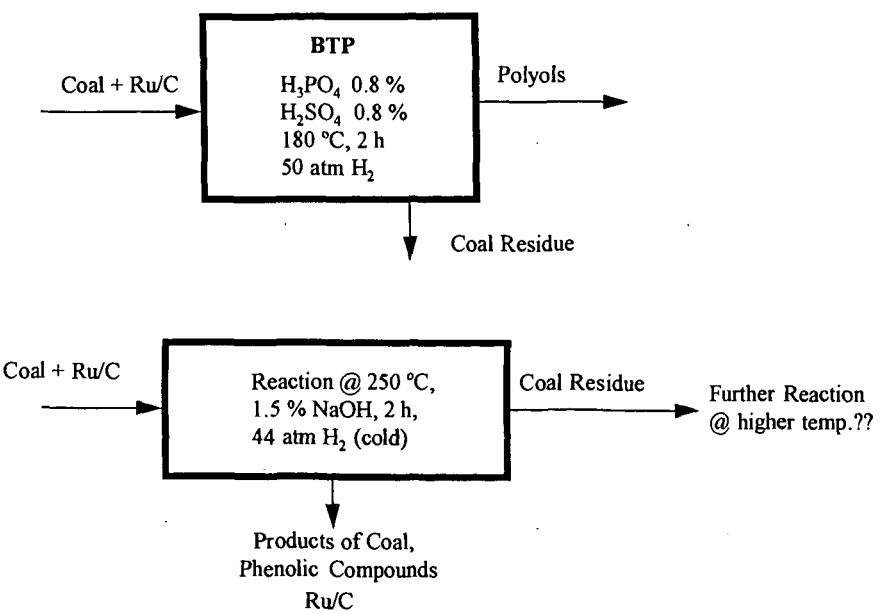

Figure 3: Schematic of BTP Process and Lignin Reaction Process Applied to Coal

CHANGES IN MOLECULAR ACCESSIBILITY IN APCS COAL OXIDIZED IN THE PRESENCE OF SUNLIGHT

R. Ding, L.D. Kispert and A.S. Jeevarajan
Department of Chemistry, Box 870336
The University of Alabama
Tuscaloosa, AL 35487-0336

KEYWORDS: Coal, Accessibility, Weathering, Spin Probes, EPR

ABSTRACT

Weathering changes the properties of coal and its utilization through oxidative and moisture loss processes. Using an EPR-spin probe method, it has been shown that the regions in Illinois # 6 coal accessible to spin probes upon *O*-alkylation increase if the coal is first exposed to sunlight in air rather than to air in the absence of sunlight. Analysis reveals that an increase in oxidation products and microporosity has occurred. One plausible cause for the increase is the formation and reaction of singlet oxygen. A study of Pocahontas #3, Lewiston-Stockton and Wyodak-Anderson coal in which the oxygen content varies from 2% to 17% shows that the accessibility of spin probes in toluene swelled oxidized coal depends also on the percent oxygen present and time of exposure to sunlight

INTRODUCTION

An EPR spin probe method developed in this lab[1] has been used to determine micropore size distribution and acid/base character during swelling[2-4], changes in pore structure and wall chemistry upon swelling at different temperatures and with solvents of various polarities[5,6], the break-up of the hydrogen bonding between the bedding planes[7], and the accessible nature of the covalently cross-linked materials during swelling[8]. This technique has been used successfully to follow changes in the micropore structure during weathering, oxidation, dehydration, and short term oxidation [9-12] of APCS coal.[13] Upon weathering the lower ranked coals (Beulah-zap and Wydak-Anderson) were observed to undergo structural collapse which precluded retention of even the smallest probes, while medium ranked coals exhibited improved retention.[9]

PREVIOUS STUDIES ON COAL OXIDATION

Eight vacuum dried APCS coals were oxidized in a pure O_2 environment as well as weathered in air so the effect of oxidation alone on coal structure could be determined.[10,11] It was shown that the removal of water was primarily responsible for the structural collapse observed in low ranked coal and for the increase in retention of polar spin probes in medium ranked coals.[10] Coals oxidized in a pure oxygen environment showed an increase in retention by as much as a factor of five.[11] Even the higher ranked coals showed significant retention of polar spin probes after four days exposure to oxygen. Short term exposure[12] of Illinois #6 to dry argon or oxygen showed a dramatic change in the coal structure in as little as thirty seconds. Long term weathering for as long as six months was carried out[14] to show that for Beulah-Zap, Illinois #6, and Upper Freeport coals little change occurs after weathering for thirty-six days. However, this is not true for Wyodak Anderson, Blind Canyon and Lewis-Stockton coals which undergo changes throughout the six months weathering period.

It has also been established that the inclusion of spin probes into the macromolecular structure of coal increases in a dramatic oscillatory manner by spiking a "poor" swelling solvent (toluene) with as little as 100 ppm of a strong swelling solvent (pyridine).[15] This has been explained in terms of four different processes: (1) disruption of weak hydrogen bonds which isolate the interconnected micropore system; (2) disruption of weak hydrogen bonds which protect individual micropores; (3) competition of pyridine for the active sites involved in the hydrogen bonds or the "poisoning" of sites; and (4) disruption of stronger hydrogen bonds within the macromolecules which causes an opening of the structure.

These processes were confirmed when the hydroxyl substituents were derivatized[16] with *n*-butyl groups in the absence of oxygen and light. The dramatic cyelic variation was eliminated due to the decrease in hydrogen bonding. It was also shown that a dramatic increase in spin probe retention occurred upon alkylation due to the existence of a more open structure (increasing microporosity) as a result of a decrease in attractive forces, and it was noted that the microporosity increased with increasing rank. In particular, upon O-alkylation, the relative value of the spin probe concentration increased by a factor of 4 for Beulah-Zap lignite (19.1% O), 2.5 for Wyodak-Anderson subbituminous (16.9% O), 5 for Illinois #6 (10.1% O), 3 for Blind Canyon (10.9% O), 1.3 for Pittsburgh #8 (6.9% O), 5.4 for Lewiston-Stockton high volatile bituminous coal (6.7% O), 10 for Upper Freeport medium volatile bituminous (4.7% O) and 6 for Pocahontas #3 low volatile bituminous (1.5% O). Previously published work by Liotta, Rose, and Hippo[17] indicated that an increase in microporosity occurs upon alkylation and that this increase is more pronounced in higher than lower ranked coals. Our measurements confirm these results. We also observed that the increase in microporosity depends on the structure of

each coal; Pittsburgh #8 and Lewiston-Stockton have almost identical oxygen content (6.9% vs. 5.7%) yet exhibit a large difference in the change in microporosity upon *O*-alkylation (1.3% vs. 5.4%). A similar effect was also observed for Illinois #6 and Blind Canyon (5% vs. 3%), although the difference is smaller for these coals which contain a higher percentage oxygen.

Oxidation processes of the coal have been studied by other methods as well. The oxygen content of coal has been determined by neutron activation analysis[18] and by XPS analysis of the coal surface.[19,20] Oxidation has also been measured by noting the relative changes in the FTIR signatures,[21] pH,[22] Gieseler fluidity,[23,24] pyrolysis response,[25,26] and free swelling index.[27] Low temperature oxidation must be quantified even though the amount of solid oxidation products is small.[28] XPS measurements in conjunction with GC analysis of the gaseous products and thermal gravimetric analysis (GA) of the fuels[29] have been useful in determining the oxidation process. Oxidation-induced structural changes of APCS at 120 °C were observed by differential scanning calorimetry (DSC) and solvent swelling.[30] The changes in the free radical character of Alberta coals upon air oxidation between 20-250 °C have been studied[31] as a function of mineral, moisture, and exinite macerate content. Water was also found to be a suitable probe molecule for the detection and measurement of coal oxidation.[32] Although a number of studies have been carried out, the influence of sunlight on the weathering process has not been studied and is the subject of this paper.

EXPERIMENTAL

The coal samples were irradiated by sunlight in the air on a clear day (30-40 °F) when the relative humidity was about 40%. A portion of the samples was swelled in toluene after exposure to sunlight, another was alkylated after exposure according to published methods[17] and a third portion was kept in the dark and then swelled.

A 40 mg unmodified sample of each APCS coal was added to a 10^{-3} M solution of the nitroxide spin probe in the swelling solvent. A spin probe was selected (in this study, VII; Tempamine[15]) depending on the dimensions (approximately spherical) of the coal pores to be studied or the substituents (amine) on the nitroxide molecule required to interact with various functionalities present in the coal.

Each coal and spin probe mixture was stirred vigorously under a nitrogen atmosphere at room temperature. After 18 hours, the mixture was filtered by suction, and residual solvent coating the coal was removed under reduced pressure at room temperature to collapse the coal around the nitroxide spin probe. The resulting material was washed with cyclohexane to remove any spin probe attached to the surface or trapped in large open pores of the coal, and the mixture was filtered and vacuum dried to remove the residual cyclohexane. The coal sample was packed into an EPR sample tube, evacuated, and sealed. The prepared spin probe-doped coal sample was stored at 77 K to prevent the slow 2-3 week decay of the nitroxide spin probe EPR signal at 300 K. EPR powder spectra were recorded on a Varian E-12 EPR spectrometer. Because of the presence of a large central signal due to radicals always present in coal, only the A_{zz} nitrogen hyperfine coupling was deduced. The magnetic field was calibrated using proton NMR markers, and the microwave frequency was measured with a frequency counter. The relative spin concentration per weight of undoped coal was determined by integrating the low field EPR line and comparing it to the integrated EPR spectrum of a frozen solution of the nitroxide spin probe under study. The absolute spin concentration was determined by comparison to a Cr(III) standard from the National Bureau of Standards.

RESULTS AND DISCUSSION

Changes in the Accessible Regions of Coal after Oxidation in Sunlight followed by Alkylation

The spin probe retention as a function of swelling solvent is plotted (Figure 1) for samples of swelled Illinois #6 O-alkylated (A) under a nitrogen atmosphere, in the absence of sunlight, (B) O-alkylated in air and in the absence of sunlight, and (C) after the coal was exposed to sunlight for 1.5 hours in air and then alkylated in air. The increase (37%) in the retained spin probe concentration upon alkylation reflects the increase in accessible regions of the coal as the coal becomes oxidized and is then alkylated. The effect of sunlight is striking. The spin probe tempamine (VII) is a base approximately spherical in shape that contains an amine substitutent capable of forming strong hydrogen bonds. Since upon alkylation the hydrogen-bonding OH substituents are converted to OR groups, the possibility of binding a trapping of tempamine by such hydrogen-bonding is excluded. The fact that nevertheless considerably greater amount of the spin probe are trapped (Figure 1 C) implies that micropores similar in size to spin probe VII are formed after alkylation of the coal that was oxidized in the presence of sunlight and air, and that the spin probe is not removed by the cyclohexane rinsing.

It was also noted that for toluene swelled Wyodak-Anderson (Figure 2), a decreasing spin probe retention occurred with increasing time of exposure to sunlight in the presence of air. In the case of toluene swelled Lewiston-Stockton (Figure 3), no dependence on spin probe concentration was found on time of exposure to air and sunlight; however, for toluene swelled

Pocahontas #3 (Figure 4), the spin probe concentration increased with increasing exposure to air and sunlight. It is apparent that an increase in OH groups occurs in high rank Pocahontas #3 upon air oxidation in the presence of sunlight, i.e., that addition sites for hydrogen bonding for spin probe VII are formed. However, the opposite trend occurs for coals with high oxygen content. In oxygen rich coal, cross-linking can occur by the combination of hydroperoxide radicals with existing radicals in the coal, reducing the microporosity with increasing exposure to sunlight. As the oxygen content decreases, the cross linking mechanism decreases in importance. Thus, it is expected that no dependence on sunlight will be observed for Lewiston-Stockton, a coal with 6.7% oxygen where the presence of cross-linking is balanced by the presence of hydrogen bonding as the exposure to sunlight is increased.

Sunlight Oxidation Mechanism

A clue to the reason for the increased numbers of OH (and perhaps carbonyl) groups in samples of coal exposed to sunlight in an air atmosphere was provided by the following observation. Upon irradiating a Blind Canyon coal suspension in dichloromethane, with filtered light (λ = 300 - 390 nm) from a 200 watt Hg cw lamp, a very intense phosphorescence peak was observed at 1277 nm. This emission is known to occur in the decay of singlet oxygen to the triplet ground state. Further such a signal was not observed upon irradiating dichloromethane (CH_2Cl_2 does not absorb above 240 nm) or a coal suspension in cyclohexane (a non-swelling solvent for coal). The formation of singlet oxygen is a result of energy transfer from the exited state (D_2 or D_1) of the radicals present in undoped coal, (Figure 5) to the excited singlet S_1 state of oxygen which then undergoes decay to the T_0 state producing the observed phosphorescence. The coal based phenoxyl and naphthalene anion radicals, for example, absorb at 390 and 340 nm, respectively. Thus, one plausible cause for the increase in oxidized products formed in coal upon exposure to sunlight is the formation and reaction of singlet oxygen. It is also possible to generate singlet oxygen by energy transfer from irradiated toluene which absorbs at 300 nm, so the choice of solvent is crucial.

CONCLUSION

Sunlight plays an important role in the weathering process. An increase in the number of OH groups in Illinois #6 occurs upon exposure to sunlight in the presence of air or oxygen. After subsequent alkylation, the micropore structure increases by 37%. One possible reason is the formation of singlet oxygen by energy transfer from excited singlet states of the radicals. The increase in microporsity decreases with time of exposure to sunlight for coals (not alkylated) with high (17%) oxygen content. For Lewiston Stockton coal not alkylated with medium (6.7%) oxygen content, there is no dependence on sunlight but for high rank coal (2%), Pocahontas #3 (not alkylated), there is an increase in microporosity with exposure to sunlight. The formation of singlet oxygen could possibly account for the increase in oxidation products in high rank coals as a function of sunlight.

ACKNOWLEDGMENT

This investigation was supported by the United States Department of Energy, University Coal Grant Program, Grant No. DE-FG22-93PC93202. Dr. Chignell at the National Institute of Environmental Health Sciences (NIEHS), Research Triangle Park, NC, is thanked for use of his equipment to measure the singlet oxygen phosphorescence from irradiated coal suspension and Dr. Elli Hand for discussions.

REFERENCES

1. Wuu, S.K.; Kispert, L.D. *Fuel* **1985**, *64*, 1681.
2. Goslar, J.; Kispert, L.D. *Energy and Fuels* **1989**, *3*, 589.
3. Goslar, J.; Cooray, L.S.; Kispert, L.D. *Fuel* **1989**, *68*, 1402.
4. Goslar, J.; Kispert, L.D. *Fuel* **1990**, *69*, 564.
5. Spears, D.R.; Kispert, L.D.; Piekara-Sady, L. *Fuel* **1992**, *71*, 1003.
6. Spears, D.R.; Sady, W.; Kispert, L.D. *Prepr. Pap. Am. Chem. Soc.,Div. Fuel Chem.* **1991**, *36*, 1277.
7. Spears, D.R.; Sady, W.; Kispert, L.D. *Fuel* **1993**, *72*, 1225.
8. Spears, D.R., Sady, W.; Tucker, D.; Kispert, L.D. *Energy and Fuels* **1993**, *7*, 1001.
9. Sady, W.; Kispert, L.D.; Spears, D.R. *Prepr. Pap. Am. Chem. Soc., Div. Fuel Chem.* **1992**, *37*, 1151.
10. Sady, W.; Tucker, D.; Kispert, L.D.; Spears, D.R. *Prepr. Pap. Am. Chem. Soc., Div. Fuel Chem.* **1993**, *38*, 1323.
11. Tucker, D.; Kispert, L.D. *Prepr. Pap. Am. Chem. Soc., Div. Fuel Chem.* **1993**, *38*, 1330.
12. Tucker, D.; Kispert, L.D.; *Prepr. Pap. Am. Chem. Soc., Div. Fuel Chem.* **1993**, *38*, 1335.
13. Vorres, K.S. *Energy and Fuels* **1990**, *4*, 420.
14. Kispert, L.D.; Tucker, D.; Sady, W. *Prepr. Pap. Am. Chem.Soc., Div. Fuel Chem.* **1994**, *39*, 54.
15. Ding, R.; Tucker, D.; Kispert, L.D. *Prepr. Pap. Am. Chem. Soc.,Div. Fuel Chem.* **1995**, *40*, 590.
16. Ding, R.; Tucker, D.; Kispert, L.D. *Prep. Pap. Am. Chem. Soc., Div. Fuel Chem.*

1995, *40*, 425.
17. Liotta, R.; Rose, K; Hippo, E. *J. Org. Chem.* **1981**, *46*, 277.
18. Ehmann, W.D.; Koppenaal, D.W.; Hamrin, C.E., Jr.; Jones, W.C.; Prasad, M.N.; Tian, W.Z. *Fuel* **1986**, *65*, 1563.
19. Perry, D.L.; Gint, A. *Fuel* **1983**, *62*, 1029.
20. Clark, D.T.; Wilson, R. *Fuel* **1983**, *62*, 1034.
21. Fredericks, P.M.; Moxon, N.T. *Fuel* **1986**, *65*, 1531.
22. Yun, Y.; Hoesterey, B.; Meuzelaar, H.I.C.; Hill, G.R. *Prepr., Pap. Am. Chem. Soc., Div. Fuel Chem.* **1987**, *32*,302.
23. Huffman, G.P.; Huggins, F.E.; Dunmyre, G.E.; Pignocco, A.J.; Lin, M. *Fuel* **1985**, *64*, 849.
24. Grint, A.; Perry, D.L. *Proc. Int. Conf. Coal Sci. 1985*, 879.
25. Ignasiak, B.S.; Clugston, D.M.; Montgomery, D.S. *Fuel* **1972**, *51*,76.
26. Iyuhara, H.; Tanibata, R.; Nishida, S. *Proc. Conf. Coal Sci.* **1985**, 491.
27. Larsen, J.W.; Dee, D.; Schmidt, T; Grint, A. *Fuel* **1986**, *65*, 595.
28. Gethner, J.S. *Fuel* **1987**, *66*, 1091; Isaacs, J.J.; Liotta, R. *Energy & Fuels* **1987**, *1*, 349.
29. Kilemen, S.R.; Freund, H. *Prepr. Pap. Am. Chem. Soc., Div. Fuel Chem.* **1988**, *33*, 706.
30. Yun, Y.; Sunberg, E. *Prepr. Pap. Am. Chem. Soc., Div. Fuel Chem.* **1992**, *37*, 1184.
31. Kudynska, J.; Buckmaster, H.A. *Fuel* **1992**, *71*, 1127.
32. Petit, J.C. in "1991 International Conference on Coal Science Proceedings," Edt. by International Energy Agency Coal Research, Butterworth-Heinemann, Oxford, 1991, p. 186.

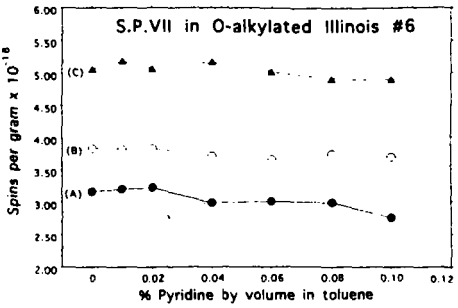

Figure 1: Spin probe VII retention concentration in O-butylated Illinois #6 versus percent pyridine by volume in toluene.

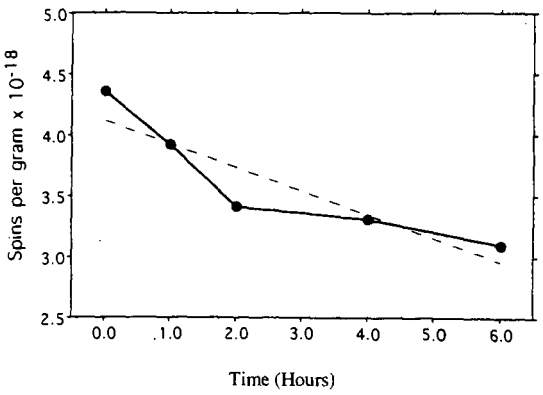

Figure 2: Toluene Swelled Wyodak-Anderson: Time of exposure to sunlight in the presence of air versus spin probe retention concentration

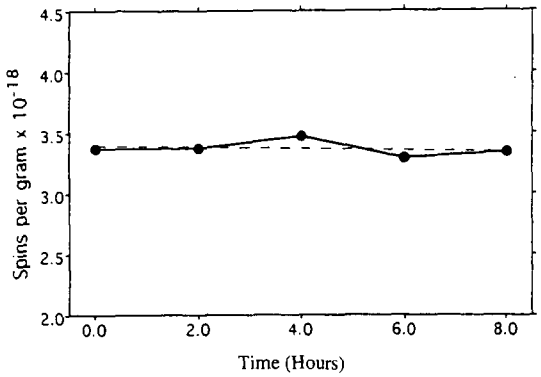

Figure 3: Toluene Swelled Lewiston-Stockton: Time of exposure to sunlight in the presence of air versus spin probe retention concentration

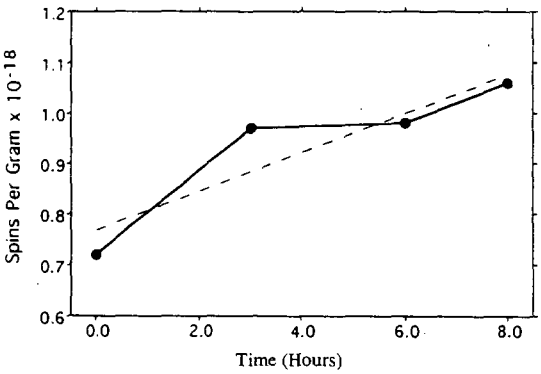

Figure 4: Toluene Swelled Pocahontas # 3: Time of exposure to sunlight in the presence of air versus spin probe retention concentration

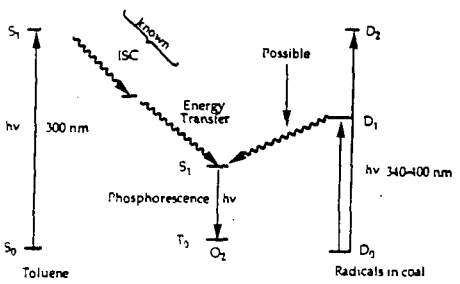

Figure 5: Energy diagram for singlet oxygen formation upon excitation of the naturally occurring radicals in coal

HIGH CONVERSION (98%) FOR THE HYDROGENATION OF 1-METHYLNAPHTHALENE TO METHYLDECALINS

Belma Demirel
U.K. Center for Applied Energy Research
3572 Iron Works Pike, Lexington, KY 40511-8433, USA
and
Wendell H. Wiser
University of Utah, Chemical and Fuels Engineering
Salt Lake City, UT 84112, USA

Keywords: Hydrogenation, 1-methylnaphthalene, methyldecalin

ABSTRACT

This work presents results from the hydrogenation of 1-methylnaphthalene. Aromatics are undesirable because of their toxicity, poor combustion characteristics and environmental impact. Saturated cyclic hydrocarbons with one or two rings show great promise for use in fuels. Methyldecalins were used as feed in the second step of a two-stage operation for the production of high octane gasoline components from 1-methylnaphthalene, which represents coal derived liquids. Experiments were conducted in a stirred batch reactor with commercial as well as previously tested non-commercial catalysts under different reaction conditions. The data shows that a NiMo catalyst supported on titania-alumina produced high yields of methyldecalins at 325°C and 1000 psi. The products were analyzed by GC/MS and ^{13}C-NMR spectroscopy. The conversion to methyldecalins were 98%. Previous methods yielded considerably lower conversion.

INTRODUCTION

It is widely agreed that the availability of petroleum in international trade is likely to diminish in the future. Research is being undertaken to develop economically competitive process for the conversion of coal, oil shale, tar sands and petroleum residues into liquid fuels. Although there has been significant advances both in improving the technology for converting coal to liquid fuels as well as in improving economics, the cost is still higher than for fuels produced from petroleum. Several of these coal liquefaction processes rely on the use of a catalyst.

Coal liquefaction processes generally involve a number of mechanical and chemical steps. Catalytic hydrogenation and cracking of the coal liquids take very important place in the development of coal liquefaction technology. The catalyst is believed to bring about the conversion of various species to molecules which are capable of cracking or depolymerizing coal particles by hydrogen transfer.

Coal liquids are very complex mixtures, mostly containing ring-type molecules, both aromatics and hydroaromatics, with various types of functional groups attached. 1-Methylnaphthalene (1-MeNAPH) was selected as a model compound representing coal-derived liquids. The immediate objective of this part of the project is to convert 1-MeNAPH to methyldecalins. Methyldecalins were in this study used as feed in the second stage of a two-stage operation for the production of high octane gasoline components from 1-MeNAPH, but they can also be used directly as a component in jet fuels.[1-6]

EXPERIMENTAL

Catalyst Preparation. NiMo/TiO_2-Al_2O_3 and NiMo/SiO_2-Al_2O_3 catalysts were prepared by incipient impregnation method. The support TiO_2-Al_2O_3 or SiO_2-Al_2O_3 was calcined in air at 540°C for 16 h, ground and sieved to -100 mesh. All prepared catalysts contained 25 mmol of Ni and 77 mmol of Mo per 100 g of support. A weighed sample was first impregnated with an aqueous solution of ammonium molybdate ($(NH_4)_6Mo_7O_{24}.4H_2O$, Alfa Product). The impregnated sample was oven-dried at 120°C for 16 h and then impregnated with a salt solution of nickel nitrate ($Ni(NiO_3)_2.6H_2O$, Fischer Scientific Co.).

NiW/TiO_2-Al_2O_3 and NiW/Al_2O_3 was impregnated in a single step with an aqueous solution containing calculated amounts of ammonium meta tungstate($(NH_4)_6H_2W_{12}O_{40}.3H_2O$, Cerac inc.) and nickelous nitrate followed by drying at 120°C for 16 h. The resulting material contained 88.9 mmol of Ni and 165.6 mmol of W per 100 g of TiO_2-Al_2O_3 or 100 g of Al_2O_3. Each catalyst was finally calcined in air at 540°C for 16 h.

NiW/SiO_2-Al_2O_3 (Harshaw Catalysts), Pt/REX and Pd/REX (proprietary) are commercial catalysts used for the experiments.

Presulfidation. All catalysts except Pt/REX and Pd/REX were sulfided in a tubular reactor prior to use. Nitrogen with a flow rate of 60 ml/min purged the sulfidation reactor to remove the air. The catalyst was heated to 400°C under nitrogen flow and kept at this temperature and inert conditions for an hour. The gas flow after this desorption step was changed to 10% (by wt) hydrogen sulfide in hydrogen. The reactor was maintained at 400°C at the same flow rate for 2 h. Subsequently, it was purged with nitrogen at the same conditions for an hour to remove the residual amount of hydrogen sulfide and then cooled to ambient temperature.

Reaction Experiments. Reaction experiments were conducted in a 300 cc batch reactor equipped with a magnetic drive stirrer, heating assembly, gas inlet and gas collector. Weighed amount of 1-MeNAPH (Aldrich Chemicals, 98%) and the sulfided catalyst in a feed to catalyst ratio of 10 to 1 were quickly dumped into the reactor. The sealed reactor was repeatedly purged with nitrogen and subsequently hydrogen to replace the air, and then pressurized with hydrogen and heated to a reaction temperature over about 20 minutes at slow stirring rate (80 rpm). Once the desired temperature was reached, the stirring speed was increased to 800 rpm and the reactor was remained at reaction temperatures for 1-10 h. Sulfided fresh catalyst was added to reaction mixture after first 5 h.

Product Analysis. Liquid products were identified by GC and GC/MS (Hewlett Packard 5890 Series II GC with a HP 5971 Mass Selective Detector). DB-5 column (30mx0.25mm i.d.x1.0μm, J&W Scientific) with a temperature program from 40 to 260°C. Gas products were analyzed by a Shimadzu GC-14A gas chromatograph, equipped with a flame ionization detector (FID) and Chromosorb 102 80/100 column (6'x1/8"x0.0085", Supelco). The column temperature ranged from 40 to 200°C. Scotty standard gases were used for calibration.

Methyldecalins from the hydrogenation of 1-MeNAPH were also identified by ^{13}C-NMR spectroscopy (VXR-400).

RESULTS AND DISCUSSION

Initial experiments were performed at 325°C and 1000 psi for 10 h with a feed to catalyst ratio of 10 to 1 by weight. The results are given in Figure 1. All conditions remained the same for all experiments, changing only the catalyst. The total conversion was defined as

$$\%\text{Total Conversion} = 100 \times \frac{\text{Feed - Feed in product}}{\text{Feed}}$$

Liquids were weighed just after completion of the reaction, and gas amounts were calculated from gas chromatograms. Liquid product distribution was calculated based on converted material. The products can be subdivided into four different groups.

(1) Cycloalkanes (*methyldecalins*, *cyclohexanes* and *cyclopentanes* which are mostly alkyl substituted and *'other cycloalkanes'* which include decalins, octahydroindenes, bicycloheptanes, etc.)
(2) Alkanes (*normal* and *branched*)
(3) Alkenes and cycloalkenes
(4) Aromatics (*Methyltetralins*, and *'other aromatics'* which include bigger than one ring aromatics)

Near 100% conversion was achieved with each catalyst but product distribution i.e. the depth of ring hydrogenation varies widely (Figure 1). $NiMo/TiO_2$-Al_2O_3 exhibited by far the highest hydrogenation activity followed by NiW/Al_2O_3 and NiW/TiO_2-Al_2O_3. Pt/REX and Pd/REX exhibited high cracking activity with a product dominated by aromatics. NiW/SiO_2-Al_2O_3 gave a mixture of hydrogenation and cracking products. Conclusively, the most effective catalyst in hydrogenation of 1-MeNAPH is $NiMo/TiO_2$-Al_2O_3 catalyst with a 97.2% conversion to methyldecalins at 325°C and 1000 psi.

Figure 2 shows the effect of temperature on the yield and distribution of liquid products from 1-MeNAPH using $NiMo/TiO_2$-Al_2O_3. The total conversion slightly decreased when the temperature was increased from 350°C to 450°C. The yield of methyltetralins and methyldecalins also showed a reverse temperature dependence. Conversion to one ring compounds, given under 'other aromatics', was observed as a result of cleavage reactions of tetralins at high temperatures.

Since reactions at higher temperatures result in cracking, the temperature was decreased to 325°C using $NiMo/TiO_2$-Al_2O_3 catalyst. Figure 3 summarizes the results under different reaction conditions, keeping only the temperature constant at 325°C. A total conversion of 100% was achieved, and the yields of methyldecalins were over 92% for each experiment. The yield of

methyldecalins only changed from 97.2 % to 98.6% as pressure was increased from 1000 psi to 1500 psi. When only the feed/catalyst ratio was changed from 10/1 to 5/1 at 1000 psi for 10 h reaction time, the conversion to methyldecalins reached to 99.5%,

Mass balances were closed with 4 to 13% error. The amount of gas products was 0.1-8.4% depending on reaction conditions. The gaseous fractions analyzed by GC were predominantly composed of methane at 325°C with $NiMo/TiO_2$-Al_2O_3, NiW/TiO_2-Al_2O_3 and NiW/Al_2O_3 catalysts because these catalysts have higher hydrogenation activities compared to NiW/SiO_2-Al_2O_3, Pt/REX and Pd/REX catalysts. The latters exhibited higher yields of C_3-C_4 hydrocarbons. The temperature effect on the distribution of gas products from hydrogenation of 1-MeNAPH at 350-450°C with $NiMo/TiO_2$-Al_2O_3 catalyst showed that the yields of C_1-C_2 hydrocarbons increased with temperature whereas those of C_3-C_4 hydrocarbons decreased.

Verification of Methyldecalin Synthesis. Primary identification of methyldecalins, separated by gas chromatography, was done by mass spectrometry and comparisons with database cracking patterns.[7] The results from GC/MS are given in Figure 4. Secondary identification was given by matching retention times with published boiling points. Figure 5 compares the present results with those of Weitkamp et al.[7-9] Filled circles represent retention times for eight isomers as measured in the present work and by Weikamp et al. Open circles represent two more isomers identified as methyldecalins by mass spectrometry in the present study and extrapolated values in Weitkamp's work. Additional support for the identification of these compounds as 9-methyldecalins was given by boiling points. Finally, consistency between different spectra was verified by comparisons with a compiled list of retention times for all identified compounds within the present project. Some uncertainties still persist for the distinction between different isomers except in the case of methyldecalins, where full agreement exists with literature.[7, 8,10-12]

Figure 6 shows the ^{13}C-NMR spectrum of the product from hydrogenation of 1-MeNAPH. The signals were integrated into two groups: (a) aliphatic carbons; chemical shift, δ=15-55 ppm, and (b) aromatic carbons; δ=125-160 ppm. It was observed that the aromaticity was about 2% and that the isomers have eleven carbon atoms in different proportions.

CONCLUSION

High conversions of methyldecalins (up to 99.5%) were obtained from the hydrogenation of 1-MeNAPH using $NiMo/TiO_2$-Al_2O_3 catalyst at 325°C and 1000 psi for 10 h reaction time. The hydrogenation processes consist of a complex array of kinetic steps involving a serious of intermediates producing methyldecalins simultaneously. The intermediate products are mixtures of methylnaphthalenes, methyltetralins and methyldecalins.

When reaction temperatures were increased, hydrocracking reactions set in as observed in Figure 4.3. The results from the present study agree with the work of Weitkamp et al.[7, 8, 13] They studied the hydrogenation of alkylnaphthalenes using a broad variety of catalysts. With most catalysts, yields of methyldecalins up to 90% range were obtained from individual methylnaphthalenes after 30-40 h reaction time over $Pt(0.6\%)/Al_2O_3$ catalyst at 200°C.

REFERENCES

1. Groot, C. K., de Beer, V. H. J., Prins, R., Stolarski, M. and Niedzwiedz, W. S. *Ind. Eng. Chem. Prod. Res. Dev.* **1986**, 25, 522
2. Patzer, II J. F., Ferrauto, R. J. and Montagna, A. A. *Ind. Eng. Chem. Process Des. Dev.* **1979**, 18, 625
3. Rosal, R., Fernando, V. D. and Herminio, S. *Ind. Eng. Chem. Res.* **1992**, 31, 1007
4. Sapre, A. V. and Gates, B. C. *Ind. Eng. Chem. Process Res. Dev.* **1981**, 20, 68
5. Gollis, M. H., Belenyessy, L. I., Gudzinowicz, B. J., Koch, S. D., Smith, J. O. and Wineman, R. J. *J. Chem. Eng. Data* **1962**, 7, 311
6. Donath, E. and Hess, M. *Chem. Eng. Progress* **1960**, 56 (4), 68
7. Weitkamp, A. W., Banas, E. M. and Johnson, G. D. *Preprints Amer. Chem. Soc. Div. Petr. Chem.* **1962**, 7, C-139
8. Weitkamp, A. W., in 'Advances in Catalysis, Volume 18', (Eds D. D. Eley, H. Pines and P. B. Weisz), Academic Press, New York, **1968**, p.1
9. Banas, E. M., Weitkamp, A. W. and Bhacca, N. S. *Analytical Chemistry* **1966**, 38 (12), 1783.
10. Meyerson, S. and Weitkamp, A. W. *Org. Mass Spectr.* **1969**, 2, 603
11. Bagrii, E. I., Musarev, I. A., Kurashova, E. K., Dolgopolova, T. N. and Sanin, P. I. *Neftekhimiya* **1968**, 8, 818
12. Stukanova, L. N., Shan'gina, T. N. and Petrov, A. A. *Neftekhimiya* **1969**, 9, 196
13. Shaptai, J., Nag, N. K. and Massoth, F. E. 'Proc. 9th International Congress on Catalysis', Calgary, **1988**, p.1

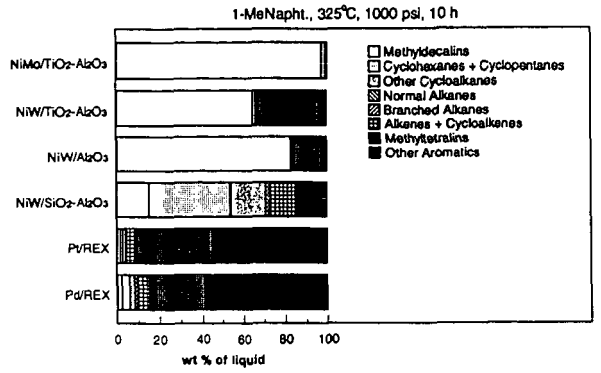

Figure 1. Yield and distribution of liquid products from hydrogenation/hydrocracking of 1-MeNAPH using different catalysts. Difference to 100% is the unconverted material. Feed/catalyst ratio is 10/1.

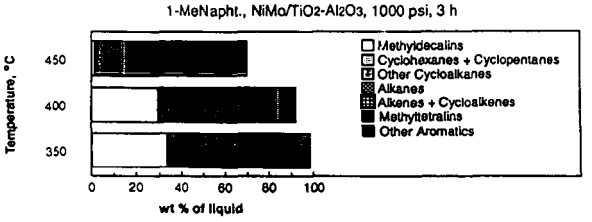

Figure 2. Effect of temperature on the yield and distribution of liquid products from hydrogenation/hydrocracking of 1-MeNAPH. Difference to 100% is the unconverted material Feed/catalyst ratio is 10/1

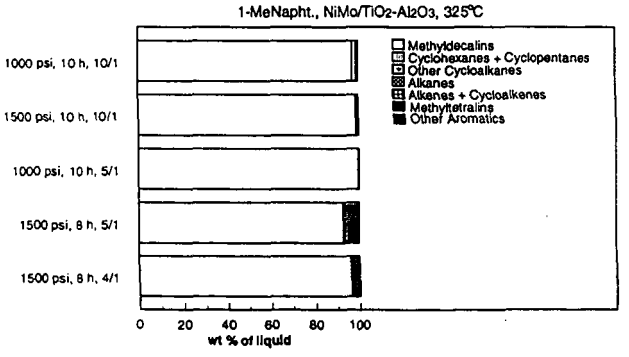

Figure 3. Effect of variable combinations on the yield and the distribution of liquid products from the hydrogenation of 1-MeNAPH using $NiMo/TiO_2$-Al_2O_3 catalyst. 10/1, 5/1 and 4/1 define feed to catalyst ratios.

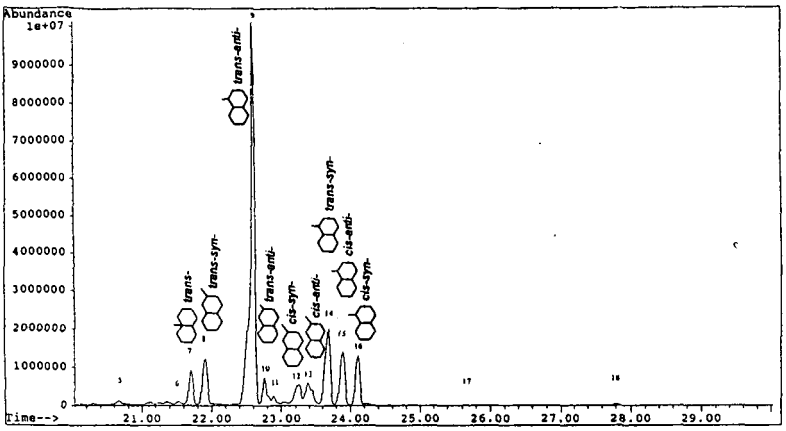

Figure 4. Identification of methyldecalins by GC/MS.

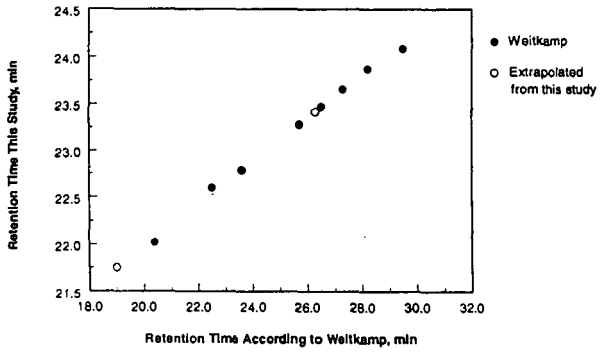

Figure 5. Identification of isomers of methyldecalins by comparison with published GC retention times.

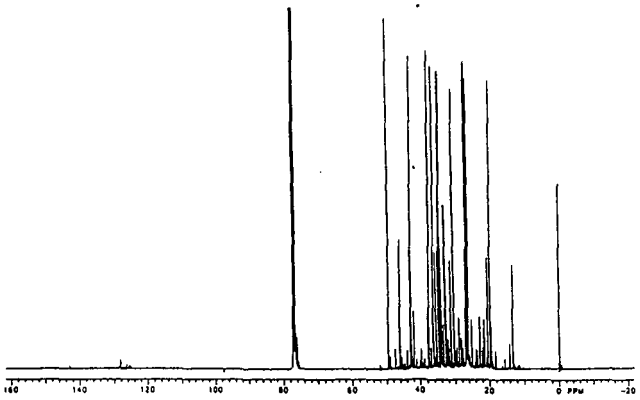

Figure 6. ^{13}C-NMR spectrum of the product from hydrogenation of 1-MeNAPH.